ALMA MATER STUDIORUM
UNIVERSITÀ DI BOLOGNA

DOTTORATO DI RICERCA IN

Scienze Chirurgiche e Tecnologie Innovative

Ciclo XXXVIII

Settore Concorsuale: 06/D2

Settore Scientifico Disciplinare: MED13/MEDS-08/A

ADVANCEMENTS IN THE APPLICATION OF LIQUID CHROMATOGRAPHY-TANDEM MASS SPECTROMETRY (LC-MS/MS) TO DRIED BLOOD SPOTS FOR THE CHARACTERIZATION OF METABOLIC AND HORMONAL DERANGEMENT IN ENDOCRINE DISEASES

Presentata da: **Greta Galante**

Coordinatore Dottorato

Prof. Emanuela Marcelli

Supervisore

Prof. Uberto Pagotto

Cosupervisore

Prof. Flaminia Fanelli

Esame finale anno 2026

ALMA MATER STUDIORUM
UNIVERSITÀ DI BOLOGNA

Table of Contents

ABSTRACT 5
1. LIQUID CHROMATOGRAPHY COUPLED TO MASS SPECTROMETRY 7
1.1. THE CHROMATOGRAPHIC METHOD 7
1.2. HIGH-PERFORMANCE LIQUID CHROMATOGRAPHY 9
1.2.1. TYPICAL COMPONENTS OF AN HPLC 9
1.2.2. THE LC-MS INTERFACE: BRIDGING THE LIQUID AND VACUUM WORLDS . 11
1.3. INTRODUCTION TO MASS SPECTROMETRY 12
1.3.1. CORE COMPONENTS OF MASS SPECTROMETERS 12
1.4. IONIZATION TECHNIQUES 13
1.4.1. ELECTRON IONIZATION (EI) 13
1.4.2. ATMOSPHERIC PRESSURE IONIZATION (API) 14
1.5. MASS ANALYZERS AND DETECTOR 18
1.5.1. MASS ANALYZERS 18
1.5.2. ION DETECTION 19
1.6. TANDEM MASS SPECTROMETRY 19
1.6.1. MULTIPLE REACTION MONITORING (MRM) 19
1.7. THE CHROMATOGRAM AND MASS SPECTRUM 20
1.7.1. THE ROLE OF THE ION RATIO IN SPECIFICITY 20
1.7.2. MATRIX EFFECT AND ION SUPPRESSION 21
1.8. QUANTITATIVE ANALYSIS IN LC-MS/MS 22
1.8.1. CALIBRATION CURVES 22
1.8.2. THE INTERNAL STANDARD METHOD 22
1.9. METHOD VALIDATION IN LC-MS/MS 23
1.9.1. LINEARITY AND MEASURABILITY RANGE 23
1.9.2. ACCURACY AND PRECISION 23
1.9.3. SELECTIVITY AND SPECIFICITY 24
1.9.4. LIMIT OF DETECTION (LOD) AND LIMIT OF QUANTITATION (LOQ) 24
1.9.5. MATRIX EFFECT 25
1.9.6. STABILITY 25
2. DRIED BLOOD SPOTS 26
2.1. GENERAL INFORMATION ABOUT DRIED BLOOD SPOT (DBS) 26
2.2. TECHNICAL SPECIFICATIONS 27
2.3. ANALYTE EXTRACTION AND ANALYSIS METHODS 28
2.4. ADVTANGES AND LIMITATIONS 28
2.5. CURRENT APPLICATIONS 31
3. ADRENAL GLANDS 33

3.1. PHYSIOLOGY OF ADRENAL GLANDS 34
3.1.1. PHYSIOLOGY OF THE ADRENAL CORTEX 34
3.1.1.1. ZONA FASCICULATA 35
3.1.1.2. ZONA GLOMERULOSA 36
3.1.1.3. ZONA RETICULARIS 38
3.1.2. PHYSIOLOGY OF ADRENAL MEDULLA 38
3.2. MAJOR ADRENAL PATHOLOGIES 42
3.2.1. PATHOLOGIES OF THE ADRENAL CORTEX 42
3.2.1.1. CUSHING SYNDROME 42
3.2.1.2. ADRENOCORTICAL ADENOMAS (ACAs) 49
3.2.1.3. MILD AUTONOMOUS CORTISOL SECRETION 50
3.2.1.4. ADRENOCORTICAL CARCINOMAS (ACCs) 51
3.2.1.5. HYPERALDOSTERONISM 52
3.2.1.6. ADRENOGENITAL SYNDROMES AND CONGENITAL ADRENAL HYPERPLASIA (CAH) 54
3.2.1.7. ADDISON'S DISEASE 55
3.2.2. PATHOLOGIES OF ADRENAL MEDULLA: PHEOCHROMOCYTOMA 58
4. STEROID HORMONES 61
4.1. CLASSES AND PHYSIOLOGICAL ROLE 61
4.2. BIOSYNTHESIS AND STRUCTURAL CLASSIFICATION 62
4.2.1. SYNTHESIS PATHWAYS AND TISSUE SPECIFICITY 62
4.2.2. STRUCTURAL CLASSIFICATION BY CARBON NUMBER 62
4.3. TRANSPORT AND MEMBRANE PERMEABILITY 63
4.3.1. CIRCULATORY TRANSPORT AND CARRIER PROTEINS 63
4.3.2. BIOLOGICAL ACTIVITY AND CLEARANCE 63
4.4. RECEPTOR BINDING AND ACTION: MOLECULAR MECHANISMS 64
4.4.1. STEROID RECEPTORS: STRUCTURE AND CLASSIFICATION 64
4.4.2. GENOMIC ACTION (SLOW PATHWAY) 64
4.4.3. REGULATION OF STEROIDOGENESIS 65
4.4.4. RAPID NON-GENOMIC ACTION (FAST PATHWAY) 65
4.5. REGULATION AND SYNTHESIS CONTROL OF STEROID HORMONES 65
4.5.1. GLUCOCORTICOIDS: THE HYPOTALAMIC-PITUITARY-ADRENAL (HPA) AXIS AND CIRCADIAN RHYTHM 66
4.5.2. MINERALOCORTICOIDS: THE RENIN-ANGIOTENSIN-ALDOSTERONE SYSTEM (RAAS) 67
4.5.3. SEX STEROID HORMONES: BIOSYNTHESIS, REGULATION, AND PHYSIOLOGICAL ROLES 68

4.6. ADVANTAGES OF LC-MS/MS OVER IMMUNOASSAY FOR STEROID ANALYSIS 69
5. METABOLOMICS 71
5.1. TARGETED AND UNTARGETED METABOLOMICS 71
5.2. CLASSES OF METABOLITES OF INTEREST IN METABOLOMICS 73
5.2.1. AMINO ACIDS 73
5.2.2. BIOGENIC AMINES 75
5.2.3. ACYLCARNITINES 77
5.2.4. GLYCEROPHOSPHOLIPIDS 79
5.2.5. SPHINGOMYELINS 80
5.3. APPLICATION OF LC-MS/MS IN STEROIDOMICS AND METABOLOMICS 82
6. AIM OF THE THESIS 83
7. MATERIALS AND METHODS 86
7.1. DEVELOPMENT AND OPTIMIZATION OF LC-MS/MS METHODS FOR ENDOGENOUS AND EXOGENOUS STEROIDS IN DRIED BLOOD SPOTS (DBS) 86
7.1.1. CHEMICALS AND REAGENTS 86
7.1.2. PREPARATION OF STOCK AND WORKING SOLUTIONS 86
7.1.3. LC-MS/MS INSTRUMENTATION AND SOURCE OPTIMIZATION 86
7.1.4. CHROMATOGRAPHIC METHOD DEVELOPMENT 87
7.1.5. CALIBRATION AND ANALYTICAL PERFORMANCE 88
7.1.6. DBS SAMPLE PREPARATION AND EXTRACTION 88
7.2. CIRCADIAN STEROID PROFILING AND COMPLEMENTARY METHOD DEVELOPMENT AT THE UNIVERSITY OF GENEVA (UNIGE) 92
7.2.1. CIRCADIAN STEROID PROFILING IN DBS 92
7.2.2. DEVELOPMENT OF AN LC-MS/MS METHOD FOR ESTROGEN ANALYSIS IN SERUM97
7.3. VALIDATION OF TARGETED METABOLOMICS IN SERUM AND DBS SPECIMENS 99
7.4. CIRCADIAN METABOLIC PROFILING IN HEALTH AND IN STATES OF CORTISOL RHYTHM DERANGEMENT 104
8. RESULTS 110
8.1. DEVELOPMENT OF LC-MS/MS METHODS FOR ENDOGENOUS AND EXOGENOUS STEROIDS IN DRIED BLOOD SPOTS (DBS) 110
8.1.1. OPTIMIZATION OF IONIZATION AND CHROMATOGRAPHIC CONDITIONS 110
8.1.2. EVALUATION OF AMMONIUM FLUORIDE CONCENTRATION 112
8.1.3. CALIBRATION AND ANALYTICAL PERFORMANCE 113
8.1.4. OPTIMIZATION OF DBS EXTRACTION PROTOCOL 118
8.2. CIRCADIAN STEROID PROFILING AND COMPLEMENTARY METHOD DEVELOPMENT AT THE UNIVERSITY OF GENEVA (UNIGE) 121

8.2.1. CHARACTERIZATION OF THE CIRCADIAN STEROIDOME IN DBS 121
8.2.2. ESTROGEN ANALYSIS IN SERUM 126
8.3. VALIDATION OF TARGETED METABOLOMICS IN SERUM AND DBS 130
8.4. CIRCADIAN METABOLIC PROFILING IN HEALTH AND IN STATES OF CORTISOL RHYTHM DERANGEMENT 136
9. DISCUSSION 143
9.1. DEVELOPMENT AND OPTIMIZATION OF AN LC-MS/MS METHOD FOR ENDOGENOUS AND EXOGENOUS STEROIDS IN DBS 143
9.2. CIRCADIAN STEROID PROFILING AND COMPLEMENTARY METHOD DEVELOPMENT AT THE UNIVERSITY OF GENEVA (UNIGE) 147
9.2.1. CHARACTERIZATION OF THE CIRCADIAN STEROIDOME IN DBS 147
9.2.2. ESTROGEN ANALYSIS IN SERUM 151
9.3. VALIDATION OF TARGETED METABOLOMIC ANALYSIS IN DBS 153
9.4. CIRCADIAN METABOLIC PROFILING IN HEALTH AND IN STATES OF CORTISOL RHYTHM DERANGEMENT 156
10. CONCLUSION 160
Bibliography 162

ABSTRACT

The present study focused on the development and application of advanced liquid chromatography-tandem mass spectrometry (LC-MS/MS) methodologies for hormonal and metabolite profiling. The project pursued four main objectives: i) optimization of analytical and pre-analytical LC-MS/MS protocols for the quantification of extended exogenous and endogenous steroid panels in dried blood spots (DBS) at the Center for Applied Biomedical Research (CRBA), University of Bologna; ii) analysis of DBS samples for a broad steroid panel using an internal calibration combined with multi-targeting strategy at the Biomedical and Metabolomics Analysis (BMA) group at the University of Geneva; iii) development of a pre-analytical and analytical procedure for the highly sensitive LC-MS/MS quantification of estrogens; iv) validation of the application in DBS of a broad targeted metabolomics method, and application to cohorts of patients with altered cortisol secretion or rhythm.

At the University of Bologna, two broad LC-MS/MS panels overall allowing the measurement of 34 among steroid hormones and drugs were optimized, and a dedicated DBS extraction protocol was refined to improve analytical recovery and matrix cleanliness. At the University of Geneva, 54 samples from a circadian steroid profiling study in 6 healthy subjects were analyzed using an internal calibration and multitargeted approach, which ensured absolute quantification of 8 key steroids. This work confirmed the feasibility of DBS sampling combined with LC-MS/MS for accurate characterization of diurnal steroidome rhythm. A second research line addressed one of the major analytical challenges of LC-MS/MS: the low ionization efficiency of estrogens. A dedicated sample purification and derivatization procedure was optimized, leading to a substantial improvement in detection sensitivity and enabling the reliable quantification of these low-abundance hormones. Finally, a targeted metabolomics approach focusing on 187 among amine and lipid compounds was applied to investigate metabolic pathway alterations associated with cortisol rhythm disorders. Building validation data demonstrating the general strong correlation of metabolite levels between DBS and serum matrices, the method was used to profile metabolites in patients with adrenal insufficiency under glucocorticoid replacement therapy, mild autonomous cortisol secretion, and Cushing's syndrome. The analysis revealed distinct metabolic patterns linked to the degree and timing of cortisol dysregulation.

Altogether, the work represents a significant methodological and translational advancement in steroidomics and metabolomics, providing robust, sensitive, and minimally invasive tools for the clinical investigation of endocrine and metabolic disorders.

1. LIQUID CHROMATOGRAPHY COUPLED TO MASS SPECTROMETRY

1.1. THE CHROMATOGRAPHIC METHOD

Chromatographic techniques comprise a set of analytical methods that enable the separation of molecules in complex samples (1). The development of this method was initiated in the early 20th century by the Russian scientist Mikhail Semyonovich Tsvet during empirical evaluations of pigments contained in chloroplasts (2) (3). From its theoretical foundation to the present day, chromatographic techniques have been significantly developed and optimized, primarily due to continuous advancements in instrumentation and materials (4).

Chromatography is based on two theoretical principles: the distribution of a molecule, called the analyte, between a mobile phase and a stationary phase, and the different migration speeds of the analytes in the sample (5). Specifically, in liquid chromatography (LC), the mobile phase is a liquid, and the stationary phase is generally a solid packed within the chromatographic column (6). Due to the specific affinity that each molecule has for the stationary phase, analytes will pass through the analytical column at different speeds and will therefore elute at different times: the higher a molecule's affinity for a given stationary phase, the greater the interactions, and the longer it will take for that molecule to detach from it (5) (6).

Currently, various combinations of mobile and stationary phases exist, which define the distinct types of liquid chromatography (7).

- Adsorption Chromatography: Utilized for the separation of non-ionic compounds insoluble in water; the stationary phase is a solid, on whose surface chemically active sites are present, capable of forming a series of non-covalent bonds with the various molecules contained in the sample under analysis (7) (8).
- Ion-Exchange Chromatography: Based on the principle of attraction between oppositely charged ions (9); the stationary phase consists of macromolecules containing ionized active sites, where counter-ions can be exchanged with others of equal charge present in the mobile phase. This establishes competition between the counter-ions of the stationary phase and those of the mixture being separated, for the ionized active sites of the stationary phase (9) (10).

- Partition Chromatography: There are two main types of partition chromatography, distinguished by the relative polarity of the stationary and mobile phases: normal-phase partition chromatography and reversed-phase partition chromatography (11). In the former case, the stationary phase is polar, and the mobile phase is non-polar; the different components of the sample are then eluted in increasing order of polarity (11) (12). In reversed-phase chromatography, the stationary phase is non-polar, while the mobile phase is polar. The first compounds to be eluted will be the most polar ones, followed by the less polar ones (12) (13).
- Size-Exclusion Chromatography**:** Size-exclusion chromatography (also known as gel filtration or gel permeation chromatography) utilizes specific materials like dextran (14); the function of these substances is that the chains of these polymers, connected by branching and cross-links, form a particular three-dimensional network. This type of chromatography behaves like a filter, allowing smaller molecules to penetrate the network meshes, while larger molecules, whose dimensions exceed the gel meshes, are eluted first (14) (15).

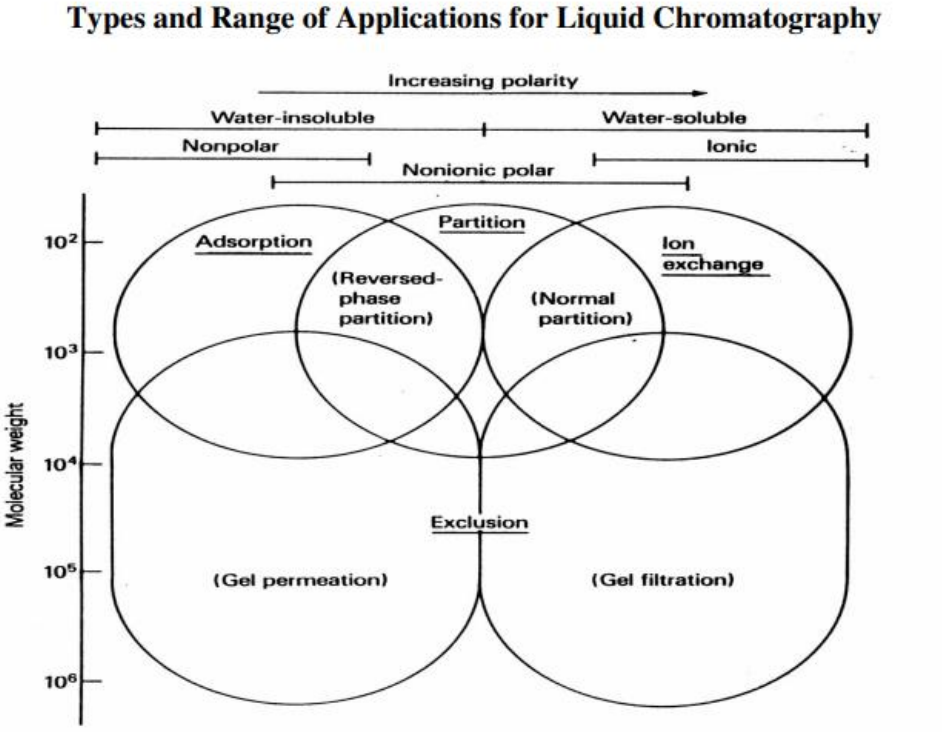

Figure 1*: Types of liquid chromatography in relation to the chemical nature of the target analyte. Reproduced from Skoog, Holler and Nieman, "Principles of Instrumental Methods, 5 th. Ed., p. 726, 1971 (251).*

1.2. HIGH-PERFORMANCE LIQUID CHROMATOGRAPHY

High-Performance Liquid Chromatography (HPLC) is an analytical technique representing the natural evolution of classical chromatography (4) (15). In HPLC, the stationary phase is packed inside an analytical column. The liquid mobile phase passes through the analytical column thanks to the high pressure applied by a pumping system positioned upstream of the column (2). The efficiency and technical evolution of modern liquid chromatography depend on the advancements of instrumentation, which requires operating pressures of several hundred atmospheres to allow the achievement of flow rates capable of ensuring efficient separation in a reasonable time (2) (16). Modern HPLC systems are composed of the following elements: mobile phase reservoirs, pumps, automated sample introduction systems (or autosamplers), analytical columns equipped with corresponding guard columns, and detection systems.

1.2.1. TYPICAL COMPONENTS OF AN HPLC

- Mobile Phase Reservoirs: These consist of glass bottles suitable for containing the mobile phases; the pumping system pushes the mobile phases into the lines by aspirating them through the solvent inlet filters placed at the bottom of the bottles. Various systems are also present to eliminate air bubbles that can cause alterations in flow continuity, referred to as degassers (17).
- Pumps: The pumping system aspirates the mobile phases from the bottles and introduces them into the lines, pushing them to the analytical column (18). Given the wide variety of solvents that can be used, it is fundamental that this pumping system be chemically resistant to most of them; moreover, it must be capable of ensuring a constant and reproducible flow, thus avoiding phenomena of variation in the liquid flow rate, an event that alters the normal flow dynamics, thereby compromising the reproducibility of the method (18). The high backpressures generated in the HPLC system primarily depend on the characteristics of the analytical column packing, the viscosity of the phases, and the diameter of the tubes connecting the various system elements (16).
- Autosampler: This component allows for the automation of the sample introduction process during analysis (19). This element is equipped with a specific thermostated

compartment to hold the samples and a needle injection system capable of ensuring repeatability and precision in the injection of micro-volumes of sample (0.1 - 100 μL) (19).

- Analytical Column: The analytical column is the element within which the separation of the molecules constituting the sample under analysis occurs (20). It consists of a cylinder of various lengths and diameters, filled with different packing materials (20). The performance of the column can be optimized by evaluating the optimal temperature of its housing, in order to provide the correct conditions for maximum possible interaction between the analytes and the binding sites of the analytical column (21). Furthermore, the analytical column must be periodically replaced due to the constant accumulation of substances within it, an event that causes a progressive increase in working back-pressures and a reduction in resolving power (22).
- Guard Column: The primary function of the guard column is to protect the analytical column from the accumulation of substances. It therefore extends the lifespan of the analytical column; this guard column is packed with the same stationary phase as the analytical column, has the same diameter but is shorter in length (22).
- Detector: This component allows for the detection of analyte passage and generates a signal proportional to the amount of analyte passing per unit of time (7). Furthermore, through its interface with a computer, it allows for the quantification of these events to deduce the analyte concentration in the sample (7). Several types of detectors exist, e.g., spectrophotometric (ultraviolet, infrared, etc.), fluorometric, and refractive index detectors (28). In recent years, the use of HPLC separation techniques coupled with mass spectrometers as detectors has gained increasing recognition (2) (23).

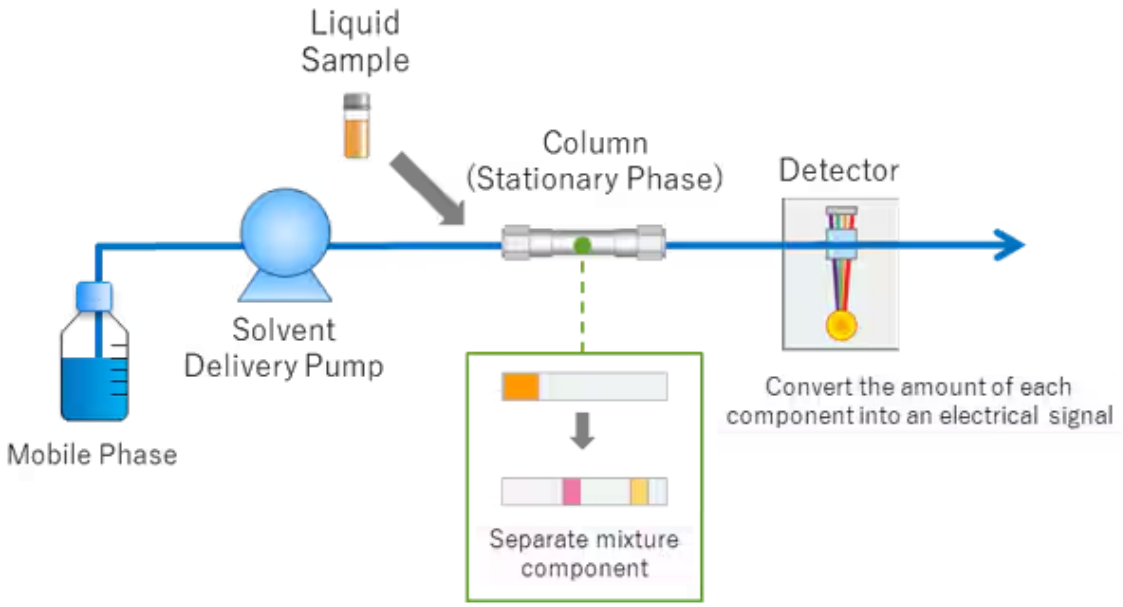

Figure 2. *Overview of HPLC. Reproduced from: Shimadzu Corporation, "What is HPLC (High Performance Liquid Chromatography)?" available at www.shimadzu.com, accessed October 2025 (24).*

1.2.2. THE LC-MS INTERFACE: BRIDGING THE LIQUID AND VACUUM WORLDS

The successful coupling of a liquid chromatography system with a mass spectrometer represents a significant technical challenge. The LC system operates by pumping a liquid mobile phase at high pressure (often several hundred atmospheres), whereas a mass spectrometer requires a remarkably high vacuum to allow ions to travel freely without collision. The LC-MS interface is the crucial component that bridges these two disparate environments. Its primary function is to efficiently remove the vast volume of solvents while simultaneously converting the neutral analyte molecules into gas-phase ions that can be analyzed by the mass spectrometer. This process is fundamentally achieved through various ionization techniques, which serve as the core of the interface itself, and that will be described in the following paragraph 1.4.

1.3. INTRODUCTION TO MASS SPECTROMETRY

Mass spectrometry (MS) is a powerful analytical technique used for the identification, characterization, and quantification of chemical compounds. It operates by measuring the molecular mass of an entire molecule and/or the mass and fragmentation pattern of its stable fragments. Its basic principle relies on the unique mass-to-charge (m/z) ratio and fragmentation signature, which serve as highly specific fingerprints, enabling the unequivocal identification of a particular compound (25).

The fundamental process of mass spectrometry can be broken down into three main stages:

- Ion Generation: The sample is first converted into a gaseous stream of charged particles (ions).
- Ion Separation: These ions are then transported through a high-vacuum environment and separated based on their mass-to-charge (m/z) ratio by a mass analyzer.
- Ion Detection: Finally, the separated ions are detected, and their abundance is measured to generate a mass spectrum.

1.3.1. CORE COMPONENTS OF MASS SPECTROMETERS

A mass spectrometer is an analytical instrument composed of five primary functional elements that interact constructively to analyze a sample. These components are (i) the sample inlet system, which prepares the sample for analysis, (ii) the ion source, where the sample molecules are ionized, (iii) the mass analyzer, which separates ions based on their mass-to-charge (m/z) ratio, (iv) the detector/recorder system, which measures the abundance of the separated ions, and (v) the vacuum system, which is essential to prevent molecular interference and ensure the free flight of ions (25). Modern mass spectrometers are also seamlessly integrated with advanced computer systems and accessories for data acquisition and analysis.

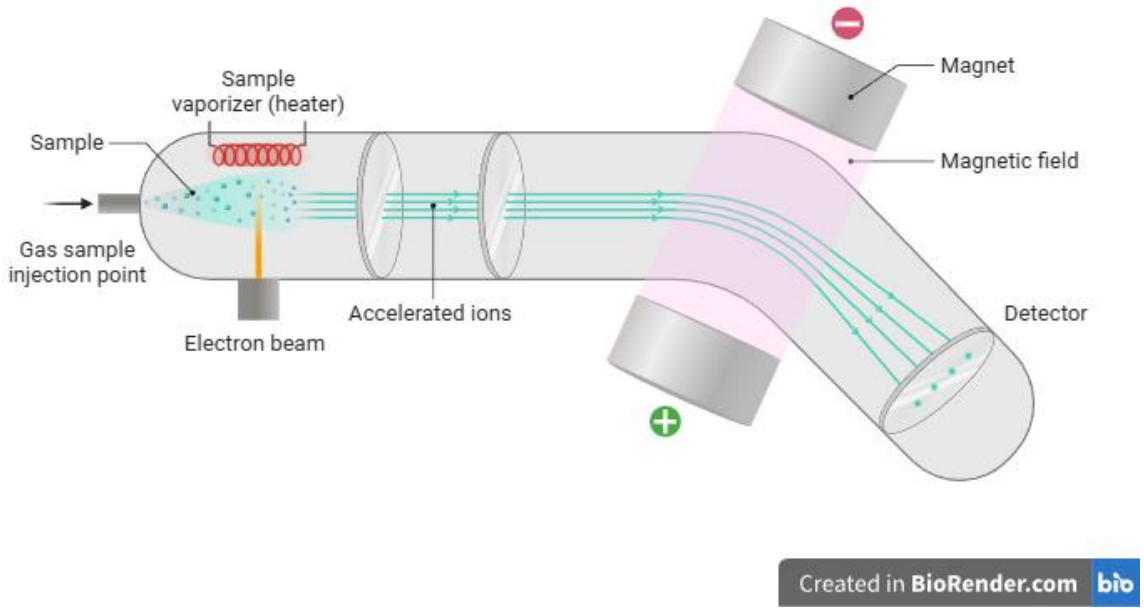

Figure 3. *Schematic representation of the mass spectrometer. Created in https://BioRender.com*

1.4. IONIZATION TECHNIQUES

The first critical step in mass spectrometry is the conversion of neutral sample molecules into gas-phase ions. The choice of ionization technique is crucial and depends on the physicochemical properties of the analyte (26).

1.4.1. ELECTRON IONIZATION (EI)

Electron Ionization (EI) is the oldest and most widely used technique, particularly for volatile, gas-phase samples. In EI, a sample vapor is bombarded with a focused beam of high-energy electrons, leading molecules to the loss of an electron and to form a molecular ion. This process is highly energetic, leading to significant fragmentation of the molecules into a characteristic pattern of fragment ions. This fragmentation pattern is invaluable for structural identification. The main limitation of EI is that it requires the analyte to be volatile, which restricts its use in

biomedical analysis to low molecular weight and non-polar compounds. It is the core technology behind gas chromatography-mass spectrometry (GC-MS) (26).

1.4.2. ATMOSPHERIC PRESSURE IONIZATION (API)

A breakthrough for biomedical applications was the development of "soft" ionization techniques that do not cause significant fragmentation. The most common of these operate at atmospheric pressure (Atmospheric Pressure Ionization, API), allowing the direct analysis of liquid-phase samples, which are ideal for biological matrices (26).

Electrospray Ionization (ESI) is a well-known ionization technique that operates at pressure which makes it the most common API method, for the analysis of polar, non-volatile and thermally labile compounds (27) (28). Its gentle nature is especially suited to biomolecules, peptides, proteins, and nucleic acids, allowing their analysis, without fragmentation. The electrospray ionization (ESI) workflow starts, by pushing the sample through a stainless-steel or fused-silica capillary at an almost imperceptible flow, typically ranging from a few nanoliters per minute up to a few microliters per minute. Simultaneously a substantial voltage, between 2 and 5 kV, is applied between the tip and the mass-spectrometer inlet generating a powerful electric field at the tip. This field drives charges to accumulate on the surface of the emerging liquid, which then reshapes into the characteristic Taylor cone (29). The solvent keeps evaporating, and each time the droplet's charge builds to the point of a Coulomb explosion the event repeats until at last analyte ions are ejected from the droplet's surface into the gas phase (3). As mentioned before, ESI ionization is defined as "soft," since it preserves the structural identity of the analyte with low amount of energy. Nevertheless, this source has the tendency to generate adducts of the analyte, above all wit sodium and chlorine, which reduce the sensitivity of the system; for this reason, it is essential to remove these interferences in the pre-analytical phase. ESI sources reach the maximum performance when they operate on analytes which can be positively charged.

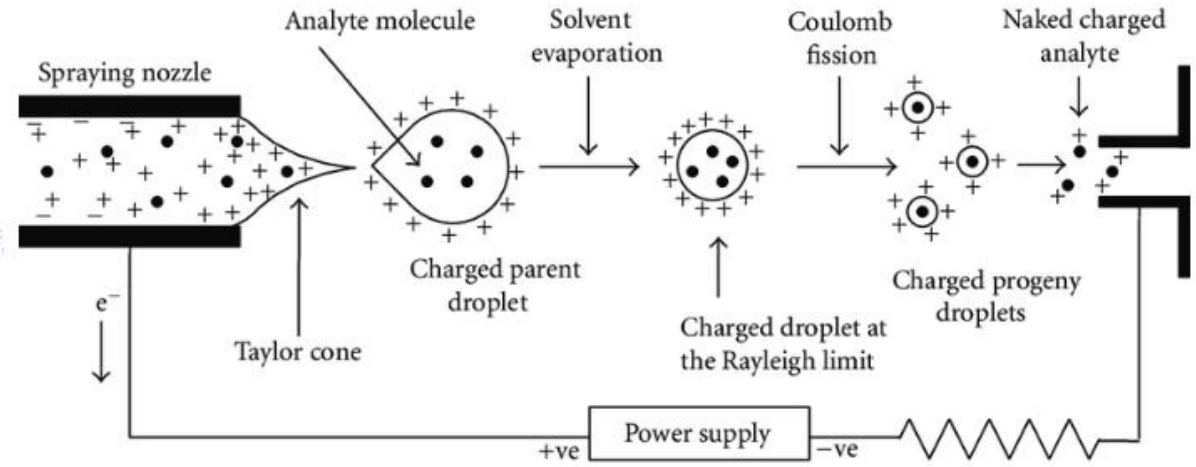

***Figure 4**. Schematic representation of the electrospray ionization process. Reproduced from: Shibdas Banerjee, Shyamalava Mazumdar, Electrospray Ionization Mass Spectrometry: A Technique to Access the Information beyond the Molecular Weight of the Analyte, International Journal of Analytical Chemistry, Year (30).*

Atmospheric Pressure Chemical Ionization (APCI) is a soft ionization technique that operates at atmospheric pressure, offering a valid alternative to electrospray ionization (ESI). It is particularly well-suited for the analysis of non-polar and thermally stable analytes (23) (31). Unlike ESI, which relies on the formation of charged droplets, APCI utilizes a gas-phase chemical ionization process. The liquid mobile phase containing the analytes is first nebulized with a gas flow (typically nitrogen) and heated in a vaporizing tube to create a fine aerosol of neutral molecules. The subsequent chemical ionization step occurs through a high-voltage corona discharge. This discharge creates a plasma in the surrounding gas, which generates highly reactive primary ions from the solvent molecules. These primary ions then react with the analyte molecules, transferring their charge and thus ionizing the analyte itself (23) (31). The ionization reaction can proceed in two main ways:

- In positive ion mode, a proton is typically transferred from the ionized solvent molecules to the analyte, forming protonated molecular ions ($[M+H]^+$).
- In negative ion mode, a proton is either removed from the analyte molecule, or a negative charge is transferred $[M-H]^-$ (32).

Because APCI requires elevated temperatures to vaporize the sample, it is best suited for analytes that are volatile and thermally stable. Furthermore, APCI is less susceptible to signal suppression from salts and buffers in the sample compared to ESI, which can simplify sample preparation (3). Many spectrometers are now equipped with hybrid sources that can be quickly

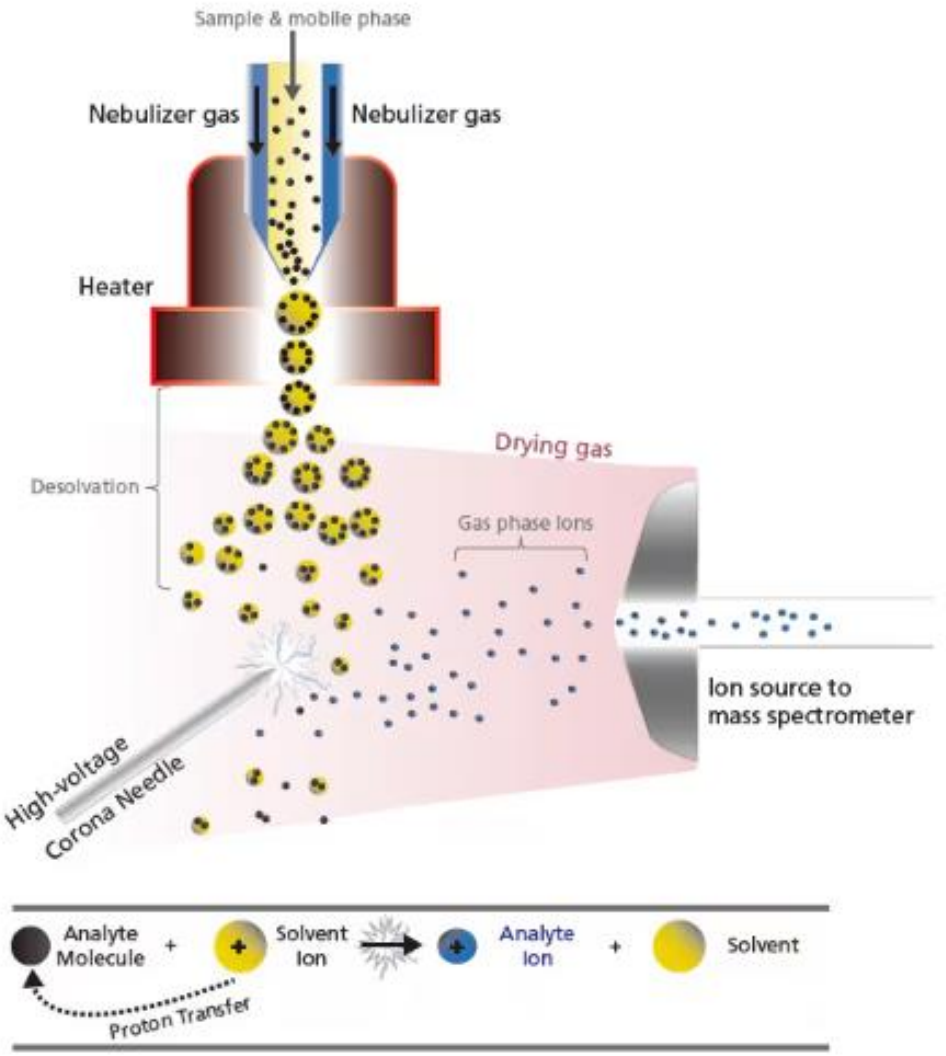

Figure 5: *Schematic of the ion-molecular reaction (e.g. proton transfer) in APCI. Reproduced from: Shimadzu Corporation, "Interfaces for LCMS", available at www.shimadzu.com, accessed October 2025 (253)*

switched between ESI and APCI configurations, providing enhanced analytical versatility based on the characteristics of the analytes of interest (31).

Atmospheric Pressure Photoionization (APPI) is a soft API technique that uses high-energy photons to ionize analytes, making it particularly suitable for less polar or non-polar compounds that are challenging to ionize with ESI or APCI (33). The core of APPI lies in its unique ionization mechanism, which is based on photoionization. In APPI, the liquid effluent from the chromatography system is converted into a gas-phase aerosol by heating and a nebulizing gas. This aerosol is then exposed to a high-intensity lamp, most commonly a krypton lamp, which emits high-energy photons (34). Analytes with an ionization potential (IP) lower than the photon energy will absorb the light and become directly ionized. A key feature of APPI is the frequent use of a dopant, typically a solvent or chemical with a low ionization potential (e.g., toluene or acetone), to significantly enhance the ionization efficiency (35). The dopant molecules are easily ionized by the photons, forming radical cations. These dopant ions then

undergo gas-phase chemical ionization reactions with the analyte molecules, transferring their charge to the analyte (32). This dopant-assisted mechanism is often more efficient than direct photoionization, especially for analytes with higher ionization potentials. APPI is highly effective for a wide range of compounds, including polycyclic aromatic hydrocarbons (PAHs), steroids, and pesticides, which are not amenable to electrospray ionization. Due to its use of a lamp, it is also a "cleaner" ionization technique than APCI, as it avoids the formation of unwanted ions that can result from the corona discharge (34).

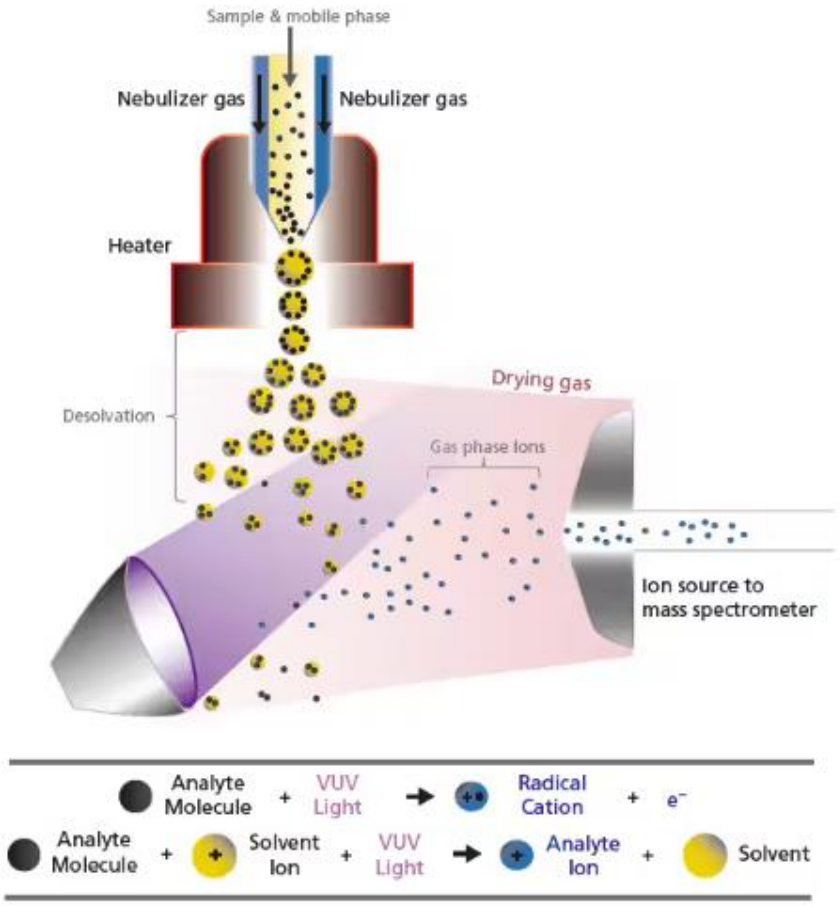

Figure 6: *Schematic of the ionization process by UV light in atmospheric pressure photoionization APPI. Reproduced from: Shimadzu Corporation, "Interfaces for LCMS", available at www.shimadzu.com, accessed October 2025 (253).*

1.5. MASS ANALYZERS AND DETECTOR

Once ions are generated, they are directed into the mass analyzer where they are separated and then detected.

1.5.1. MASS ANALYZERS

The mass analyzer is the heart of the mass spectrometer, where ions are separated based on their m/z ratio within a high-vacuum environment. Three common types are used:

- Quadrupole: This is the most common analyzer for clinical analysis. It consists of four parallel metal rods. By applying radiofrequency and direct current (DC) voltages to the rods, a mass-selective filter is created, allowing only ions with a specific m/z ratio to pass through. The voltages can be varied over time to perform a "mass scan" and measure a wide range of ions (26). Quadrupole is commonly used for quantitative analysis.
- Ion Trap: in this type of mass spectrometers, ions are "trapped" and stored in a three-dimensional quadrupolar field formed by ring electrodes. The ions are then ejected from the trap sequentially based on their m/z ratio. Ion traps require slightly higher pressure to "cool" the ions and improve performance. Ion traps are commonly used to identify the structure of molecules.
- Time-of-Flight (TOF): In a TOF analyzer, a pulse of ions is accelerated into a flight tube. Because ions with a lower mass-to-charge ratio travel faster than heavier ions, they arrive at the detector at separate times. The time of flight is measured and used to determine the m/z ratio of the ions. TOF analyzers are known for their high resolution and speed. Time-of-flight is commonly used for the calculation of the exact mass of the analyte.

1.5.2. ION DETECTION

After leaving the mass analyzer, the ions are detected by a single ion-detecting device, typically an electron multiplier. This detector converts the ion signal into an electrical signal proportional to the number of ions that strike it, allowing for the quantitative measurement of each analyte.

1.6. TANDEM MASS SPECTROMETRY

The principle of Tandem Mass Spectrometry (MS/MS) represented a significant breakthrough in LC-MS. This technique compensates for the limited chromatographic resolution of LC by providing highly specific mass spectrometric detection, thereby enabling the reliable analysis of complex biological samples (26). The most common instrument for MS/MS is the triple quadrupole (3Q) mass spectrometer. It consists of three main sections:

- First Quadrupole (Q1): This acts as a mass filter, selecting only the intact, ionized analyte molecules, known as parent ions, based on their specific mass-to-charge (m/z) ratio. All other ions are filtered out.
- Collision Cell (Q2): The selected parent ions are then transferred into this chamber, where they collide with a trace amount of inert gas (e.g., argon or nitrogen). These high-energy collisions cause the parent ions to fragment into smaller, more stable ions, known as daughter ions.
- Third Quadrupole (Q3): This second mass filter selects only one or more specific daughter ions from the mixture of fragments generated in the collision cell.

This parent-to-daughter ion selection process is called a mass transition, and it provides an exceptional level of specificity for identifying and quantifying an analyte.

1.6.1. MULTIPLE REACTION MONITORING (MRM)

The ability of the triple quadrupole to rapidly change the selected mass transitions allows for Multiple Reaction Monitoring (MRM). In MRM mode, the instrument sequentially monitors a large number of specific mass transitions within a single analytical run. This enables the

simultaneous quantification of multiple different compounds with very high sensitivity and specificity (26).

1.7. THE CHROMATOGRAM AND MASS SPECTRUM

The LC-MS/MS system combines liquid chromatography (LC) with a mass spectrometer, such as the triple quadrupole (3Q), often operating in Multiple Reaction Monitoring (MRM) mode. This tandem mass spectrometry (MS/MS) approach allows for the generation of a chromatogram, which plots the signal intensity over time for specific analytes. The information from the chromatographic peak at a given retention time is combined with the structural and identifying information provided by the MRM transition (23). This important coupling ensures that the signal measurement for the analyte of interest is guaranteed by three distinct levels of specificity:

- Retention Time: The analyte elutes from the LC column at a highly specific and reproducible time.
- Parent Ion Selection: The first quadrupole (Q1) selects only the molecular ion (or parent ion) of the analyte.
- Fragment Ion Selection: The third quadrupole (Q3) isolates a specific and characteristic fragment ion (or daughter ion) produced in the collision cell (Q2).

By monitoring a specific parent-to-daughter ion transition, the system can selectively detect only the compound of interest, greatly minimizing background noise and interference.

1.7.1. THE ROLE OF THE ION RATIO IN SPECIFICITY

A fourth and crucial layer of specificity can be achieved by monitoring two separate MRM transitions for the same molecule. This involves selecting two different and characteristic fragment ions produced from the same parent ion, namely, transitions (36). In consistent fragmentation conditions, the ratio of the abundances of these two fragments is constant and unique to the thermodynamic properties of the molecule. This ion ratio (IR) is a fundamental tool to confirm the identity of the analyte. Monitoring the ion ratio in complex biological samples, where compositional variability can be significant, is extremely helpful in ruling out

signal contributions from other molecules that may have a similar retention time or mass-to-charge ratio and therefore interfere with the accurate quantification of the analyte of interest. This ensures the integrity and reliability of quantitative measurement, setting the stage for discussion on how external factors, like the matrix, can still influence the signal, as it will be described in the following paragraph (36).

1.7.2. MATRIX EFFECT AND ION SUPPRESSION

In quantitative LC-MS/MS analysis, the matrix, i.e., all compounds in the sample other than the analyte of interest, can significantly affect the accuracy and precision of the results (37). The matrix is a particular issue in complex biological samples (e.g., plasma, urine), which contain a multitude of substances that can co-elute with the analyte of interest. The term matrix effect refers to the alteration of the analyte's ionization efficiency due to the presence of co-eluting compounds. This can manifest as either a decrease (ion suppression) or an increase (ion enhancement) in the mass spectrometer signal (2). Ion suppression is more common and is a major source of analytical variability. It occurs when co-eluting substances compete with the analyte for charge or space on the surface of electrospray droplets, thereby reducing the number of analyte ions that are able to reach the mass analyzer (23). The severity of matrix effects is influenced by several factors, including the properties of the analyte, the composition of the matrix, and the LC conditions. While using highly specific detection modes like MRM helps, it does not eliminate the problem. Therefore, it is essential to implement analytical strategies to mitigate matrix effects, such as:

- Effective Sample Clean-up: using techniques like solid-phase extraction (SPE) or liquid-liquid extraction (LLE) to remove as many interfering matrix compounds as possible before LC-MS analysis.
- Isotope-Dilution Internal Standardization: the use of a stable isotope-labeled internal standard (IS) is the gold standard for correcting matrix effects. Since the IS has the same physicochemical properties as the analyte, it is affected by ion suppression to the same extent, allowing to accurately determine the analyte concentration based on the ratio of the analyte to the IS signal (3).

1.8. QUANTITATIVE ANALYSIS IN LC-MS/MS

Quantitative analysis with LC-MS/MS is a rigorous process used to determine the exact concentration of a target analyte within a sample. Unlike qualitative analysis, which simply identifies a substance, quantification provides a numerical value for its abundance, reported in a determined unity of measurement. This is achieved by creating a mathematical relationship between the instrument's signal response and the analyte's known concentration (38). Given the potential for variability from sample to sample, particularly in complex biological matrices, achieving accurate quantification requires meticulous preparation and the use of specific analytical methods, such as calibration curves and internal standards (38).

1.8.1. CALIBRATION CURVES

A calibration curve is the fundamental tool for quantitative analysis. It is a relationship between the measured signal intensity at known concentration of the analyte in a series of standard solutions, which can be represented in a plot displaying the first on the y-axis and the second on the x-axis. To create this curve, a set of standard samples are prepared at increasing concentrations of the analyte. These are then analyzed under the exact same conditions as the unknown samples. The resulting data points are used to generate a regression line. This line provides a formula that allows to calculate the concentration of the analyte in any unknown sample by simply measuring its signal intensity. A well-defined calibration curve is essential for ensuring the linearity and accuracy of the measurements over the entire analytical range.

1.8.2. THE INTERNAL STANDARD METHOD

While a calibration curve is crucial for quantification, it does not account for all sources of analytical variability. The Internal Standard (IS) method is therefore considered the gold standard for achieving accurate and precise quantification, particularly within complex matrices. An IS is a compound added at a fixed, known concentration to all samples, including calibrators, quality controls, and unknowns, prior to sample preparation and analysis (37). The ideal IS is a stable isotope-labeled analogue of the analyte of interest. Being chemically identical, it behaves in the same manner as the analyte throughout the entire analytical

workflow, from sample extraction to ionization. This parallel behavior allows the IS to serve as a correction factor for fluctuations in sample recovery, instrument performance, and, most importantly, matrix effects (3). By normalizing the analyte's signal to the IS signal, variations in ion suppression or enhancement are mitigated, thereby ensuring a highly accurate and reproducible final concentration value (39).

1.9. METHOD VALIDATION IN LC-MS/MS

Method validation is a critical and regulated process that ensures an analytical method is reliable, robust, and suitable for its intended purpose (37). For quantitative LC-MS/MS analysis, the method must be rigorously validated according to established guidelines, such as those provided by the U.S. Food and Drug Administration (FDA), the European Medicines Agency (EMA), and the Clinical and Laboratory Standards Institute (CLSI) (40) (41) (42). This systematic process confirms that the data generated is valid and can be used to draw scientifically defensible conclusions. The validation process involves the evaluation of several key performance parameters.

1.9.1. LINEARITY AND MEASURABILITY RANGE

Linearity and measurability range define the concentration interval over which the analytical method provides results that are directly proportional to the analyte's concentration. Linearity is evaluated by analyzing a series of test samples with known and increasing concentrations and constructing a calibration curve. The quantitative range is the interval between the lower limit of quantitation (LLOQ) and the upper limit of quantitation (ULOQ). It is essential that the instrumental response is linear and that the correlation coefficients are sufficiently high to ensure the reliability of the quantitative data.

1.9.2. ACCURACY AND PRECISION

Accuracy represents the total measurement error of an analytical method and reflects the closeness of the measured values to the true value. It is a combination of trueness and precision,

thus encompassing both systematic and random error components (ISO 5725-1:1994; CLSI C62-A, 2014). Trueness describes the closeness of agreement between the average value obtained from a large series of test results and the true or accepted reference value of the analyte. It is typically expressed as percent bias or percent recovery.

Precision, on the other hand, refers to the closeness of agreement between independent test results obtained under stipulated conditions. It is expressed as the coefficient of variation (CV%) and can be subdivided into:

- Repeatability, which assesses variability under the same operating conditions (same analyst, instrument, and day);
- Reproducibility, which assesses variability under changed conditions, such as different days, analysts, or instruments.

Both accuracy and precision are evaluated using replicate quality control (QC) samples at multiple concentration levels. Together, they ensure that the analytical method produces results that are both true and consistent across analytical runs.

1.9.3. SELECTIVITY AND SPECIFICITY

The selectivity and specificity of an LC-MS/MS method refer to its ability to measure the analyte of interest without interference from other compounds present in the sample, such as endogenous or exogenous substances or metabolites. Selectivity is evaluated by injecting matrix blank samples (not containing the analyte) to check for the absence of interfering signals at the analyte's retention time and its specific MRM transition. The high selectivity offered by tandem MS is one of the main advantages of this technique.

1.9.4. LIMIT OF DETECTION (LOD) AND LIMIT OF QUANTITATION (LOQ)

The limit of detection (LOD) and the limit of quantitation (LOQ) define the lowest analyte concentrations that can be reliably detected or quantified by an analytical method, respectively. The LOD represents the smallest amount of analyte that produces a signal distinguishable from background noise, although quantification at this level may not be accurate. In contrast, the

LOQ corresponds to the lowest concentration that can be quantified with acceptable accuracy and precision under the established validation criteria (40) (42) (41). In LC-MS/MS methods, both parameters are commonly determined using the signal-to-noise (S/N) ratio approach, where LOD is defined as the concentration giving an S/N of approximately 3:1, and LOQ as the concentration giving an S/N of approximately 10:1. Alternatively, when blank samples are not representative or when noise cannot be easily measured, LOD and LOQ can be calculated statistically from the standard deviation of the response (σ) and the slope of the calibration curve (S) according to ICH Q2(R2) guidelines, using the following formulas:

$$LOD = 3.3 \times \frac{\sigma}{S} \qquad LOQ = 10 \times \frac{\sigma}{S}$$

where σ is the standard deviation of the intercepts or of replicate low-level measurements. The experimental determination of LOD and LOQ should be performed under routine analytical conditions to ensure the values reflect the true sensitivity of the method. These parameters are crucial for defining the quantitative range, assessing the method's suitability for low-abundance analytes, and establishing the lower limit of the calibration curve (43).

1.9.5. MATRIX EFFECT

As discussed previously, the matrix effect is the influence determined by co-eluting substances on the ionization efficiency of the analyte. This can lead to signal suppression or, less commonly, signal enhancement. The assessment of the matrix effect is a critical aspect of validation, especially for complex biological samples. It is typically measured by comparing the analyte signal in a neat solvent with the signal obtained from a matrix sample that has been spiked with the analyte and processed through the entire workflow.

1.9.6. STABILITY

The stability of the analyte in the sample is a critical factor for ensuring the reliability of analytical results over time. Stability studies evaluate whether the analyte degrades under various conditions, such as during freeze-thaw cycles, short-term and long-term storage, or after being prepared for analysis. Stability must be demonstrated for both the analyte and the IS in all relevant sample types, storage conditions, and pre-analytical and analytical procedures.

2. DRIED BLOOD SPOTS

2.1. GENERAL INFORMATION ABOUT DRIED BLOOD SPOT (DBS)

Dried blood spot (DBS) technique consists of a membrane on whose surface a biological sample corresponding to drops of capillary blood is absorbed; after drying, various analytical methods can be applied to study the sample (**Figure 7**). In recent years, DBS has become a useful tool for biological analyses, so much so that it has been described as the most appropriate method for collecting biological samples, thanks to specific advantages such as the need for a small volume of biological material, the possibility, in many cases, of storing and transporting the sample at room temperature, the greater stability of the analytes, and the reduced risk of infection for operators (44). DBS originated from Bang's idea of using cellulose sheets to collect blood samples. This collection method was first used in clinical practice in the early 1960s, when it was applied to neonatal screening for phenylketonuria, according to Guthrie's idea (44) (45).

Figure 7: *Representation of dried blood spot from finger-prick. Reproduced from Clinical Lab Products, Implementing Dried Blood Spot (DBS) Testing in the Clinical Laboratory, available at clpmag.com, accessed in October 2025 (261).*

2.2. TECHNICAL SPECIFICATIONS

In general, there are two types of sorbent membranes used for DBS in modern research procedures: fiberglass or cellulose and paper (pulp and paper), as in the case of Whatman 903; the latter is produced from pure cotton fibers without additives and is among the most commonly used types of paper for DBS, especially for neonatal screening (44) (45). Several companies offer diverse types of membranes with different treatments depending on the objectives of the study. A requirement for the use of a sorbent membrane is its ability to effectively absorb a biological fluid, distribute it evenly over its surface, and ensure the safety of the dry biological material. The presence of excessively rough and/or porous layers significantly alters the wettability of the membrane and, consequently, its ability to distribute biological material evenly over its surface. Therefore, the materials chosen should exhibit marked hydrophilic properties and a homogeneous structure, which allows for uniform and reversible absorption of blood components, including proteins and other biologically active compounds, in the pores of the membrane. To improve these capabilities, treatments can be applied. For example, the surface can be treated with nanoparticles and water-soluble polymers, increasing the stability of the sample and providing some antibacterial properties. Alternatively, treating the membrane with zinc oxide improves the stability of the absorbed sample during storage. Another possible treatment is with antibacterial agents, which prevents the degradation of the biological sample. Finally, treatments with hydrophilic glass fibers not only provide the antibacterial properties necessary for the stability of the biological material but also increase the hydrophilicity of the membrane surface (44). The general principle of sample collection involves impregnating the membrane with drops of blood (44) . Blood drops are obtained by pricking the patient's heel, fingertip, or big toe with a safety lancet. After the prick, the blood drop is placed directly on the membrane, in the pre-printed circles, ideally applying one drop per circle so that it fills it evenly and symmetrically. Coagulation, stratification, and supersaturation must be avoided, and the circle must not be touched either before or after depositing the blood. Potentially, blood can also be applied to the card using a calibrated pipette (45). It is generally recommended to incubate the sample for 2-3 hours at room temperature (15-22°C), allowing the blood to dry before transporting and storing the membrane. The drying time depends on the sample volume and the type of membrane. It is important that the sample is not heated or stacked and that it does not meet other samples or surfaces. In addition, samples should be kept away from direct light sources and areas of high humidity, as these can cause

bacterial growth, alter extraction efficiency during analysis, or contribute to the degradation of unstable analytes (44).

Once the sample has dried, it is recommended to use sealable bags with desiccants for transport and long-term storage of DBS at room temperature. Samples containing unstable compounds should be stored at low temperatures, such as 2-8°C, but also -15°C or even below -60°C (44).

2.3. ANALYTE EXTRACTION AND ANALYSIS METHODS

DBS extraction involves punching one or more discs from the dried blood spot on the membrane, which are then placed in test tubes or extraction plates. The extraction procedure for LC-MS/MS analysis involves adding a solvent, such as methanol, containing internal standards. The extraction solvent must be strong enough to break the bond between the analyte and the matrix proteins or the membrane. The reaction is facilitated by imparting a certain degree of oscillation, using a vortex or sonication, to improve its efficiency. After centrifugation to remove any corpuscles and precipitates, the extracts can be transferred manually or automatically to new test tubes or autosampler plates for subsequent LC-MS/MS analysis (45).

2.4. ADVTANGES AND LIMITATIONS

In order to obtain satisfactory results from analyses conducted on any biological material, it is essential to standardize the procedures for collecting, transporting, and storing it, to improve the reproducibility of results and reduce potential procedural errors. DBS reduces possible errors in the pre-analytical phase and offers several advantages:

- It requires a blood volume of 10-40 µL, significantly less than the minimum 0.5 mL required for conventional blood collection. This small volume of blood can also be obtained via capillary collection, reducing the invasiveness of the procedure and allowing, after minimal training, independent collection by the patient, which in turn reduces biological risks and costs. It also favors sample collection from fragile patients.
- It can be shipped to laboratories at variable temperatures, between +5°C and -35°C, without necessarily requiring compliance with the cold chain, which reduces transportation costs, even over long distances;

- It is resistant to long-term storage and takes up little space, facilitating the creation of biobanks;
- Drying blood reduces the risk of contamination with infectious biological agents or other types of pathogens, which makes DBS preferable to whole blood in clinical practice.
- It allows a large number of biomarkers such as cells, viruses, nucleic acids, RNA, antibodies, as well as small molecules and proteins to be analyzed in a single sample.

Thanks to these advantages, DBS has significantly improved blood sample collection in resource-limited settings. Despite the specific limitations discussed below, the DBS collection method is currently the most ethical and least expensive method for collecting, transporting, and storing biological material (44).

Below are some biological and pre-analytical factors that need to be considered when working with DBS. The concentration of analytes in capillary blood may differ from that in venous blood, depending on the analyte in question. For example, paracetamol has significantly higher concentrations in capillary blood than in venous blood. In addition, DBS has several aspects that can influence quantitative investigations. DBS is a special matrix in which the analyte of interest is distributed after the drop is applied. Although each DBS puncture should represent a specific and homogeneous blood volume, sample quality may vary from point to point. The risk of such heterogeneity must be considered when developing quantitative methods (45). Factors affecting the distribution of the blood drop and analytes on the membrane are hematocrit, blood viscosity, nature of the analyte, type of membrane, thin-layer chromatography migration effect, ambient temperature, and humidity. The factor that most influences the physical behavior of the blood drop is hematocrit, i.e., the percentage of blood volume occupied by red blood cells, which in the healthy adult population varies between 41 and 51% in men and between 37 and 47% in women; capillary blood tends to have a higher hematocrit than venous blood, around 61% (45). Blood viscosity is directly proportional to hematocrit, and it influences the diffusion properties of the blood drop on the membrane and, consequently, the uniformity of the drop, the drying time, and the reproducibility of the analyses. When hematocrit is high, distribution on the membrane is poor, generating a smaller distribution area but causing blood stratification. Therefore, for the same punch diameter, there will be more blood, potentially leading to a falsely high quantification of the analytes, and vice versa. The effect of hematocrit also depends on the analyte: for example, vitamin D shows no or slight variations in relation to hematocrit. Differences in the volume of the blood drop

deposited on the membrane can also influence the results of quantitative analyses, even if the hematocrit is the same. For example, it has been observed that the concentration of phenylalanine measured in a DBS obtained from 35 µL of blood is lower than that measured in one obtained from 100 µL (45). This phenomenon is thought to depend on the ratio between the area of dispersion of the drop on the membrane and its weight and the amount of blood deposited, where a linear relationship between these two variables indicates a uniform distribution of blood on the card (45). Punching a 3 mm diameter disc can hold approximately 4.3 µL of blood and absorb approximately 1.46 µL of serum (46); however, the volumes of blood and serum absorbed in a defined membrane area depend on the hematocrit and the initial volume of the drop. One way to reduce this variability is to deposit the precise volume of whole blood required on the card, as indicated by the dotted line. In addition, to reduce the uneven distribution of analytes in the DBS, the membrane must meet stringent quality standards, including uniformity, absence of chemical leaching, and minimal chromatographic effect (44). The chromatographic effect, or distribution effect, is due to the possible interaction between the analytes and the membrane material, and migration of the former such as determining differences in concentration based on the position from which the puncture is obtained, i.e., central or peripheral with respect to the adsorbed blood drop. The chromatographic effect is considered negligible if there is good reproducibility, with a coefficient of variation <15% between the various sampled areas. However, Holub et al. described how it can have a major impact on the quantification of amino acids and acylcarnitines in DBS samples with low hematocrit (47). Regarding punching, the use of a large-diameter punch (generally up to 9 mm) or multiple punches makes it possible to increase the sensitivity of the procedure. In general, where possible, it is preferable to apply a large-diameter punch to cover as much of the DBS as possible, thereby minimizing the various effects due to hematocrit or migration and thus increasing reproducibility and accuracy. An additional distribution effect is vertical, found in analytes and membranes with particular chemical-physical properties. According to this phenomenon, some analytes may permeate and concentrate on the thickness of the support much more than on the surface, thus altering extraction efficiency. The pretreatment of membranes, for example, with impregnation with pasteurized plasma proteins, allows for the deactivation of active absorption sites in the membrane. However, the massive addition of protein material could lead to a significant matrix effect depending on the method (45). When handling DBS cards, it is important to consider the possibility of cross-contamination between samples because of contact between stacked cards and repeated use of the same punch. It is recommended to clean the punch or to punch on a clean matrix between samples (44). As for

stability, although drying the sample promotes stability, exceptional circumstances have been observed. For example, carnitine levels increase by 7.6% per year for the first 5 years, then decrease by 1.4% per year in subsequent years (44) . In general, the stability of the analyte absorbed onto the membrane during drying and storage should always be evaluated (44). Some compounds are prone to rapid enzymatic degradation, which could occur during blood collection, sometimes even before the drop is placed on the card. Furthermore, DBS is not suitable for the analysis of volatile and/or air-sensitive compounds. For an analyte to be effectively stored in DBS, it must be stable in whole blood for at least 2-3 hours without pretreatment, which is the time required to collect and dry the blood drop on the membrane (45).

2.5. CURRENT APPLICATIONS

DBS technique is increasingly used for the collection and storage of blood samples in various clinical and scientific fields, given that, in addition to the practical advantages already described, DBS allows for the identification and quantification of a large number of analytes. One of the classic applications of DBS in the clinical setting is neonatal screening, a comprehensive system that, starting with the collection of capillary blood from the heel of the newborn at 24-48 hours of life, allows for the diagnosis and monitoring of congenital diseases that are asymptomatic at birth but require early diagnosis, such as metabolic, endocrine, hematological, and genetic diseases. The application of MS on DBS is especially useful in the search for congenital metabolic disorders. The most modern applications allow the simultaneous evaluation of more than 30 metabolic disorders from a single DBS sample (48). Among the most recent applications of DBS are population studies in which the analysis of several types of physical-chemical biomarkers, i.e., protein, genetic, or metabolic, is of interest. Furthermore, the use of DBS is particularly successful in metabolomics studies, in which large numbers of samples, requiring enormous resources for collection and storage, must be analyzed using highly informative techniques. Recent improvements in the materials used for membranes have made it possible to achieve greater sample stability during transport and long-term storage and have also improved the extractability of small molecules. For example, using various LC-MS techniques, it has been possible to measure the concentration of substances such as adrenal corticosteroids, amino acid profiles, carnitines and acylcarnitines, creatine, and others (49) (50). The improvements described above have also enabled the application of DBS

in fields such as toxicology, doping control, and therapy monitoring. Another application is serological diagnosis, which searches for antibodies that are markers of infectious diseases. Other applications include the assessment of hormonal status, food intolerances, and the dose-dependent effects that environmental pollutants can have on human health. Another fairly widespread application, also due to the lower biological risks associated with DBS, concerns the diagnosis of HIV-1 infection and the monitoring of antiretroviral therapy (51). In conclusion, DBS is currently increasingly used for small molecule research, thanks in part to LC-MS technologies and their superiority over immunoassays in terms of better selectivity and specificity, which is very often a source of false positives for the latter (45).

3. ADRENAL GLANDS

The adrenal glands are paired endocrine organs, located in the retroperitoneum, within the perirenal space, immediately above and in front of the upper pole of each kidney, from which they are separated by a small amount of fibrous tissue (52). They are immersed in perirenal adipose tissue and surrounded by the renal fascia. With regard to microscopic anatomy, when sectioned, we can observe that the adrenal gland is divided into two parts: the cortex and the medulla, with different macro and microscopic characteristics. The cortex occupies about 90% of the glandular section and has a characteristic golden yellow appearance due to the abundance of cholesterol, from which steroid hormones are produced. The medulla, on the other hand, occupies the middle portion of each adrenal gland and has a dark red or grayish color, depending on its blood content. The medulla is completely surrounded by the cortex, except for the region corresponding to the hilum. The gland has a thick collagen connective capsule, from which some trabeculae extend into the cortex (52). In addition, the capsule contains the rich subcapsular arterial plexus. The adrenal cortex consists of three zones: the outer *zona glomerulosa*, the intermediate *zona fasciculata*, and the inner *zona reticularis*. The glomerular zone, located under the capsule, consists of a narrow region of small polyhedral and basophilic cells, distributed in spherical clusters. At the ultrastructural level, we see an abundance of smooth endoplasmic reticulum, a typical feature of cells that synthesize steroids. The *zona fasciculata* which is larger, occupies about 75% of the cortex and consists of large polyhedral basophilic cells arranged in continuous cords, two cells thick, between which fenestrated venous sinuses run parallel. In this case too, the cells have abundant smooth endoplasmic reticulum, as well as lipid droplets, giving them a “foamy” appearance. Lipid droplets are composed of cholesterol esters. Finally, the reticular zone is composed of round cells organized in interconnected branched cords. Inside the cells, there is abundant smooth endoplasmic reticulum, many lysosomes, and aggregates of brown lipofuscin pigments, which accumulate with age. The cells of the *zona fasciculata* and *reticularis* are rich in ascorbic acid. The adrenal medulla is composed of pheochromocytes, or chromaffin cells, and supporting cells, called sustentacular cells (53). Chromaffin cells owe their name to their reaction to staining with dichromate fixatives; they are part of the neuroendocrine system and are functionally equivalent to postganglionic sympathetic neurons. Chromaffin cells are voluminous, with large nuclei and slightly granular basophilic cytoplasm, due to the presence of granules containing chromogranins, proteins associated with catecholamines, and enkephalins, opiate-like proteins

that in some circumstances can have endogenous analgesic effects. Pheochromocytes are arranged in single rows along the venous sinuses. On the surfaces not facing the sinuses, they receive the synapses of the sympathetic nerve endings. Neuroendocrine cells similar to chromaffin cells are widely distributed in an extra-adrenal system composed of cell clusters and nodules which, together with the adrenal medulla, form part of the paraganglia system. These extra-adrenal paraganglia are intricately connected to the autonomic nervous system and can be divided into three groups based on their anatomical distribution: branchial, intraganglionic, and aortic sympathetic. The branchiomeric and intraganglionic paraganglia, associated with the parasympathetic system, are located near the major arteries and cranial nerves of the head and neck, and include the carotid glomus. Specifically, the intraganglionic paraganglia are distributed along the course of the vagus nerve. The aortic sympathetic chain, on the other hand, is associated with the segmental ganglia of the sympathetic system; therefore, it is distributed mainly along the course of the abdominal aorta. The Zuckerlandl organs, adjacent to the aortic bifurcation, belong to this group.

3.1. PHYSIOLOGY OF ADRENAL GLANDS

The adrenal cortex and medulla perform distinctly different functions. Specifically, the medulla is responsible for the production of catecholamines, especially adrenaline, under sympathetic control; while the cortex is responsible for the production of three different types of steroid hormones, one for each zone: the *zona glomerulosa* produces mineralocorticoids, the *zona fasciculata* produces glucocorticoids, and the *zona reticularis* produces sex steroids and also participates to a small extent in the production of glucocorticoids (54).

3.1.1. PHYSIOLOGY OF THE ADRENAL CORTEX

A distinction must be made between the different zones of the adrenal gland, as they are responsible for producing diverse types of hormones, with different regulatory mechanisms. **Figure 8** summarizes the mechanisms of adrenal steroidogenesis.

3.1.1.1. ZONA FASCICULATA

The *zona fasciculata* is responsible for the production of glucocorticoids, the main representative of which is cortisol, using cholesterol as a substrate. The cells of the *zona fasciculata* are capable of synthesizing cholesterol in modest quantities. They mainly draw on blood cholesterol present in low-density lipoprotein (LDL) and high-density lipoprotein (HDL) particles. The cholesterol is then esterified and stored in lipid droplets, to be continuously transformed into new free cholesterol thanks to cholesterol ester hydrolase. This process is enhanced in response to stimuli that promotes cortisol synthesis, especially in response to adrenocorticotropic hormone (ACTH), the main regulator. Cholesterol is stored in the cytoplasm, but the first enzyme in the synthetic pathway, CYP11A1, is located at the level of the inner mitochondrial membrane. Therefore, the reaction that limits the speed of the biosynthetic sequence is the transfer of cholesterol from the outer mitochondrial membrane to the inner membrane (55). The steroidogenic acute regulatory protein (StAR), which has a short half-life and is activated by pituitary trophic hormones, is essential for this transfer process. In the *zona fasciculata*, cholesterol is sequentially converted into pregnenolone, progesterone, 17-hydroxyprogesterone (17-OHP), 11-deoxycortisol, and cortisol. Steroidogenic enzymes belong to two superfamilies:

- the cytochrome P-450 monooxygenase family, known as CYP, located in the inner mitochondrial matrix or smooth endoplasmic reticulum. CYP enzymes function as hydroxylases, lyases, oxidases, and aromatases, and some CYP enzymes perform more than one function. All these enzymes require the transfer of electrons through specific enzymatic cofactors with reducing power: P450 oxidoreductase (POR) for microsomal CYP enzymes, and adrenodoxin/adrenodoxin reductase (ADX/ADR) for mitochondrial CYP enzymes;
- the hydroxysteroid dehydrogenase (HSD) family. Among these, the enzyme 3β-HSD2 plays a key role in adrenal steroidogenesis.

More specifically, the cholesterol side chain cleavage enzyme, CYP11A1, generates pregnenolone, which is then converted into progesterone by 3β-HSD2 (56). This is followed by conversion to 17-OHP by CYP17A1, further hydroxylation at carbon 21 by CYP21A2, and finally 11β-hydroxylation by CYP11B1, producing active cortisol. The cortisol synthesized in the *zona fasciculata* is transported in the blood, 90% bound to corticosteroid-binding globulin (CBG), also known as transcortin, and 5-7% bound to albumin; the remaining fraction

circulates as a free hormone. It is believed that free cortisol, due to its lipophilicity, enters cells without the need for active transport mechanisms. With regard to the mechanism of action of cortisol, it acts on target cells mainly through the glucocorticoid receptor (GR), which belongs to the family of nuclear receptors (57). When the hormone is not present, the GR forms a stable cytoplasmic complex with many chaperonins. The cortisol-GR bond promotes the dissociation of chaperonins, followed by the translocation of the cortisol-GR complex into the nucleus. The final effect is the regulation of gene transcription: on the one hand, there is an increase in the transcription of a series of target genes; on the other hand, glucocorticoids can repress the gene transcription of other genes, such as pro-inflammatory genes, either by interfering with other transcription factors or by recruiting proteins that act as co-repressors (57). Through these mechanisms, cortisol exerts a wide range of actions related to the definition of stress responses. In general, cortisol regulates blood glucose levels and the functions of the central nervous system and cardiovascular system during fasting, increases blood sugar during stress, and stimulates muscle protein catabolism (54). Cortisol is also involved in regulating the immune system to protect the body from the adverse effects of excessive inflammatory and immune responses.

3.1.1.2. ZONA GLOMERULOSA

This is a thin area of the adrenal cortex responsible for producing mineralocorticoids. The most important hormone in this class is aldosterone, which regulates the homeostasis of salts and body fluids, and therefore plasma osmolarity. The *zona glomerulosa* does not express CYP17, so it is unable to synthesize cortisol and adrenal androgens. Instead, this is the only zone that expresses the enzyme CYP11B2, called aldosterone synthase, which catalyzes the last three reactions that convert DOC to aldosterone (55). Pregnenolone is converted to progesterone and then to DOC by the enzymes 3β-HSD and CYP21A2, respectively. Subsequently, thanks to CYP11B2, 11-hydroxylation of DOC occurs with the formation of corticosterone, followed by 18-hydroxylation with the consequent formation of 18-hydroxycorticosterone, and finally 18-oxidation with the production of aldosterone. Once synthesized, aldosterone binds with low affinity to albumin and CBG and has a half-life of approximately 20 minutes. Almost all aldosterone is inactivated by the liver in a single pass of glucuronidation and then excreted by the kidney (58). The *zona glomerulosa* is marginally influenced by ACTH, while it is mainly regulated by the renin-angiotensin-aldosterone system (RAAS), potassium levels, and atrial

natriuretic peptide (ANP). ANP is produced and released by atrial myocytes in response to cardiac dilation and acts by causing vasodilation and reduced renal reabsorption of sodium and water. The latter function is performed by antagonizing the RAAS. In fact, ANP inhibits aldosterone secretion both directly, by acting on the adrenal cortex, and indirectly, by reducing circulating renin levels. Regarding the RAAS, the juxtaglomerular cells of the afferent arterioles of the kidney synthesize, store, and release the proteolytic enzyme renin in response to three types of stimuli: a reduction in renal perfusion pressure; activation of the sympathetic fibers that innervate the afferent arterioles via β-adrenergic receptors; a reduction in sodium concentration in the macula densa (58). Renin and aldosterone secretion varies with posture, increasing when standing upright. Furthermore, this secretion decreases with age and, in women, depends on the phase of the menstrual cycle, with maximum secretion during the luteal phase. Renin acts as a proteolytic enzyme on a circulating protein substrate, angiotensinogen, produced by the liver, in order to release angiotensin I. This, in turn, is cleaved into angiotensin II by the angiotensin converting enzyme (ACE), present on the surface of endothelial cells, especially those in the lungs and kidneys. Angiotensin II has a number of important biological effects: it increases sodium reabsorption; causes vasoconstriction of the arterioles, leading to an increase in blood pressure; stimulates ADH secretion and thirst; stimulates aldosterone secretion by the adrenal cortex, activating the angiotensin II receptor type 1 (AT1R). The binding of angiotensin II to the AT1R receptor causes depolarization of the glomerular cell membrane through the inhibition of adenosine triphosphate (ATP)-dependent sodium-potassium pumps, i.e., ATPase-dependent pumps, and through the inhibition of potassium channels, resulting in an increase in intracellular sodium (58). Depolarization is followed by an increase in intracellular calcium levels, caused both by the opening of voltage-dependent calcium channels and by the inhibition of ATPase-dependent calcium pumps. Calcium then acts as a second messenger, stimulating the intracellular signaling pathway that leads to CYP1 and CYP11B2 transcription. Aldosterone acts by binding to the intracellular MR. The aldosterone-MR complex enters the nucleus and regulates the expression of specific genes, in a manner very similar to that of cortisol. In particular, activated MR increases the transcription of the epithelial sodium channel (ENaC) and serum/glucocorticoid-regulated kinase 1 (SGK-1) (58). Aldosterone has several important effects on the kidneys, which together lead to increased reabsorption of water and sodium, resulting in increased blood pressure. More specifically, aldosterone stimulates sodium reabsorption by the thick ascending limb of Henle's loop, the distal tubule, and the collecting duct, with a predominant effect on the latter two portions. Aldosterone also increases renal perfusion pressure, which in turn negatively regulates renin

release. Aldosterone reduces potassium levels in the blood by acting on two levels: on the one hand, it induces an increase in cellular potassium absorption, and on the other, it increases renal excretion. Finally, aldosterone has a pro-inflammatory and pro-fibrotic effect on the cardiovascular system, causing hypertrophy and remodeling of the left ventricle, not only linked to increased blood pressure (58). Physiologically, an oral or intravenous sodium load leads to aldosterone suppression; an attenuated or absent response occurs in patients with excess mineralocorticoids from autonomous secretion.

3.1.1.3. ZONA RETICULARIS

The zona reticularis is the innermost layer of the adrenal cortex, located deep within the zona fasciculata and superficially to the adrenal medulla. The cells in this region are organized into irregularly arranged cords, which intertwine to form a network (from the Latin reticulum, "network") (59). The cells in the reticular zone synthesize precursor androgens, including dehydroepiandrosterone (DHEA) and androstenedione, from cholesterol (60). DHEA is subsequently converted to DHEA sulfate by the enzyme sulfotransferase SULT2A1 (61). Since the enzyme 17β-hydroxysteroid dehydrogenase is absent here, these precursors are not further converted into active androgens within the adrenal cortex but are released into the bloodstream to be used by the testes and ovaries in the production of testosterone and estrogen, respectively. The secretion of adrenal androgens is partially regulated by adrenocorticotropic hormone (ACTH) and, to a lesser extent, by corticotropin-releasing hormone (CRH) (62). In humans, the reticular zone contains the enzyme 17α-hydroxylase, which catalyzes the hydroxylation of pregnenolone; the resulting compound can then be converted to cortisol by a mixed oxidase system. A deficiency of 17α-hydroxylase leads to a reduction in plasma levels of estrogen, androgens, and cortisol, with a consequent compensatory increase in ACTH, which stimulates the production of 11-deoxycorticosterone and corticosterone (63). In rodents, the absence of 17α-hydroxylase leads to compensatory synthesis of corticosterone instead of cortisol.

3.1.2. PHYSIOLOGY OF ADRENAL MEDULLA

The adrenal medulla is responsible for the production of catecholamines: approximately 80% of the cells in the adrenal medulla secrete adrenaline, while the remaining 20% secrete

noradrenaline (54). The adrenal medulla produces 100% of the adrenaline in circulation, but only 30% of the norepinephrine: the remaining 70% is released by postganglionic sympathetic nerve endings and diffuses into the circulatory system (64). The fact that the medulla is not the only source of circulating catecholamines means that it is not essential for survival. The catecholamines produced by the adrenal medulla are not released near a target organ and do not function as neurotransmitters, but as hormones, being secreted into the bloodstream. The hormone adrenaline acts rapidly in response to various forms of stress, both physical and psychological, with the aim of triggering a systemic sympathetic response of the "fight or flight" type (65). To do this, it regulates numerous physiological processes, including energy metabolism and cardiac output. The cells of the adrenal medulla can synthesize the catecholamine neurotransmitter norepinephrine from tyrosine, which is then converted into adrenaline (66). More specifically, the synthesis process begins with the transport of the amino acid tyrosine into the cytoplasm of chromaffin cells. Subsequently, tyrosine is hydroxylated into dihydroxyphenylalanine (DOPA) by the enzyme tyrosine hydroxylase, which represents the rate-limiting step of the entire biosynthetic sequence (66). DOPA is then converted into dopamine by the enzyme aromatic amino acid decarboxylase, a cytoplasmic enzyme. Dopamine is transported into secretory vesicles, called chromaffin granules, where it is converted into norepinephrine by the enzyme dopamine β-hydroxylase. In most medullary cells, almost all norepinephrine diffuses into the cytoplasm by facilitated transport to be methylated to epinephrine by the cytoplasmic enzyme phenylethanolamine N-methyltransferase (PNMT) (67). Epinephrine is then transported back into the chromaffin granules. Thanks to the vascular organization of the adrenal gland, cortisol-rich cortical secretions diffuse through chromaffin cells and permeate them before entering the inferior vena cava. Cortisol inhibits the differentiation of medullary cells into neurons, preventing them from forming dendrites and axons. In addition, cortisol induces the expression of the PNMT enzyme (67).

The secretion of catecholamines by the medulla is mainly regulated by stress conditions, either already present or anticipated, thanks to descending sympathetic signals, mainly from centers of the autonomic nervous system located in the hypothalamus and brainstem, which in turn receive afferent signals from the cerebral cortex, the limbic system, and other regions of the hypothalamus and brainstem (68). When activated, these centers cause the release of acetylcholine by preganglionic cholinergic sympathetic neurons that innervate the cells of the adrenal medulla. Acetylcholine binds to the nicotinic receptors of chromaffin cells, causing

increased transcription of the enzyme tyrosine hydroxylase, thus speeding up the entire biosynthetic sequence, and of dopamine β-hydroxylase, and stimulates the exocytosis of chromaffin granules through depolarization and consequent activation of voltage-dependent calcium channels (68). The synthesis of adrenaline and noradrenaline is closely linked to their secretion, without significant changes in their intracellular concentrations in chromaffin cells: increased levels of intracellular catecholamines reduce the activity of tyrosine hydroxylase, while the release of catecholamines causes negative feedback to cease (66).

The biological effects of catecholamines vary depending on the receptors on which they act. In general, we must distinguish between α- and β-adrenergic receptors, which are in turn divided into α_1 and α_2, β_1, β_2, and β_3 (69). Adrenaline and noradrenaline are potent agonists of α receptors and β_1 and β_3 receptors, while adrenaline is more potent than noradrenaline on β_2 receptors. It should be noted that several types of receptors predominate in different tissues, and this different expression determines the variety of functions of catecholamine hormones. Many organs and tissues are influenced by sympathetic-medullary activity. A significant example is its role in physical exercise, which is similar to the "fight or flight" response, but without the subjective element of fear (65). The overall action of the sympathetic-medullary system during physical exercise is to cope with the increased energy requirements of the skeletal muscles and heart muscle, while ensuring adequate amounts of glucose and oxygen to the brain. In response to physical exercise, numerous events mediated by catecholamines occur, such as increased blood flow to the muscles, thanks to the integrated action of catecholamines on the heart, veins, lymphatic vessels, and arterioles of non-muscular and muscular areas; the promotion of muscle glycogenolysis and lipolysis in adipose tissue, which leads to an increase in circulating lactate and glycerol levels, used by the liver to increase gluconeogenesis, a process that, together with ketogenesis, increases during exercise; increased glucagon secretion, thanks to β_2 receptors, and reduced insulin secretion, thanks to α_2 receptors, which contribute to increased blood sugar levels, also thanks to increased glycogenolysis and gluconeogenesis; the relaxation of bronchial smooth muscle, with the aim of providing adequate levels of oxygen to the tissues; the decrease in the energy requirements of visceral smooth muscle, thanks to the reduction in the overall motility of the smooth muscles of the gastrointestinal and urinary tracts, thus ensuring the conservation of energy for the tissues that need it (65). Catecholamines have a short half-life, ranging from 10 to 100 seconds. Approximately half of the catecholamines circulating in plasma form a labile bond with albumin (67). Catecholamines are removed from circulation mainly through reuptake

processes, 90% of which are conducted by the same synapses that released them, and 10% by extra-neuronal tissues. Another possibility is the metabolization of catecholamines by the action of two enzymes: monoamine oxidases (MAO) and catechol-O-methyltransferase (COMT), which determine the production of a series of metabolites such as 3,4-dihydroxymandelic acid, metanephrine, vanillylmandelic acid, normetanephrine, and 3-methoxy-4-hydroxyphenylglycol. Most catecholamines are metabolized by COMT, which is the main source of metanephrine and normetanephrine in the adrenal medulla, where the two compounds are obtained from the degradation of epinephrine and norepinephrine, respectively. Metanephrine and normetanephrine are then oxidized by MAO to produce vanillylmandelic acid. MAO can also oxidize epinephrine and norepinephrine to 3,4-dihydroxymandelic acid, which is subsequently converted to vanillylmandelic acid by COMT. Vanillylmandelic acid and metanephrine can be measured in urine or plasma to assess the patient's catecholamine production level, although these derive not only from medullary metabolism but also from neuronal metabolism (70).

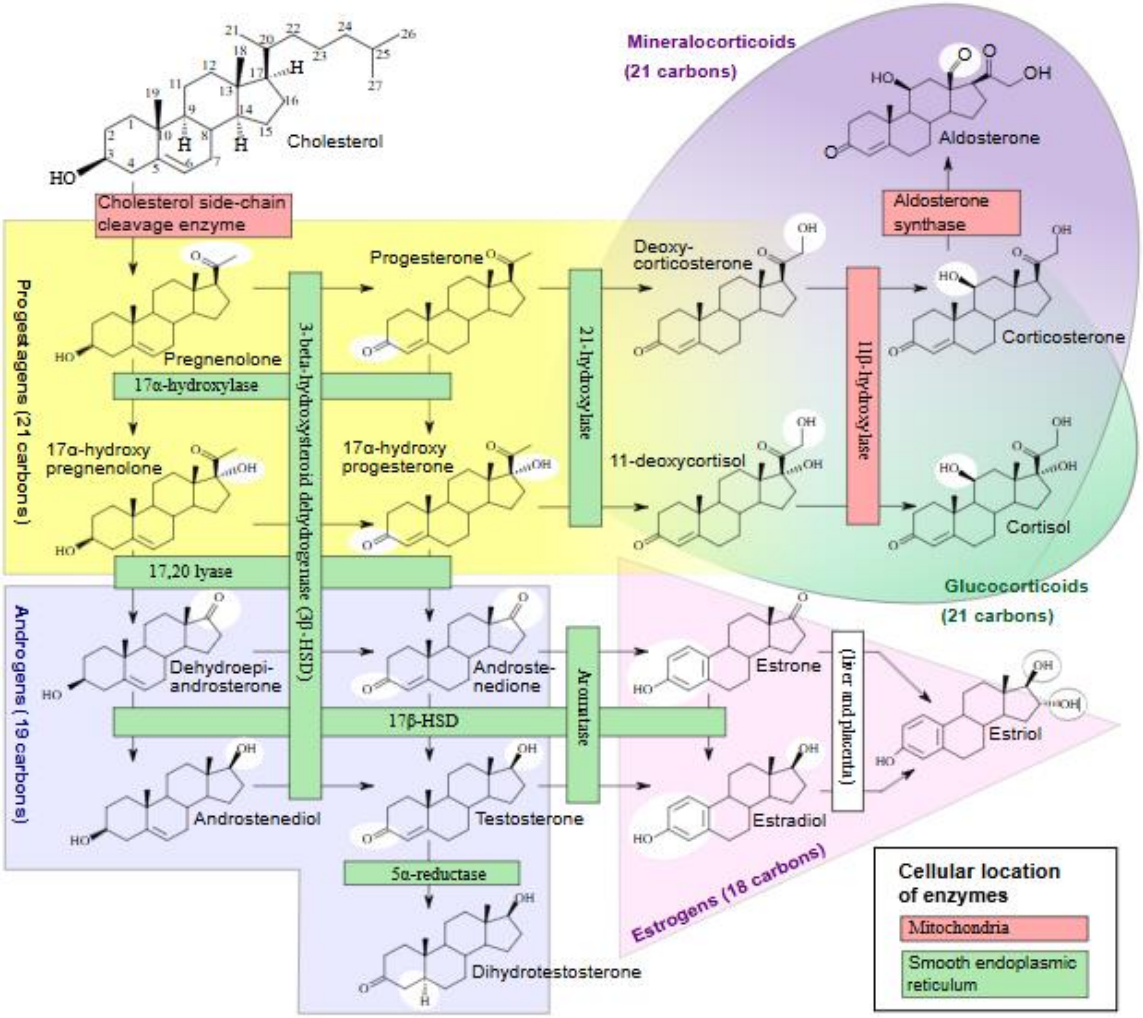

Figure 8. *Adrenal steroidogenesis pathway. Reproduced by Häggström, Mikael; Richfield, David, Diagram of the pathways of human steroidogenesis, Wiki Journal of Medicine, 2014 (71).*

3.2. MAJOR ADRENAL PATHOLOGIES

Adrenal disorders can be classified primarily according to their location in the cortex or medulla, and then according to their secretory function.

3.2.1. PATHOLOGIES OF THE ADRENAL CORTEX

Adrenal cortex disorders can be linked to both increased and decreased hormone synthesis. Specifically, adrenal hypofunction is responsible for Addison's disease, while adrenal hyperfunction, depending on the hormone pathway most affected, can manifest itself in: Cushing's syndrome, with excess glucocorticoids; adrenogenital syndrome, with excess adrenal sex steroids; hyperaldosteronism, with excess aldosterone.

3.2.1.1. CUSHING SYNDROME

Cushing's syndrome is defined as the cluster of clinical manifestations resulting from chronic exposure to excess cortisol. Cushing's syndrome is generally considered a rare disease, with an annual incidence of 1-2 cases per 100,000 inhabitants, but this is probably underestimated (72). Excess cortisol can result from various causes, which is why a distinction is made between exogenous Cushing's, which is the most common, and endogenous Cushing's, which is further divided into ACTH-dependent and ACTH-independent forms (73). More specifically, we distinguish between:

- Primary Cushing's syndrome, associated with the presence of adrenal lesions such as secreting hyperplasia adenoma, secreting carcinoma, or hyperplasia, or with rare congenital mutations in the context of a primary nodular pigmented adrenal syndrome or McCune-Albright syndrome. Adrenal adenomas and carcinomas (adrenocortical carcinoma, ACC) are responsible for 10% and 5% of endogenous Cushing's syndromes, respectively, and are more common in women (73);

- Secondary Cushing's syndrome, better known as Cushing's disease, resulting from excessive ACTH production by an ACTH-secreting pituitary adenoma, usually a microadenoma, i.e., less than 1 cm in diameter, which then stimulates bilateral adrenal hyperplasia. This form accounts for about 70% of endogenous hypercortisolism (73);
- Tertiary Cushing's syndrome, caused by excess CRH, which causes hyperplasia of corticotropic cells, excess ACTH, and consequent adrenal hyperplasia (73);
- Ectopic Cushing's syndrome, generally due to ACTH production by non-pituitary neoplastic lesions, such as small cell lung cancer, carcinoids, medullary thyroid carcinoma, and islet cell tumors, which are often difficult to detect due to their small size. Ectopic ACTH production is responsible for approximately 10% of ACTH-dependent Cushing's syndromes. More rarely, ectopic CRH production occurs (73);
- Iatrogenic Cushing's syndrome, or Cushing's-like syndrome, linked to pharmacological exposure to substantial amounts of cortisol or ACTH for prolonged periods (73).

Regarding adrenal lesions that may be associated with Cushing's syndrome, adenomas and carcinomas are the most common causes of ACTH-independent Cushing's syndrome, while hyperplasia is more often a manifestation of an ACTH-dependent form. ACCs generally cause more pronounced hypercortisolism than adenomas and hyperplasias. Furthermore, in forms of ACTH-independent Cushing's, if the lesion is unilateral, the contralateral adrenal gland and the unaffected ipsilateral parenchyma will appear atrophic, as the trophic stimulus of ACTH is lost, its secretion being suppressed by negative feedback from excess cortisol (55). Even in forms of Cushing's syndrome caused by exogenous glucocorticoids, the suppression of endogenous ACTH causes bilateral cortical atrophy, with only the glomerular zone maintaining its normal thickness. Adrenal hyperplasia can be diffuse, macro-, or micro-nodular. Diffuse adrenal hyperplasia is found in individuals with ACTH-dependent Cushing's syndrome. Both glands are enlarged to varying degrees, reaching a weight of up to 30 g. Microscopically, an expanded reticular zone with a scarcity of lipids is observed, comprising compact eosinophilic cells surrounded by vacuolated cells rich in lipids. In macronodular adrenal hyperplasia, the glands are almost completely replaced by prominent nodules of assorted sizes, but generally greater than 3 mm in diameter, containing a mixture of poor and lipid-rich cells (73). In addition, the areas between the macroscopic nodules show evidence of microscopic nodularity. In micronodular adrenal hyperplasia, micronodules with a diameter of 1-3 mm are found, with dark pigmentation, ranging from brown to black, likely due to the presence of lipofuscin. The micronodules are interspersed with atrophic areas. Furthermore, it has been observed that, in

ACTH-independent forms, hyperplasia is never completely autonomous but is rather regulated by circulating hormones such as luteinizing hormone and ADH, whose receptors are overexpressed on adrenal cortical cells by an unknown mechanism. Primary functioning adrenal neoplasms that secrete cortisol are morphologically indistinguishable from non-functioning neoplasms. Functioning neoplasms that cause Cushing's syndrome can be benign or malignant and are more common in women between the ages of 30 and 60. Adrenal cortical adenomas are yellow tumors, surrounded by a capsule of varying thickness, generally weighing less than 30 g. Microscopically, they consist of cells very similar to those of the normal *zona fasciculata*. On imaging, especially computed tomography (CT), adenomas can be distinguished as typical or atypical, where typical adenomas have a density of less than 10 Hounsfield units (HU) and an absolute washout of more than 60% on delayed scanning at 15 minutes. ACCs associated with Cushing's syndrome tend to reach larger sizes, often reaching 200-300 g; they are non-encapsulated tumors with all the atypical features typical of carcinomas (73). The clinical manifestations of Cushing's syndrome are varied and do not differ depending on the cause. Glucocorticoids affect almost all cells in the body, so excess cortisol involves multiple physiological systems. The following may be observed, varying from patient to patient:

- weight gain. This fairly common trait is characterized by an accumulation of abdominal adipose tissue, in the face and back, resulting in a pendulous abdomen with central obesity, moon face, and dorsal hump, respectively;
- diastolic hypertension, hypokalemia, and edema, due to the acquired mineralocorticoid effect of cortisol, as the inactivation capacity of the enzyme 11β-HSD2 is exceeded. The resulting water and sodium retention contributes transiently to weight gain;
- glucose intolerance, caused by the induction of insulin resistance and stimulation of gluconeogenesis. Full-blown diabetes mellitus develops in 20% of individuals with hypercortisolism;
- polyuria, due to hyperglycemia and consequent glycosuria;
- protein loss and reduction in muscle mass. Fast-twitch type 2 muscle fibers are most affected. This also causes a reduction in the circumference of the proximal limbs, which therefore appear thin, in contrast to the bulging abdomen. Muscle loss causes weakness, especially in the proximal muscles;

- reduction in bone matrix, with osteopenia followed by osteoporosis, resulting in low back pain and increased risk of fracture. Increased bone resorption also causes hypercalciuria, which can lead to kidney stones;
- loss of collagen, leading to weakening of the integuments, which makes the underlying vessels more visible. This, together with the increase in hematocrit and the more frequent rupture of small vessels, explains the appearance of facial telangiectasias and striae rubrae, purplish stretch marks usually visible at the abdominal level;
- increased vascular sensitivity to catecholamines, resulting in vasoconstriction and hypertension;
- suppression of the immune system, leading to increased susceptibility to infections and inefficient wound healing;
- neurological effects: high cortisol levels in the hippocampus cause alterations in mental state, with negative effects on learning, memory, and other neurological functions, manifesting as symptoms ranging from irritability to depression, and even severe psychiatric disorders such as schizophrenia;
- in women, signs and symptoms related to suppression of gonadotropins may be present, resulting in hypogonadism associated with hyperandrogenism, with hirsutism, acne, and oligomenorrhea, and in some cases infertility. These effects are particularly common in the presence of ACC;
- Alteration of the hypothalamic-pituitary-thyroid axis, leading to decreased secretion of thyroid-stimulating hormone (TSH);
- Bronze or brownish hyperpigmentation of the skin, mucous membranes, and hair, but only in ACTH-dependent forms, since the increased production of ACTH is associated with higher levels of melanocyte-stimulating hormone, derived from the maturation of a common pre-prohormone (72) (73).

Based on all these effects, these patients are at higher risk of metabolic syndrome and therefore of adverse cardiovascular events. Patients with Cushing's syndrome develop a state of hypercoagulability, which can lead to deep vein thrombosis with subsequent pulmonary embolism. Even after treatment, depending on the duration and degree of exposure to excess cortisol, the patient may experience long-term reduced quality of life and an increased risk of cardiovascular disease and osteoporosis (73).

Diagnosis

The diagnostic work-up of Cushing's syndrome follows a structured, stepwise approach aimed first at confirming the presence of endogenous hypercortisolism and subsequently identifying its etiology (72) (74) (75). Clinical suspicion arises from the presence of multiple, progressive, and disproportionate features of cortisol excess (such as facial rounding, proximal myopathy, wide violaceous striae, or easy bruising) or from an adrenal incidentaloma that requires hormonal evaluation (72). Before biochemical testing, exogenous glucocorticoid exposure, systemic, inhaled, intra-articular, or topical, must always be excluded. Current Endocrine Society and European Society of Endocrinology guidelines recommend using at least two different first-line tests to confirm cortisol excess (72) (76) :

- 24-hour urinary free cortisol (UFC): measured on at least two separate collections; values above the assay-specific upper limit (typically >50 µg/24 h or >138 nmol/24 h) support the diagnosis.
- Low-dose dexamethasone suppression test (DST): 1 mg dexamethasone is administered at 11 p.m., and plasma cortisol is measured at 8 a.m. the following morning. A cortisol level >50 nmol/L (1.8 µg/dL) indicates lack of suppression and is consistent with Cushing's syndrome (72) (74).
- Late-night salivary or plasma cortisol: loss of the normal circadian rhythm is a sensitive marker. A salivary cortisol >5.5 nmol/L (2 ng/mL) or plasma cortisol >200 nmol/L (7.5 µg/dL) is considered abnormal etiology (72) (75).

Potential confounding factors include pseudo-Cushing states (e.g., depression, alcoholism, severe obesity), incomplete urine collection, or drug interference with dexamethasone metabolism (e.g., phenytoin, carbamazepine, rifampicin) (72). Once hypercortisolism is confirmed, plasma ACTH measurement differentiates between ACTH-independent and ACTH-dependent forms (72) (75):

- Suppressed ACTH (<1 pmol/L) → suggests an adrenal (ACTH-independent) source.
- Normal or elevated ACTH (≥2 pmol/L) → indicates ACTH-dependent Cushing's syndrome, requiring further localization studies.

Imaging is then performed based on ACTH results:

- Non-contrast adrenal CT for ACTH-independent cases, to identify adenomas, carcinomas, or nodular hyperplasia.

- Pituitary MRI with gadolinium for ACTH-dependent forms, noting that up to 40% of ACTH-secreting microadenomas may be undetectable on imaging (72) (74) (77).

If MRI findings are inconclusive, dynamic endocrine tests are used to distinguish between pituitary and ectopic ACTH production:

- High-dose dexamethasone suppression test (8 mg overnight or 2 mg q6h for 48 h): suppression of serum cortisol >50% from baseline supports Cushing's disease (pituitary origin) (72) (76).
- CRH (or desmopressin) stimulation test: a rise in plasma ACTH >40% and cortisol >20% from baseline is also consistent with a pituitary source (75) (78).
- Inferior petrosal sinus sampling (IPSS) remains the gold standard when biochemical and imaging results are discordant. A central-to-peripheral ACTH ratio >2 at baseline or >3 after CRH administration confirms pituitary origin, whereas absence of gradient indicates ectopic secretion (72) (78).

In ACTH-dependent forms where ectopic secretion is suspected, high-resolution CT or MRI of the chest and abdomen (especially targeting lungs, thymus, and pancreas) should be performed, followed by 68Ga-DOTATATE PET/CT or octreotide scintigraphy if no lesion is identified (75).

Treatment and prognosis of Cushing's Syndrome

The treatment approach for Cushing's syndrome depends on the original cause of the condition and the severity of cortisol overproduction. The first treatment choice for Cushing's syndrome involves surgical removal of the disease-causing lesion when possible: patients with ACTH-independent adrenal disease undergo adrenalectomy and patients with pituitary adenomas (Cushing's disease) receive transsphenoidal surgery. The initial surgical treatment of Cushing's syndrome leads to fast biochemical remission, but patients experience frequent relapses which require ongoing monitoring. The preferred treatment for localized ectopic ACTH-producing tumors involves surgical removal of the tumor but patients with non-resectable or non-localized tumors receive bilateral adrenalectomy or medical therapy. Patients need glucocorticoid replacement therapy after definitive treatment because their HPA axis needs time to recover which spans from several months to multiple years (74) (79). Medical therapy becomes necessary when surgery proves unsuitable or produces incomplete results or when patients need

immediate treatment during their wait for surgery in severe cases. The three main categories of medical treatment for Cushing's syndrome include steroidogenesis inhibitors which block adrenal cortisol production (e.g. ketoconazole, metyrapone, mitotane, etomidate) and pituitary-directed agents which decrease ACTH production (e.g. pasireotide, cabergoline) and glucocorticoid receptor antagonists which block cortisol receptor action (e.g. mifepristone) and glucocorticoid receptor signaling modulators (e.g. relacorilant). The selection of treatment depends on individual patient needs and the need for fast results and drug interactions and availability in the patient's area (79) (80). The oral 11β-hydroxylase inhibitor osilodrostat has proven to be an effective treatment for normalizing cortisol levels in patients with endogenous Cushing's syndrome. The LINC program included randomized and open-label studies which showed that osilodrostat treatment led to significant and enduring decreases in urinary free cortisol (UFC) levels which resulted in better blood pressure management and glycemic control and symptom reduction. The initial dosing schedule in clinical trials used 2 mg twice daily but real-world practice shows that patients often start with 4 mg daily as a single dose or 2 mg twice daily. The risk of adrenal insufficiency requires constant and close observation because it can develop during dose adjustments or at any time even when the medication dose appears stable. The monitoring process for patients includes both clinical evaluations and serum cortisol/UFC tests and electrolyte checks for hypokalemia and ECG assessments when necessary for QTc risk evaluation. The "block-and-replace" method involves adding physiological glucocorticoid replacement to patients who need dose escalation to prevent adrenal insufficiency (81) (82) (83). The treatment of pituitary disorders in Cushing's disease involves two main options: pasireotide (a somatostatin analog with SSTR5 affinity) and cabergoline (a dopamine agonist). The subcutaneous and long-acting injectable formulations of pasireotide help patients with Cushing's disease achieve better UFC levels and improved clinical symptoms but patients commonly develop hyperglycemia which requires active treatment. The treatment of Cushing's disease with cabergoline shows effectiveness for particular patients who receive this medication as a standalone therapy or in combination with ketoconazole or pasireotide to enhance biochemical control (84) (85). The GR antagonist mifepristone helps patients with hypercortisolism by improving their blood sugar control and cortisol-related symptoms even when their cortisol levels stay elevated. The treatment provides immediate relief from cortisol action symptoms, but patients need to undergo complex biochemical tests because their cortisol and ACTH levels will remain elevated. The selective glucocorticoid receptor modulator relacorilant demonstrated positive results in its phase 2/3 clinical trials by controlling blood pressure and glucose levels without causing adrenal

insufficiency like steroidogenesis inhibitors do. The phase-3 randomized-withdrawal GRACE trial demonstrated that relacorilant provided significant clinical advantages to patients who had hypertension and/or hyperglycemia because of endogenous hypercortisolism. The therapeutic role of relacorilant in medical practice will become clearer through ongoing post-marketing research and extended clinical studies (86). The monitoring of steroidogenesis inhibitors (metyrapone and ketoconazole and osilodrostat) requires regular checks of cortisol levels (UFC and serum) and potassium levels and liver function tests (especially for ketoconazole) and adrenal insufficiency symptoms; patients who receive QT-prolonging medications need ECG monitoring (81) (83). The management of pasireotide requires patients to receive close glycemic monitoring since they need active hyperglycemia management (84). The GR modulators/antagonist's mifepristone and relacorilant require clinical endpoint monitoring of blood pressure and glycemic control and signs and symptoms because cortisol and ACTH levels may increase paradoxically (86). Untreated chronic hypercortisolism confers markedly increased risk of cardiovascular disease, infections, metabolic complications, osteoporosis and venous thromboembolism; successful treatment (surgical or medical) reduces but may not fully normalize long-term morbidity risks. Lifelong surveillance for recurrence, management of comorbidities, and attention to bone health and cardiovascular risk factors are mandatory components of post-remission care (74) (81).

3.2.1.2. ADRENOCORTICAL ADENOMAS (ACAs)

Most ACAs are clinically silent, found accidentally during imaging, so-called adrenal incidentalomas (≥5 mm). Typical adenomas are well-circumscribed nodules, up to 2.5 cm in diameter, expanding the adrenal gland. Functioning adenomas are associated with atrophy of the residual cortex, unlike non-functioning ones (75). On gross examination, adenomas appear yellow to brownish yellow due to lipid content. Microscopically, they consist of cells resembling normal adrenal cortex, with small nuclei, mild pleomorphism ("endocrine atypia"), and low mitotic activity. Cytoplasm shows eosinophilic to vacuolated appearance based on the amount of lipid present in the cells. The majority of adenomas do not produce cortisol, but some cases show minimal cortisol production without developing Cushingoid symptoms which now fall under the definition of mild autonomous cortisol secretion (MACS).

3.2.1.3. MILD AUTONOMOUS CORTISOL SECRETION

Among patients with incidentally discovered adrenocortical adenomas, a relevant subset displays mild but autonomous cortisol secretion without the clinical phenotype of Cushing's syndrome. The European Society of Endocrinology (ESE) and European Network for the Study of Adrenal Tumors (ENSAT) established MACS as the official term for this condition in their 2023 guidelines. MACS is characterized by mild, autonomous cortisol excess leading to partial hypothalamic-pituitary-adrenal (HPA) axis suppression and an increased prevalence of cardiometabolic comorbidities such as hypertension, type 2 diabetes, and osteoporosis.

Diagnosis

The diagnosis of MACS relies primarily on hormonal evaluation, particularly the 1 mg overnight dexamethasone suppression test (DST), integrated with clinical and radiological assessment.

- Overnight 1 mg DST: Patients receive 1 mg dexamethasone orally at 23:00, and serum cortisol is measured at 08:00-09:00 the following morning.
- A post-DST cortisol > 1.8 µg/dL (50 nmol/L) indicates loss of normal feedback suppression and supports the diagnosis of MACS (75).
- Levels between 1.8 and 5 µg/dL (50-138 nmol/L) indicate possible mild autonomy, while values > 5 µg/dL (> 138 nmol/L) suggest more pronounced autonomous secretion.

Additional tests (performed if DST results are equivocal or if clinical suspicion persists):

- Late-night salivary cortisol: loss of diurnal rhythm supports cortisol excess.
- 24-hour urinary free cortisol (UFC): may be normal or mildly elevated.
- Plasma ACTH: typically, suppressed, or low-normal, confirming ACTH-independent secretion.
- Serum DHEAS: often low, reflecting chronic ACTH suppression.

Before confirming MACS, exogenous glucocorticoid exposure and factors interfering with dexamethasone metabolism (e.g., CYP3A4 inducers, oral estrogens) must be excluded (72).

Most MACS cases are discovered incidentally during imaging for unrelated conditions. Lesions are generally ≤ 4 cm, homogeneous, and lipid-rich, with unenhanced CT density < 10 HU, consistent with benign adenomas. Although patients are typically asymptomatic, subtle

features such as weight gain, hypertension, impaired glucose tolerance, or osteopenia may be present due to chronic low-grade cortisol exposure (87).

Treatment

Management of MACS depends on the degree of cortisol autonomy, patient comorbidities, and surgical risk. The 2023 ESE/ENSAT guidelines recommend the following approach:

- Conservative management (observation) is appropriate for most patients with mild cortisol excess and no or stable comorbidities.

Regular follow-up should include:

- Annual reassessment of cortisol secretion (DST),
- Monitoring blood pressure, glucose metabolism, and bone density.

Adrenalectomy should be considered in patients with biochemically confirmed MACS and clinically relevant comorbidities potentially attributable to cortisol excess (e.g., hypertension, diabetes, osteoporosis) that cannot be adequately controlled by medical therapy (75) (88). Post-surgical follow-up includes evaluation for hypocortisolism, which may require transient hydrocortisone replacement therapy until recovery of the HPA axis. For non-surgical candidates or persistent cortisol hypersecretion, medical therapy with steroidogenesis inhibitors such as metyrapone, osilodrostat, or ketoconazole can be considered. MACS is associated with increased cardiometabolic risk compared to non-functioning adrenal adenomas, including higher rates of hypertension, insulin resistance, dyslipidemia, and fragility fractures (89). However, timely recognition and management, whether conservative or surgical, can mitigate long-term morbidity.

3.2.1.4. ADRENOCORTICAL CARCINOMAS (ACCs)

Adrenocortical carcinoma is rare (1-2 cases per million annually), occurring at any age, including childhood. ACCs are more frequently functioning than adenomas and frequently cause virilization or Cushing-like syndromes (90). Tumors are typically large (>20 cm), invasive, and destructive to the adrenal. Although generally highly malignant, biological behavior varies significantly between patients. Somatic TP53 mutations are present in ~25% of sporadic ACCs, while germline TP53 mutations cause Li-Fraumeni syndrome, predisposing to multiple solid tumors including ACC (90). Additional alterations involve the Wnt/β-catenin

pathway and IGF-2 overexpression, the latter seen in ~90% of cases. Macroscopically, ACCs are heterogeneous, with necrotic, hemorrhagic, and cystic areas. They tend to invade the adrenal vein, inferior vena cava, and lymphatics, leading to regional and distant metastases (lungs and other viscera). Microscopically, differentiation varies, from adenoma-like cells to pleomorphic giant cells resembling metastatic carcinoma (90). Biochemically, 60-70% of ACCs produce excess steroids, although clinical features may be subtle due to inefficient steroid synthesis. Overproduction of both glucocorticoids and androgen precursors is common and often indicative of malignancy (90).

3.2.1.5. HYPERALDOSTERONISM

Hyperaldosteronism is a condition characterized by excessive aldosterone production from the adrenal cortex. Screening studies in hypertensive populations reveal a prevalence of 5–12%, increasing in hypertensive patients with hypokalemia (91). It is the most common cause of secondary hypertension. Primary hyperaldosteronism (Conn's syndrome) arises from intrinsic adrenal pathology, leading to suppression of the renin-angiotensin-aldosterone system (RAAS):

- Bilateral adrenal hyperplasia (idiopathic hyperaldosteronism, IHA) accounts for ~60% of cases, typically in older patients with milder hypertension.
- Aldosterone-producing adenomas (~35%) are generally small (<2 cm), often left-sided, and histologically resemble *zona fasciculata* cells.
- Adrenocortical carcinoma (ACC) is a rare cause, mainly in young patients with large lesions.

Glucocorticoid-remediable hyperaldosteronism is a rare familial form in which ACTH drives aldosterone synthesis, suppressible by dexamethasone (92). Secondary hyperaldosteronism results from extra-adrenal stimuli, usually renin-dependent, as seen in renal artery stenosis, renin-secreting tumors, or diuretic use, and may also occur with excessive licorice consumption (93). Excess aldosterone causes sodium and water retention, leading to hypervolemia and hypertension, and potassium excretion, potentially causing hypokalemia. Late-stage hypertension is also aggravated by aldosterone-mediated vasoconstriction. Hypokalemic metabolic alkalosis can cause muscle weakness, paresthesia, myopathy, cramps, tetany, and paralysis (92). Long-term consequences include resistant hypertension, metabolic syndrome,

insulin resistance, endothelial dysfunction, cardiovascular remodeling, and increased risk of stroke, myocardial infarction, osteoporosis, type 2 diabetes, and cognitive impairment (92).

Diagnosis

Routine screening for hyperaldosteronism is not recommended for all hypertensive patients but is indicated in those with resistant hypertension, early-onset hypertension (<40 years), a family history of hypertension or stroke, hypokalemia, or incidentally discovered adrenal masses (91). The diagnostic protocol involves three stages: screening, confirmation, and subtype characterization. Screening relies on measuring plasma aldosterone and renin levels (or plasma renin activity, PRA) to calculate the aldosterone-renin ratio (ARR), preferably in the morning after correcting potassium levels. Medication adjustments are recommended to avoid false positives or negatives (91). Secondary hyperaldosteronism is suggested by elevated PRA and aldosterone with ARR <10. Primary hyperaldosteronism is suspected if PRA is suppressed (<1 ng/mL/h) and plasma aldosterone is elevated (>10 ng/dL). Confirmation tests include intravenous saline infusion, oral sodium loading, or fludrocortisone suppression, which demonstrate autonomous aldosterone secretion if levels fail to suppress appropriately. Once diagnosed, adrenal imaging, preferably thin-slice CT, is used to identify lesions. For surgical candidates, adrenal vein sampling (AVS) distinguishes unilateral adenomas from bilateral hyperplasia. AVS relies on aldosterone/cortisol ratios to confirm lateralization (92). Genetic testing is indicated for familial glucocorticoid-remediable hyperaldosteronism, and urinary steroid metabolite profiling via GC-MS may refine diagnosis in atypical cases (92).

Treatment

Surgery is the preferred treatment for patients with lateralized adrenal lesions on CT or AVS, particularly those under 40 years old. The favored approach is laparoscopic adrenalectomy (92). Patients not eligible for surgery or with bilateral disease are managed medically. The first-line therapy is the mineralocorticoid receptor (MR) antagonist spironolactone, starting at 12.5-50 mg twice daily and titrated up to 400 mg/day to control blood pressure and normalize potassium (94) (95). Side effects include menstrual irregularities, decreased libido, and gynecomastia (96) (97). Other options include eplerenone, a more selective MR antagonist (25 mg twice daily up to 200 mg/day), and amiloride, a sodium channel blocker (5-10 mg twice daily) (96) (97). In glucocorticoid-remediable hyperaldosteronism, treatment consists of low-dose dexamethasone, sometimes combined with an MR antagonist for optimal blood pressure control (98).

3.2.1.6. ADRENOGENITAL SYNDROMES AND CONGENITAL ADRENAL HYPERPLASIA (CAH)

Congenital adrenal hyperplasia (CAH) is an autosomal recessive disorder caused by enzymatic defects in cortisol biosynthesis, leading to excess androgen production. In about 90% of cases, the defect involves 21-hydroxylase (CYP21A2) deficiency (99). The resulting loss of cortisol feedback causes chronic ACTH elevation, which induces bilateral adrenal hyperplasia and overproduction of adrenal androgens. Histologically, the adrenal cortex appears thickened, nodular, and lipid-depleted, with eosinophilic, lipid-poor proliferating cells mixed with lipid-rich clear cells. Hyperplasia of pituitary corticotrope cells is also frequent. The androgen excess leads to variable clinical presentations, ranging from severe virilization of female external genitalia at birth to mild hirsutism, acne, and oligomenorrhea in non-classical forms (100). When the enzymatic defect also affects aldosterone synthesis, patients experience salt-wasting, with hyponatremia, hyperkalemia, acidosis, and hypotension, potentially leading to cardiovascular collapse. Severe CAH may also impair catecholamine synthesis, further predisposing to hypotension. Three clinical variants of 21-hydroxylase deficiency are described (99):

- Salt-wasting (classic) CAH: complete deficiency of glucocorticoids and mineralocorticoids, presenting in neonates with salt loss, hypotension, and virilization (in females).
- Simple virilizing CAH: partial enzyme defect affecting glucocorticoid synthesis only; causes androgen excess without salt loss.
- Non-classic (late-onset) CAH: mild, partial deficiency with preserved cortisol production, resulting in mild hyperandrogenism during adolescence or adulthood, often mimicking polycystic ovary syndrome (PCOS).

Diagnosis

CAH should be suspected in any newborn presenting with ambiguous genitalia. Targeted newborn screening programs now allow early detection of severe forms before clinical symptoms appear. Diagnosis is based on the measurement of steroid precursors accumulated upstream of the enzymatic block, performed in serum and urine, typically using immunoassays, though mass spectrometry (MS) is preferred for greater specificity and accuracy (101).

Differential diagnosis includes other adrenogenital syndromes caused by sex hormone-secreting adrenal tumors, mainly adrenocortical carcinomas (ACC). The resulting clinical picture depends on which hormone is secreted, as well as the patient's sex and age at the onset of hypersecretion.

Treatment

Treatment with glucocorticoids in CAH is more complex than in other forms of primary adrenal insufficiency, as it must both replace deficient cortisol and suppress excessive ACTH secretion, which drives androgen overproduction. Current therapy is limited by the lack of glucocorticoid formulations that mimic the physiological circadian rhythm of cortisol, leading to early-morning ACTH stimulation and androgen excess (100). In children, therapy aims to optimize growth and pubertal development, prevent adrenal crises, and manage 46, XX disorders of sex development (102). In adults, the focus is on maintaining fertility and avoiding glucocorticoid-related side effects such as metabolic syndrome and osteoporosis. Fertility may be reduced in women due to chronic anovulation, while men may develop testicular adrenal rest tumors (TARTs), which impair spermatogenesis and can lead to irreversible fibrosis (103). Hydrocortisone is generally used to prevent adrenal crises, while prednisolone or prednisone may be required to control androgen excess. In children, hydrocortisone is given in divided doses at 1-1.5× the normal cortisol production rate. Adults may need intermediate-acting glucocorticoids at the lowest effective dose, while dexamethasone can be used short-term to restore fertility, minimizing adverse effects (102). During stressful events (surgery, acute illness, trauma), glucocorticoid doses should be doubled or tripled. Biochemical monitoring includes androstenedione, testosterone, and 17-hydroxyprogesterone (17-OHP) levels; normalization of 17-OHP suggests glucocorticoid overtreatment, which must be carefully titrated to avoid hypothalamic-pituitary-gonadal axis suppression (102). Mineralocorticoid requirements are higher in childhood due to relative renal resistance, necessitating salt and mineralocorticoid replacement. After puberty, therapy should be reassessed by measuring plasma renin activity, maintaining it within the upper half of the normal range (102).

3.2.1.7. ADDISON'S DISEASE

Addison's disease is a chronic primary adrenal insufficiency caused by the destruction or dysfunction of the adrenal cortex, leading to deficient glucocorticoid and mineralocorticoid

production with elevated ACTH levels. It affects roughly 2 out of 10,000 people (104). Causes include autoimmune adrenalitis (most common), infections (tuberculosis, HIV, fungi), bilateral adrenal hemorrhage, metastases, or genetic disorders such as X-linked adrenoleukodystrophy and congenital adrenal hypoplasia. In autoimmune Addison's disease, antibodies against 21-hydroxylase and 17-hydroxylase destroy adrenal tissue (105). It can occur alone or as part of autoimmune polyglandular syndromes (APS):

- APS type I (APECED)-autosomal recessive (AIRE gene), childhood onset with Addison's disease, hypoparathyroidism, and chronic mucocutaneous candidiasis.
- APS type II - polygenic, adult onset, including Addison's disease with autoimmune thyroiditis, type 1 diabetes, celiac disease, and sometimes vitiligo.

Symptoms develop gradually and include fatigue, weakness, weight loss, hypotension, salt craving, hyponatremia, hyperkalemia, and hyperpigmentation due to excess ACTH/POMC (104). Secondary adrenal insufficiency, caused by pituitary or hypothalamic disease or prolonged glucocorticoid therapy, presents without hyperpigmentation or major electrolyte imbalance since aldosterone secretion is preserved. An Addisonian crisis (acute adrenal failure) may occur during physical stress, after sudden withdrawal of corticosteroids, or following massive adrenal hemorrhage, as in Waterhouse-Friderichsen syndrome from meningococcal sepsis (105). Histologically, autoimmune adrenalitis shows small, atrophic glands with lymphocytic infiltration; infectious causes produce granulomatous inflammation, while metastatic involvement leads to enlarged, infiltrated glands (104).

Diagnosis

The short ACTH (cosyntropin) stimulation test using 250 µg of cosyntropin is the standard diagnostic tool for adrenal insufficiency (104). Serum cortisol is measured 30-60 minutes after administration, and a peak below 450-550 nmol/L (16-18 µg/dL) indicates adrenal failure. The exact threshold varies by assay, with lower cutoffs for LC-MS/MS methods. In early pituitary insufficiency (within ~4 weeks), patients may still respond to exogenous ACTH, so the insulin tolerance test (ITT) can be used as an alternative, though it is more invasive and contraindicated in diabetes, cardiovascular disease, or seizure history (106). Random cortisol levels are not reliable because of circadian variation. Many patients with secondary adrenal insufficiency have normal basal cortisol but fail to mount an adequate ACTH-stimulated response. Testing should never delay treatment: in a suspected adrenal crisis, measure baseline cortisol, start

replacement therapy immediately, and postpone functional testing. After confirming adrenal insufficiency, plasma ACTH measurement distinguishes the cause:

- High ACTH: primary adrenal failure.
- Low/inappropriately normal ACTH: secondary (pituitary or hypothalamic) insufficiency.

In primary adrenal insufficiency, elevated plasma renin supports mineralocorticoid deficiency. Patients with newly diagnosed Addison's disease should undergo autoimmune screening for anti-adrenal (anti-21-hydroxylase) antibodies (104). If negative, CT imaging is indicated to assess hemorrhage, infection, or neoplasia. In males without autoantibodies, testing for very-long-chain fatty acids helps exclude X-linked adrenoleukodystrophy. When ACTH is low, MRI of the hypothalamic-pituitary region is recommended to evaluate central causes.

Treatment

Acute adrenal insufficiency (adrenal crisis) requires immediate rehydration with normal saline (1 L/hour initially) under continuous cardiac monitoring (104). Glucocorticoid replacement should start promptly with an initial 100 mg IV bolus of hydrocortisone, followed by 200 mg over 24 hours, either as continuous infusion or divided IV/IM doses. Mineralocorticoid therapy is introduced once the daily hydrocortisone dose is reduced below 50 mg, since higher doses already provide sufficient mineralocorticoid activity. For chronic adrenal insufficiency, glucocorticoid replacement aims to mimic normal daily cortisol production: 15-25 mg of oral hydrocortisone in 2-3 divided doses, with at least half the dose in the morning. Dosage must be individualized to achieve good quality of life using the lowest effective dose (104). In the third trimester of pregnancy, hydrocortisone requirements may rise by ~50%. Patients should be educated to increase their glucocorticoid dose during stress, doubling the dose for fever or illness, and using 100 mg IV hydrocortisone daily during surgery, trauma, or prolonged vomiting. Diet should include at least 150 mEq sodium/day, increasing intake during heat exposure or diarrhea. Current glucocorticoid formulations do not replicate the physiological circadian rhythm, and long-acting agents (prednisolone, dexamethasone) are generally avoided. Therapy is monitored clinically, based on symptoms, body weight, blood pressure, and orthostatic hypotension. Over-replacement may lead to metabolic and bone complications, so patients on ≥30 mg/day hydrocortisone require osteoporosis surveillance. In isolated primary adrenal insufficiency, periodic autoimmune screening is recommended (104). Mineralocorticoid replacement uses fludrocortisone 100-150 µg daily, with higher doses in hot

climates. Adequacy is assessed by orthostatic testing, serum sodium and potassium, and plasma renin, which should remain in the upper normal range. Adjustments in glucocorticoid dose can affect mineralocorticoid needs (40 mg hydrocortisone ≈ 100 μg fludrocortisone). During pregnancy, fludrocortisone dose may require a modest increase due to progesterone's MR-antagonist effect, though renin cannot be used for monitoring because it rises physiologically (104). Adrenal androgen replacement may benefit patients, especially women, with persistent fatigue or reduced libido despite optimal steroid therapy. DHEA 25-50 mg once daily can be used, monitored by DHEAS, androstenedione, testosterone, and SHBG levels 24 hours after dosing.

3.2.2. PATHOLOGIES OF ADRENAL MEDULLA: PHEOCHROMOCYTOMA

Pheochromocytoma is a rare tumor of the adrenal medulla's chromaffin cells, with an incidence of 2-8 cases per million per year and a mean diagnostic age of around 40 years, though it may also occur in childhood or late adulthood (107). Classically known as the "10% tumor", it is malignant in 10%, extra-adrenal (paraganglioma) in 10%, bilateral in 10%, and non-hypertensive in 10%. Familial forms, once thought to represent 10%, are now estimated at about 25%. Pheochromocytomas can be sporadic or hereditary, and in the latter situation, genetic forms are often more aggressive. Among the genetic syndromes associated to an increased risk of pheochromocytoma, it is important to mention the Multiple Endocrine Neoplasia type 2 (MEN2), caused by RET proto-oncogene mutations, and characterized by medullary thyroid carcinoma, pheochromocytoma, primary hyperparathyroidism, mucosal neuromas, and marfanoid habitus (108). Macroscopically, pheochromocytomas have a variable presentation, ranging from small, well-circumscribed nodules to large hemorrhagic masses up to 1-4 kg, often encapsulated and compressing surrounding tissue (109). They display a yellow-brown cut surface, sometimes with necrotic or cystic areas. Fresh tissue darkens with potassium dichromate due to catecholamine oxidation. Microscopically, histologically characteristics of pheochromocytomas are diverse, but generally exhibit the characteristic "zellballen" pattern, nests of polygonal or spindle-shaped chromaffin cells surrounded by sustentacular (S-100 positive) cells and a rich vascular stroma (109). Chromaffin cells stain positively for chromogranin and synaptophysin. No specific histologic feature reliably predicts malignancy; the presence of metastases to lymph nodes, liver, lung, or bone is the only definitive criterion

of malignancy. The clinical presentation of pheochromocytoma is so variable that it has earned the nickname “the great mimicker.” Generally, pheochromocytoma is responsible for hypersecretion of catecholamines, with a possible prevalence of adrenaline or, more frequently, noradrenaline, resulting in hyperactivation of the sympathetic nervous system. Among these, the main effect is hypertension, which can manifest as stable hypertension or hypertensive peaks, with a predominant increase in diastolic pressure in cases where norepinephrine prevails, and in systolic pressure if adrenaline prevails. Tachycardia, sweating, severe headache, constipation, and weight loss may also occur despite a possible increase in caloric intake.

Hypertensive peaks are caused by a sudden release of catecholamines, which can lead to congestive heart failure, acute myocardial infarction, pulmonary edema, ventricular fibrillation, or acute cerebrovascular events. Cardiac complications are attributable to ventricular arrhythmias or catecholamine-induced heart disease, also known as catecholamine-induced myocardial instability; this may be due to both the direct toxic effects of catecholamines and the indirect coronary vasoconstrictive effect. During episodes of catecholamine release, patients appear anxious and pale and complain of tachycardia and palpitations. These paroxysmal crises generally last less than an hour and can be precipitated by surgery, changes in position, exercise, pregnancy, urination, and medication. In some cases, pheochromocytomas secrete other hormones, such as ACTH and somatostatin, which can lead to other associated clinical manifestations. About 5% of patients are asymptomatic, with tumors that appear non-functioning, though they may release catecholamines under stress (e.g., during surgery) (107). Occasionally, tumors may also secrete ACTH or somatostatin, leading to mixed endocrine syndromes.

Diagnosis

Patients presenting with the classic triad of palpitations, headache, and profuse sweating, especially when associated with hypertension, should be strongly suspected of having a pheochromocytoma (107). Diagnosis relies on two equally important steps: biochemical confirmation of catecholamine excess and tumor localization through imaging. The hormonal activity of the tumor fluctuates, causing considerable variability in serial catecholamine measurements. However, most tumors continuously release O-methylated metabolites, which are detected by measuring metanephrines. Catecholamines and metanephrines can be detected using various methods, and when values are three times higher than the upper limit of normal,

the diagnosis is highly probable, regardless of the method used. In patients with values close to the normal limits, the choice of method becomes important. Urinary tests for the determination of total or fractionated metanephrines are widely available and commonly used as initial tests; among these, fractionated metanephrine and catecholamine assays are the most sensitive. Plasma tests are more practical and include the measurement of catecholamines and metanephrines. Plasma metanephrine assays are the most sensitive and are less prone to false positives due to stress, including that caused by venipuncture. In any case, it is important to reduce the risk of false positives through proper preparation, excluding dietary factors and medication that could interfere. If results are still uncertain, a clonidine suppression test can be performed, in which normetanephrine is measured in plasma three hours after oral administration of 300 μg of clonidine (110). For imaging, CT and MRI have comparable sensitivity and specificity, with MRI being slightly superior; both should be performed with contrast enhancement. When standard imaging is inconclusive, PET scans with 18F-FDG or 68Ga-DOTATATE can provide additional diagnostic information (110).

Treatment

The goal of therapy is complete surgical removal of the tumor, achieved through partial or total adrenalectomy (110). Minimally invasive approaches are preferred for smaller, localized lesions, whereas open surgery is indicated for large tumors or suspected metastases. In malignant pheochromocytoma, curative treatment is rare; management focuses on cytoreductive surgery combined with adjuvant radiotherapy or chemotherapy. When possible, adrenal cortical preservation is recommended to prevent Addison's disease, particularly in hereditary or bilateral forms. Preoperative management is critical to ensure hemodynamic stability. Blood pressure should be maintained below 160/90 mmHg for at least a week before surgery, typically using α-blockade (phenoxybenzamine) for 2-3 weeks (110). A β-blocker may be added if tachycardia persists after α-blockade optimization. Additional antihypertensives, such as calcium channel blockers, may also be employed. Adequate hydration before surgery prevents postoperative hypotension or hypovolemic shock due to the sudden fall in circulating catecholamines. Postoperatively, normalization of catecholamine levels confirms successful tumor removal. In patients undergoing bilateral adrenalectomy with cortical-sparing surgery, an ACTH stimulation test should be performed to rule out cortisol deficiency.

4. STEROID HORMONES

4.1. CLASSES AND PHYSIOLOGICAL ROLE

Steroids are ubiquitous hormones defined structurally by a characteristic arrangement of four fused, non-aromatic rings (111). The precursor to all major mammalian steroids is cholesterol. Steroid hormones are systematically categorized into five distinct classes, based primarily on the specific receptor types to which they bind: glucocorticoids, mineralocorticoids, androgens, estrogens, and progestogens. While structurally related, vitamin D derivatives are often studied separately as they do not strictly fall under the definition of steroids. Furthermore, the inherent complexity of studying these lipids is amplified by the existence of multiple molecular variants within each primary class, representing slight modifications of the parent steroid molecule. Steroids exert control over a wide array of vital physiological processes, including the regulation of metabolism, inflammatory and immune responses, maintenance of salt and water balance, development of secondary sexual characteristics, reproduction and the body's capacity to cope with stress and injury (112). All steroid hormones are metabolic derivatives of the ubiquitous structural membrane lipid, cholesterol. It is noteworthy that cholesterol itself, through its essential role in cellular membrane dynamics (e.g., lipid rafts), influences many of the same physiological pathways via a distinct mechanism separate from that of its hormone derivatives.

Table 1: *Examples of Each of the Five Classes of Steroid Hormones. Adapted from: William Stillwell, Chapter 20 - Bioactive Lipids, An Introduction to Biological Membranes (Second Edition), 2016 (111).*

Steroid hormone class	Example	Moniker
Glucocorticoids	Cortisol	Stress hormone
Mineralocorticoids	Aldosterone	Blood pressure hormone
Androgens	Testosterone	Male hormone
Estrogens	Estradiol	Female hormone
Progestogens	Progesterone	Pregnancy hormone

4.2. BIOSYNTHESIS AND STRUCTURAL CLASSIFICATION

4.2.1. SYNTHESIS PATHWAYS AND TISSUE SPECIFICITY

Steroid hormones are synthesized predominantly within the adrenal cortex and gonads, with minor contributions from adipose tissue, the central nervous system, and the placenta (112). All steroidogenesis originates from the common precursor, cholesterol. The process involves multiple enzymes characterized by distinct expression profiles across different organs and tissues. The first rate-limiting step is the conversion of cholesterol into pregnenolone (P5), which takes place on the inner mitochondrial membrane, catalyzed by cytochrome P450scc (CYP11A1) (113). P5 then serves as the universal precursor for all subsequent, tissue-specific biosynthetic pathways. The specific type of steroid produced is governed by the local expression of key enzymes, such as P450C17 (CYP17) which drives the synthesis of cortisol and sex steroids, and 3β-hydroxysteroid dehydrogenase (3β-HSD) which directs synthesis toward progesterone and aldosterone (113). This enzymatic specificity dictates that:

- glucocorticoids are produced in the *zona fasciculata.*
- mineralocorticoids are produced in the *zona glomerulosa*.
- sex steroids (androgens and estrogens) are produced in the *zona reticularis* and the gonads.

4.2.2. STRUCTURAL CLASSIFICATION BY CARBON NUMBER

Aside from their classification by receptor type, steroid hormones are also structurally categorized based on their carbon backbone (113), reflecting their position in the biosynthetic pathway:

- **C-21** steroids: these include the glucocorticoids, mineralocorticoids, and progestogens, containing 21 carbon atoms.
- **C-19** steroids: these include androgens, containing 19 carbon atoms.
- **C-18** steroids**:** these include estrogens, which have 18 carbon atoms due to the aromatization of the A-ring, making them the only class with an aromatic ring structure.

4.3. TRANSPORT AND MEMBRANE PERMEABILITY

4.3.1. CIRCULATORY TRANSPORT AND CARRIER PROTEINS

Due to their pronounced lipophilicity and minimal water solubility, steroid hormones circulate in the bloodstream in two forms: free (unbound) and protein-bound (114). The binding affinity of these hormones to various transport proteins dictates their distribution. They generally exhibit high affinity for specific globulins and lower affinity for non-specific carrier proteins, such as albumin. Key examples of high-affinity carrier proteins include:

- Corticosteroid-Binding Globulin (CBG), also known as transcortin, which is primarily responsible for transporting cortisol (F) and progesterone (P4) (114)
- Sex Hormone-Binding Globulin (SHBG), which is dedicated to the transport of testosterone (T) and estradiol (E2) (114).

It is notable that aldosterone lacks specific high-affinity carrier proteins; consequently, only about half of the circulating hormone is complexed with transport proteins.

4.3.2. BIOLOGICAL ACTIVITY AND CLEARANCE

The free fraction of the circulating hormone is the biologically active form, capable of mediating the hormone's biological action and driving feedback regulation (114). This physiological mechanism dictates that as the total circulating hormone levels increase; the unbound, active fraction will also rise. Furthermore, only the free fraction is subject to metabolic modifications, such as sulfation and glucuronidation, which determine the hormone's clearance and ultimate excretion from the body. Upon reaching the target tissues, the hormone's lipophilic nature allows the free form to readily and passively diffuse across the cellular plasma membrane. Within the cell membrane, steroids exhibit high lateral mobility and can undergo flip-flop movements to rapidly access their intracellular receptors (111).

4.4. RECEPTOR BINDING AND ACTION: MOLECULAR MECHANISMS

4.4.1. STEROID RECEPTORS: STRUCTURE AND CLASSIFICATION

The receptors that mediate the hormonal action of steroids belong to the nuclear receptor (NR) superfamily, specifically Type 3 receptors (115). These include the two estrogen receptors (ERα and ERβ), the glucocorticoid receptor (GR), the mineralocorticoid receptor (MR), the progestin receptor (PR), and the androgen receptor (AR). Inactive receptors are located in the cytosol as monomers (115). All steroid receptors share a modular structure defined by key functional domains: the central DNA-Binding Domain (DBD), which targets the Hormone Responsive Element (HRE) on the DNA, and the terminal Ligand-Binding Domain (LBD), which serves as an activation domain. The highly flexible Hinge region (D), situated between the DBD and LBD, engages in receptor dimerization dynamics. All steroid receptors, when unliganded, are associated with multi-protein complexes containing heat shock proteins (Hsp90, Hsp70, and Hsp56), which maintain the receptor in an inactive, hormone-binding-competent conformation (116).

4.4.2. GENOMIC ACTION (SLOW PATHWAY)

The receptor activation process begins when the receptor binds to its ligand which enables dimerization and nuclear entry. The receptor complex binds to the HRE site after activation to control gene transcription by either promoting or blocking target gene expression. The transcriptional machinery recruitment depends on the synergistic action between Activation Function 1 (AF-1) and AF-2 (AF-2) domains. The recruitment of co-activator protein complexes enables chromatin remodeling and pre-initiation complex assembly (117). The process leads to prolonged genomic responses that develop at a slower rate.

4.4.3. REGULATION OF STEROIDOGENESIS

The expression of steroidogenic enzymes depends on specific transcription factors which control their gene activation. The Steroidogenic Factor 1 (SF-1) shows high expression levels in tissues that produce steroids including the adrenal glands and gonads (118). SF-1 is a critical transcriptional regulator for several key steroidogenic enzymes by direct binding to their promoters.

4.4.4. RAPID NON-GENOMIC ACTION (FAST PATHWAY)

Steroid hormones produce fast non-genomic effects through a separate pathway which operates independently of gene transcription and protein synthesis. The "fast pathway" of steroid hormone action depends on specific nuclear receptors (ERα, GR, PR, etc.) which reside near the plasma membrane (119). The membrane-associated receptors activate signaling pathways through different mechanisms which include G-protein-coupled receptors (GPCRs) and Src kinase activation and ion channel modifications. The rapid effects of estrogen trigger changes in intracellular calcium (Ca2+) levels and trigger immediate activation of Mitogen-Activated Protein Kinase/Extracellular-signal-Regulated Kinase (MAPK/ERK) pathways (119). The non-genomic effects of steroid hormones enable immediate cellular responses which can interact with the slow genomic pathway to achieve precise cellular outcomes.

4.5. REGULATION AND SYNTHESIS CONTROL OF STEROID HORMONES

The delicate balance of steroid hormone concentrations is maintained by sophisticated, organ-specific endocrine axes that govern the synthesis, secretion, and concentration of each distinct class (55).

4.5.1. GLUCOCORTICOIDS: THE HYPOTALAMIC-PITUITARY-ADRENAL (HPA) AXIS AND CIRCADIAN RHYTHM

The hypothalamic-pituitary-adrenal (HPA) axis controls glucocorticoid secretion through its negative feedback mechanism which operates at multiple hierarchical levels. The suprachiasmatic nucleus (SCN) sends circadian signals to the hypothalamus which releases corticotropin-releasing hormone (CRH) to activate anterior pituitary ACTH production (120) (121). ACTH binds to melanocortin-2 receptors (MC2R) on adrenal cortical cells, activating the cAMP–PKA pathway and stimulating StAR-dependent cholesterol transport and the expression of steroidogenic enzymes (120) (121). Once secreted, cortisol binds to glucocorticoid receptors (GRs), ubiquitously expressed transcription factors that modulate the expression of genes involved in glucose metabolism, inflammation, and cell survival (120). Cortisol also binds with lower affinity to mineralocorticoid receptors (MRs), particularly in the kidney, though local inactivation of cortisol by 11β-hydroxysteroid dehydrogenase type 2 (11β-HSD2) prevents inappropriate MR activation (120) (121). Cortisol exerts negative feedback at both hypothalamic and pituitary levels, suppressing CRH and ACTH release and thus preventing excessive hormone accumulation (121). The HPA axis maintains adaptive stress responses through its feedback mechanism which prevents harmful hormone exposure However, chronic stress or dysregulation of the HPA axis can result in maladaptive hypercortisolemia or hypocortisolemia, with important metabolic, immune, and neuropsychiatric consequences (121) (122). Importantly, HPA axis activity is deeply shaped by circadian rhythmicity. Cortisol levels follow a robust daily pattern characterized by the Cortisol Awakening Response (CAR), a sharp surge within 30-45 minutes after awakening, followed by a progressive decline across the day and a nadir in the late evening (123). This rhythm is driven by SCN output and supported by intrinsic adrenal clocks, ensuring that glucocorticoid release is tightly aligned with behavioral cycles of activity, feeding, and rest (124). Through these oscillatory dynamics, glucocorticoids synchronize peripheral clocks in metabolic tissues with the central circadian pacemaker (125) (126). This coordination allows optimal timing of gluconeogenesis, lipid metabolism, and energy mobilization in anticipation of the active phase of the day (124) (125). Moreover, glucocorticoids exert crucial immunomodulatory functions, promoting immune readiness during the morning surge while suppressing excessive inflammation during the nocturnal decline (124) (127). Disruption of this rhythm, as observed in shift work, chronic stress, depression, or metabolic disorders, is strongly associated with cardiometabolic disease, immune dysfunction, and accelerated aging (124) (127).

4.5.2. MINERALOCORTICOIDS: THE RENIN-ANGIOTENSIN-ALDOSTERONE SYSTEM (RAAS)

The principal mineralocorticoid in humans is aldosterone, synthesized exclusively in the *zona glomerulosa* of the adrenal cortex. Its production relies on a specialized enzymatic machinery that includes CYP11A1 for cholesterol side-chain cleavage, CYP21A2 for 21-hydroxylation, and most critically CYP11B2 (aldosterone synthase), which catalyzes the final steps unique to aldosterone biosynthesis (128). Unlike glucocorticoids, mineralocorticoids secretion is largely independent of the HPA axis and is predominantly controlled by the Renin-Angiotensin-Aldosterone System (RAAS) together with plasma potassium concentration (129). RAAS is initiated when reduced renal perfusion pressure, sympathetic nervous activation, or decreased sodium delivery to the distal tubule stimulates juxtaglomerular cells of the kidney to release renin. Renin cleaves circulating angiotensinogen into angiotensin I, which is subsequently converted to angiotensin II by angiotensin-converting enzyme (ACE). Angiotensin II exerts potent trophic and secretory effects on *zona glomerulosa* cells, stimulating aldosterone biosynthesis through calcium-dependent pathways and upregulation of CYP11B2 expression. In parallel, elevated extracellular potassium directly depolarizes glomerulosa cells, providing another strong physiological signal for aldosterone secretion. Although ACTH can acutely increase aldosterone release, its role is minor and transient compared to RAAS and potassium (128) (129). Aldosterone acts primarily by binding to the MR, highly expressed in the distal nephron, colon, salivary glands, and cardiovascular tissues. Through MR activation, aldosterone promotes transcription of genes encoding ion transporters such as ENaC and Na^+/K^+-ATPase, thereby enhancing sodium reabsorption and potassium excretion. Because circulating cortisol can bind MR with high affinity, specificity is ensured by the local activity of 11β-hydroxysteroid dehydrogenase type 2 (11β-HSD2), which inactivates cortisol to cortisone in aldosterone-sensitive tissues (130). Like glucocorticoids, aldosterone secretion also displays a circadian rhythm, with levels peaking in the early morning, though the pattern is more variable and heavily dependent on RAAS activity and posture (58). Dysregulation of mineralocorticoid production has important clinical consequences: primary hyperaldosteronism (due to aldosterone-producing adenoma or bilateral adrenal hyperplasia) is a leading cause of secondary hypertension, whereas secondary hyperaldosteronism occurs in conditions with chronic RAAS activation such as heart failure, cirrhosis, or nephrotic syndrome.

4.5.3. SEX STEROID HORMONES: BIOSYNTHESIS, REGULATION, AND PHYSIOLOGICAL ROLES

Sex steroid hormones, including androgens, estrogens, and progesterone, constitute a major class of steroid hormones. Their biosynthesis begins with the conversion of cholesterol to pregnenolone, catalyzed by the mitochondrial cytochrome P450scc (CYP11A1) and regulated by the steroidogenic acute regulatory protein (StAR). Subsequent enzymatic steps involving 3β-hydroxysteroid dehydrogenase, 17α-hydroxylase/17,20-lyase (CYP17A1), and aromatase define the synthesis of progesterone, androgens (e.g., testosterone, dihydrotestosterone), and estrogens (mainly estradiol) in gonads, adrenal glands, and, during pregnancy, the placenta (131). In males, Leydig cells in the testes represent the primary site of testosterone production, whereas in females, estrogens and progesterone are secreted mainly by ovarian follicles and the corpus luteum, with additional synthesis in the placenta during gestation. The adrenal *zona reticularis* contributes to circulating androgens such as dehydroepiandrosterone (DHEA), DHEA-sulphate and androstenedione, which can be further converted to active sex steroids in peripheral tissues (132). The secretion of sex steroids by the gonads is tightly regulated by the hypothalamic-pituitary-gonadal (HPG) axis. Pulsatile release of gonadotropin-releasing hormone (GnRH) from the hypothalamus stimulates the anterior pituitary to release luteinizing hormone (LH) and follicle-stimulating hormone (FSH), which in turn act on gonadal cells to drive steroidogenesis. In Leydig cells, LH activates cAMP/PKA signaling to promote cholesterol transport via StAR, the rate-limiting step in steroid hormone biosynthesis. In ovarian granulosa and theca cells, coordinated action of LH and FSH regulates the production of estrogens and progesterone across the menstrual cycle (133). Importantly, the temporal dynamics of sex steroid secretion exhibit both pulsatility and circadian modulation. Testosterone levels in men display a robust circadian rhythm, peaking in the early morning hours and declining throughout the day, a rhythm that is partially dependent on sleep–wake cycles and GnRH/LH pulsatility. Estrogen and progesterone secretion, although primarily cyclical across the menstrual cycle, also show daily fluctuations influenced by hypothalamic input and peripheral metabolic cues (134). Such rhythmicity ensures synchronization of reproductive function with broader metabolic and behavioral states. Sex steroid hormones exert their functions primarily through intracellular nuclear receptors: AR, estrogen receptors α and β (ERα/ERβ), and PRs A and B (PRA/PRB). Once bound to their ligands, these receptors act as transcription factors regulating gene expression, while additional non-classical mechanisms involve membrane-associated receptors such as GPER1 and ZIP9, mediating rapid signaling

cascades (135) (136). Notably, progesterone receptors are widely distributed across reproductive and non-reproductive tissues, highlighting pleiotropic roles beyond reproduction, including in the nervous, endocrine, and immune systems (137). Functionally, sex steroids regulate reproductive development and fertility but also extend their influence on multiple physiological systems. Testosterone and its metabolite dihydrotestosterone direct male sexual differentiation, spermatogenesis, and maintenance of secondary sexual traits, while also modulating muscle metabolism, bone homeostasis, and neurocognitive processes (134) (132). Estrogens, conversely, are essential for female reproductive function, but they also regulate cardiovascular physiology, bone density, and neuroprotection, with dysregulation implicated in diverse pathologies (136). Progesterone, traditionally associated with pregnancy maintenance, also exerts neuroprotective and immunomodulatory functions, emphasizing its broad biological relevance (133). Altogether, sex steroid hormones are versatile regulators linking reproductive biology to systemic physiology, with their biosynthesis, secretion, and receptor-mediated actions providing a complex framework that integrates endocrine, metabolic, and neural functions.

4.6. ADVANTAGES OF LC-MS/MS OVER IMMUNOASSAY FOR STEROID ANALYSIS

Immunoassays (IA) represent the traditional analytical approach for quantifying hormones, such as steroids, in clinical practice. These methods rely on the selective binding between an antibody and the target analyte, with detection based on colorimetric, chemiluminescent, or fluorescent signals. The combination of straightforward operation and affordable prices and automated features have established immunoassays as the standard for endocrine testing during the last few decades (138). However, immunoassays suffer from well-documented analytical limitations, including cross-reactivity with structurally related compounds, susceptibility to matrix effects, and restricted dynamic range. These issues are particularly problematic at low concentrations (e.g., testosterone in women and children, adrenal precursors, or estrogens in men and postmenopausal women), where antibody specificity is often insufficient (138) (139). By contrast, LC-MS/MS offers unmatched specificity, achieved through chromatographic separation coupled with selective mass transitions, minimizing interference and enabling resolution of isobars and isomers (140). Furthermore, it supports multiplexing, i.e., the simultaneous measurement of dozens of analytes in a single run, enabling comprehensive

steroid panels or targeted metabolomics assays (138). When paired with stable isotope-labeled IS, LC-MS/MS provides robust quantitation across wide concentration ranges, reducing matrix effects and variability. Moreover, IA are available for a tiny number of molecules, in contrast to LC-MS/MS, where the method allows flexible expansion of analytical panels to include new endogenous metabolites or exogenous drugs without the need for new antibodies, making it a versatile and future-proof technology (138).

5. METABOLOMICS

Metabolomics is the extensive analysis of all metabolites in a biological system (141). Metabolites have a crucial role in cellular energy production by providing substrates for glycolysis, fermentation, and oxidative phosphorylation. Additionally, they function as building blocks for large biomolecules and cell membranes, as well as signaling messengers. A biological sample can contain thousands of metabolites, covering a diverse range of biochemical classes, such as amino acids, biogenic amines, organic acids, nucleotides, and lipids (142). The alteration in metabolite levels is deeply linked to different pathologies, allowing the investigation of disease etiology, status, therapeutic response, and biological process changes (143). The metabolome, defined as the complete set of metabolites within a biological system or sample, is shaped by both intrinsic and extrinsic factors. On the one hand, it reflects the underlying genomic and cellular activity unique to everyone; on the other, it is strongly influenced by environmental inputs such as pharmacological treatments, dietary habits, lifestyle, and microbiome. By characterizing this complex and dynamic metabolic network, metabolomics enables the detection of variations in metabolite levels and compositions, thereby uncovering specific molecular phenotypes that mirror the organism's physiological condition or pathological alterations (141) (144). Analytical approaches for metabolomics investigations include, but are not limited to, 1H and 13C nuclear magnetic resonance (1H- and 13C-NMR) spectroscopy, gas chromatography-mass spectrometry (GCMS), gas chromatography-flame ionization detection (GC-FID), direct infusion-mass spectrometry (DI-MS), and liquid chromatography-mass spectrometry (LC-MS) (145).

5.1. TARGETED AND UNTARGETED METABOLOMICS

Metabolomic strategies can be divided into two distinct approaches, untargeted and targeted, each with their own advantages and disadvantages (146). Untargeted metabolomics is a high-throughput approach that measures all detectable metabolites in a given sample, including unknown analytes. It is typically performed using LC-MS or gas chromatography-mass spectrometry (GC-MS) platforms, while nuclear magnetic resonance (NMR) spectroscopy can also be employed when broad structural information is desired. In broad terms, metabolomics is employed for two main investigative strategies: metabolite fingerprinting and metabolite

profiling. The fingerprinting approach focuses on the rapid characterization of samples through global patterns in metabolite signals, without requiring prior identification of individual compounds. Conversely, metabolite profiling targets specific metabolites, quantifying them individually and enabling the detection of those whose concentrations differ significantly across experimental or clinical groups (147). Because of its broad coverage, untargeted metabolomics typically requires integration with advanced chemometric tools, such as multivariate statistical analysis (principal component analysis (PCA) and partial least squares-discriminant analysis, PLS-DA), to condense the vast datasets produced into a smaller number of interpretable signals (145). These signals must then be annotated through computational libraries or experimental validation, followed by definitive identification using analytical chemistry approaches. This strategy provides a powerful avenue for novel biomarker and pathway discovery, since the scope of detection is limited only by sample preparation strategies and by the sensitivity and specificity of the analytical platform employed. Nevertheless, untargeted metabolomics presents significant challenges, including the time- and protocol-intensive nature of data processing, the complexity of characterizing previously unknown metabolites, the dependency on the intrinsic analytical window of the method, and the inherent bias toward detecting the most abundant molecular species (145). On the other hand, targeted metabolomics focuses on the measurement of specific, chemically defined and biochemically annotated metabolites. It is most commonly performed using LC-MS/MS in multiple reaction monitoring (MRM) mode, although GC-MS and capillary electrophoresis-mass spectrometry (CE-MS) are also used for specific classes of metabolites. By employing IS, analyses can be performed in either a quantitative or semi-quantitative fashion (145). This approach leverages the extensive knowledge of metabolic enzymes, their kinetics, and the biochemical pathways in which they are involved. A major advantage of targeted strategies is the possibility to tailor sample preparation to the metabolites of interest, thereby minimizing the predominance of highly abundant compounds and avoiding matrix effects. Moreover, because the analytes under investigation are explicitly defined, analytical artifacts are less likely to propagate into downstream analyses. Studying predefined panels of metabolites can also uncover novel relationships between them, offering new insights into physiological and pathological states.

***Table 2**: Comparison between untargeted and targeted metabolomics approaches.*

Feature	Untargeted metabolomics	Targeted metabolomics
Objective	Comprehensive detection of all measurable metabolites, including unknowns	Quantification of predefined, chemically characterized metabolites
Scope	Broad, hypothesis-generating	Focused, hypothesis-driven
Data output	Relative abundances, global metabolic patterns	Absolute or semi-quantitative concentrations
Strengths	Discovery of novel biomarkers and pathways Broad coverage of metabolic space	High specificity and sensitivity Accurate quantification using internal standards. Reduced influence of matrix effects and abundant molecules
Challenges	Data processing is complex and time-consuming. Difficult identification of unknown metabolites Bias toward abundant compounds	Restricted to known metabolites Requires prior biochemical knowledge of pathways
Typical applications	Disease classification, biomarker discovery, metabolic phenotyping	Clinical diagnostics, validation of biomarkers, pathway-focused studies

5.2. CLASSES OF METABOLITES OF INTEREST IN METABOLOMICS

Among the numerous metabolites present in plasma and other biological tissues, certain classes represent the main indicators of physiological and pathological processes. In human metabolomics, these molecules are often studied for their biological and clinical relevance. The most important classes considered in this work include amino acids, biogenic amines, acylcarnitines, glycerophospholipids, and sphingomyelins.

5.2.1. AMINO ACIDS

Amino acids function as protein building blocks because they contain two functional groups which include an amino group (-NH_2) and a carboxyl group (-COOH). The α-carbon atom in all common amino acids bonds to four distinct groups which include a carboxyl group and an amino group and a side chain (R group) and a hydrogen atom (113). The chemical properties and biological functions of amino acids depend on their R group structure (**Figure 9**). The α-

carbon atom functions as a chiral center which produces two non-superimposable mirror images known as enantiomers except for glycine because it has a hydrogen atom as its R group. The human body contains 20 proteinogenic amino acids which exist only in the L-configuration and scientists divide them into two categories based on their ability to be synthesized endogenously: essential amino acids (histidine, isoleucine, leucine, lysine, methionine, phenylalanine, threonine, tryptophan, valine) and non-essential amino acids (alanine, arginine, asparagine, aspartate, cysteine, glutamate, glutamine, glycine, proline, serine, tyrosine) (113). The occurrence of D-amino acids remains scarce because they appear in specific peptides and bacterial cell walls and molecules with antibiotic properties. Amino acids contribute to energy metabolism through oxidative degradation, particularly under three conditions: during normal protein turnover, when dietary protein exceeds biosynthetic needs, or during fasting and uncontrolled diabetes. In these situations, amino acids lose their amino groups and are converted into α-keto acids, forming carbon skeletons that are oxidized to CO_2 and H_2O or transformed into gluconeogenic intermediates. The breakdown process directs amino acids into central catabolic pathways which enable them to generate energy when required.

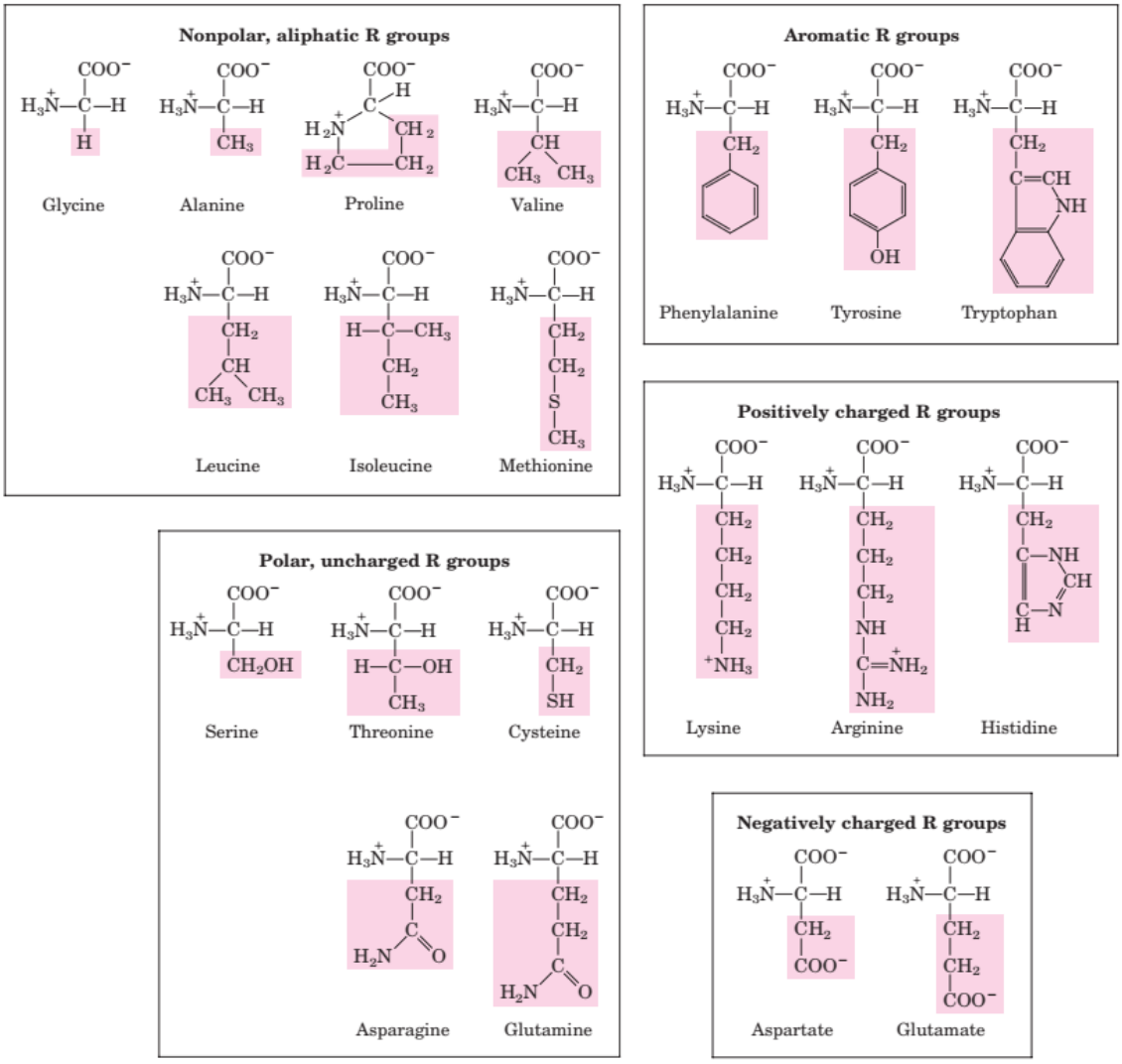

***Figure 9**. Structure of amino acids. Reproduced from: David L Nelson, Michael M Cox, Lehninger Principles of Biochemistry, 2017 (113).*

5.2.2. BIOGENIC AMINES

Biogenic amines are biomolecules containing one or more amino (-NH_2) groups, primarily produced through the oxidative decarboxylation of amino acids, but also via amination and transamination of aldehydes and ketones. Their structures can be aliphatic, as in putrescine; aromatic, as in tyramine; or heterocyclic, as in histamine. Biogenic amines can also be classified according to the number of amino groups they contain: phenylethylamine (PEA) and tyramine are monoamines, cadaverine and putrescine are diamines, and spermine and spermidine are classified as polyamines (148). In some contexts, di-amines are also included within the polyamine category.

The formation of these compounds occurs through specific biosynthetic pathways which are shown in **Figure 10**. Tyrosine produces a family of catecholamines, including dopamine, norepinephrine, and epinephrine. Glutamate is converted by glutamate decarboxylase into γ-aminobutyric acid (GABA), an inhibitory neurotransmitter. The neurotransmitter serotonin originates from tryptophan which serves as its precursor molecule. The decarboxylation of histidine produces histamine, which is released in substantial amounts during allergic responses. Furthermore, polyamines such as spermine and spermidine are derived from proline, glutamine, methionine, and arginine through a series of reactions, with the rate-limiting step catalyzed by ornithine decarboxylase.

Biogenic amines are crucial to multiple physiological functions, and disturbances in their metabolism can have profound effects on homeostasis (149). They serve as precursors of hormones, alkaloids, proteins, and nucleic acids, and function as a source of nitrogen as well. Based on their physiological effects in humans, biogenic amines can be classified as psychoactive or vasoactive: the former are involved in nervous system function, as in histamine, putrescine, and cadaverine, while the latter influence vascular processes, as in tyramine, tryptamine, and β-phenylalanine. Histamine interacts with target cells via receptors such as H1, H2, and H3, which belong to the G protein-coupled receptor family. The binding of histamine to these receptors triggers vasodilation and smooth muscle contraction which starts inflammatory responses. Putrescine is responsible for the synthesis of spermine and spermidine and is primarily produced from arginine metabolism in some microorganisms and plants. Polyamines are low molecular weight, positively charged molecules that act as mediators of various biological processes, including cell growth, oxidative stress response, and cortisol-induced inflammatory responses. The four polyamines putrescine, cadaverine, spermine and spermidine function as cell growth promoters and differentiation agents while controlling gene expression. The molecules interact with multiple sites on DNA, RNA, nucleotides, phospholipids, and proteins to control signal transduction through DNA condensation and gene expression regulation. The proper maintenance of polyamine levels inside cells depends on their biosynthesis and catabolism pathways and cellular homeostasis mechanisms. The proper development of the gastrointestinal tract depends on dietary polyamines which also help prevent food allergies. The effects of other biogenic amines in humans are less well understood, and current knowledge is primarily derived from their study as food contaminants.

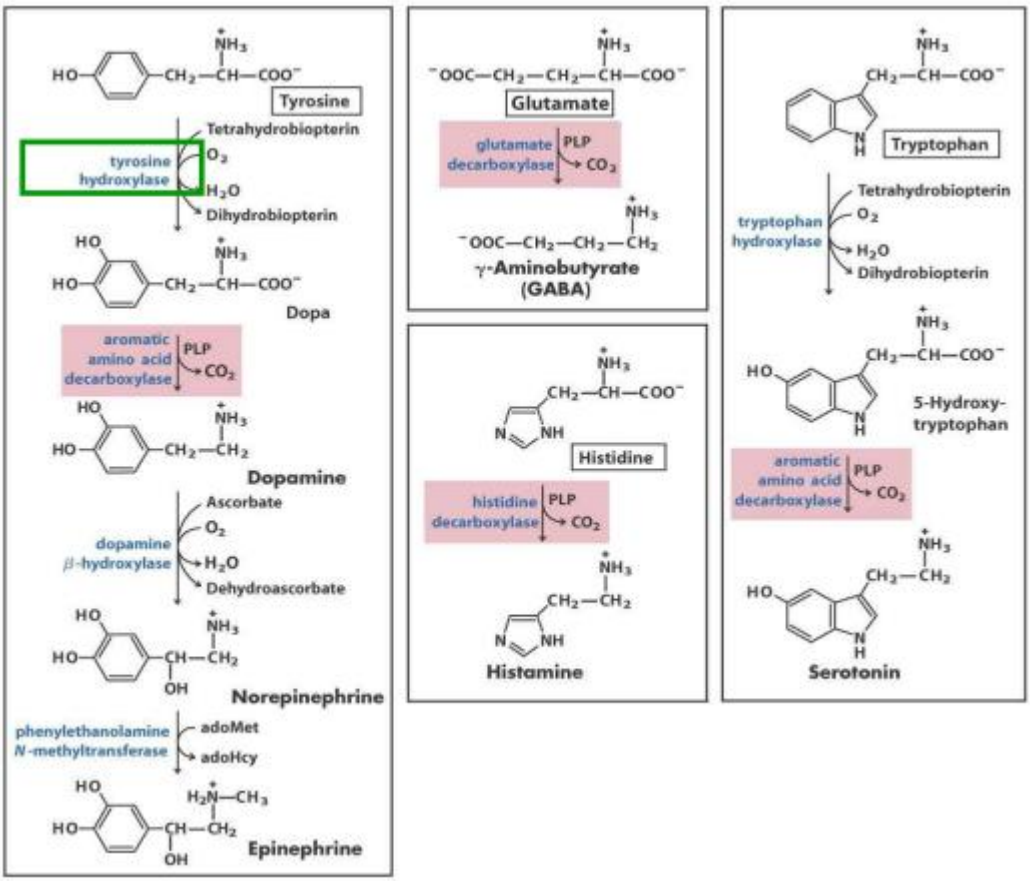

Figure 10. *Synthetic processes of the main biogenic amines. Reproduced from: David L Nelson, Michael M Cox, Lehninger Principles of Biochemistry, 2017 (113).*

5.2.3. ACYLCARNITINES

Acylcarnitines are esters formed by the conjugation of fatty acids (acyl groups) with L-carnitine, and they play a significant role in energy metabolism. The main function of acylcarnitines involves transporting acyl groups from cytosol into mitochondrial matrices where β-oxidation produces ATP (150) (151). Research conducted during the last few decades has revealed that acylcarnitines perform multiple biological functions beyond their traditional energy metabolism role. In particular, long-chain acylcarnitines have been implicated in insulin resistance and cardiovascular disease, and they are increasingly recognized as biomarkers in both clinical and research contexts (152) (153) (154).

Acylcarnitine plasma measurements serve as a standard tool for newborn screening to identify fatty acid oxidation disorders and other metabolic disorders (155) (156). Metabolomics uses acylcarnitine profile changes to identify disease conditions and nutritional imbalances which

make them useful for diagnosis and prognosis. The classification of acylcarnitines depends on their fatty acyl chain length which follows the same system as fatty acid classification (**Figure 11**): short-chain (C2-C5), medium-chain (C6-C12), long-chain (C13-C20), and very long-chain (>C21) species (157) (158) The classification system for acylcarnitines includes saturation degree (saturated vs. unsaturated) and configuration (cis/trans) and functional substitution types such as hydroxyl and carboxyl groups. The structurally diverse family of acylcarnitines includes branched dicarboxylic acylcarnitines and hydroxylated unsaturated acylcarnitines as well as simple acylcarnitines like acetyl-, propionyl-, and palmitoyl-carnitine which make up the majority of the acylcarnitine pool. Biosynthetically, carnitine acyltransferase system produces acylcarnitines through its ability to transfer activated acyl-CoA groups onto L-carnitine. The three mechanisms that control carnitine homeostasis include: endogenous biosynthesis, dietary uptake and renal reabsorption through the organic cation/carnitine transporter 2 (OCTN2) (159) (160) (161). Importantly, therapeutic use of carnitine availability modulation helps decrease acylcarnitine levels in metabolic disorders.

Figure 11. *Representative structures of various acylcarnitine classes. Reproduced from Dambrova M. et al, Acylcarnitines: Nomenclature, Biomarkers, Therapeutic Potential, Drug Targets, and Clinical Trials, Pharmacol Rev, 2022 (162).*

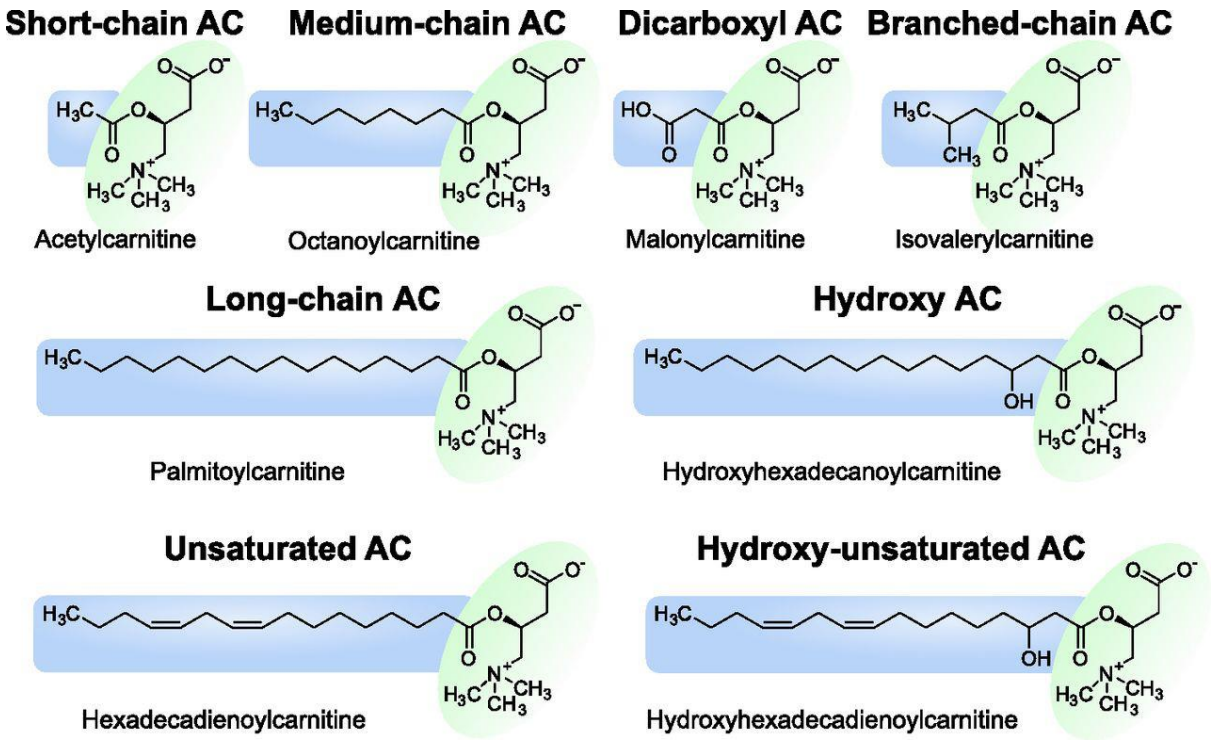

5.2.4. GLYCEROPHOSPHOLIPIDS

Glycerophospholipids (GPLs) are the most abundant lipids in biological membranes, accounting for nearly half of membrane lipid mass (163) (164). For example, in human erythrocyte membranes, GPLs constitute over 43% of total lipids, with phosphatidylcholine (PC, ~17%), phosphatidylethanolamine (PE, ~18%), phosphatidylserine (PS, ~7%), and phosphatidylinositol (PI, ~1%), followed by cholesterol (~23%), sphingomyelin (~18%), and minor components (165). However, in general, PC represents 45-55% of total cellular GPLs, PE contributes 17-25%, and PS ~5%, whereas PI and its phosphorylated derivatives vary widely between 2% and 20%, depending on the tissue and cellular context (165). Structurally, the glycerol backbone serves as the foundation for these amphiphilic molecules which organize their structure. The sn-1 and sn-2 positions of GPLs receive fatty acid esterification while the sn-3 carbon links to a phosphate group that binds different polar head groups (166). The main GPL classes derive their names from their head group composition which includes phosphatidic acid (PA) and PC and PE and PS and PI and cardiolipin (CL). GPLs containing a single fatty acyl chain are referred to as lysophospholipids (LPLs). The shape of GPL molecules depends on the size relationship between their head group and acyl chain segments which produces cylindrical shapes for PC and conical shapes for PA, PE, and CL and inverted conical shapes for lyso-GPLs and PI and its derivatives. These structural differences directly affect membrane properties such as curvature, packing, fluidity, and stiffness. Diverse types of glycerophospholipids can be observed in **Figure 12**. Beyond their structural role in membranes, GPLs are highly dynamic and participate in numerous cellular processes. They regulate vesicle trafficking, neurotransmission, and signaling through G protein-coupled receptors (GPCRs) and ion channels (167). They are also key mediators in calcium homeostasis, protein translocation, apoptosis, inflammation, and neurogenesis. Enzymatic cleavage of head groups by phospholipases (C or D) generates bioactive lipid intermediates, such as diacylglycerol (DAG) or PA, whichfunction ass potent second messengers (166). The biosynthesis of GPLs occurs across multiple cellular compartments, including the endoplasmic reticulum (ER), Golgi apparatus, and mitochondria. Of particular importance are mitochondria-associated membranes (MAMs), specialized contact sites between the ER and mitochondria that coordinate lipid exchange and signaling (166). GPLs also undergo continuous remodeling through cycles of fatty acid hydrolysis and re-esterification, processes that diversify acyl chain composition and fine-tune membrane biophysical properties. Finally, although GPLs appear structurally simple,

their stereochemistry and the chemical lability of phosphate esters make them challenging to study. Spontaneous acyl migration between the sn-1 and sn-2 positions can occur, complicating both synthetic strategies and analytical interpretation. Despite these challenges, GPLs remain a central focus in lipidomics, as their compositional changes are tightly linked to alterations in cellular physiology and pathology.

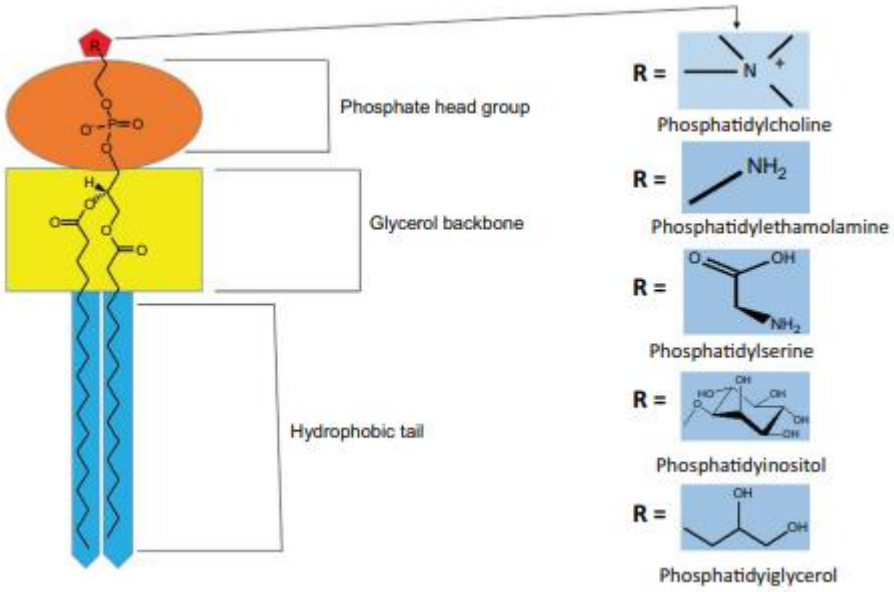

***Figure 12**. Diverse types of glycerophospholipids. Reproduced from: Mukherjee P.K. et al, Chapter 4 - Phospholipid complexation: A versatile technique for delivery of phytomedicine, Evidence-Based Validation of Herbal Medicine (Second Edition), 2022 (168).*

5.2.5. SPHINGOMYELINS

Sphingomyelins (SMs) are a class of sphingolipids widely present in the plasma membranes of mammalian cells where they play major structural and functional roles. One of their defining structural features is the backbone: an N-acyl-D-erythro-sphingosyl moiety bound to a phosphocholine head group. The N-acyl chain lengths typically range between 16-24 carbons and are often saturated; some monounsaturated chains (e.g., 24:1) also occur (169) (170) (171). Examples of types of sphingomyelins can be observed in **Figure 13**. DiA key property of sphingomyelins, distinguishing them from many glycerophospholipids, is their capacity for hydrogen bonding. Both intra- and intermolecular hydrogen bonds are present: for example, the 3-hydroxyl group of the long-chain base can form bonds with phosphate oxygens of the head group, and the amide NH may also be involved in intermolecular interactions. These hydrogen bonding capabilities contribute significantly to membrane stability, ordering, and

interaction with cholesterol and ceramide (169) (171). The molecular structure of SMs (e.g., saturation, chain length mismatch between sphingosine base and N-acyl chain, hydroxylation or branching of the acyl chains) strongly influences membrane biophysical properties. For instance, SMs with saturated and long acyl chains tend to increase membrane order, elevate the melting temperature (Tm), and promote formation of liquid-ordered domains with cholesterol. In contrast, chain mismatch (one chain significantly longer than the other), unsaturation, or presence of hydroxyl groups reduce packing efficiency, influence interdigitation between leaflets, and modulate the dynamics of bilayer fluidity (171) (172) (173) . Functionally, SMs contribute not only to membrane structure, influencing fluidity, membrane thickness, barrier properties, and curvature, but also to cell signaling. Their arrangement affects the formation of lipid rafts (membrane microdomains enriched in cholesterol and sphingolipids), which serve as platforms for receptor signaling, endocytosis, and protein sorting. SM metabolism (via sphingomyelinases and sphingomyelin synthases) yields bioactive lipids such as ceramide, which influence processes like apoptosis, growth arrest, inflammation, and membrane trafficking (174) (170) (169). In summary, subtle differences in sphingomyelin molecular structure (head group interactions, acyl chain length/unsaturation/match, hydroxylation) are directly translated into functional consequences at the membrane level. These structure-function relationships make SMs a critical class of lipids in studies of membrane biology, disease states, and potentially, metabolomic profiling in health and pathologies involving membrane dysfunction (171) (169).

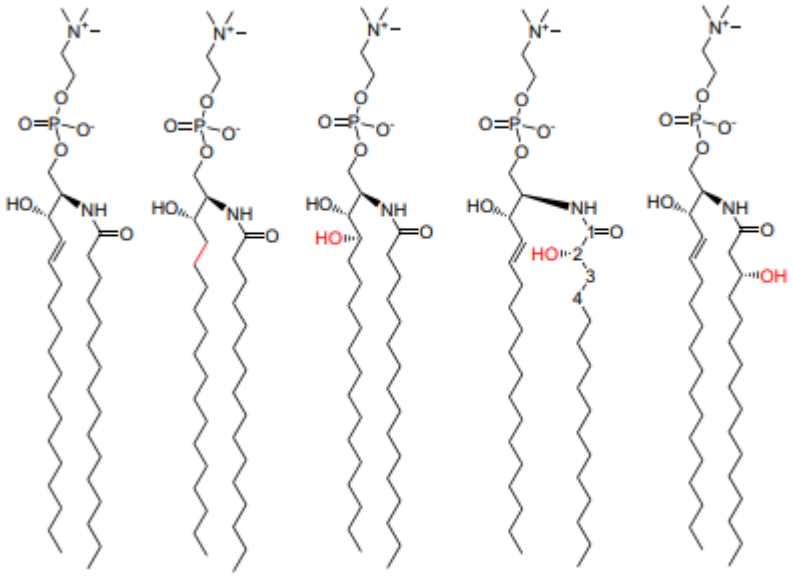

Figure 13. *Examples of types of sphingomyelins. Reproduced from: Peter Slotte J, Molecular properties of various structurally defined sphingomyelins -- correlation of structure with function, Prog Lipid Res., 2013 (169).*

5.3. APPLICATION OF LC-MS/MS IN STEROIDOMICS AND METABOLOMICS

LC-MS/MS has become a pillar technology in endocrinology because of its ability to provide high analytical specificity and multiplexing capacity compared to traditional immunoassays. The clinical use of LC-MS/MS technology enables healthcare providers to diagnose and track various endocrine disorders through adrenal and gonadal steroid measurements in patients with congenital adrenal hyperplasia and polycystic ovary syndrome and primary aldosteronism and Cushing's syndrome and sex development disorders (175) (176). The multiplexed assay technology enables researchers to measure twenty or more steroids at once which generates complete hormonal profiles for better disease identification and treatment planning (177). Beyond classical endocrinology, LC-MS/MS also plays an expanding role in metabolomics. The targeted metabolomic platforms measure steroids, amino acids, acylcarnitines, bile acids and additional metabolites during a single analytical run to show complete metabolic pathway information (175). In the context of steroidomics, technology enables the characterization of subtle alterations in steroid biosynthesis and clearance under both physiological and pathological conditions (176). Recent advancements have further demonstrated the feasibility of combining LC-MS/MS with alternative and convenient sampling strategies such as dried blood spots (DBS), enabling minimally invasive, high-throughput monitoring of steroid profiles in newborns, adults, and patients with adrenal or gonadal disorders (178) (179). The integration of LC-MS/MS in endocrinology and metabolomics research provides unique opportunities for the simultaneous investigation of endocrine axes and metabolic pathways. This approach could not only improve diagnostic accuracy in endocrine diseases but also support the discovery of novel biomarkers, the exploration of circadian rhythmicity of hormones, and the development of precision medicine strategies.

6. AIM OF THE THESIS

Steroid hormones are key regulators of metabolism, immune response, stress adaptation, and reproduction. Measuring their circulating concentrations is crucial for untangling endocrine pathophysiology and for diagnosing and managing disorders of the hypothalamic-pituitary-adrenal (HPA) axis, such as Cushing's syndrome, adrenal insufficiency, and mild autonomous cortisol secretion (MACS). Alongside endogenous steroids, synthetic glucocorticoids rank among the widely prescribed therapeutic agents worldwide prized for their anti-inflammatory and immunosuppressive properties. Nevertheless, their pharmacokinetics and pharmacodynamics remain highly variable among individuals, and long-term exposure can lead to metabolic complications resembling endogenous hypercortisolism. Traditional steroid quantification relies on immunoassays performed on serum or plasma samples obtained by venipuncture. Although these methods are widely used, their specificity is hampered by antibodies that often cross-react among structurally similar steroids. In addition, repeated venous sampling is invasive and impractical for dynamic investigations such as the circadian rhythm assessment. Dried blood spot (DBS) sampling represents a valuable alternative: it requires only a few drops of capillary blood collected by finger prick, allows easy storage and transport, and can be self-performed by the patient. However, the use of DBS for steroid profiling remains technically challenging, as it demands overly sensitive and selective analytical procedures to overcome the small sample volume, matrix interferences, and the presence of isomeric compounds. Liquid chromatography coupled with tandem mass spectrometry (LC-MS/MS) has emerged as the gold standard for steroid analysis, providing high specificity, sensitivity, and multiplexing capacity. Yet, few validated LC-MS/MS methods exist for the comprehensive quantification of both endogenous and exogenous steroids in DBS, limiting their clinical translation and use in home-based monitoring.

Metabolomics has gained increasing attention as a powerful approach for identifying molecular signatures of disease within the framework of predictive, preventive, personalized, and participatory medicine (180). Advances in LC-MS platforms now allow for broad metabolite coverage with high analytical precision. Nevertheless, most metabolomic investigations still rely on serum or plasma, while DBS, despite its advantages, has been marginally explored for global metabolic profiling. Establishing the equivalence between DBS and conventional matrices is therefore essential to extend metabolomic applications to minimally invasive settings. Alterations in cortisol secretion deeply affect systemic metabolism. Chronic

hypercortisolism, as observed in Cushing's syndrome or MACS, is associated with insulin resistance, dyslipidemia, protein catabolism, and increased cardiovascular risk. On the other hand, adrenal insufficiency requires life-long glucocorticoid replacement therapy (GRT), and it is often associated with increased risk of adrenal crisis and cardiometabolic consequences, since several studies have observed that continuous glucocorticoid therapy fails to mimic physiologic fluctuation, determining either over- and under-exposure in different part of the day (181). Recent studies have demonstrated circadian oscillations in several metabolite classes, including amino acids, acylcarnitines, and phospholipids, reflecting the rhythmic control of metabolic pathways (182). Moreover, in pathological states characterized by chronic cortisol excess, such as Cushing's syndrome and mild autonomous cortisol secretion (MACS), broad alterations in the circulating metabolome have been reported. In particular, member of the Endocrinology research group of the University of Bologna demonstrated that patients with hypercortisolism exhibit specific metabolic abnormalities in fasting serum samples, including impaired protein synthesis, incomplete β-oxidation of fatty acids, and dysregulated polyamine metabolism, the extent of which correlates with the severity of hypercortisolism (183). These findings point to a state of metabolic inflexibility, independent of diabetes status, and highlight the profound systemic impact of glucocorticoid excess. However, despite these insights, it remains unclear whether, and to what extent, the disruption of cortisol circadian rhythmicity is associated with corresponding alterations in the circadian fluctuation of the circulating metabolome.

Based on these considerations, the present PhD project aimed to develop and validate LC-MS/MS methods to be applied to DBS sampling for the targeted quantification of a vast panel of endogenous steroid hormones and metabolites, exogenous steroid drugs, and a broad panel of metabolites from amine and lipid classes, and to apply these methods to the characterization of the circadian fluctuations of the steroidome and of the metabolome in health and in conditions of disrupted cortisol secretion. This integrated analytical and translational approach sought to establish DBS as a reliable microsampling tool for both steroidomic and metabolomic investigations, thereby enabling minimally invasive monitoring of hormonal and metabolic dynamics in endocrine disorders.

As a complementary component of the PhD work, a research period was conducted at the Biomedical and Metabolomics Analysis (BMA) Group at the University of Geneva (UNIGE), with the goal of broadening analytical and methodological expertise in steroidomics. During this stay, the BMA's LC-MS/MS method for up to 200 steroids was applied to DBS samples

from healthy subjects to assess the feasibility of capturing circadian steroid fluctuations through minimally invasive sampling. Furthermore, a dedicated LC-MS/MS method for ultra-sensitive quantification of estrogens in serum was developed to overcome analytical challenges associated with low abundance, matrix effects, and limited ionization efficiency. The methodological knowledge and technical expertise acquired during this experience were subsequently transferred to the endocrinology research group at the University of Bologna, reinforcing the integration of steroidomics and metabolomics capabilities within the broader framework of endocrine research.

7. MATERIALS AND METHODS

7.1. DEVELOPMENT AND OPTIMIZATION OF LC-MS/MS METHODS FOR ENDOGENOUS AND EXOGENOUS STEROIDS IN DRIED BLOOD SPOTS (DBS)

7.1.1. CHEMICALS AND REAGENTS

Analytical-grade steroid standards and the corresponding isotopically labeled internal standards were purchased from certified suppliers (see **Table 3** for details on analytes and vendors). LC-MS grade methanol, acetonitrile, water, methyl tert-butyl ether (MTBE), ethyl acetate, hexane, formic acid (≥99%), and ammonium fluoride (NH_4F) were obtained from Merck (Darmstadt, Germany). Merck (Darmstadt, Germany) supplied protein Saver 903 cards. Glass tubes of 12x75 mm were purchased from Laboindustria SPA (Arzergrande, Italy); PYREX® 13x100mm tubes were purchased from Sigma Aldrich (St. Louis, USA); autosampler vials were purchased from Phenomenex (Torrance, CA, USA). Solid-phase extraction cartridges (C18, 100 mg, 1 mL) were obtained from Biotage (Uppsala, Sweden). All reagents and solvents were of LC-MS or analytical grade and used without further purification.

7.1.2. PREPARATION OF STOCK AND WORKING SOLUTIONS

Individual stock solutions of each steroid and the corresponding isotopic internal standard were prepared in methanol at concentrations ranging from 1 to 10 mg/mL. For lyophile compounds, concentration was determined gravimetrically using an analytical balance (AX105 DeltaRange®, Mettler-Toledo, Novate Milanese, Italy). Working solutions (0.01-100 µg/mL) were obtained by serial dilution in methanol. All solutions were stored at -20 °C in glass vials (V-Vial® Grad, Duran Wheaton Kimble, Millville, NJ, USA).

7.1.3. LC-MS/MS INSTRUMENTATION AND SOURCE OPTIMIZATION

Analyses were performed using an HPLC Series 200 system (PerkinElmer, Shelton, Connecticut, U.S.A.) coupled to a triple quadrupole mass spectrometer (API 4000 QTrap,

Sciex, Concord, Canada) available at the Center for Applied Biomedical Research (CRBA), University of Bologna. Each steroid was individually infused into the ion source at 1-100 µg/mL using a syringe pump (TurboIonSpray®, Sciex) at 10 µL/min. Both atmospheric pressure chemical ionization (APCI) and electrospray ionization (ESI) sources were evaluated in positive and negative ion modes. For APCI, a make-up flow of 50% methanol (400 µL/min) was added to stabilize the spray. For each analyte, full-scan and product ion spectra were acquired to identify the precursor ion and the most abundant and specific fragment ions. Compound-dependent parameters, including declustering potential (DP, 50-120 V), collision energy (CE, 15-60 eV), and cell exit potential (CXP, 6-12 V), were optimized to define two multiple reaction monitoring (MRM) transitions per analyte on each source. Instrumental settings were as follows: curtain gas, 20 psi; nebulizer gas (GS1), 35 psi; auxiliary gas (GS2), 50 psi; ion spray voltage, 5500 V (ESI+) or -4500 V (ESI-); and source temperature, 550 °C.

7.1.4. CHROMATOGRAPHIC METHOD DEVELOPMENT

Chromatographic optimization was conducted to ensure adequate retention, resolution, and selectivity for all target compounds, particularly for isobaric or structurally related steroids. Several stationary phases were systematically evaluated for their ability to provide satisfactory separation and peak symmetry, including the columns Kinetex® Luna C8 100 Å (2.6 µm, 100 × 3 mm), Kinetex® Biphenyl 100 Å (2.6 µm, 100 × 3 mm), Kinetex® Luna-C8(2) (3µm, 100 × 3 mm), Kinetex® Luna-PFP(2) (5µm, 100 × 4.6mm) (all by Phenomenex, Torrance, CA, USA), and the Eclipse-XD8-C18 (3.5µm, 100 × 3 mm; Agilent, Santa Clara, CA, USA). Water, methanol, and acetonitrile were evaluated as mobile phases. To improve ionization efficiency and peak shape, various mobile-phase additives were evaluated, including formic acid (0.05-0.1%), acetic acid (0.05-0.1%), ammonium formate (1-5 mM), and ammonium fluoride (5-100 µM). The column temperature was set to 50 °C. Each analyte was injected individually (10–50 ng/mL; 1-10 µL injection volume) to determine retention times and assess chromatographic resolution. The final gradients were designed to ensure optimal separation of isobaric compounds, such as cortisol, 20α-dihydrocortisone and 20β-dihydrocortisone; cortisone and prednisolone; 11-keto-testosterone and 11-keto-androstenedione; 21-deoxycortisol, corticosterone and 11-deoxycortisol; 16-hydroxy-progesterone, 11α-hydroxy-progesterone, 11-deoxycorticosterone, 11β-hydroxyprogesterone and 17-hydroxyprogesterone, which exhibited overlapping MRM transitions. During method refinement, acquisition parameters

were monitored to balance dwell time, which influences the sensitivity of the method. Dwell time is the period during which the mass spectrometer collects data for a specific analyte. If it is too short, it may reduce data quality; if it is too long, it can compromise the detection efficiency of other compounds. By dividing the analysis into time periods, it is possible to precisely define the number of data points per chromatographic peak required to ensure good resolution and sensitivity for each analyte, thus optimizing the balance between dwell time and the number of analytes. Therefore, optimization was carried out, ensuring a sufficient number of data points per chromatographic peak (typically 10-15 points) for accurate quantification across all analytes included in the MRM panels.

7.1.5. CALIBRATION AND ANALYTICAL PERFORMANCE

Calibration curves were prepared in 50% methanol (v/v) to evaluate analytical linearity under simplified matrix conditions. Each calibration curve consisted of serial dilutions prepared with a 1:2 dilution step, spanning a concentration range appropriate to the expected pathophysiological or pharmacological levels of each steroid. Each calibration point was analyzed in triplicate in a single run, and linear regression models were generated using 1/x weighting, based on peak area ratios between analytes and their corresponding IS. A preliminary evaluation of method linearity was performed by registering curve R^2 within the measurement range, and precision and accuracy at each calibration point.

7.1.6. DBS SAMPLE PREPARATION AND EXTRACTION

Whole blood was collected in K2-EDTA tubes (BD Vacutainer®, REF 367525, Becton Dickinson, Franklin Lakes, NJ, USA), and 30 µL aliquots were spotted onto Whatman® Protein Saver 903 cards (Merck, Darmstadt). The cards were air-dried for 24 hours at room temperature in a dust-free environment and stored in sealed plastic bags with desiccant until analysis. Circular punches (6 mm diameter) were obtained using a manual puncher and transferred into PYREX® 13 x 100 mm tubes. To identify the most effective extraction strategy, several conditions were systematically evaluated. First, a simple DBS soaking in solvent approach, popular in literature, was evaluated by using water, methanol, acetonitrile, and mixtures. In parallel, two extraction systems were compared, such as the multi-tube vortex

mixing (Benchmark Scientific, Sayreville, NJ, USA) and the ultrasonic bath (Starsonic 90 ultrasonic bath, Liarre, Bologna, Italy). In addition to soaking-based approaches, liquid-liquid extraction (LLE) with methyl tert-butyl ether (MTBE), and solid-phase extraction (SPE) using C18 cartridges (100mg/1mL, 220-0010-A; Biotage, Uppsala, Sweden) was also evaluated. For each condition, extraction efficiency, reproducibility, background signal, and matrix effect were assessed on spiked IS to determine the most suitable approach for DBS steroid detection.

Table 3. *Analytes and Internal Standards.*

Analyte	Brand	Product ID	Purity / Isotopic Purity
11-Deoxycorticosterone	Cerilliant®, Certified Reference Material	D-105	>99.9%
11-Deoxycortisol	Cerilliant®, Certified Reference Material	D-061	>99.9%
11-Deoxycortisol-d2	Cambridge Isotope Laboratories	DLM-7209-PK	
11-Ketoandrostenedione	Steraloids	A7250-000	
11-Ketotestosterone	Steraloids	A6720-000	
11β-Hydroxyandrostenedione	Steraloids	A6630-000	
11β-Hydroxytestosterone	Steraloids	A5760-000	
11-α-OH-Progesterone	Steraloids	Q3240-000	
11-β-OH-Progesterone	Steraloids	Q3270-000	
16α-Hydroxyestrone	Cymit Quimica	TR-H941900	
16-OH-Progesterone	Steraloids	Q3330-000	
17-OH-Pregnenolone	Cerilliant®, Certified Reference Material	H-105	>99.9%
17-OH-Progesterone	Cerilliant®, Certified Reference Material	H-085	>99,9%
17-OH-Progesterone-d8	Cambridge Isotope Laboratories	DLM-6598-PK	98%
18-Oxo-Cortisol	MedChemExpress	HY-113151	
20-α-Dihydrocortisone	Steraloids	Q3930-000	
20-β-Dihydrocortisone	Steraloids	Q3960-000	
21-Deoxycortisol	Cerilliant®, Certified Reference Material	D-062	>99.9%
6-α-Methylprednisolone (MPS)-D6	ClearSynth	CS-O-14401	not less than 90%
Aldosterone	Steraloids	Q2000-000	
Aldosterone-D7	Merck	706035	≥98 atom % D, ≥98% (CP)
Androstenedione	Cerilliant®, Certified Reference Material	A-075	>98.9%
Androstenedione-d5	CDN Isotopes	DLM-8330-0	≥98% D
Beclomethasone Dipropionate	Merck	1048506	
Budesonide	Merck	B1157300	
Corticosterone	Cerilliant®, Certified Reference Material	C-117	>99.9%
Corticosterone-d8	Cambridge Isotope Laboratories	DLM-7347-PK	98%
Cortisol	Cerilliant®, Certified Reference Material	C-106	>99.9%
Cortisol-d4	Cambridge Isotope Laboratories	DLM-2218-PK	98%
Cortisone	Cerilliant®, Certified Reference Material	C-130	>99.9%
Cortisone-d7	Cambridge Isotope Laboratories	DLM-9142-C	
Dexamethasone (DEX)	Merck	PHR1526	99.30%
Dexamethasone (DEX)-D4	CDN Isotopes	D-5559	99,00% / 98.10%
DHEA	Cerilliant®, Certified Reference Material	D-063	99.70%
DHEA-S	Merck	700086P	98%
DHEA-S-13C3	Merck	929980	
Estradiol	Cerilliant®, Certified Reference Material	E-060	

Estradiol-13C3	Cerilliant®, Certified Reference Material	E-073	
Estradiol-Sulfate	Cymit Quimica	TM-T40580	
Estradiol-Sulfate-D4	Cymit Quimica	3U-D5287	
Estrone	Cerilliant®, Certified Reference Material	E-075	
Estrone-13C3	Cerilliant®, Certified Reference Material	E-108	
Estrone-3-sulfate	Merck	1001428169	>98%
Estrone-3-Sulfate-D4	Merck	524956	
Methylprednisolone (MPS)	Merck	PHR1717	99.00%
Prednisolone (PNL)	Merck	P6004	99%
Prednisolone-d6	CDN Isotopes	D-6447	
Prednisone (PNS)	Merck	P2900000	
Prednisone-d8	CDN Isotopes	D-7418	
Progesterone	Cerilliant®, Certified Reference Material	P-069	
Progesterone-13C2	Cambridge Isotope Laboratories	CLM-457-PK	90%
Testosterone	Cerilliant®, Certified Reference Material	T-037	
Testosterone-13C2	Cambridge Isotope Laboratories	CLM-159-0.01	99%

7.2. CIRCADIAN STEROID PROFILING AND COMPLEMENTARY METHOD DEVELOPMENT AT THE UNIVERSITY OF GENEVA (UNIGE)

7.2.1. CIRCADIAN STEROID PROFILING IN DBS

Study Design and Sample Collection

The DBS samples analyzed at the Biomedical and Metabolomics Analysis (BMA) Group, University of Geneva (UNIGE), originated from a prospective, multicenter observational pharmacological study (GC-KINE-PRO, approved by the local Ethic Committee with id 766/2022/Oss/AOUBo) coordinated by Prof. Uberto Pagotto, Dept. of Medical and Surgical Sciences, University of Bologna. The study was conducted in collaboration with three Italian clinical centers and university partners, including the Department of Experimental Medicine of the Sapienza University of Rome, the Department of Medical Sciences of the University of Turin, and the Department of Clinical Medicine and Surgery of the University of Naples "Federico II." The study aimed to investigate endogenous and exogenous steroid profiling across different patient cohorts: individuals with normal weight, overweight or obesity, suspected hypercortisolism, patients with Graves' ophthalmopathy undergoing glucocorticoid therapy, and patients with overweight or obesity or impaired glucose or lipid metabolism. Within this framework, finger-prick DBS was collected for steroidomics. In particular, to provide a refined characterization of the circadian fluctuations of the steroidome, each patient collected up to 9 DBS samples on a single observation day.

DBS Analysis at UNIGE

A subset of DBS samples collected in Bologna was analyzed at the BMA group in UNIGE, where a method for the detection of up to 200 steroid hormones is available (184). This method enables the absolute quantification of 8 steroids (cortisol, cortisone, 11-deoxycortisol, 11-deoxycorticosterone, testosterone, androstenedione, 17α-hydroxyprogesterone and progesterone) by applying an internal calibration strategy using ^{13}C3-labelled internal standards (IS) (185). The aim of the collaboration, therefore, was to assess the applicability of this method to DBS sampling to enable the detection of the largest possible steroid panel, along with the high-throughput, ease-of-quantification of major steroids. Such a proof-of-concept was conducted on DBS samples from 6 subjects (3 males and 3 females) from the GC-KINE-

PRO study, including 3 normal-weight and 3 overweight/obese subjects, for a total of 54 DBS samples.

One-point absolute quantification and IS working mixture preparation

A distinctive and innovative aspect of the protocol presented here is the systematic use of one-point internal calibration (IC) using ^{13}C3-labelled IS for absolute quantification of endogenous steroids (185). This original approach represents an alternative to traditional external calibration based on curves prepared in surrogate matrices, such as serum depleted with charcoal, which may introduce variability due to matrix effects or inadequate similarity to the authentic matrix. Instead, the use of IC allows:

- direct quantification in the real biological sample, eliminating the need for an analyte-free matrix,
- faster and more efficient sample preparation, particularly advantageous in clinical settings, excellent reproducibility, and stability over time.

The implementation of single-point IC is based on some basic requirements:

- Selection of appropriate ISs as internal calibrant: it is crucial to select stable isotopes with high chemical purity (>97%) and isotopic enrichment (>99%) to minimize interference and signal crosstalk. Isotopes labeled with ^{13}C or ^{15}N are preferable to deuterium (^{2}H) because of their higher stability and chromatographic and ionization behavior more similar to native analytes.
- Evaluation of the Response Factor (RF): The RF, which represents the ratio of analyte signal to the IS signal at the same concentration, must be determined and verified over different concentration levels to ensure its consistency over the analytical range. A historical RF (hRF) can be calculated to monitor stability over time and between analytical batches.
- Optimal IS concentration: the concentration of IS added to the sample must be carefully set at about one-third of the upper limit of the expected concentration range of the respective analyte, to avoid competitive ion suppression phenomena or interference with low analyte signal.

The following equation calculates the analyte concentration ([A]) in a sample:

$$[\mathrm{A}] = \frac{YA}{YSIL} \times \frac{[\mathrm{SILeq}]}{hRF}$$

where A is the analyte, Y is the measured signal, and [SIL]_eq is the SIL-analyte concentration equivalent. [SIL]_eq can be calculated as follows:

$$[\text{SILeq}] = [\text{SIL}] \times [\text{SIL}]\_\text{CP} \times [\text{SIL}]\_\text{enrichment} \times \text{A\_MW} \div [\text{SIL}]\_\text{MW}$$

Where MW is the molecular weight, CP is the chemical purity, and enrichment is the percentage of isotopic substitution. This equivalence compensates for errors arising from potential limitations in chemical purity and isotopic enrichment.

For absolute quantification, a mix of ISs including 17α-hydroxyprogesterone, androstenedione, 11-deoxycortisol, testosterone, progesterone, cortisone, 11-deoxycorticosterone, cortisol ^{13}C3-isotopes, was prepared. The target concentrations of these isotopes were determined based on the expected physiological serum levels of the corresponding endogenous steroids. To define the absolute concentrations for the SIL mix, the calculation assumed, as previously reported in the literature, that two 6 mm DBS discs contained approximately 25 µL of whole blood, corresponding to 12.5 µL of serum, where steroids predominantly reside (179) (186). The IS working solution was therefore formulated so that, when applied to the extraction solvent, the final concentration of each isotope reflected the amount expected in 12.5 µL of serum (**Table 4**).

Table 4. *Mix IS preparation.*

	Reference IS concentration in serum* (ng/mL)	IS concentration calculated for DBS soaking in 500 µL (ng/mL)	Spiked amount per DBS extract (ng)
17A-Hydroxyprogesterone-13C3	0.167	0.008	0.004
Androstenedione-13C3	0.443	0.022	0.011
17A-Hydroxypregnenolone-13C2-d2	1.121	0.056	0.028
11-Deoxycortisol-13C3	0.961	0.048	0.024
Testosterone-13C3	1.280	0.064	0.032
Progesterone-13C3	1.667	0.083	0.042
Pregnenolone-13C2-d2	2.013	0.101	0.050
Cortisone-13C3	3.000	0.150	0.075
11-Deoxycorticosterone-13C3	4.036	0.202	0.101
Cortisol-13C3	18.500	0.925	0.463

* Calculated as 1/3 of the upper limit of biological distribution according to the Human Metabolome Database.

Estimation of Blood and Serum Content in 6mm DBS Punches

To empirically estimate the actual blood volume represented by a 6 mm DBS punch, 30 µL of whole blood obtained from a K2-EDTA tube (BD Vacutainer®, REF 367525, Becton Dickinson, Franklin Lakes, NJ, USA) was spotted onto DBS cards (Whatman® Protein Saver 903 cards, Merck, Darmstadt) and dried for 24 h. The blood area was precisely excised and weighed to determine the total blood mass of the original spot (average ± SD: 19.5 ± 0.2 mg, determined on 10 replicates). Afterward, a 6 mm punch was excised and weighed (average ± SD: 7.41 ± 0.20 mg; 10 replicates). The proportional blood volume per punch was then calculated using a simple mass-volume relationship:

$$\frac{weight\ of\ 6mm\ punch\ (mg)}{total\ spot\ weight\ (mg)} = \frac{volume\ of\ 6mm\ disc\ \ (\mu L)}{Spotted\ volume\ (30\mu L)}$$

yielding an estimated mean blood volume of 11.4 ± 0.3 µL per punch (CV = 2.4%). During sample preparation, two 6 mm punches were collected for each time point and weighed individually. The total blood volume extracted from each pair was then estimated using the proportional relationship:

$$Sample\ 6\ mm\ disc\ blood\ volume\ (\mu L) = \frac{Sample\ 6mm\ disc\ weight\ (mg) \times average\ 6mm\ disc\ volume(\mu L)}{average\ 6mm\ disc\ weight\ (mg)}$$

From the blood volume estimated from two 6 mm punches, the actual serum volume was derived assuming an average hematocrit of 45%.

Therefore, a correction factor was computed to normalize the observed vs the expected serum volume, defined as:

$$Correction\ factor = \frac{12.5\mu L}{estimated\ serum\ volume\ in\ two\ 6mm\ discs}$$

This factor was finally applied to the raw analyte concentrations to yield weight-normalized and serum-equivalent values, ensuring comparability across samples with variable spot size or blood density.

Sample Preparation

Sample preparation was carried out at the Centre for Applied Biomedical Research (CRBA), University of Bologna, building on the extraction workflow that had been optimized in the preliminary development phase. In particular, the procedure refined in Bologna was established to ensure sufficient recovery and reproducibility prior to the abroad period, enabling the reliable

analysis of clinical study samples in Geneva. Two 6 mm discs were punched from each card, weighed for concentration normalization, and extracted with methanol/water (80:20, v/v) containing ^{13}C3-labelled isotopes. Extraction efficiency was improved through sequential vortex mixing, sonication, and centrifugation, followed by solid-phase extraction on C18 cartridges (IST Isolute C18 100 mg/1mL 220-0010-A Biotage Uppsala, Sweden). Steroids were eluted with methanol, evaporated to dryness, and reconstituted in 50µl of 50% methanol prior to LC-MS/MS analysis.

Analytical phase and data processing

The analytical phase was conducted at the Biomedical and Metabolomics Analysis (BMA) group, University of Geneva, using an Acquity H-Class UPLC System coupled to a Xevo TQ-XS Triple Quadrupole (Waters Corp., Milford, MA, USA). Single-point IC with ^{13}C3-labelled standards was systematically applied, enabling direct quantification in real matrices of cortisol, cortisone, 11-deoxycortisol, 11-deoxycorticosterone, androstenedione, 17-hydroxyprogesterone, testosterone and progesterone, using an automated in-house workflow implemented in Python 3.9 (187). For all targeted compounds, both those quantified by internal calibration and those detected semi-quantitatively, quantifier-to-qualifier MRM ion ratios were systematically evaluated to flag out-of-range values and ensure the specificity of analyte detection. Blank and QC samples were used to monitor background levels, signal retention, and analytical reproducibility. Data were reported in ng/mL for analytes with absolute quantification, whereas non-quantified compounds were expressed as normalized peak areas. The multitargeted dataset was processed using a dedicated workflow implemented in R (version 4.3.1; R Core Team, 2023), which performed quality control, data normalization, and signal drift correction. Drift correction was achieved through a LOESS (Locally Estimated Scatterplot Smoothing) normalization, a non-parametric, locally weighted regression approach applied to QC samples across the analytical sequence. This method models and corrects non-linear signal intensity drifts due to instrumental fluctuations or batch effects, ensuring intra- and inter-batch signal comparability. The corrected data were then used to generate normalized quantitative tables, QC metrics, and graphical summaries for downstream statistical analyses (e.g., Friedman test for temporal trends).

7.2.2. DEVELOPMENT OF AN LC-MS/MS METHOD FOR ESTROGEN ANALYSIS IN SERUM

All methodological development for estrogens was conducted during the research stay at the Biomedical and Metabolomics Analysis (BMA) group, University of Geneva, under the supervision of Prof. Serge Rudaz. The initial focus was on improving the sensitivity and selectivity for the LC-MS/MS detection of estrone (E1), 17β-estradiol (E2), and estriol (E3). These compounds are particularly challenging to analyze due to their low physiological concentration, pronounced matrix effect, and poor MS/MS ionization and fragmentation efficiency (188). To overcome these limitations, a derivatization strategy was employed, which involves the chemical modification of the target molecules. This approach was chosen because the derivatization reaction introduces a specific chemical tag that significantly enhances the ionization efficiency of the steroid molecules, thereby increasing the analytical signal and allowing for their detection at extremely low concentrations. This modification also improves their chromatographic behavior and fragmentation patterns, which is essential for accurate and selective quantification. Two derivatization reagents were evaluated, namely dansyl chloride and 2-fluoro-1-methylpyridinium p-toluenesulphonate (FMPTS), both supplied by Sigma Aldrich (St. Louis, USA). Derivatization conditions were systematically optimized using neat standards, varying solvent composition, water content, the sequence of reagent addition. In the specific case of dansyl-chloride, the compound concentration was optimized, and the catalytic base was selected between triethylamine (TEA, Sigma Aldrich, St. Louis, USA) and sodium bicarbonate (Sigma Aldrich, St. Louis, USA).

Formation of the derivatized compounds was confirmed by direct injection into the mass spectrometer and monitoring the expected precursor ions, while product ion scans allowed the identification of the most abundant and reproducible fragments, which were subsequently used to define MRM transitions. Source and collision parameters, including declustering voltage, collision energy, and collision cell exit potential, were fine-tuned to maximize sensitivity and minimize background noise. Moreover, the efficacy of NH4F post-column infusion (20 mmol/L in MeOH, 5 µL/min) to enhance ionization was evaluated of steroids.

Volumes of 250 µL of serum were used to optimize the extraction protocol preceding the derivatization. Two strategies were evaluated. The first one leaned on the laboratory's usual steroid workflow involving protein precipitation followed by SPE (HLB 30 mg, Oasis, Waters Corporation). The second approach tailored on estrogens, developed on purpose during the

research stay, employed LLE using 0.8 mL MTBE at a 1:4 serum-to-solvent ratio. After derivatization, extracts were redissolved in 100 µL of 80% methanol, and 5 µl were injected in the LC-MS/MS system.

The employed platform was an Acquity H-Class UPLC System coupled to a Xevo TQ-XS Triple Quadrupole (Waters Corp., Milford, MA, USA). Chromatographic separation was performed with a Raptor™ Inert Biphenyl 2.7µm 100x2.1mm (Restek Corporation, Bellefonte, Pennsylvania, USA) column. Column temperature was set on 45°C. Mobile phases were water 0.01% formic acid (mobile phase A) and methanol 0.01% formic acid (Mobile phase B). Mobile phase B was ramped up linearly from 40% to 100% in 18 min. Mobile phase composition was then quickly brought back to 40% B and re-equilibrated for the next run. The total run time was 24 min with a flow rate of 0.4 mL/min. Analyses were conducted in positive electrospray (ESI) mode (capillary voltage at 1.7kV), with MRM transitions optimized for each estrogen derivative. Retention times, signal intensities, and fragmentation patterns were systematically examined to ensure selectivity and reproducibility.

Finally, human authentic serum samples were used as test samples as fortified with known concentrations of neat standards, post-extraction or /and pre-extraction, at four distinct levels concentration, from 100 pg/mL to 100 ng/mL, to evaluate the performance of the method and to assess matrix effects, recovery, and process efficiency.

7.3. VALIDATION OF TARGETED METABOLOMICS IN SERUM AND DBS SPECIMENS

Study design and sample collection

To verify the feasibility of using dried blood spot (DBS) samples for targeted metabolomic profiling, a preliminary validation study was conducted assessing the feasibility of DBS extraction and analysis with a commercial kit later described, and the comparison of DBS results with those obtained in conventional serum samples. The study was approved by the Ethic Committee (ProSteroSal study; 213/2015/O/Tess). After providing their informed consent, 6 healthy volunteers (3 males and 3 females), aged 26-50 years, with body mass index (BMI) between 18.5 and 25.0 kg/m², were enrolled. None of the participants reported chronic or acute illnesses or the use of medications during the three months prior to sampling. For one week prior to the observation day, volunteers followed a standardized, normocaloric Mediterranean diet. On the seventh day, each participant underwent peripheral venous blood collection from the antecubital vein and simultaneous DBS sampling at six predefined time points corresponding to 30 minutes before and two hours after breakfast (07:30), lunch (13:30), and dinner (19:30). Specifically, samples were collected at 07:00, 09:30, 13:00, 15:30, 19:00, and 21:30. The samples were collected at the Unit of Endocrinology and Prevention and Treatment of Diabetes of the Sant'Orsola-Malpighi University (IRCCS) Polyclinic of Bologna. Blood samples were collected into Vacutainer® SST II Advance tubes (REF 366468, BD, Franklin Lakes, NJ, USA), allowed to clot, and centrifuged at 3000 rpm for 10 min at room temperature. Serum was aliquoted (3 × 700 µL) into 1.5 mL polypropylene tubes (Eppendorf®, Hamburg, Germany) and stored at −80°C until analysis. At the same time-points, DBS were obtained by finger prick using sterile lancets (30 G, 1.2 mm needle; Mylife Lancets, Switzerland) and blood drops were spotted onto Whatman® 903 protein saver cards (Merck, Darmstadt, Germany). The cards were air-dried for 24 h at room temperature and stored in sealed plastic bags with desiccant at -80°C. In-house DBS quality controls (QC) were prepared from a single K2EDTA blood sample (BD Vacutainer®, REF 367525, Becton Dickinson, Franklin Lakes, NJ, USA) by spotting 40 µL onto paper cards, dried for 24 h at room temperature, and stored at -80°C until analysis.

Analytical platform and LC-MS/MS workflow

Targeted metabolomic profiling was performed using the AbsoluteIDQ® p180 kit (Biocrates Life Sciences AG, Innsbruck, Austria). The assay enables the quantitative analysis of 187 small molecules across multiple metabolite classes, including 21 amino acids, 21 biogenic amines, 40 acylcarnitines, 90 glycerophospholipids and 15 sphingomyelins. The list of all metabolites with the full biochemical name and abbreviation is reported in **Tables 5-9**. Sample preparation and analysis were conducted according to the manufacturer's protocol (https://biocrates.com/absoluteidq-p180-kit/). Each 96-well plate included blanks, zero samples, seven-point calibration standards, and three levels of kit-provided QC (low, medium, high). Paired serum and DBS samples from each volunteer were analyzed within the same analytical run, distributed across two independent runs using kits from the same lot. For DBS samples, three 3-mm discs were punched and weighed. The discs were transferred into the corresponding wells of the kit plate, dried under a gentle stream of nitrogen, and derivatized with 50 µL of 5% phenyl isothiocyanate (PITC) (Sigma Aldrich St. Louis, USA) for 1 h at room temperature. After drying, metabolites were extracted with 300 µL of 38% g ammonium acetate in methanol (Merck, Darmstadt, Germany). Part of the eluates were transferred in a clean 96 well plate and diluted with 1:5 (v/v) with ultrapure water (Milli-Q Gradient A10 system, Millipore, Switzerland) FIA.

Undiluted extracts were used for the quantitation of metabolites belonging to amino acids and biogenic amine classes were analyzed by liquid chromatography-tandem mass spectrometry (MS/MS) and quantified by isotopic dilution on a 7-point calibration curve. A 10 µL aliquot was injected into an Eclipse XDB-C18 column (3.0 × 100 mm, 3.5 µm; Agilent, Santa Clara, CA, USA) maintained at 50°C, using a 9.5-minute gradient with mobile phase A (water + 0.2% formic acid) and B (acetonitrile + 0.2% formic acid). The LC–MS/MS system consisted of a PerkinElmer Series 200 HPLC coupled to an API 4000 QTrap mass spectrometer (Sciex, Toronto, Canada) operating in positive electrospray ionization and multiple reaction monitoring (MRM) mode. Metabolites belonging to acylcarnitines, phospho- and sphingolipids were analyzed in the water diluted extracts by flow injection analysis-MS/MS (FIA) and quantified by their relative intensity over the chosen isotopically labeled internal standard. Two injections, one in positive and the second in negative ion mode, were done to capture both lipid and exose species. The quantification of this subset of compounds determined by flow injection analysis-MS/MS (FIA) was stated as semiquantitative by the supplier. Data were acquired using Analyst 1.7 (Sciex) and processed with MetIDQ software (Oxygen-DB110-3023,

Biocrates), which is an integral part of the AbsoluteIDQ p180 Kit, following the manufacturer instructions (Biocrates Life Sciences AG).

Quality control and data processing

The numerical data obtained for each DBS sample were corrected for its weight and converted into µmol/L unit. In-house DBS QC were used as a reference for this purpose. According to the Biocrates guidelines (www.biocrates.com), three 3 mm DBS punches are equivalent to 9 µL of blood. The blood volume of each unknown DBS sample was determined using the formula:

$$volume\ of\ unknown\ sample\ (\mu L) = \frac{weight\ of\ unknown\ sample\ \times 9}{average\ weight\ of\ DBS\ QC\ sample}$$

The final concentration of each analyte in each unknown DBS sample was then calculated as:

$$Final\ concentration(\mu mol/L)\ = \frac{raw\ concentration \times 10}{volume\ of\ unknown\ sample}$$

This formula accounts for the difference between the estimated DBS volume and the 10 µL of liquid calibrators specified by the kit.

Data validation and Statistics

Each analytical plate is generated with its own set of calibration curves. Based on signals in the blank and in the zero samples, the MetIDQ software generated plate specific limits of detection (LOD) and quantification (LOQ).

Given the non-normal nature of the distribution of most of the source variables, we adopted a non-parametric approach for data analysis. Therefore, median, interquartilic range, minimum and maximum values were used as descriptive statistics. Correlation between serum and DBS concentrations were performed by the Spearman's rank test. $P < 0.05$ was statistically significant and $0.05 < P < 0.10$ was considered a trend.

***Table 5**. List of amino acids.*

Amino acids			
Ala	Alanine	Lys	Lysine
Arg	Arginine	Met	Methionine
Asn	Asparagine	Orn	Ornithine
Asp	Aspartate	Phe	Phenylalanine
Cit	Citrulline	Pro	Proline
Glu	Glutamate	Ser	Serine
Gln	Glutamine	Thr	Threonine
Gly	Glycine	Trp	Tryptophan
His	Histidine	Tyr	Tyrosine
Ile	Isoleucine	Val	Valine
Leu	Leucine		

***Table 6.** List of biogenic amines.*

Biogenic Amines			
Ac-Orn	Acetylornithine	Met-SO	Methionine sulfoxide
Alpha-AAA	Arginine	Nitro-Tyr	Nitrotyrosine
ADMA	Alpha-Aminoadipic acid	PEA	Phenylethylamine
Carnosine	Carnosine	Putrescine	Putrescine
Creatinine	Creatinine	Serotonin	Serotonin
DOPA	Dihydroxyphenylalanine	Spermidine	Spermidine
Dopamine	Dopamine	Spermine	Spermine
Histamine	Histamine	SDMA	Symmetric dimethylarginine
c4-OH-Pro	cis-4-Hydroxyproline	Taurine	Taurine
T4-OH-Pro	trans-4-Hydroxyproline		
Kynurenine	Kynurenine		

***Table 7**. List of acylcarnitines.*

Acylcarnitines			
C0	Carnitine	C5-DC	Glutarylcarnitine (Hydroxyhexanoylcarnitine)
C2	Acetylcarnitine	C5-M-DC	Methylglutarylcarnitine
C3	Propionylcarnitine	C5-OH	Hydroxyvalerylcarnitine (Methylmalonylcarnitine)
C3-OH	Hydroxypropionylcarnitine	C5:1	Tiglylcarnitine
C3:1	Propenoylcarnitine	C5:1-DC	Glutaconylcarnitine
C4	Butyrylcarnitine	C6	Hexanoylcarnitine (Fumarylcarnitine)
C4-OH	Hydroxybutyrylcarnitine (Malonylcarnitine)	C6:1	Hexenoylcarnitine
C4:1	Butenylcarnitine	C7-DC	Pimeloylcarnitine
C5	Valerylcarnitine	C8	Octanoylcarnitine

C9	Nonaylcarnitine	C14:2-OH	Hydroxytetradecadienylcarnitine
C10	Decanoylcarnitine	C16	Hexadecanoylcarnitine
C10:1	Decenoylcarnitine	C16-OH	Hydroxyhexadecanoylcarnitine
C10:2	Decadienylcarnitine	C16:1	Hexadecenoylcarnitine
C12	Dodecanoylcarnitine	C16:1-OH	Hydroxyhexadecenoylcarnitine
C12:1	Dodecanedioylcarnitine	C16:2	Hexadecadienylcarnitine
C14	Dodecenoylcarnitine	C16:2-OH	Hydroxyhexadecadienylcarnitine
C14:1	Tetradecanoylcarnitine	C18	Octadecanoylcarnitine
C14:1	Tetradecenoylcarnitine	C18:1	Octadecenoylcarnitine
C14:1-OH	Hydroxytetradecenoylcarnitine	C18:1-OH	Hydroxyoctadecenoylcarnitine
C14:2	Tetradecadienylcarnitine	C18:2	Octadecadienylcarnitine

Table 8. *List of glycerophospholipids.*

Glycerophospholipids			
lysoPC a C14:0	PC aa C34:1	PC aa C42:0	PC ae C38:2
lysoPC a C16:0	PC aa C34:2	PC aa C42:1	PC ae C38:3
lysoPC a C16:1	PC aa C34:3	PC aa C42:2	PC ae C38:4
lysoPC a C17:0	PC aa C34:4	PC aa C42:4	PC ae C38:5
lysoPC a C18:0	PC aa C36:0	PC aa C42:5	PC ae C38:6
lysoPC a C18:1	PC aa C36:1	PC aa C42:6	PC ae C40:1
lysoPC a C18:2	PC aa C36:2	PC ae C30:0	PC ae C40:2
lysoPC a C20:3	PC aa C36:3	PC ae C30:1	PC ae C40:3
lysoPC a C20:4	PC aa C36:4	PC ae C30:2	PC ae C40:4
lysoPC a C24:0	PC aa C36:5	PC ae C32:1	PC ae C40:5
lysoPC a C26:0	PC aa C36:6	PC ae C32:2	PC ae C40:6
lysoPC a C26:1	PC aa C38:0	PC ae C34:0	PC ae C42:0
lysoPC a C28:0	PC aa C38:1	PC ae C34:1	PC ae C42:1
lysoPC a C28:1	PC aa C38:3	PC ae C34:2	PC ae C42:2
PC aa C24:0	PC aa C38:4	PC ae C34:3	PC ae C42:3
PC aa C26:0	PC aa C38:5	PC ae C36:0	PC ae C42:4
PC aa C28:1	PC aa C38:6	PC ae C36:1	PC ae C42:5
PC aa C30:0	PC aa C40:1	PC ae C36:2	PC ae C44:3
PC aa C30:2	PC aa C40:2	PC ae C36:3	PC ae C44:4
PC aa C32:0	PC aa C40:3	PC ae C36:4	PC ae C44:5
PC aa C32:1	PC aa C40:4	PC ae C36:5	PC ae C44:6
PC aa C32:2	PC aa C40:5	PC ae C38:0	
PC aa C32:3	PC aa C40:6	PC ae C38:1	

Table 9. *List of sphingomyelins.*

Sphingomyelins			
SM (OH) C14:1	SM C18:0	SM (OH) C22:2	SM (OH) C24:1
SM C16:0	SM C18:1	SM C22:3	SM C26:0
SM C16:1	SM C20:2	SM C24:0	SM C26:1
SM (OH) C16:1	SM (OH) C22:1	SM C24:1	

7.4. CIRCADIAN METABOLIC PROFILING IN HEALTH AND IN STATES OF CORTISOL RHYTHM DERANGEMENT

Study population

The study was approved by the Ethical Committee of the CE-AVEC (ProSteroSal, id: 213/2015/O/Tess). All subjects gave written informed consent. The volunteers, after providing written informed consent, were recruited among patients attending the Unit of Endocrinology and Diabetes Prevention and Care of the S. Orsola University Hospital in Bologna (IRCCS) between 2020 and 2022, for the evaluation and subsequent clinical management of suspected or confirmed adrenal or thyroid disorders.

Participants were divided into four groups:

- patients with adrenal insufficiency (AI, n=8) under once-daily dual-release hydrocortisone therapy;
- patients with mild autonomous cortisol secretion (MACS, n=12);
- patients with Cushing's syndrome (CS, n=9);
- healthy subjects (HS, n=10) recruited from the general population.

All participants met the following inclusion criteria:

- age ≥ 18 years;
- Caucasian ethnicity;
- complete sexual development;
- stable body weight during the previous three months;
- normal thyroid function (based on age and/or etiology);
- ability to provide informed consent;
- for women in reproductive age, regular menstrual cycles (11–13 per year) were required.

General exclusion criteria were established to avoid comorbidities or lifestyle conditions potentially influencing the circadian hormone rhythm or metabolism, and included:

- untreated gastrointestinal disease or malabsorption;
- assumption of drugs interfering with gastrointestinal absorption and/or motility;

- diagnosis of type II diabetes;
- drug or alcohol abuse;
- pregnancy or lactation;
- competitive sport activity;
- night-shift work;
- recent transoceanic flights;
- severe medical conditions contraindicating study participation;
- for women in reproductive age, use of estrogen-progestins (combined oral contraceptives).

Further exclusion criteria were established for HS, including:

- use of any medication in the 4 weeks preceding the study (except for occasional antipyretics or nonsteroidal anti-inflammatory drugs, and stable L-thyroxine replacement in primary hypothyroidism);
- use of exogenous steroid medication or medications altering steroid secretion or metabolism within the last 3 months;
- endocrine (except for simple goiter or adequately treated hypothyroidism), hepatic, renal, cardiovascular, autoimmune, neurological, psychiatric, or hematological disorders.

Patients with MACS or CS were selected among those performing a 1 mg dexamethasone suppression test (DST) for a suspicion of cortisol excess, as per guidelines (72) (189). Those who displayed a post-DST cortisol level > 50 nmol/L, in absence of typical clinical signs and symptoms, were diagnosed as MACS. At variance, those patients displaying a post-DST cortisol level > 50 nmol/L along with typical clinical signs and symptoms were diagnosed as CS. MACS and CS patients participated in the study before starting any disease specific surgical or pharmacological treatments. Exclusion criteria included:

- use of exogenous steroid medication or medications altering steroid secretion or metabolism within the last 3 months;
- presence of pheochromocytoma, primary aldosteronism, or suspected adrenal malignancy.

For patients with AI, diagnosis was defined according to European Society of Endocrinology guidelines (104). Glucocorticoid replacement therapy (GRT) type and dose were assigned by an expert endocrinologist. Only patients with a disease history lasting more than 6 months and under once-daily dual-release hydrocortisone therapy were included in the study.

Experimental protocol

All participants underwent a clinical evaluation, during which anthropometric parameters were recorded. Height and weight were measured using a mechanical scale equipped with a stadiometer, while waist circumference was measured with a non-stretchable flexible tape measure, without compressing the soft tissues. Subsequently, all volunteers underwent body composition assessments using bioimpedance analysis. In addition, patients with suspected MACS or Cushing's syndrome underwent first-line tests for the evaluation of hypercortisolism.

Bioimpedance Analysis and Diet Calculation

Basal metabolic rate (BMR) and body composition were determined using bioimpedance analysis with the BIA101BIVA device (Akern, Pisa, Italy) and the associated BodygramPlus software. Based on the BMR, each participant's total daily energy expenditure (TDEE) was calculated using the formula TDEE = BMR × PAL, where PAL stands for Physical Activity Level and was set to 1.3. Using the BMR and TDEE values, a standardized normocaloric Mediterranean diet was designed for each participant with the help of the Metadieta nutritional software. Bioimpedance analysis also provided the following body composition parameters:

- Fat-free mass (FFM): evaluated both in absolute terms (kg) and as a percentage of total body weight. FFM includes all non-fat components of the body, such as skeleton, approximately 73% of body fluids, muscles, skin, and organs. A healthy physical condition typically corresponds to an FFM of 77-85% of total body weight, depending on age.
- Fat mass (FM): evaluated both in absolute terms (kg) and as a percentage of total body weight. A healthy physical condition typically corresponds to an FM of 15-23% of total body weight, depending on age.

Diet

For one week prior to sample collection, participants were instructed to follow a normocaloric Mediterranean diet, designed based on their bioimpedance results as described above. The general principles of this diet included five daily meals, three main meals and two snacks, with the following daily caloric distribution: breakfast 15-20%, snacks 5-10%, lunch 30-35%, and dinner 30-35%. Macronutrient distribution consisted of 50-60% carbohydrates, 25–30% fats, and the remaining percentage from proteins, providing 0.9-1.1 g of protein per kg of ideal body weight according to the Lorentz formula. During the same week, participants were asked to maintain a regular sleep-wake cycle.

Dexamethasone suppression test

In patients with suspected CS or MACS, a 1 mg dexamethasone suppression test (DST) was performed by administering two 0.5 mg tablets of dexamethasone (Decadron®) at 23:00, followed by venous blood sampling between 08:00 and 09:00 of the following morning to determine serum cortisol levels. Analyses were carried out at the Laboratorio Unico Metropolitano di Bologna according to routine clinical procedures.

Observation day and Sample Collection

Participants were provided with all necessary materials, including sterile single-use safety lancets (30 G, 1.2 mm needle; Mylife Lancets, Switzerland) and seven progressively numbered Whatman 903 cards (Merck, Darmstadt). On the observation day, volunteers self-collected DBS at seven specific time points: 30 minutes before and two hours after breakfast (07:30), lunch (13:30), and dinner (19:30), and at 23:00, corresponding to 07:00, 09:30, 13:00, 15:30, 19:00, 21:30, and 23:00. DBS collection instructions were as follows:

- wash hands with warm water
- disinfect the fingertip with an alcohol-based sanitizer;
- allow the finger to dry;
- prick the fingertip and gently squeeze to obtain a drop of blood;
- apply the blood drop to the designated circle on the card corresponding to the collection time, filling the entire outlined area (approximately three drops of blood were required).

At each time point, participants collected two DBS per time, depositing a drop of blood in two outlined areas on a Whatman 903 card. After completing the collection, the participants stored the cards in a dry place at room temperature until delivery, which occurred in the

following days at the Unit of Endocrinology and Diabetes Prevention and Care, S. Orsola University Hospital, IRCCS, Bologna. DBS collected from each participant were placed in an envelope and stored at -80°C until analysis at the Applied Biomedical Research Center, Department of Medical and Surgical Sciences, University of Bologna. Targeted metabolomic profiling of 187 molecules was performed as previously described.

Statistical analysis

Continuous anthropometric, clinical, and metabolic variables were reported as mean ± standard deviation (SD). Data obtained from the metabolic profiling of DBS samples were explored and analyzed using a structured multi-step approach, aimed at identifying circadian fluctuations in molecular patterns and distinguishing between different clinical groups. This approach was designed not only to reduce data dimensionality but also to retain biologically relevant information for downstream analysis.

1. Feature selection with BORUTA

The first step involved selecting the most informative metabolic features using the BORUTA algorithm (190). BORUTA is a wrapper method built around random forest classifiers, which evaluates the importance of each variable by comparing it to randomized shadow features. Features that consistently show higher importance than the randomized controls are retained. In our study, Healthy Subjects (HS) and Cushing's Syndrome (CS) patients were chosen as the comparison groups, because they represent the extremes of the metabolic phenotype spectrum. This step allowed us to prune uninformative variables while retaining features that most effectively capture differences between HS and CS, ensuring that subsequent analyses focused on relevant molecular patterns.

2. Dimensionality reduction with Factor Analysis (FA). Following feature selection, Factor Analysis (FA) (191) was applied to reduce the complexity of the dataset and to identify latent factors representing correlated molecular patterns. FA identifies underlying dimensions (factors) that explain shared variance among the selected metabolites, allowing correlated features to be combined into single composite scores. These composite scores represent biologically meaningful patterns and facilitate comparison of circadian dynamics across individuals and groups.

3. Characterization of circadian fluctuations. The composite scores derived from FA were evaluated at all seven time points of DBS collection (07:00, 09:30, 13:00, 15:30, 19:00,

21:30, 23:00) to characterize circadian fluctuations of relevant metabolic patterns. This step enabled the identification of temporal trends in metabolite concentrations and the assessment of intra-day variations within each study group.

4. Comparative analysis across clinical groups. Once circadian patterns were established in HS and CS, these same composite scores were analyzed in patients with Adrenal Insufficiency (AI) and Mild Autonomous Cortisol Secretion (MACS). This allowed us to evaluate how metabolic circadian rhythms in these patient groups deviate from healthy controls and from overt Cushing's syndrome, highlighting both preserved and altered temporal patterns.

5. Kinetic modeling of metabolite fluctuations. To quantitatively describe the circadian profiles of molecular patterns, multiple kinetic models were assessed for each composite score. Model selection was based on goodness-of-fit criteria and estimation error of parameters. The three best-performing models, second-order polynomial, third-order polynomial, and power-law functions ($y = Ax^k + c$), were applied to fit temporal dynamics in each group. This approach enabled an objective comparison of the shape, amplitude, and timing of metabolic fluctuations across different clinical conditions.

6. Implementation and significance. The entire data analysis pipeline was developed in python 3.8, employing the BORUTApy (https://github.com/scikit-learn-contrib/boruta_py) package for feature selection and ScikitLearn (https://scikit-learn.org/stable/) for dimensionality reduction. Fitting, modelling, and validation of kinetics was developed using custom scripts and the LMfit (https://lmfit.github.io/lmfit-py/) package. This multi-step approach ensured that the final analyses focused on relevant, biologically interpretable patterns, while accounting for the complexity of the metabolomic dataset. Statistical significance for group comparisons was set at $p < 0.05$.

8. RESULTS

8.1. DEVELOPMENT OF LC-MS/MS METHODS FOR ENDOGENOUS AND EXOGENOUS STEROIDS IN DRIED BLOOD SPOTS (DBS)

8.1.1. OPTIMIZATION OF IONIZATION AND CHROMATOGRAPHIC CONDITIONS

In the developmental phase, tests were performed to compare electrospray ionization (ESI) and atmospheric pressure chemical ionization (APCI) sources. ESI provided higher signal intensity for most analytes and was therefore selected as the ionization mode for all subsequent experiments. Based on the preferred ionization polarity of the studied compounds, two LC-MS/MS methods were developed: one in negative (ESI-) and the other in positive (ESI+) mode (**Tables 10** and **12**). This analytical division into two separate LC-MS/MS methods was necessary because the API 4000 QTrap mass spectrometer does not permit polarity switching during a single acquisition cycle.

A significant challenge in both analytical panels consisted in achieving the chromatographic separation of steroidal compounds that generated cross-reactive signals in the MS/MS detection. Within the steroid family, this typically occurs between steroids sharing the same molecular weight, i.e., isobars or isomers. Indeed, such compounds will not only generate a parental ion with the same m/z, but also an overlapping fragmentation pattern, as expected by the similarity of the core structure of the steroid class. Therefore, a specific steroid might produce a signal in MRM transitions optimized for an isobar or isomer congener. Due to natural isotope distributions, MS/MS cross-reactivity can also occur between molecules with mass differences of 1 or 2 amu. Finally, cross-reactivity may also result upon source-fragmentation, such as in the case of water loss or loss of the conjugated sulphate group in positive ionization.

Chromatographic optimization was initially carried out using a Kinetex® Luna C8 100 Å (2.6 µm, 100 × 3 mm) column for both methods. However, with this stationary phase, cortisone and prednisolone, both with a molecular weight of 360.45 Da, as well as cortisol, 20α-dihydrocortisone, and 20β-dihydrocortisone, all with a molecular weight of 362.46 Da, were not baseline-separated. To improve separation, the first attempt consisted in the modification of the chromatographic gradient; however, it was not possible to obtain the expected resolution.

Subsequently, several columns were evaluated, and separation was finally achieved using the Kinetex® Biphenyl 100 Å (2.6 µm, 100 × 3 mm) column, which was therefore selected for the ESI- panel, while the mentioned C8 column was used confirmed for the ESI+ panel. For both methods, mobile phase A consisted of 20% methanol in water, and phase B was 100% methanol. The flow rate was maintained at 300 µL/min, except during the washing steps, where it was increased to 400 µL/min. For the ESI- method, the gradient started at 5% B, increased to 47% B at 1 min, maintained until 4 min, then to 90% B at 10 min, and finally to 100% B at 10.5 min. After a 2-minute wash, the system was returned to its initial condition for the last minutes, giving a total runtime of 18 min. For the ESI+ method, the gradient started at 2% B, increased to 45% B at 0.5 min, maintained until 6 min, then rose to 92% B at 13.5 min and to 100% B at 13.7 min. After 1.3 min washing, the system was re-equilibrated to the initial composition for 5 min, with a total runtime of 20 min. Both gradients were divided into acquisition periods, three for the ESI- and five for the ESI+ method, to optimize the dwell time and cycle time and maintain adequate sensitivity and peak definition for all monitored transitions. Representative chromatograms of the optimized ESI- and ESI+ panels are shown in **Figures 14** and **15**.

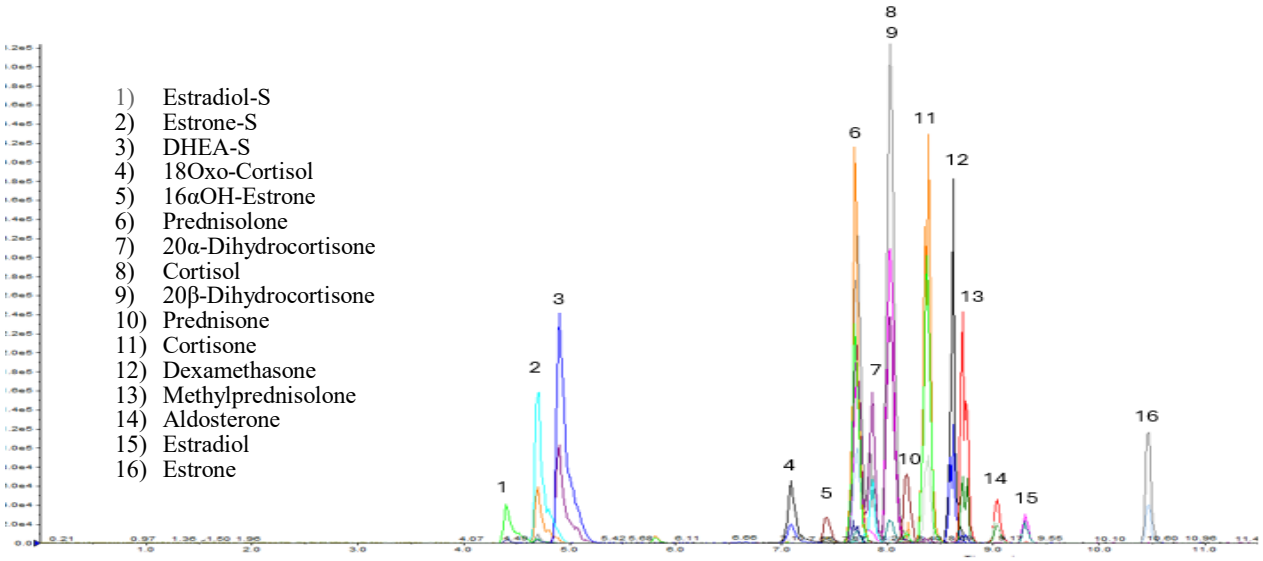

Figure 14. *Chromatogram of ESI- panel.*

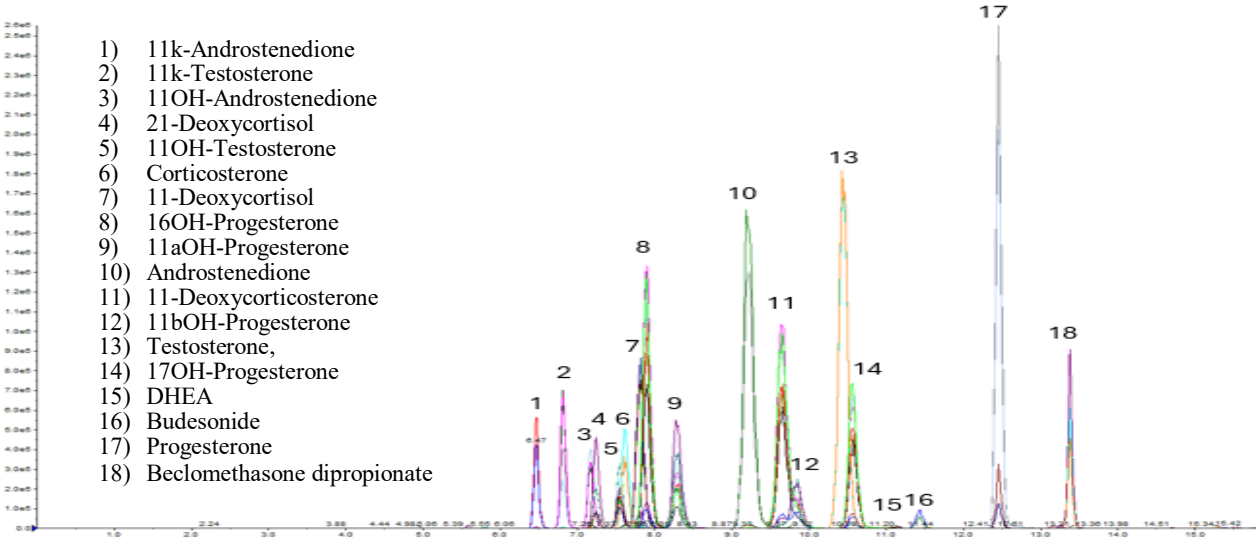

Figure 15. *Chromatogram of ESI+ panel.*

8.1.2. EVALUATION OF AMMONIUM FLUORIDE CONCENTRATION

To boost ionization efficiency, ammonium fluoride (NH_4F) was evaluated as a mobile-phase additive. A systematic series of runs covered NH_4F concentrations of 0, 10, 20, 50, 100, and 200 µM. The signal intensity rose steadily to 50 µM, emerging as a compromise across the steroid panel, with most analytes showing enhanced responses. At concentrations of 100 µM or higher, the signal plateaued, providing no improvement. Unfortunately, we found that keeping NH_4F at 50 µM or above for a period gradually drove the system's back-pressure. To preserve the platform, we ultimately settled on a 10 µM NH_4F concentration for the analysis. Consequently, the mobile phase was defined as 20 % methanol in water containing 10 µM NH_4F (phase A) and pure methanol (phase B).

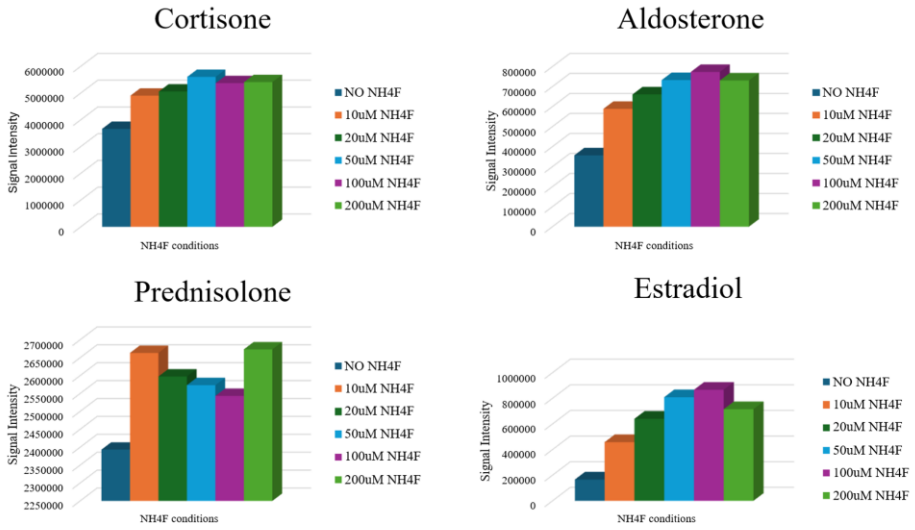

Figure 16. *Comparison of analyte yields at different levels of NH4F concentrations reported for four analytes.*

8.1.3. CALIBRATION AND ANALYTICAL PERFORMANCE

Calibration curves for each analyte were generated using a weighted (1/x) regression. The linearity was satisfactory across the measurement range, with all R^2 values exceeding 0.99. Accuracy and precision were assessed at concentration tiers as displayed in **Tables 11 and 13**. The accuracy ranged between 85 and 118%, whereas CV stayed below 15 %, reflecting intra-assay consistency.

Table 10. *Compound dependent LC and MS parameters for representative analytes in ESI- panel.*

Analyte	Retention Time	Transition	Q1/Q3	DP	CE	CXP
Estradiol-Sulphate	4.40	Quantifier	350.9/271.0	-110	-45	-15
		Qualifier	350.9/145.0	-110	-75	-11
Estrone-Sulphate	4.70	Quantifier	349.2/269.2	-80	-45	-12
		Qualifier	349.2/145.1	-80	-75	-10
DHEA-Sulphate	4.90	Quantifier	367.1/97.0	-100	-40	-8
		Qualifier	367.1/80.0	-130	-120	-10

18-Oxo-Cortisol	7.09	Quantifier	375.2/317.0	-70	-20	-15
		Qualifier	375.2/345.1	-70	-15	-15
16alpha-hydroxyestrone	7.42	Quantifier	285.1/145.0	-100	-80	-10
		Qualifier	385.1/158.7	-100	-55	-10
Prednisolone	7.69	Quantifier	359.1/329.2	-90	-13	-8
		Qualifier	359.1/280.0	-90	-38	-15
20α-dihydrocortisone	7.72	Quantifier	361.0/271.1	-105	-25	-3
		Qualifier		-80	-20	-10
Cortisol	7.86	Quantifier	361.2/331.2	-75	-18	-10
		Qualifier	361.1/297.1	-75	-35	-10
20βdihydrocortisone	7.72	Quantifier	361.1/315.5	-130	-40	-7
		Qualifier	361.1/331.2	-80	-20	-10
Prednisone	8.18	Quantifier	357.2/327.2	-130	-11	-5
		Qualifier	357.2/123.0	-130	-20	-6
Cortisone	8.39	Quantifier	359.0/329.1	-65	-13	-9
		Qualifier	359.0/301.1	-65	-22	-11
Dexamethasone	8.62	Quantifier	391.1/361.3	-90	-15	-15
		Qualifier	391.1/307.1	-90	-35	-15
Methylprednisolone	8.71	Quantifier	373.1/343.3	-80	-20	-14
		Qualifier	373.1/309.0	-80	-35	-15
Estradiol	9.30	Quantifier	271.1/145.0	-125	-55	-5
		Qualifier	271.1/183.1	-125	-55	-7
Aldosterone	9.03	Quantifier	359.2/189.1	-75	-25	-15
		Qualifier	359/297.2	-75	-20	-15
Estrone	10.46	Quantifier	269.1/145.0	-130	-55	-5
		Qualifier	269.1/142.9	-130	-70	-10
DHEA-Sulphate-D6	4.90	Quantifier	373.0/98.2	-60	-65	-5
		Qualifier	373.0/255.0	-60	-20	-10
		Qualifier	365.1/284.1	-60	-40	-16
Prednisone-D8	8.18	Quantifier	365.1/333.2	-60	-15	-14
		Qualifier	365.1/123.6	-60	-50	-18
Dexamethasone-D4	8.62	Quantifier	395.2/363.3	-60	-15	-20
		Qualifier	395.2/309.1	-60	-35	-13
MPS-D6	8.71	Quantifier	379.2/349.2	-60	-15	-15
		Qualifier	379.2/315.1	-60	-35	-15
Estradiol-^{13}C3	9.30	Quantifier	274.0/148.1	-115	-50	-10
		Qualifier	274.0/186.1	-115	-50	-10
Aldosterone-D7	9.37	Quantifier	366.2/194.2	-90	-30	-10
		Qualifier	366.2/338.3	-90	-25	-15
Estrone-^{13}C3	10.47	Quantifier	272.1/148.1	-100	-50	-10
		Qualifier	272.1/146.1	-100	-75	-10

Cortisol-D4	7.86	Quantifier	367.3/97.2	-90	-50	-5
		Qualifier	367.3/121.2	-90	-35	-8
Cortisone-D7	8.39	Quantifier	369.3/169.3	-90	-35	-11
		Qualifier	369.3/125.2	-90	-40	-8

Table 11. *Measurement range for representative analytes in ESI- panel.*

Analyte	Measurement range (ng/ml)	CV%	Accuracy %	Linearity
Estrone-Sulphate	0.078 - 20	1.17 - 9.9	90.9 - 113.7	0.9988
DHEA-Sulphate	2.44 - 312.5	0.24 - 12.3	86.7 - 101.2	0.9970
Cortisol	0.488 - 62.5	0.11 - 12.4	95.8 - 105.5	0.9990
Prednisone	0.195 - 50	4.23 - 14.6	88.5 - 110.4	0.9980
Cortisone	0.488 - 6.25	2.31 - 14.3	87.5 - 112.5	0.9980
Dexamethasone	0.098 - 12.5	0.41 - 13.0	93.7 - 117.8	0.9987
Methylprednisolone	2.44 - 625	0.20 - 14.7	94.5 - 104.9	0.9988
Estradiol	0.078 - 20	0.61 - 10.7	92.1 - 114.9	0.9980
Aldosterone	0.078 - 5	2.78 - 11.1	93.7 - 106.1	0.9980
Estrone	0.0098 - 5	0.60 - 8.80	92.8 - 110.6	0.9985

Table 12. *Compound dependent LC and MS parameters for representative analytes in ESI+ panel.*

Analyte	Retention Time	Transitions	Q1/Q3	DP	CE	CXP
11-Keto-Androstenedione	6.45	Quantifier	301.3/121.2	90	35	3
		Qualifier	301.3/257.2	90	30	13
11-Keto-Testosterone	6.80	Quantifier	303.3/121.2	100	35	3
		Qualifier	303.3/259.3	100	30	12
11-Hydroxy-Androstenedione	7.15	Quantifier	303.3/267.4	90	25	13
		Qualifier	303.3/121.1	90	35	3
21-Deoxycortisol	7.23	Quantifier	347.2/121.2	80	35	7
		Qualifier	347.2/311.1	70	20	10

11-Hydroxy-Testosterone	7.53	Quantifier	305.3/121.2	90	35	3
		Qualifier	305.3/105.2	90	60	5
Corticosterone	7.61	Quantifier	347.3/121.1	60	35	8
		Qualifier	347.3/97.1	85	33	4
11-Deoxycortisol	7.61	Quantifier	347.2/109.1	95	40	7
		Qualifier	347.2/97.2	100	38	7
16-Hydroxy-Progesterone	7.87	Quantifier	331.4/97.1	110	40	2
		Qualifier	331.4/109.1	110	40	2
11-α-Hydroxy-Progesterone	8.28	Quantifier	331.3/91.2	110	70	1
		Qualifier	331.3/97.1	11	40	2
Androstenedione	9.21	Quantifier	287.2/97.1	110	35	5
		Qualifier	287.2/109.1	110	35	7
11-Deoxycorticosterone	9.65	Quantifier	331.3/109.2	95	40	7
		Qualifier	331.3/97.1	95	30	4
11-β-Hydroxy-Progesterone	9.83	Quantifier	331.4/121.3	70	30	5
		Qualifier	331.4/295.3	70	20	7
Testosterone	10.44	Quantifier	289.3/97.1	90	30	5
		Qualifier	289.3/109.0	90	35	10
17-Hydroxy-Progesterone	10.57	Quantifier	331.3/97.1	90	40	5
		Qualifier	331.3/109.1	90	40	4
17-Hydroxy-Pregnenolone	12.45	Quantifier	315.2/159.2	55	35	9
		Qualifier	315.2/91.2	55	75	4
DHEA	11.08	Quantifier	271.3/213.2	65	23	10
		Qualifier	271.3/197.3	65	30	10
Budesonide	11.42	Qualifier	431.0/227.2	70	20	5
		Quantifier	431.0/159.1	70	35	8
Progesterone	12.46	Quantifier	315.2/97.1	115	30	2
		Qualifier	315.2/109.2	115	35	2
Beclomethasone Dipropionate	13.38	Qualifier	521.2/57.2	70	55	10
		Quantifier	521.2/411.1	70	20	10
Cortisol-D4	6.50	Quantifier	367.3/97.2	90	50	5
		Qualifier	367.3/121.2	90	35	8
Cortisone-D7	6.17	Quantifier	369.3/169.3	90	35	11
		Qualifier	369.3/125.2	90	40	8
Corticosterone-D8	7.61	Quantifier	355.3/125.3	80	45	6
		Qualifier	369.3/125.2	80	35	8
Androstenedione-D5	9.21	Quantifier	292.3/100.2	90	30	6
		Qualifier	292.3/113.2	90	35	8
Testosterone-^{13}C2	10.44	Quantifier	291.3/99.1	90	30	6
		Qualifier	291.3/111.1	90	35	7
17-Hydroxy-Progesterone-D8	10.57	Quantifier	339.4/100.2	90	35	6

		Qualifier	339.4/113.2	90	40	7
Progesterone-^{13}C2	12.46	Quantifier	317.4/99.2	90	35	6
		Qualifier	317.4/111.2	90	35	6

Table 13. *Measurement range for representative analytes in ESI+ panel.*

Analyte	Measurement range (ng/ml)	CV%	Accuracy %	Linearity
11-Keto-Androstenedione	0.098-200	0.66-6.4	97.6-105.4	0.9993
11-Keto-Testosterone	0.049-50	0.67-6.2	97.8-102.6	0.9999
11-Hydroxy-Androstenedione	0.049-200	0.01-8.8	90.5-102.1	0.9996
21-Deoxycortisol	0.098-50	0.07-10.0	85.6-109.7	0.9979
11-Hydroxy-Testosterone	0.024-200	0.80-11.5	90.4-104.0	0.9991
Corticosterone	0.049-200	0.47-6.4	94.4-107.5	0.9995
11-Deoxycortisol	0.098-25	1.69-7.3	97.5-105.7	0.9993
16-Hydroxy-Progesterone	0.049-25	0.86-11.7	89.2-105.9	0.9990
11-α-Hydroxy-Progesterone	0.098-50	2.29-5.9	85.6-108.7	0.9990
Androstenedione	0.024-200	0.71-8.9	89.0-103.4	0.9991
11-Deoxycorticosterone	0.049-200	0.35-10.8	96.7-101.9	0.9993
11-β-Hydroxy-Progesterone	0.195-200	0.69-9.3	96.6-102.3	0.9989
Testosterone	0.024-12.5	1.58-5.2	97.6-102.1	0.9989
17-Hydroxy-Progesterone	0.024-200	0.35-8.9	89.5-105.5	0.9995
17-Hydroxy-Pregnenolone	0.098-25	0.46-8.7	85.6-104.6	0.9994
DHEA	6.25-200	0.77-13.9	92.9-102.3	0.9984
Budesonide	1.56-200	1.28-9.9	91.7-113.2	0.9992

Progesterone	0.024-25	0.34-6.0	95.6-107.6	0.9989
Beclomethasone Dipropionate	0.049-25	0.70-8.2	85.5-105.6	0.9992

8.1.4. OPTIMIZATION OF DBS EXTRACTION PROTOCOL

Different extraction procedures were compared based on the analytical signal (peak area) obtained for each analyte. According to a simple DBS soaking in solvent approach, mixtures of acetonitrile and methanol at 50:50 and 80:20 (v/v), and methanol and water at 95:5 (v/v) were tested as extraction solutions with both sonic bath and vortex incubation. Results obtained for representative analytes are shown in **Figure 17**. The optimal condition consisted of 500 µL of acetonitrile: methanol 80:20 (v/v), followed by 20 minutes of ultrasonic agitation. However, the utilization of this simple extraction procedure was not sufficient to ensure satisfactory sensitivity in authentic samples. Therefore, supplementary purification steps were evaluated, such as LLE with MTBE and SPE with C18 cartridges. Experiments conducted on labelled IS demonstrated that while MTBE ensured high efficiency for several analytes, it caused a substantial loss of steroid sulfates and cortisol (**Figure 18**). SPE with C18 cartridges was proved to provide a more balanced recovery profile and was thus selected as the reference protocol for DBS processing.

The optimized workflow was finally defined as follows: first, two 6-mm discs from each DBS card were punched and transferred into PYREX® tubes; afterward, 500 µL of MeOH/H_2O (80:20, v/v) containing labeled IS were added. Samples were vortexed for 5 min, sonicated for 20 min at room temperature and further diluted with 500 µL of deionized water. After the SPE, samples were eluted with MeOH, dried under nitrogen, and reconstituted in 50 µL of 50% MeOH before LC-MS/MS analysis.

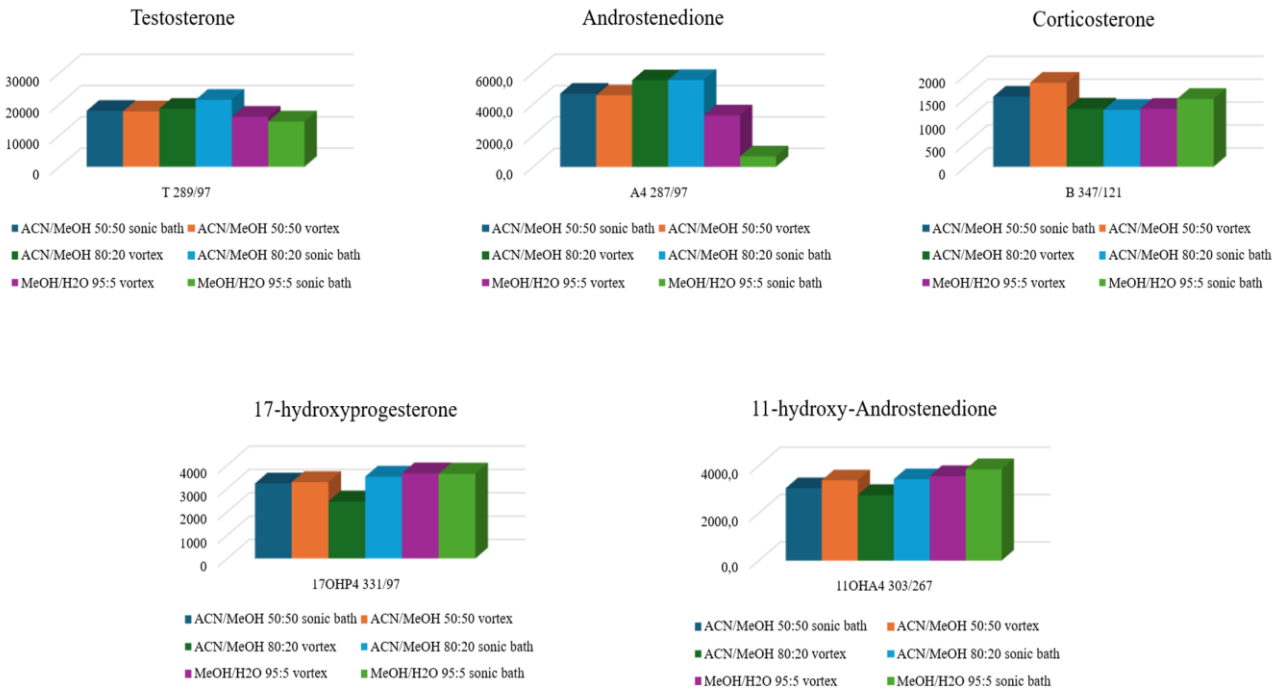

Figure 17. *Extraction efficiency of representative analytes in different extraction conditions.*

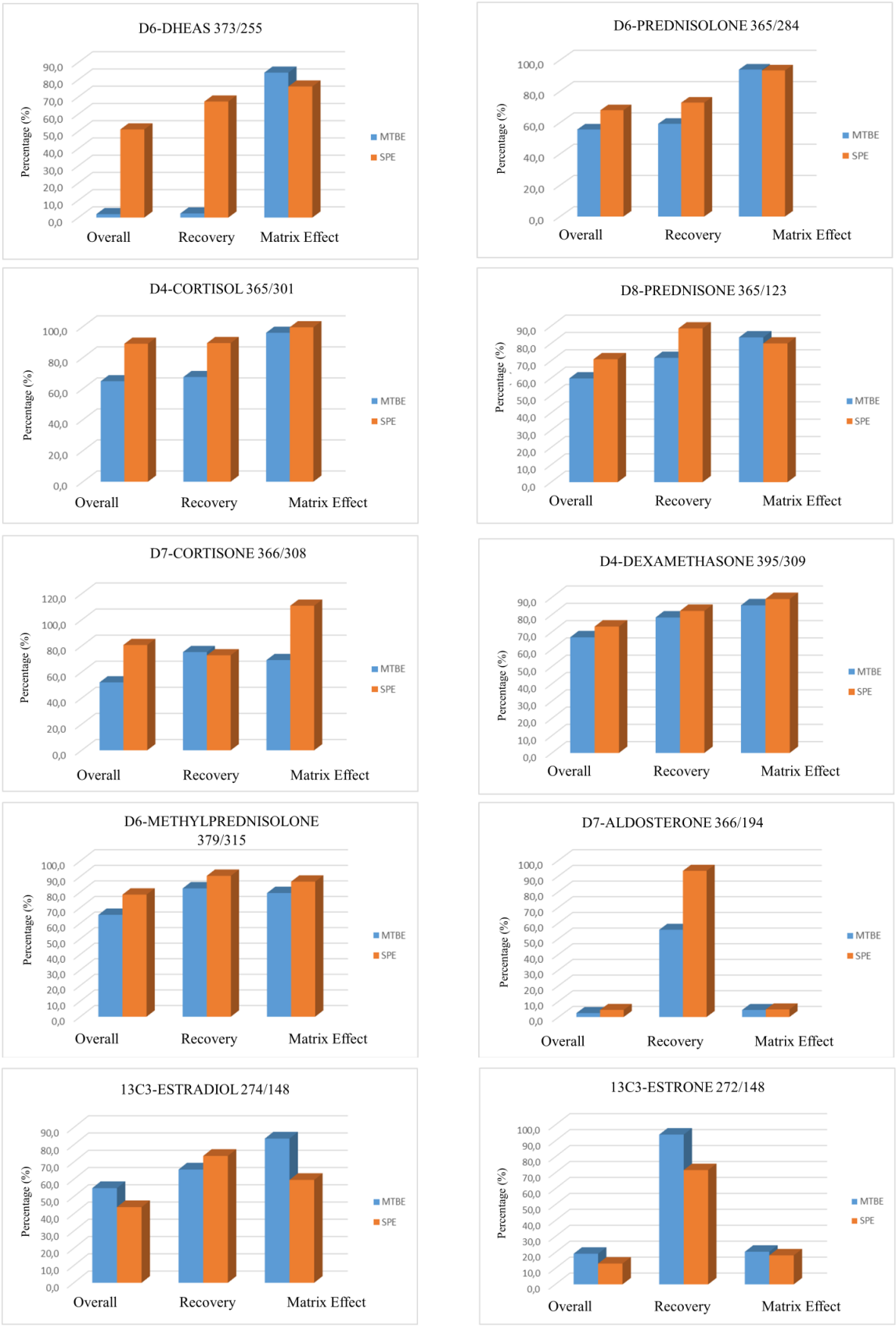

Figure 18. *Comparison of overall efficiency, recovery and matrix effect between MTBE and SPE extraction in main internal standards.*

8.2. CIRCADIAN STEROID PROFILING AND COMPLEMENTARY METHOD DEVELOPMENT AT THE UNIVERSITY OF GENEVA (UNIGE)

8.2.1. CHARACTERIZATION OF THE CIRCADIAN STEROIDOME IN DBS

The application of the LC-MS/MS method used at the BMA of UNIGE for the analysis of DBS enabled the absolute quantification of eight key steroids, including cortisol, cortisone, 11-deoxycortisol, 11-deoxycorticosterone, testosterone, androstenedione, 17α-hydroxyprogesterone and progesterone, along with the detection of 25 other steroids. In details, the following metabolites were detected among corticosteroids: 18-hydroxycortisol, 20α-hydroxycortisol, 20β-hydroxycortisol, 5α-hydroxycortisol, 5β-hydroxycortisol, 20α-cortolone, 20β-cortolone, 20α-dihydrocortisone, 20β-dihydrocortisone, corticosterone, 5βdihydro-11-dihydrocorticosterone, 11-dihydrocorticosterone; progestogens: 17α,20α-dihydroxyprogesterone, 11βhydroxyprogesterone, pregnenolone, pregnanediol-glucuronide, estrone; androgens: androstenediol, etiocholanedione, androsterone sulfate, androsterone-3-glucuronide, etiocholanolone, 5α-androstane-3α-17β-diol, 11βandrostenedione, 11βetiocholanolone)

In order to verify the ability of the UNIGE method applied to DBS to detect small diurnal variations in a broad steroid panel, samples from three men and three women (healthy subjects, aged 20-55 years) collected across the nine time points were collected. Cortisol, cortisone, and 11-deoxycortisol showed the expected circadian fluctuation (all $p<0.001$), characterized by higher levels in the morning and lower levels throughout the day, reaching a minimum at bedtime; moreover, a post-prandial rise was detected (at 14.00), as illustrated in **Figure 19**. Whether analyzed separately by sex, these trends remain significant in both men and women (cortisol $p<0.001$ and 0.033; cortisone $p<0.001$ and 0.005; respectively). Androstenedione and testosterone also exhibited significant time-dependent changes ($p < 0.001$ and 0.027, respectively); when analyzed separately by gender, only males displayed significant temporal trend ($p=0.013$ for androstenedione; p 0.048 for testosterone), while significance was lost in females (**Figure 19**). In line with androgens, 17-hydroxyprogesterone lacked a circadian fluctuation in females, but displayed a rhythm in males ($p=0.015$). By contrast,

11-deoxycorticosterone and progesterone showed no fluctuations both in males and females (**Figure 20-22**).

Exploratory analyses performed on other detected, but not quantified, steroid metabolites revealed that most glucocorticoid metabolites followed the same temporal patterns as the two major hormones of the class. Indeed, cortisol and cortisone metabolites and precursors, such as 20α-dihydrocortisol, 20β-dihydrocortisol, 5β-dihydrocortisol, 18-hydroxycortisol, and 11-dihydrocorticosterone, exhibited significant reduction from morning to evening (all $p<0.005$), confirming the rhythmicity of glucocorticoid metabolism (**Figure 20**).

Concerning the detected androgen metabolites (**Figure 21**), consistently with its specific adrenal origin, only 11βOH-androstenedione ($p<0.001$) showed the typical diurnal fluctuation above described for testosterone, androstenedione, and corticosteroids. At variance, androstenediol ($p=0.027$), androsterone-3α-glucuronide ($p=0.003$) and 11βOH-etiocholanolone ($p=0.023$) showed significant, though different temporal trends, with apparent increase of circulating levels from morning to evening. As shown in heatmaps in **Figure 22**, progestogen metabolites did not display a diurnal rhythm, apart from 17α,20α dihydroxyprogesterone ($p=0.013$), whereas estrone showed a significant fluctuation with apparently higher levels at awakening and bedtime, lowering at midday ($p=0.04$).

Figure 19. *Temporal diurnal profiles of cortisol, cortisone, 11-deoxycortisol, testosterone, androstenedione and 17hydroxyprogesterone. Mean concentrations at each time point ± SD.*

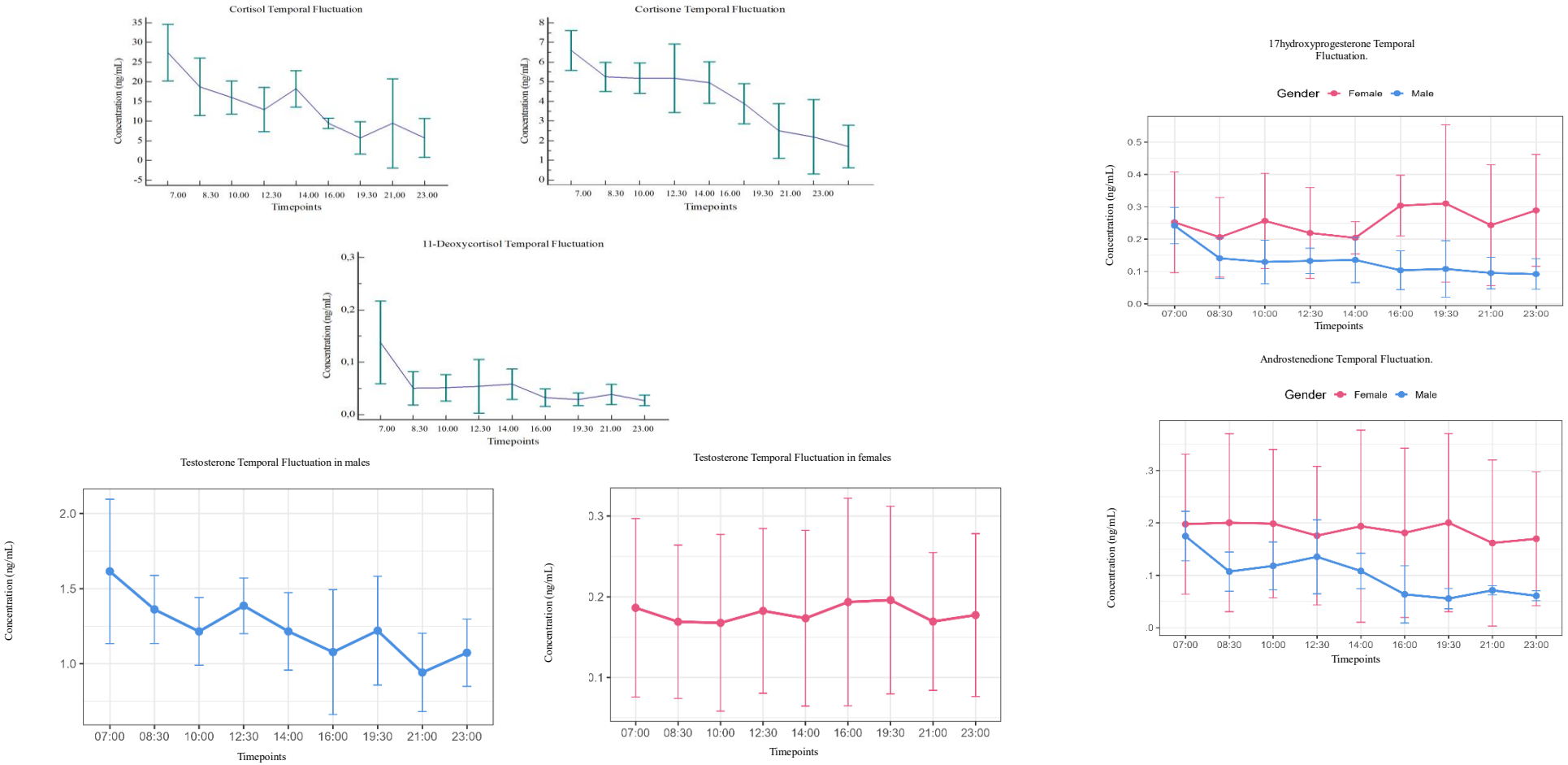

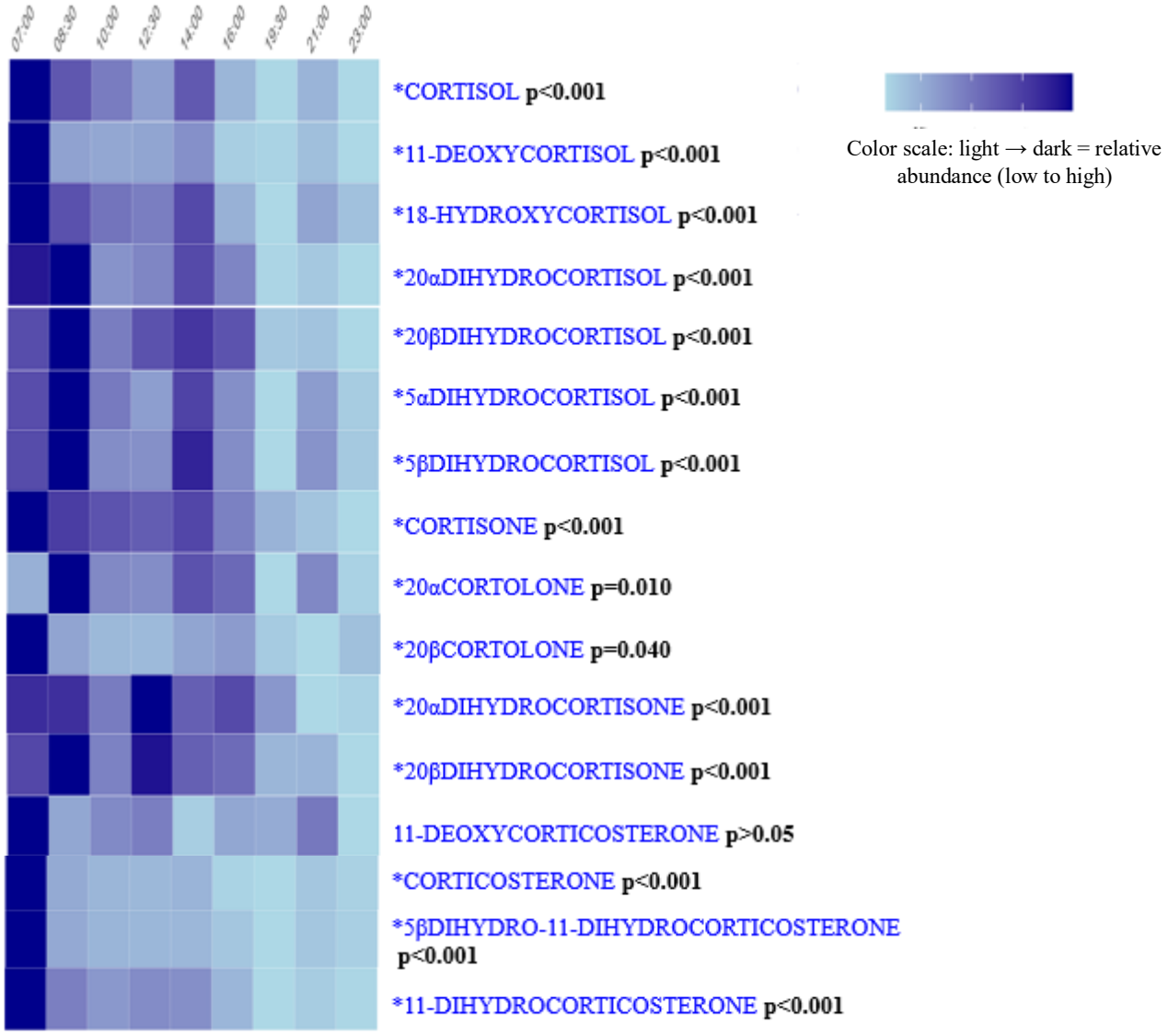

Figure 20. *Heatmaps showing temporal trend of glucocorticoids, using normalized mean peak areas across the indicated time points.* ***** *Denote statistically significant differences (*p < 0.05).*

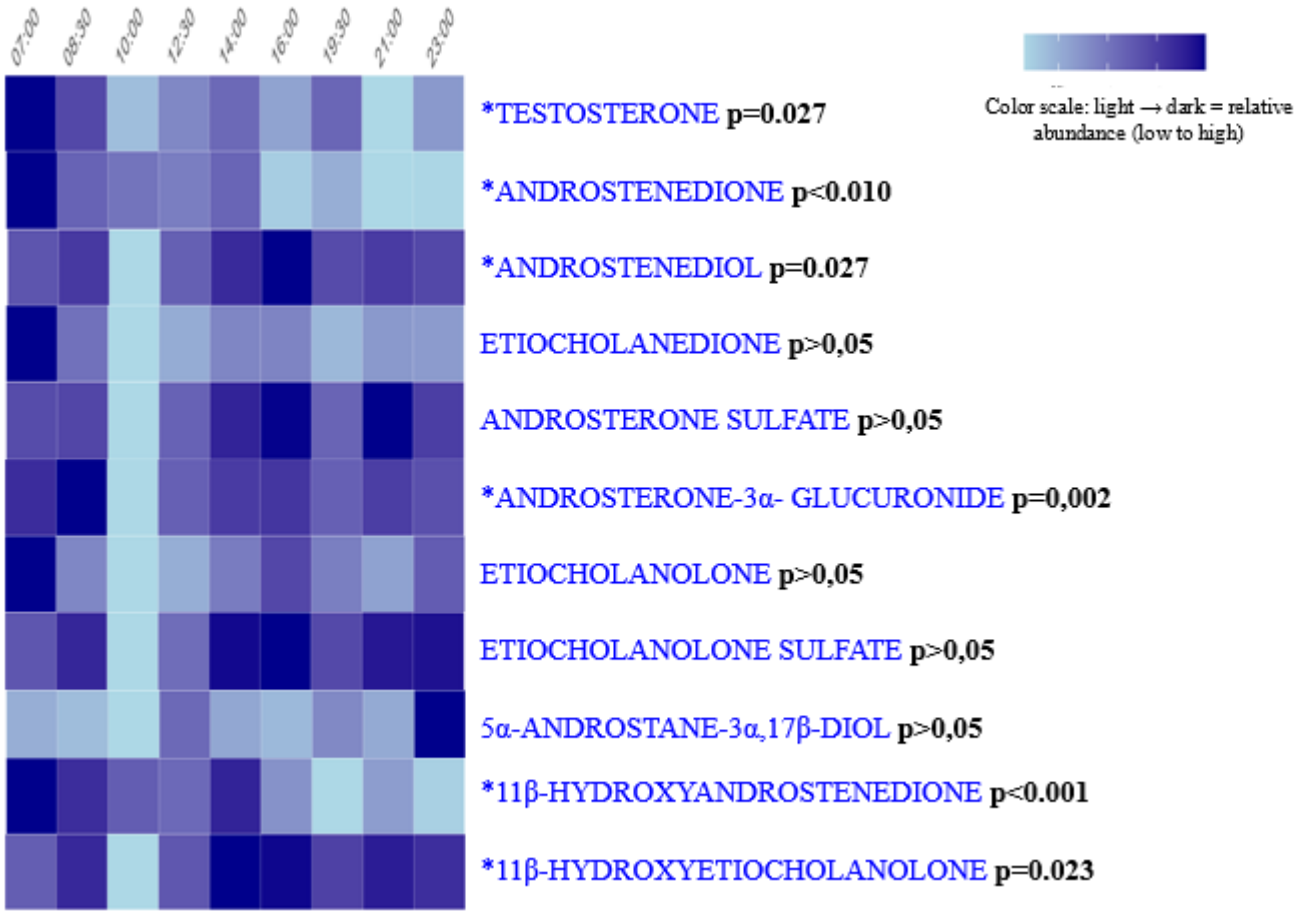

Figure 21. *Heatmaps showing temporal trend of androgens and androgens-related metabolites, using normalized mean peak areas across the indicated time points. * Denote statistically significant differences (*p < 0.05).*

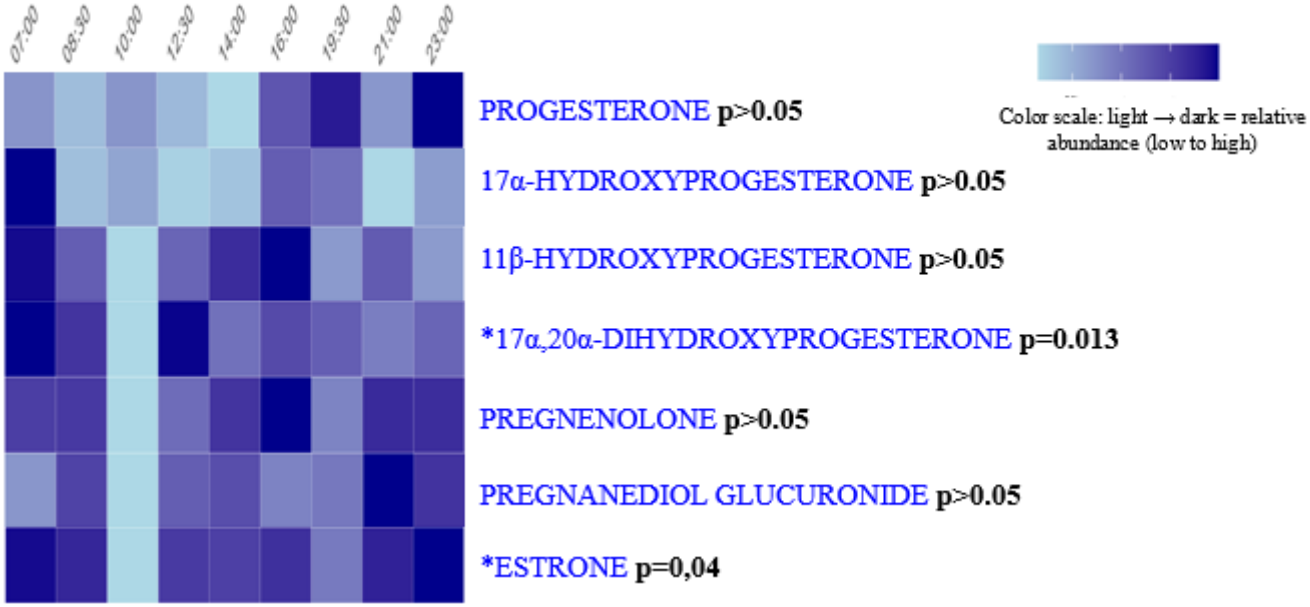

Figure 22. *Heatmaps showing temporal trend of progestogens and estrone, using normalized mean peak areas across the indicated time points. * Denote statistically significant differences (*p < 0.05).*

8.2.2. ESTROGEN ANALYSIS IN SERUM

The development of the method for estrogen measurement in serum began with experiments on neat standards, which clearly demonstrated that derivatization with dansyl chloride substantially increased signal intensity and produced more effective fragmentation pattern than FMPTS (**Figure 23**) (**Table 14**).

Afterward, the optimal concentration of dansyl chloride, along with the ideal buffer between bicarbonate vs TEA, were determined (**Figure 24**). The best was the condition with dansyl chloride 0.5 mg/mL with sodium bicarbonate 100mM.

The efficacy of dansyl chloride on boosting the MS/MS detection of neat standards is reported in **Figure 25**, where peak areas are compared between derivatized and native estrogen analytes injected at 100 ng/mL (500 pg on column), along with the post columns infusion of NH4F. Dansylation resulted in a substantial enhancement of estrogen ionization efficiency, with signal intensities increasing approximately 3-fold for estrone, nearly 80-fold for estradiol, and up to 4000-fold for estriol compared to the corresponding native analytes. Overall, the dansyl chloride derivatization protocol allowed the detection of estrone, estradiol, and estriol standards at concentrations from 0.1 to 100 ng/mL.

When the procedure was applied on authentic serum, matrix effects, recovery, and process efficiency were evaluated. This assessment demonstrated that the existing steroid protocol, consisting of protein precipitation and SPE before derivatization, was insufficient for the reliable estrogen quantification. Poor recovery and strong matrix effects at low concentrations highlighted the need for a more extensive workflow (**Figure 26**).

Therefore, these challenges led to the establishment of a dedicated pre-derivatization extraction procedure that enabled robust and reproducible quantification of estrone, 17β-estradiol, and estriol. Optimal results were obtained by using the LLE with MTBE and derivatization with dansyl chloride (0.5 mg/mL) in bicarbonate buffer (100 mM).

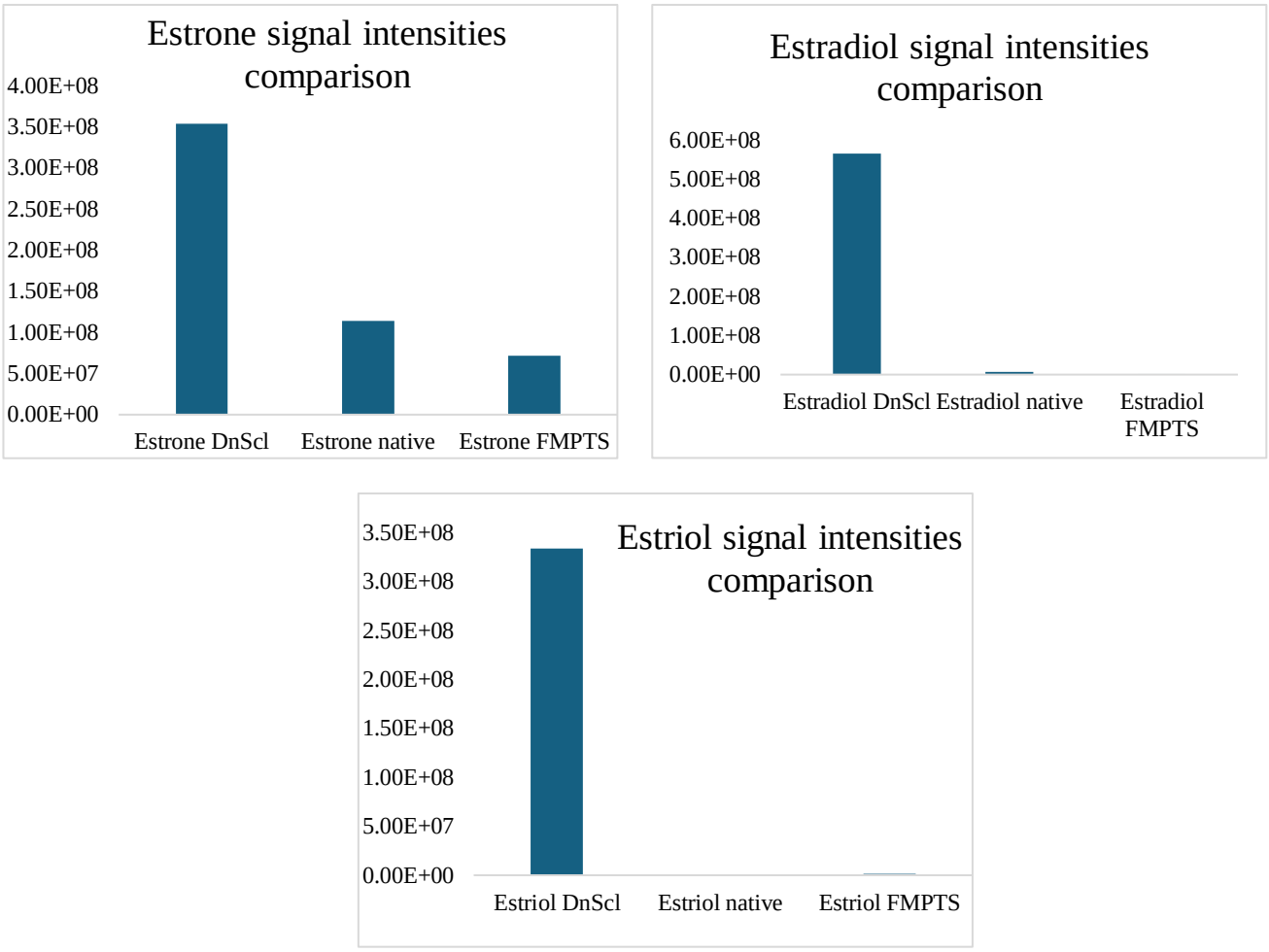

Figure 23. *Comparison of signal intensities in native estrogens and in derivatization conditions with dansyl chloride and FMPTS in estrone, estradiol and estriol.*

Table 14. *Signal intensities in native estrogens and derivatization conditions with Dansyl Chloride and FMPTS in estrone, estradiol and estriol.*

Estrone DnScl	**Estrone native**	**Estrone FMPTS**
3,54E+08	1,14E+08	7,16E+07
Estradiol DnScl	**Estradiol native**	**Estradiol FMPTS**
5,66E+08	7,28E+06	1,38E+06
Estriol DnScl	**Estriol native**	**Estriol FMPTS**
3,34E+08	8,36E+04	1,58E+06

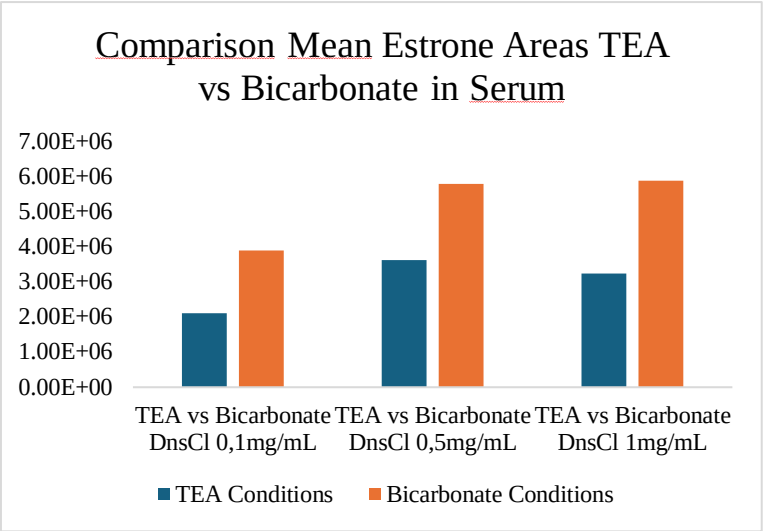

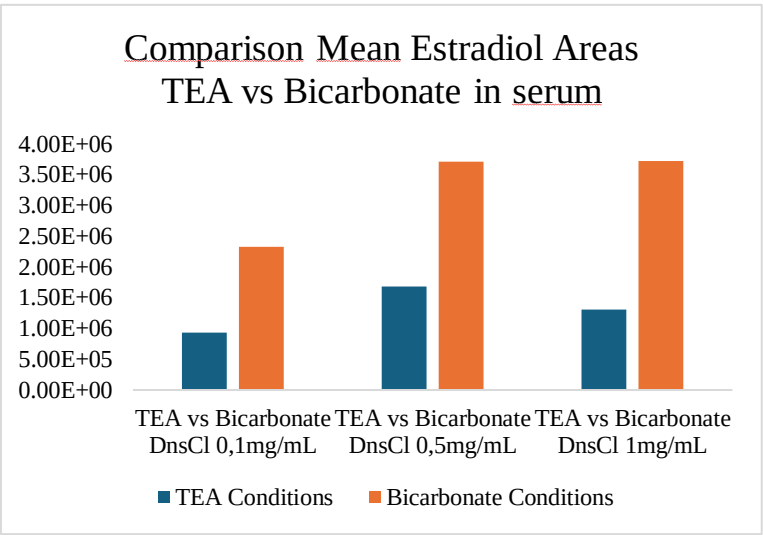

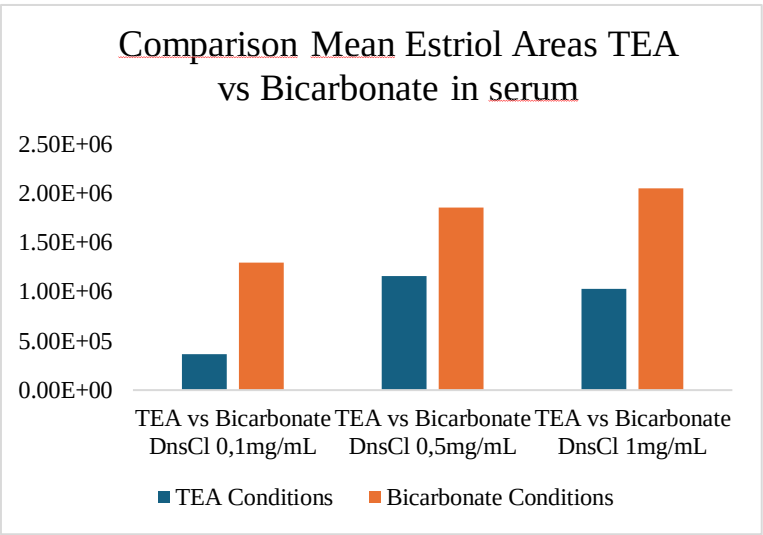

Figure 24. *Comparison of signal intensities in derivatized estrogens with Dansyl Chloride at different concentrations in estrone, estradiol and estriol using TEA and bicarbonate conditions as buffer for the derivatization reaction.*

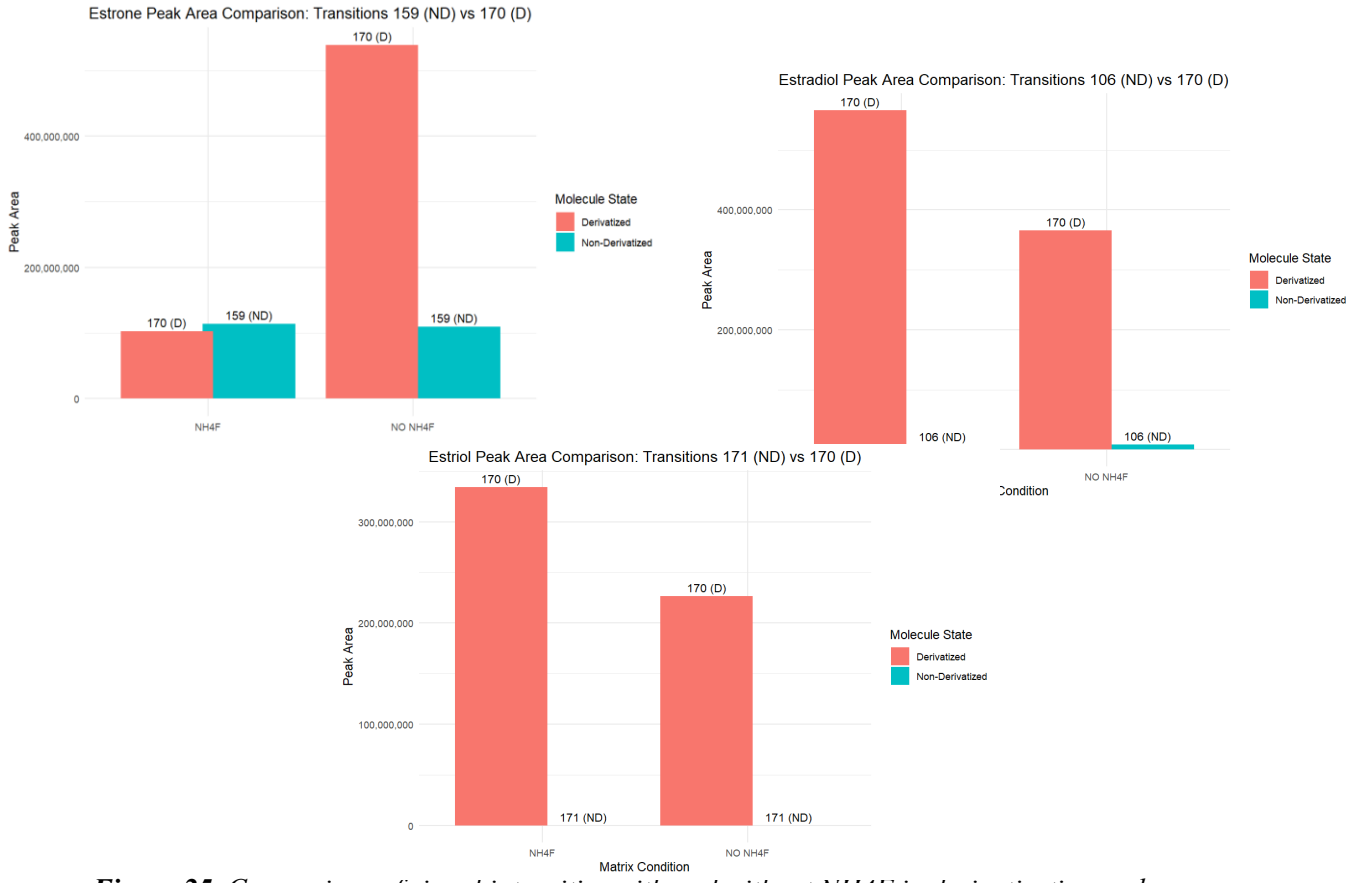

Figure 25. *Comparison of signal intensities with and without NH4F in derivatization and no derivatization conditions in estrone, estradiol and estriol.*

Figure 26. *Comparison of matrix effect, recovery and process efficiency obtained using MTBE and SPE extraction in estrone, estradiol and estriol.*

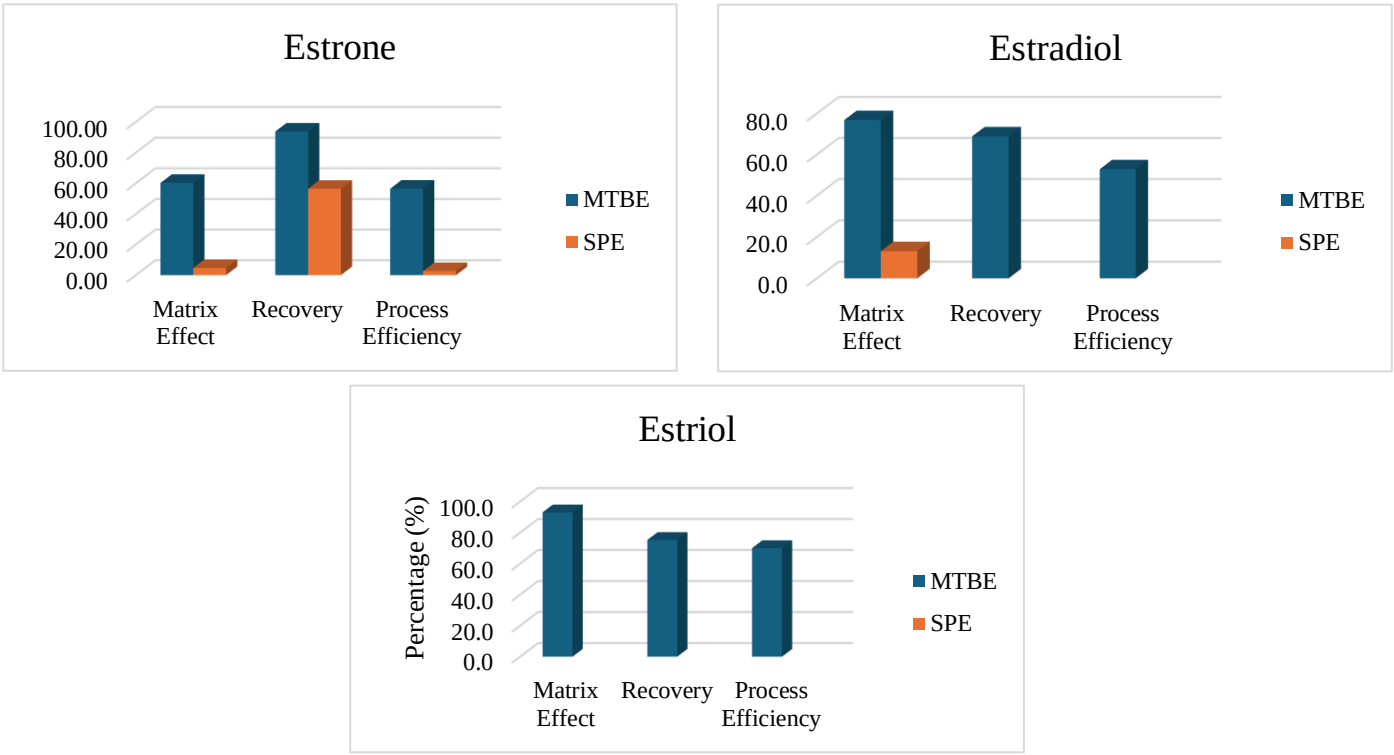

8.3. VALIDATION OF TARGETED METABOLOMICS IN SERUM AND DBS

The correlation analysis between DBS and serum concentrations for amino acids (AA) and biogenic amines (BA) revealed variable agreement across analytes (**Table 15**). Overall, several AA showed moderate-to-strong positive correlations. Among them, branched-chain AA such as isoleucine (ρ=0.773), leucine (ρ=0.774), valine (ρ 0.729), and methionine (ρ=0.655) exhibited the highest correlations, indicating consistent proportionality between DBS and serum levels. Among BA, acetyl-ornithine showed an excellent correlation (ρ=0.900), whereas serotonin (ρ=0.535), histamine (ρ=0.481), and spermine (ρ=0.581) exhibited moderate associations between matrices. Amine levels were generally less concentrated in DBS vs serum (16 to 90% relative abundance), apart from serine, histamine and spermine (1.31, 12.8 and 35.56 higher levels in DBS vs serum, respectively).

Regarding acylcarnitines (AC) (**Table 16**), all short-chain ones (C0-C5) showed moderate to strong correlations (ρ range: 0.476 - 0.803), with carnitine (C0) displaying the strongest relationship, indicating consistent proportionality between DBS and serum Moderate correlations were found for most of mid-chain AC (C6-C10), with the general exception of dicarboxylic (DC) species, and for a few long-chain (C12-C18) ACs. Curve slopes demonstrate overall lower abundance of acylcarnitine in DBS compared to serum, with approximate relative abundance ranging from <1% to 95%, and only C18:1 and C18:2 displaying 1.71- and 2.53-fold increase in DBS vs serum, respectively.

As to glycerophospholipids (**Table 17**), almost all lysophosphatidylcholines (LysoPCs) (ρ range: 0.334-0.830) and phosphatidylcholines (PC) (ρ range: 0.342-0.800) displayed significant correlation between DBS and serum levels. Compared to DBS levels, serum levels of lysoPC displayed 15 to 100% abundance. Among PC, levels in DBS were generally lower than in serum, with lower proportion found for PCaaC38:5 (18% abundance in DBS vs serum) and larger at PCaeC38:1 (4.55-fold increase in DBS vs serum).

Sphingomyelins (SM) exhibited heterogeneous and generally weaker correlations between DBS and serum levels compared to other lipid classes (**Table 18**). Among hydroxylated species, SM(OH) C22:2 showed the strongest association (ρ=0.625), followed by SM(OH) C22:1 (ρ=0.373). For the non-hydroxylated SM, correlation was observed for species between length C16:1 to C22:3 (ρ=0.384 - 0.646), while no correlation was found for those with longer

chains. According to the observed slope coefficients, DBS levels were about 18-43% of serum levels.

Correlations were also analyzed at each timepoint to verify whether the circadian rhythm could influence the comparability between DBS and serum levels. After this evaluation, we found correlations were consistent in each time point in DBS and serum.

***Table 15**. Correlation between DBS and serum in amino acids and biogenic amines.*

Analyte	Rho			Slope		Intercept	
	Coeff.	IC 95	P-value	Coeff.	IC 95	Coeff	IC 95
Alanine	0,535	0,251 - 0,735	<0,001	0,55	0,28 - 0,82	60,5	-56,6 - 177,8
Arginine	0,443	0,134 - 0,674	0,007	0,16	0,06 - 0,27	14,5	0,1 - 28,9
Aspartate	-0,195	-0,492 - 0,143	0,255	-3,81	-8,63 - 1,02	207,9	131,9 - 283,9
Citrulline	0,588	0,321 - 0,768	<0,001	0,62	0,35 - 0,88	5,0	-3,9 - 13,8
Glutamine	0,047	-0,286 - 0,369	0,788	-0,00	-0,24 - 0,24	483,7	287,5 - 679,9
Glutamate	-0,043	-0,367 - 0,289	0,802	-0,30	-1,21 - 0,62	170,2	133,0 - 207,4
Glycine	0,463	0,159 - 0,687	0,004	0,75	0,30 - 1,20	59,1	-55,8 - 174,1
Histidine	0,360	0,035 - 0,615	0,031	0,29	0,03 - 0,55	43,0	16,2 - 69,9
Isoleucine	0,773	0,596 - 0,879	<0,001	0,55	0,40 - 0,69	11,7	-1,4 - 24,8
Leucine	0,774	0,597 - 0,879	<0,001	0,42	0,27 - 0,57	27,5	0,1 - 55,0
Lysine	0,364	0,041 - 0,619	0,029	0,32	0,09 - 0,55	58,8	14,8 - 102,8
Methionine	0,655	0,416 - 0,809	<0,001	0,39	0,23 - 0,56	4,7	-0,3 - 9,7
Ornithine	0,274	-0,061 - 0,552	0,107	0,28	-0,25 - 0,81	84,6	44,5 - 124,7
Phenylalanine	0,563	0,287 - 0,752	<0,001	0,41	0,20 - 0,61	19,5	2,7 - 36,2
Proline	0,710	0,497 - 0,842	<0,001	0,44	0,32 - 0,55	29,3	5,3 - 53,2
Serine	0,330	0,002 - 0,594	0,049	1,31	0,09 - 2,53	15,6	-176,2 - 207,5
Threonine	0,663	0,428 - 0,814	<0,001	0,39	0,24 - 0,54	29,6	5,2 - 53,9
Tryptophan	0,576	0,306 - 0,761	<0,001	0,24	0,12 - 0,36	17,1	8,3 - 26,0
Tyrosine	0,572	0,300 - 0,758	<0,001	0,46	0,24 - 0,68	19,1	3,7 - 34,5
Valine	0,729	0,526 - 0,853	<0,001	0,49	0,30 - 0,67	46,9	-1,0 - 94,8
Acetyl-Ornithine	0,900	0,812 - 0,948	<0,001	0,90	0,84 - 0,96	0,1	-0,1 - 0,4
Asymmetric Dimethylarginine	0,262	-0,072 - 0,544	0,122	0,45	0,02 - 0,87	0,1	-0,1 - 0,3
Alpha-AAA	0,515	0,225 - 0,722	<0,001	0,53	0,11 - 0,95	0,5	0,1 - 0,8
Creatinine	0,660	0,423 - 0,812	<0,001	0,37	0,24 - 0,50	10,7	-0,4 - 21,9
Histamine	0,481	0,181 - 0,699	0,003	12,80	8,94 - 16,66	-0,1	-0,2 - 0,1
Kynurenine	0,512	0,221 - 0,719	<0,001	0,19	0,04 - 0,34	0,4	0,1 - 0,8
Methionine Sulfoxide	0,312	-0,018 - 0,581	0,064	0,60	-0,03 - 1,24	1,1	0,8 - 1,5
Putrescine	0,537	0,253 - 0,736	<0,001	0,74	-0,02 - 1,50	0,1	-0,0 - 0,2
Symmetric Dimethylarginine	0,075	-0,260 - 0,394	0,663	0,00	-0,08 - 0,08	0,3	0,7 - 0,4
Serotonin	0,535	0,250 - 0,734	<0,001	0,30	0,20 - 0,41	0,1	-0,0 - 0,3
Spermidine	-0,080	-0,398 - 0,255	0,642	2,64	-6,62 - 11,89	4,1	2,3 - 5,9
Spermine	0,581	0,313 - 0,764	<0,001	35,56	15,64 - 55,47	-2,5	-6,7 - 1,7
Trans-Hydroxy-Proline	0,481	0,181 - 0,699	0,003	0,35	0,20 - 0,49	1,1	0,0 - 2,1
Taurine	0,103	-0,234 - 0,417	0,551	0,13	-0,23 - 0,48	140,0	108,0 - 171,9

Total DMA	0,345	0,018 - 0,605	0,040	0,29	0,017 - 0,56	0,5	0,2 - 0,8

***Table 16**. Correlation between DBS and serum in acylcarnitines.*

Analyte	**Rho**			**Slope**		**Intercept**	
	Coeff.	**IC 95**	**p-value**	**Coeff.**	**IC 95**	**Coeff.**	**IC 95**
C0	0.803	0.645 - 0.895	<0.001	0.32	0.23 - 0.40	7.3	3.7 - 10.9
C2	0.516	0.226 - 0.722	0.001	0.40	0.21 - 0.58	4.8	3.5 - 6.0
C3	0.619	0.364 - 0.787	<0.001	0.94	0.36 - 1.52	0.5	0.3 - 0.74
C3_OH	0.676	0.447 - 0.822	<0.001	0.01	-0.01 - 0.03	0.5	0.52 - 0.55
C3_1	0.676	0.447 - 0.822	<0.001	0.19	0.10 - 0.28	0.03	0.03 - 0.04
C4	0.632	0.383 - 0.795	<0.001	0.27	0.14 - 0.39	0.08	0.06 - 0.1
C4_1	0.492	0.195 - 0.706	0.002	0.12	0.02 - 0.21	0.03	0.03 - 0.04
C5	0.476	0.175 - 0.696	0.003	0.34	0.07 - 0.62	0.09	0.05 - 0.1
C5_DC_C6_OH_	0.676	0.447 - 0.822	<0.001	0.00	-0.03 - 0.04	0.05	0.05 - 0.06
C5_1	0.676	0.447 - 0.822	<0.001	0.02	-0.03 - 0.07	0.10	0.10 - 0.12
C5_1_DC	0.073	-0.262 - 0.392	0.671	0.11	-0.13 - 0.35	0.03	0.02 - 0.05
C7_DC	0.295	-0.0372 - 0.568	0.080	0.19	0.05 - 0.33	0.02	0.01 - 0.02
C8	0.543	0.261 - 0.740	<0.001	0.16	0.10 - 0.22	0.07	0.06 - 0.08
C10	0.030	-0.301 - 0.355	0.860	0.16	0.07 - 0.24	0.13	0.11 - 0.15
C10:1	0.375	0.0534 - 0.627	0.024	0.05	0.02 - 0.09	0.06	0.06 - 0.07
C12	0.047	-0.286 - 0.370	0.785	0.22	0.11 - 0.33	0.04	0.03 - 0.05
C12:1	0.124	-0.214 - 0.434	0.472	0.14	0.07 - 0.20	0.06	0.06 - 0.07
C14	-0.11	-0.423 - 0.227	0.523	-0.70	-2.69 - 1.29	0.22	0.01 - 0.4
C14:1	0.547	0.267 - 0.742	<0.001	0.09	0.01 - 0.16	0.11	0.10 - 0.12
C16	0.299	-0.0328 - 0.571	0.076	1.05	-0.37 - 2.49	0.44	0.2 - 0.6
C16_OH	0.042	-0.290 - 0.366	0.804	0.05	-0.46 - 0.56	0.03	0.01 - 0.05
C18	0.150	-0.188 - 0.456	0.383	3.02	-4.01 - 10.07	0.12	-0.4 - 0.6
C18:1	0.418	0.104 - 0.657	0.011	1.71	0.41 - 3.01	1.00	0.6 - 1.3
C18:2	0.486	0.188 - 0.703	0.002	2.53	1.13 - 3.92	0.24	0.02 - 0.4

***Table 17**. Correlation between DBS and serum in glycerophospholipids.*

Analyte	Rho			Slope		Intercept	
	Coeff.	IC 95	p-value	Coeff.	IC 95	Coeff.	IC 95
LysoPCaC14:0	0.512	0.220 - 0.719	0.001	0.17	0.11 - 0.23	1.08	0.96 - 1.21
LysoPCaC16:0	0.334	0.006 - 0.597	0.046	0.15	0.01 - 0.28	27.99	13.24 - 42.73
LysoPCaC16:1	0.511	0.219 - 0.719	0.002	0.27	0.17 - 0.37	0.32	-0.01 - 0.65
LysoPCaC17:0	0.338	0.011 - 0.600	0.044	0.19	0.01 - 0.36	0.72	0.35 - 1.08
LysoPCaC18:0	0.623	0.371 - 0.790	<0.001	0.32	0.17 - 0.47	5.07	0.48 - 9.66
LysoPCaC18:1	0.830	0.690 - 0.911	<0.001	0.33	0.25 - 0.41	2.167	-0.65 - 4.97
LysoPCaC18:2	0.787	0.619 - 0.887	<0.001	0.27	0.20 - 0.34	4.48	-0.29 - 9.24
LysoPCaC20:3	0.684	0.459 - 0.827	<0.001	0.21	0.13 - 0.29	0.56	0.22 - 0.9
LysoPCaC20:4	0.647	0.404 - 0.804	<0.001	0.18	0.10 - 0.26	1.78	0.86 - 2.67
LysoPCaC26:0	-0.055	-0.377 - 0.278	0.749	0.10	-1.74 - 1.93	2.89	2.00 - 3.73
LysoPCaC26:1	0.287	-0.046 - 0.563	0.084	3.18	-0.92 - 7.28	-0.31	-1.55 - 0.92
LysoPCaC28:0	0.396	0.078 - 0.641	0.017	1.08	0.08 - 2.09	1.37	0.72 - 2.03
LysoPCaC28:1	0.549	0.269 - 0.743	<0.001	0.84	0.36 - 1.33	0.88	0.54 - 1.22
PCaaC24:0	-0.273	-0.552 - 0.062	0.108	-1.14	-2.86 - 0.58	1.05	0.83 - 1.28
PCaaC26:0	0.215	-0.122 - 0.508	0.207	2.39	0.47 - 4.32	0.32	-1.14 - 1.79
PCaaC28:1	0.570	0.297 - 0.757	<0.001	0.39	0.19 - 0.60	2.05	1.38 - 2.71
PCaaC30:0	0.673	0.442 - 0.820	<0.001	0.39	0.26 - 0.51	2.36	1.76 - 2.95
PCaaC30:2	0.279	-0.055 - 0.556	0.100	0.12	-0.14 - 0.38	0.30	0.24 - 0.36
PCaaC32:0	0.142	-0.196 - 0.450	0.409	0.14	-0.15 - 0.43	20.84	16.30 - 25.38
PCaaC32:1	0.719	0.511 - 0.847	<0.001	0.32	0.22 - 0.42	3.16	1.78 - 4.54
PCaaC32:2	0.658	0.420 - 0.811	<0.001	0.26	0.176 - 0.35	0.56	0.20 - 0.92
PCaaC32:3	0.551	0.272 - 0.745	<0.001	0.26	0.11 - 0.42	0.32	0.23 - 0.41
PCaaC34:1	0.417	0.102 - 0.655	0.012	0.24	0.09 - 0.39	100.90	66.78 - 135.02
PCaaC34:2	0.730	0.528 - 0.854	<0.001	0.36	0.23 - 0.48	53.17	2.84 - 103.51
PCaaC34:3	0.697	0.477 - 0.834	<0.001	0.27	0.18 - 0.36	2.70	1.40 - 3.99
PCaaC34:4	0.706	0.491 - 0.840	<0.001	0.19	0.12 - 0.27	0.32	0.17 - 0.47
PCaaC36:0	0.641	0.396 - 0.801	<0.001	1.74	1.00 - 2.49	3.41	1.26 - 5.55
PCaaC36:1	0.428	0.116 - 0.663	0.009	0.25	0.10 - 0.40	33.50	26.52 - 40.53
PCaaC36:2	0.800	0.640 - 0.894	<0.001	0.32	0.24 - 0.41	34.79	12.75 - 56.84
PCaaC36:3	0.705	0.489 - 0.839	<0.001	0.28	0.20 - 0.35	17.35	6.35 - 28.36
PCaaC36:4	0.485	0.186 - 0.701	0.003	0.21	0.13 - 0.29	22.01	7.05 - 36.97
PCaaC36:5	0.741	0.545 - 0.860	<0.001	0.20	0.14 - 0.27	1.40	0.55 - 2.26
PCaaC36:6	0.635	0.387 - 0.797	<0.001	0.21	0.13 - 0.29	0.16	0.09 - 0.22
PCaaC38:0	0.688	0.464 - 0.829	<0.001	0.67	0.37 - 0.98	1.85	0.53 - 3.17
PCaaC38:1	0.631	0.381 - 0.795	<0.001	1.80	0.90 - 2.70	2.35	1.14 - 3.56
PCaaC38:3	0.737	0.539 - 0.858	<0.001	0.29	0.19 - 0.39	7.87	3.77 - 11.97
PCaaC38:4	0.728	0.525 - 0.853	<0.001	0.22	0.15 - 0.29	9.76	3.26 - 16.25
PCaaC38:5	0.654	0.415 - 0.809	<0.001	0.18	0.10 - 0.26	5.74	2.33 - 9.15
PCaaC38:6	0.731	0.529 - 0.854	<0.001	0.19	0.12 - 0.25	6.65	1.57 - 11.73
PCaaC40:1	0.381	0.061 - 0.631	0.022	3.68	0.59 - 6.78	-1.05	-2.92 - 0.82
PCaaC40:2	0.358	0.034 - 0.615	0.032	1.29	0.19 - 2.39	0.66	0.33 - 0.98
PCaaC40:3	0.342	0.015 - 0.603	0.041	0.88	0.10 - 1.66	1.02	0.57 - 1.47

PCaaC40:4	0.657	0.419 - 0.811	<0.001	0.36	0.21 - 0.50	0.80	0.33 - 1.27
PCaaC40:5	0.636	0.388 - 0.798	<0.001	0.20	0.11 - 0.29	1.13	0.45 - 1.81
PCaaC40:6	0.779	0.605 - 0.882	<0.001	0.20	0.14 - 0.26	1.97	0.49 - 3.46
PCaaC42:1	0.433	0.122 - 0.667	0.008	0.43	0.12 - 0.74	0.40	0.29 - 0.51
PCaaC42:2	0.486	0.187 - 0.702	0.003	0.93	0.36 - 1.49	0.34	0.19 - 0.49
PCaaC42:4	0.475	0.173 - 0.695	0.003	0.77	0.26 - 1.27	0.16	0.08 - 0.25
PCaaC42:5	0.637	0.390 - 0.798	<0.001	0.70	0.38 - 1.03	0.12	0.03 - 0.20
PCaaC42:6	0.480	0.179 - 0.698	0.003	0.51	0.17 - 0.86	0.31	0.19 - 0.43
PCaeC30:0	0.569	0.295 - 0.756	<0.001	0.55	0.30 - 0.81	0.42	0.31 - 0.53
PCaeC30:1	0.414	0.099 - 0.654	0.012	0.39	0.10 - 0.68	0.18	0.12 - 0.24
PCaeC32:1	0.737	0.540 - 0.858	<0.001	0.36	0.25 - 0.48	0.89	0.49 - 1.28
PCaeC32:2	0.738	0.540 - 0.858	<0.001	0.43	0.29 - 0.57	0.36	0.23 - 0.49
PCaeC34:0	0.386	0.065 - 0.634	0.020	0.29	0.032 - 0.51	2.08	1.76 - 2.41
PCaeC34:1	0.572	0.300 - 0.758	<0.001	0.32	0.18 - 0.47	4.77	3.12 - 6.43
PCaeC34:2	0.677	0.449 - 0.823	<0.001	0.29	0.20 - 0.38	3.67	2.13 - 5.20
PCaeC34:3	0.682	0.456 - 0.826	<0.001	0.24	0.17 - 0.32	1.77	0.78 - 2.75
PCaeC36:0	0.402	0.085 - 0.645	0.015	0.87	0.21 - 1.53	1.83	1.23 - 2.42
PCaeC36:1	0.534	0.249 - 0.734	<0.001	0.84	0.36 - 1.32	7.91	3.50 - 12.31
PCaeC36:2	0.725	0.520 - 0.851	<0.001	0.50	0.33 - 0.66	5.18	2.26 - 8.10
PCaeC36:3	0.705	0.489 - 0.839	<0.001	0.26	0.19 - 0.34	1.62	0.78 - 2.45
PCaeC36:4	0.711	0.499 - 0.843	<0.001	0.20	0.13 - 0.28	2.79	1.21 - 4.37
PCaeC36:5	0.676	0.446 - 0.822	<0.001	0.20	0.13 - 0.27	1.59	0.57 - 2.60
PCaeC38:0	0.575	0.304 - 0.760	<0.001	0.50	0.26 - 0.74	1.01	0.56 - 1.46
PCaeC38:1	0.614	0.357 - 0.784	0.001	4.55	2.51 - 6.60	2.60	2.04 - 3.16
PCaeC38:2	0.674	0.444 - 0.821	<0.001	1.61	1.08 - 2.14	1.52	0.39 - 2.66
PCaeC38:3	0.617	0.362 - 0.786	<0.001	0.60	0.33 - 0.87	2.09	0.96 - 3.22
PCaeC38:4	0.592	0.328 - 0.771	0.001	0.22	0.13 - 0.31	2.41	1.07 - 3.74
PCaeC38:5	0.680	0.453 - 0.824	<0.001	0.20	0.12 - 0.27	2.38	0.80 - 3.96
PCaeC38:6	0.795	0.631 - 0.891	<0.001	0.22	0.17 - 0.27	0.71	0.25 - 1.19
PCaeC40:1	0.538	0.255 - 0.737	<0.001	0.95	0.44 - 1.46	1.14	0.48 - 1.80
PCaeC40:2	0.268	-0.066 - 0.548	0.114	0.46	-0.14 - 1.05	2.41	1.45 - 3.38
PCaeC40:3	0.545	0.264 - 0.741	<0.001	0.99	0.47 - 1.50	0.85	0.33 - 1.36
PCaeC40:4	0.696	0.476 - 0.834	<0.001	0.41	0.23 - 0.59	0.67	0.19 - 1.14
PCaeC40:5	0.619	0.364 - 0.787	0.001	0.36	0.21 - 0.52	0.84	0.15 - 1.52
PCaeC40:6	0.753	0.565 - 0.867	<0.001	0.25	0.18 - 0.32	0.53	0.15 - 0.927
PCaeC42:0	0.430	0.118 - 0.664	0.009	0.81	0.23 - 1.39	0.25	0.03 - 0.47
PCaeC42:1	0.277	-0.056 - 0.555	0.101	1.92	0.19 - 3.65	0.53	-0.04 - 1.10
PCaeC42:2	0.162	-0.176 - 0.465	0.346	0.48	-0.12 - 1.08	1.23	0.86 - 1.59
PCaeC42:3	0.553	0.274 - 0.746	<0.001	0.62	0.33 - 0.90	0.53	0.27 - 0.79
PCaeC42:4	0.631	0.381 - 0.795	<0.001	0.45	0.25 - 0.64	0.26	0.07 - 0.46
PCaeC42:5	0.584	0.316 - 0.766	<0.001	0.28	0.15 - 0.41	0.75	0.41 - 1.08
PCaeC44:3	0.511	0.220 - 0.719	0.001	0.91	0.33 - 1.48	0.14	0.06 - 0.21
PCaeC44:4	0.647	0.405 - 0.805	<0.001	0.38	0.17 - 0.59	0.21	0.12 - 0.29
PCaeC44:5	0.686	0.461 - 0.828	<0.001	0.24	0.17 - 0.30	0.26	0.10 - 0.41
PCaeC44:6	0.728	0.525 - 0.852	<0.001	0.26	0.18 - 0.34	0.21	0.11 - 0.31

Table 18. *Correlation between DBS and serum in sphingomyelins.*

Analyte	Rho			Slope		Intercept	
	Coeff.	**IC 95**	**p-value**	**Coeff.**	**IC 95**	**Coeff.**	**IC 95**
SM OH C14:1	0.303	-0.027 - 0.575	0.072	0.26	0.06 - 0.46	5.52	3.95 - 7.09
SM OH C16:1	0.269	-0.065 - 0.549	0.113	0.33	0.07 - 0.59	2.62	1.67 - 3.58
SM OH C22:1	0.373	0.050 - 0.625	0.025	0.19	0.04 - 0.35	6.00	3.89 - 8.12
SM OH C22:2	0.625	0.374 - 0.791	<0.001	0.28	0.17 - 0.40	3.42	2.01 - 4.84
SM OH C24:1	-0.012	-0.339 - 0.318	0.944	-0.13	-0.57 - 0.31	2.27	1.70 - 2.84
SM C16:0	0.207	-0.130 - 0.501	0.225	0.21	-0.009 - 0.43	95.00	67.92 - 122.08
SM C16:1	0.646	0.403 - 0.804	<0.001	0.37	0.23 - 0.50	6.02	3.57 - 8.47
SM C18:0	0.384	0.063 - 0.632	0.020	0.39	0.19 - 0.60	9.45	5.04 - 13.86
SM C18:1	0.514	0.223 - 0.721	0.001	0.43	0.27 - 0.59	2.92	1.20 - 4.64
SM C20:2	0.619	0.364 - 0.787	0.001	0.27	0.14 - 0.40	0.14	0.07 - 0.20
SM C22:3	0.474	0.173 - 0.695	0.003	0.18	0.09 - 0.26	0.09	0.012 - 0.17
SM C24:0	-0.158	-0.462 - 0.180	0.357	-0.28	-0.86 - 0.30	48.35	36.19 - 60.51
SM C24:1	0.122	-0.215 - 0.433	0.477	0.22	-0.27 - 0.73	56.57	31.67 - 81.46
SM C26:0	-0.181	-0.481 - 0.156	0.289	-1.11	-4.72 - 2.48	2.18	1.46 - 2.90
SM C26:1	-0.080	-0.399 - 0.255	0.640	-1.12	-3.97 - 1.72	3.36	2.10 - 4.62

8.4. CIRCADIAN METABOLIC PROFILING IN HEALTH AND IN STATES OF CORTISOL RHYTHM DERANGEMENT

Targeted analysis of 187 metabolites in DBS samples was performed to reveal distinct circadian metabolic patterns across the four investigated cohorts, including healthy subjects (HS), and patients with adrenal insufficiency (AI) under glucocorticoid replacement, mild autonomous cortisol secretion (MACS), and overt Cushing Syndrome.

Anthropometric characteristics of the study population are summarized in **Table 19.**

Factor analysis (FA) identified two major molecular patterns explaining most of the variance, in terms of abundance and fluctuation, between HS and CS, which were considered the two extreme phenotypes. Pattern A is mostly dominated by phosphatidylcholines (PCs), whereas pattern B is mostly dominated by acylcarnitines (ACs), amino acids (AAs), and biogenic amines (BAs). The list of compounds driving the information within pattern A and B, and the associated FA-derived coefficient are reported in **Figures 27** and **28**. Among these, the top five molecules with the highest FA-derived coefficients were selected from each pattern in order to maximize the differences between HS and CS, and used to model the circadian fluctuation equations in each group. These were PC-aa-C38:0, PC-ae-C44:3, PC-aa-C38:6, PC-ae-C42:5, and PC-aa-C36:0 for pattern A, and carnitine (C0), histidine, creatinine, asparagine, and spermidine for pattern B.

In HS, pattern A followed a well-defined U-shaped circadian rhythm, with molecule concentrations reaching their lowest levels before lunch and gradually increasing toward the evening back to levels of early morning (**Figure 29**). A second-order polynomial equation provided the best fit for these kinetics. In contrast, CS patients showed markedly lower levels of pattern A molecules, with a nearly monotonic increase throughout the day and a plateau in the late evening, best modeled by a third-order polynomial equation (**Figure 29**). These differences resulted in a complete lack of overlap between HS and CS from midday to night hours, highlighting a disrupted phospholipid rhythmicity under sustained hypercortisolism (**Figure 29**). For pattern B, HS again exhibited a second-order polynomial trend, with similar levels in early morning and late evening and low levels at midday (**Figure 30**). CS patients, instead, displayed higher overall concentrations compared to HS, with a monotonous trend best captured by a power-law model (**Figure 30**). Maximum divergences in concentrations between CS and HS were detected around midday and early afternoon (**Figure 30**).

AI patients under once-a-day glucocorticoid replacement therapy presented mixed behaviors. Pattern A metabolites in AI showed concentration levels lower than HS but similar to CS. At variance from CS, however, AI exhibited pronounced morning oscillations, possibly consistent with glucocorticoid medication intake after awakening, and a sharp rise toward the evening (**Figure 31**). Pattern B metabolites, instead, displayed concentration levels similar to HS, though with increased complexity of the morning fluctuation (**Figure 32**).

In MACS patients, an intermediate metabolic scenario appeared. Indeed, pattern A metabolites displayed an overall abundance lower than HS and similar to CS, although with a second order polynomial rhythm resembling the one of HS (**Figure 33**). Significant differences are found between MACS and CS in the evening (19:30 and 21:30). As to pattern B molecules, MACS displayed concentrations between those of HS and CS (**Figure 34**). A third order polynomial trend was found for these metabolites in MACS, paralleling the morning trend of HS and the evening trend of CS.

Table 19. *Anthropometric characteristics of the study population.*

Clinical Variables	Total Population (n=39)	HS (n=10)	MACS (n=12)	CS (n=9)	AI (n=8)	ANOVA (P)
Age (years)	51,9±15,5	41,6±18,5	66,9±6,8[a, d]	53,1±8,0	45,7±15,6	**0,001**
Weight (kg)	69,5±14,04	63,1±8,2	66,9±14,0	77,8±15,2	71,0±20,3	0,171
Height (m)	1,65±0,09	1,67±0,08	1,65±0,10	1,59±0,05	1,62±0,10	0,21
Waist (cm)	88,2±14,4	75,1±9,9	88,0±11,9[a]	102,7±12,7[b]	89,7±16,4	**0,001**
BMI (Kg/m2)	25,7±5,2	22,5±3,3	24,2±3,0	30,6±5,1[b, c]	26,9±7,8	**0,006**
FFM (Kg)	50,7±8,6	49,8±6,7	51,9±9,4	48,9±6,7[b]	48,2±10,7	**0,011**
FFM (%/Weight)	74,0±10,4	79,2±8,0	77,0±7,9	64,3±6,5[b, c]	69,7±13,2	**0,005**
FM (Kg)	18,8±10,6	13,4±6,0	15,9±7,2	28,3±10,2	23,2±15,4	0,093
FM (%/Weight)	25,9±10,4	20,8±8,0	22,9±7,9	35,7±6,5[b, c]	30,2±13,2	**0,005**
Fasting blood glucose (mg/dl)	97,8±44,0	90,0±6,5	80,7±10,0	101,7±48,2	81,1±10,4	0,324
Glycated Hb (mmol/mol)	38,4±6,8	-	37,9±5,0	42,8±10,5	35,9±2,9	0,246
Insulin (mU/ml)	5,86±2,67	-	5,2±2,62	7,85±2,63	4,31±1,54[e]	**0,026**
Triglycerides (mg/dl)	107±55,9	85,2±31,6	84,4±34,2	92,4±47,0	167,6±81,4[d, e, f]	**0,026**
Total Cholesterol (mg/dl)	202±53	198±48	183±53	183±49	245,5±48	0,100
HDL Cholesterol (mg/dl)	60,8±17,7	76,4±18,9	59,7±15,7	51,8±10,6[b]	65±11,7	**0,032**
LDL Cholesterol (mg/dl)	124±41	110±28	106±41	119±44	157±29	0,099
Basal Cortisol (ng/ml)	148±46	-	132±25	169±59		0,062
post-DST Cortisol (ng/ml)	76,0±61,6	-	46,8±30,2	122,6±62,7[c]		**0,01**

a: MACS vs HS, p<0,050; b: CS vs HS, p<0,050; c: CS vs MACS, p<0,050 d: AI vs MACS; e: AI vs HS, p<0.050; f: AI vs CS, p<0.05

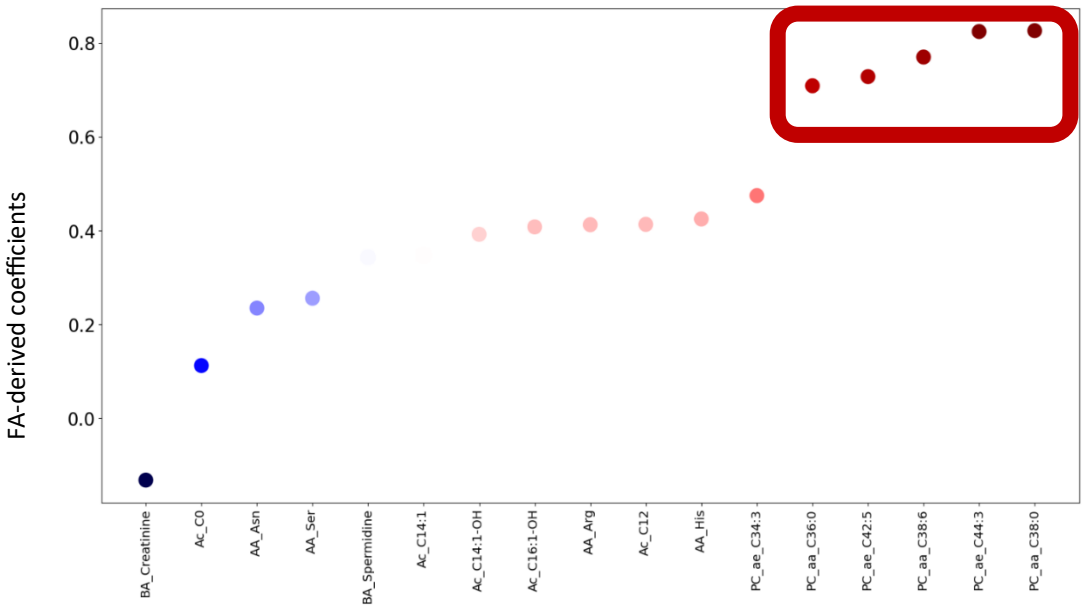

Figure 27. *list of compounds (x axis) that predominantly drive the information in pattern A. Highlighted in red, there are the five top molecules with the highest FA-derived coefficients.*

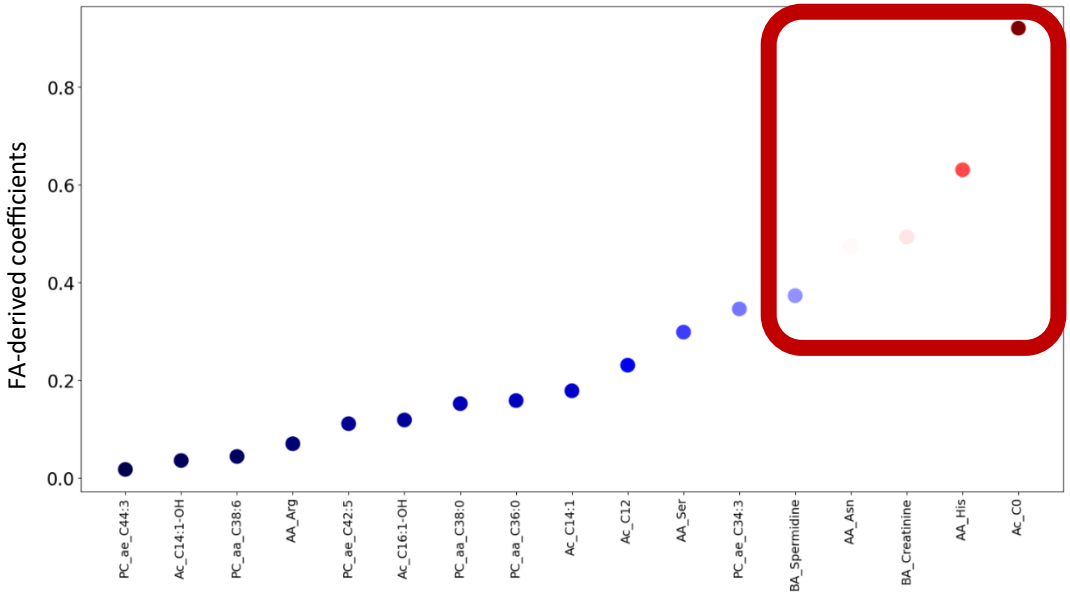

Figure 28. *list of compounds (x axis) that predominantly drive the information in pattern B. Highlighted in red, there are the five top molecules with the highest FA-derived coefficients.*

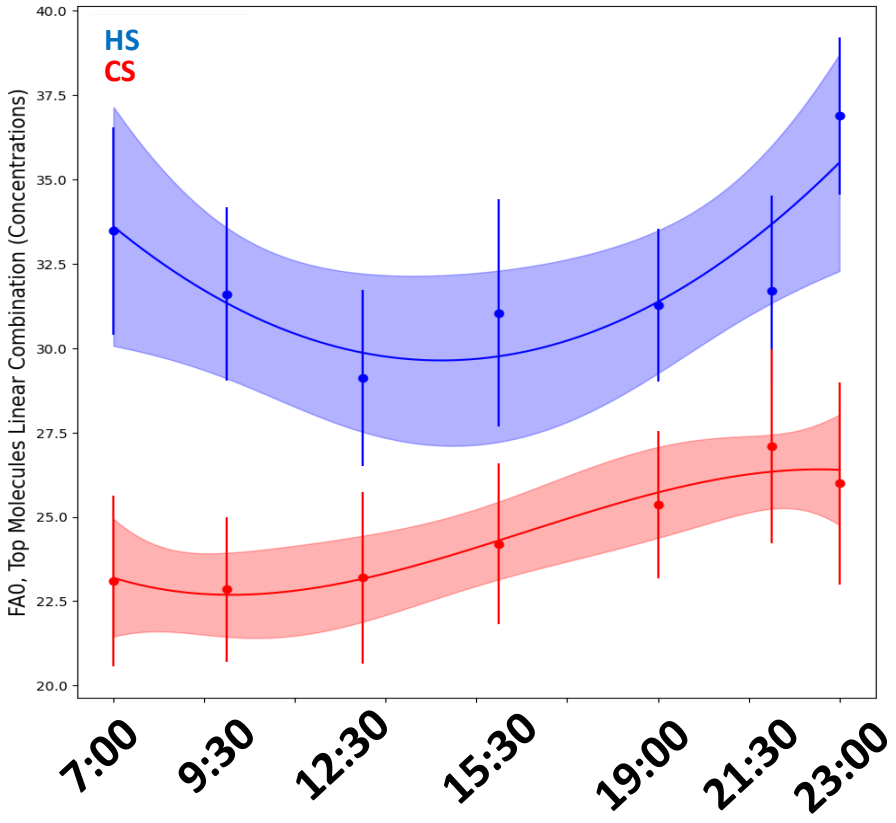

Figure 29. *Pattern A daily fluctuation in HS (blue) and CS (red) across the seven timepoints. Dots and bars: mean and st.dev. Shades: 95% CI. p<0.05 for each time point.*

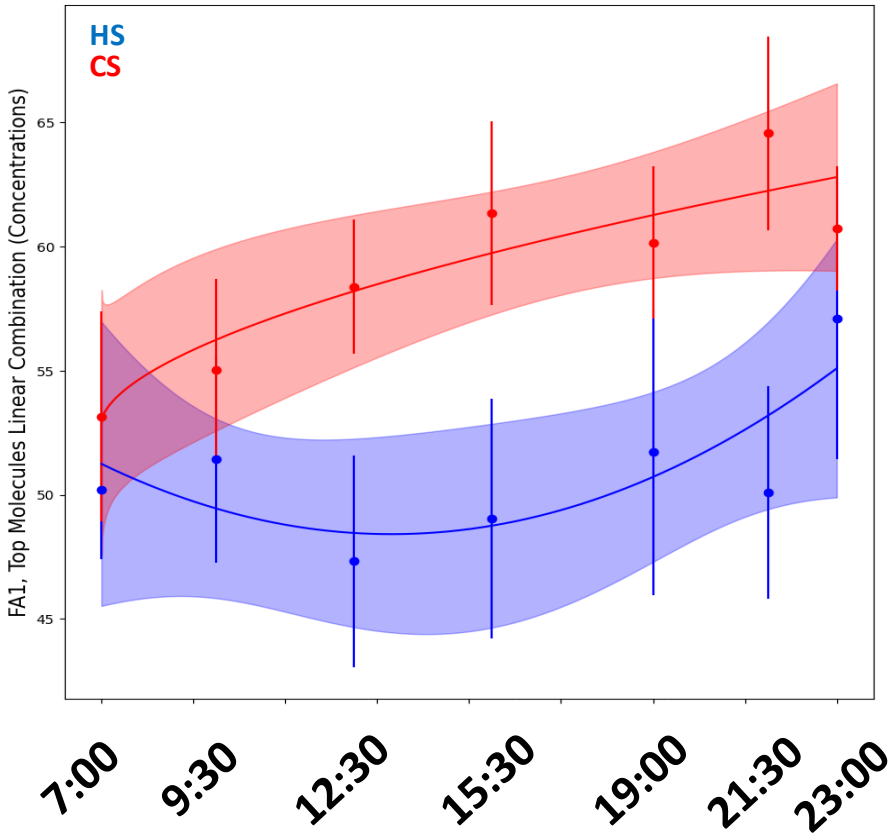

Figure 30. *Pattern B daily fluctuation in HS (blue) and CS (red) across the seven timepoints. Dots and bars: mean and st.dev. Shades: 95% CI. p<0.05 for each time point.*

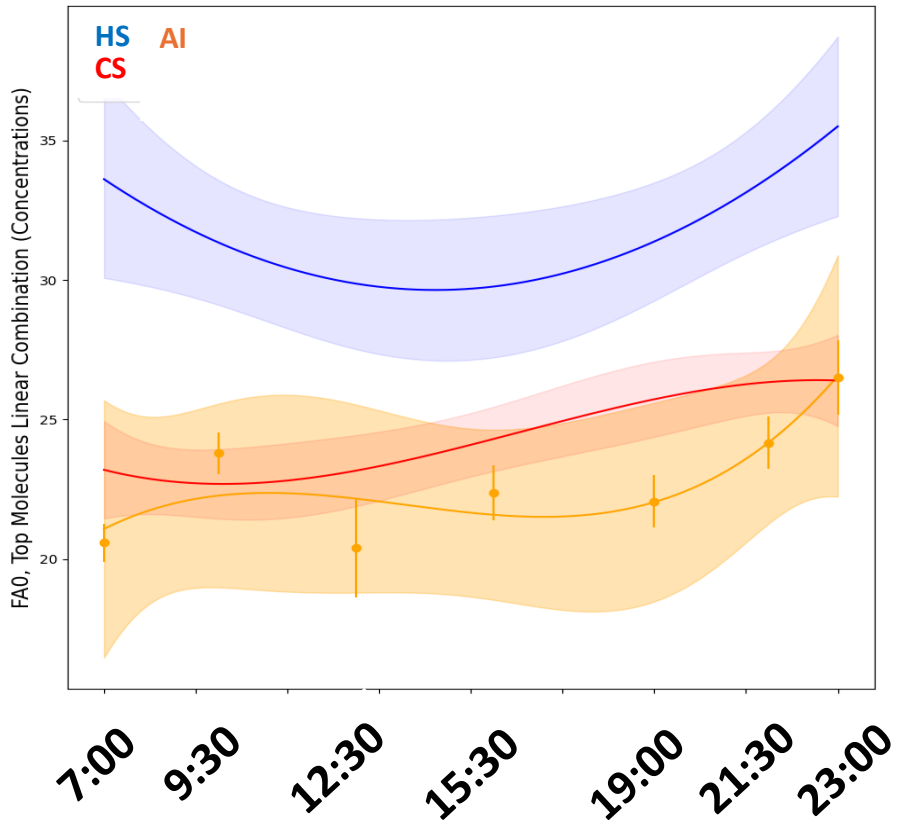

Figure 31. *Pattern A daily fluctuation in AI (orange) across the seven timepoints. Dots and bars: mean and st.dev. Shades: 95% CI. p<0.05 for each time point.*

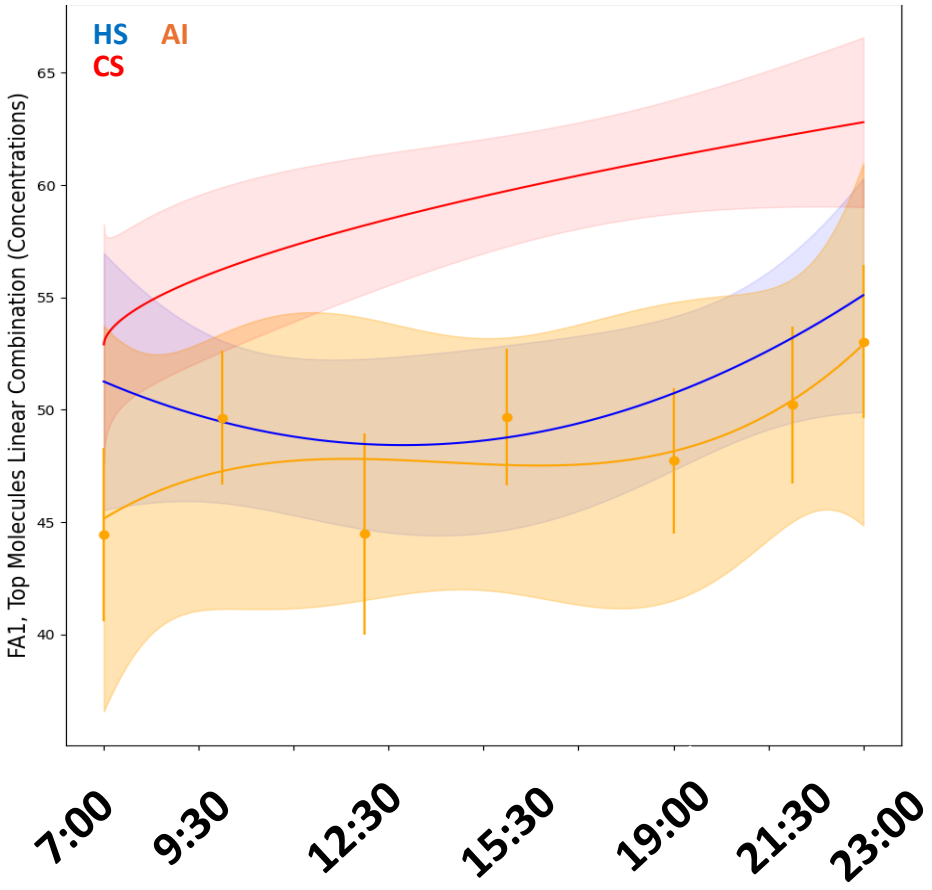

Figure 32. *Pattern B daily fluctuation in AI (orange) across the seven timepoints. Dots and bars: mean and st.dev. Shades: 95% CI. p<0.05 for each time point.*

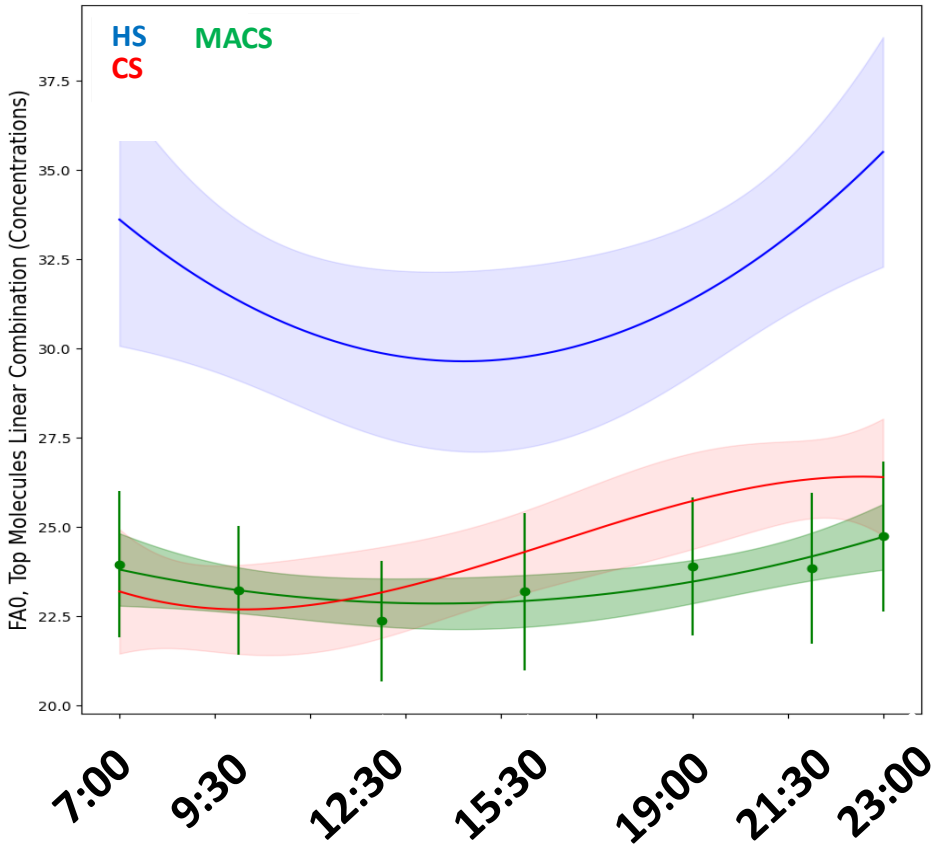

Figure 33. *Pattern A daily fluctuation in MACS (green) across the seven timepoints. Dots and bars: mean and st.dev. Shades: 95% CI. p<0.05 for each time point.*

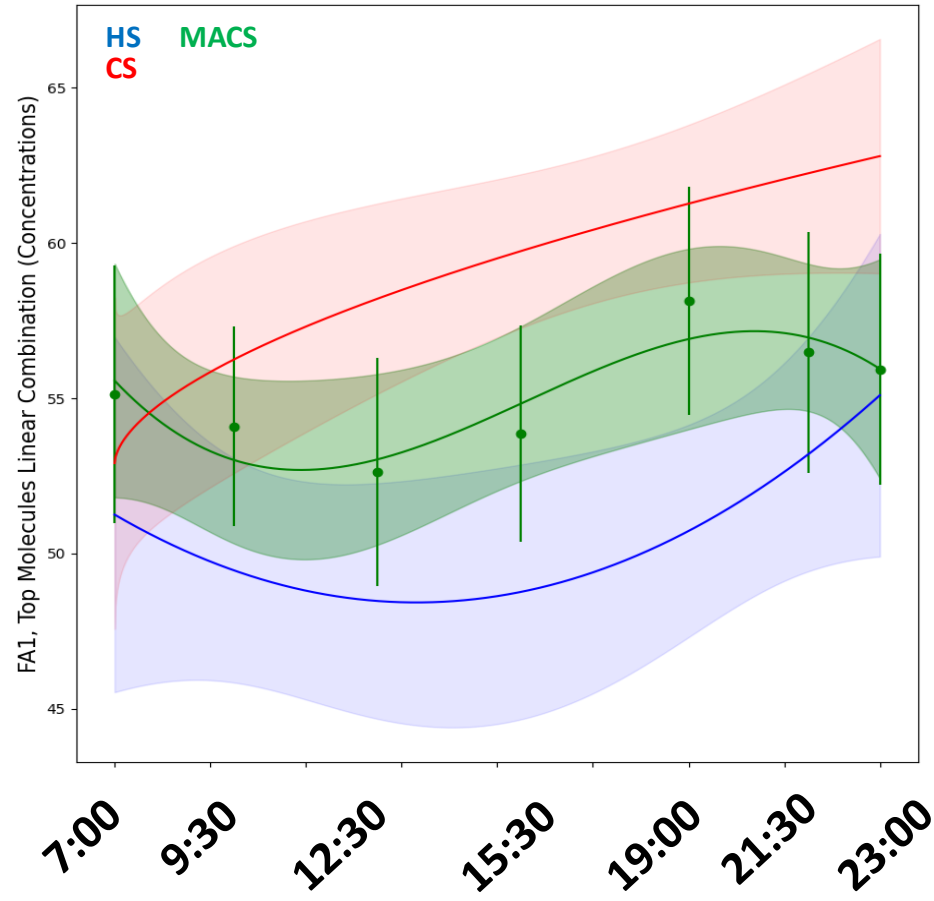

Figure 34*. Pattern B daily fluctuation in MACS (green) across the seven timepoints. Dots and bars: mean and st.dev. Shades: 95% CI. p<0.05 for each time point.*

9. DISCUSSION

9.1. DEVELOPMENT AND OPTIMIZATION OF AN LC-MS/MS METHOD FOR ENDOGENOUS AND EXOGENOUS STEROIDS IN DBS

Endogenous steroids are key molecules produced by various glands that play a fundamental role as hormones in all stages of life, regulating body and brain development, sexual behavior, fertility, physical activity, stress response, inflammatory response, and carbohydrate homeostasis. Steroid hormones are metabolized by several districts and tissues, generating a vast set of molecules contained in biological fluids, which are nowadays defined as steroidome. Based on the type of action they perform, steroid hormones are classified into five groups: mineralocorticoids, glucocorticoids, androgens, progestogens and estrogens (175). Alterations in the release, metabolization and bioavailability of these hormones are known to play a role in the etiopathogenesis of chronic non-communicable diseases, including cardiovascular diseases, obesity, and diabetes. In addition, conditions of excess or deficiency in the function of the adrenal gland can give rise to endocrine diseases such as hypercortisolism, hyperaldosteronism, congenital adrenal hyperplasia (CAH), or adrenal insufficiency. On the other hand, hyperandrogenism in women and hypogonadism in men are among the most frequent endocrine disorders in the adult population, representing a major cause of infertility and metabolic disorders. Exogenous steroids such as synthetic corticosteroids are used in hormone replacement therapy for adrenal insufficiency, as well as for immunosuppressive and anti-inflammatory purposes in numerous non-endocrine diseases. Overall, in 2019 corticosteroid drugs accounted for 15-23% of all drug prescriptions in Italy (192). In the OsMed 2023 Report, systemic corticosteroids and inhalers continue to be among the most prescribed therapeutic categories, with stable consumption compared to previous years and a slight increase in overall expenditure related to chronic use in adults and the elderly (193). Nevertheless, the pharmacokinetics of these molecules have not yet been clearly defined. In fact, it is unclear how body composition or liver and kidney function may influence the absorption, distribution, metabolism, and excretion of corticosteroids. Furthermore, drug doses are determined based on inflammatory parameters, without taking into account actual circulating drug levels, residual hypothalamic-pituitary-adrenal (HPA) axis function and circadian rhythm alterations. Constant monitoring of endogenous and exogenous steroid levels

would provide an opportunity to avoid overdosing patients, which would lead to a condition of iatrogenic hypercortisolism (175). Long term consequences of medium-term therapies with corticosteroids on the HPA axis are such that it may remain suppressed for an indefinite time, thereby posing the patient in a condition of induced adrenal insufficiency.

While benefits of monitoring the corticosteroid therapy and its effect on the endogenous steroidome are easily foreseen, the practicability of it is still far from being achieved. Indeed, therapeutic monitoring would require frequent blood sampling, which is difficult to obtain in fragile or home-based patients, especially those living in remote areas. Furthermore, Italian clinical laboratories rarely offer the possibility of measuring exogenous steroids, making monitoring virtually impossible.

Phlebotomy procedure involves a certain degree of invasiveness and discomfort for patients, at the same time requiring access to hospital facilities. A convenient alternative to venipuncture is blood drops obtained from finger pricks and absorbed onto cardboard, i.e.: dried blood spots (DBS). The use of DBS has several advantages: first, finger-prick sampling is less painful for the patient and requires a very small volume of blood. This is particularly important in newborns, children, or adults in critical condition. In addition, DBS collection is easy to perform and could be done independently by the patient at home, with significant advantages in terms of quality of life and of cost savings for healthcare facilities (194). From a logistic point of view, transporting DBS is easier than transporting venous blood samples: no refrigeration systems are required, resulting in lower costs and fewer risks for sample preservation (194). In fact, the absorption and solid nature of DBS make the analytes typically less reactive than in liquid blood, showing excellent stability even at room temperature, from a minimum of a few days to several months in some cases (194).

Measuring steroids has always represented an important analytical challenge. In fact, there are numerous compounds that belong to the steroid family, and they are so similar in terms of structure and physical-chemical properties that it is extremely difficult to identify and quantify them correctly. In many Italian centers, steroids are still measured using immunometric methods, which have significant limitations in terms of sensitivity and specificity, making these techniques obsolete and difficult to reproduce, often leading to incorrect diagnoses and inappropriate therapeutic choices. In addition, the panel of steroids measured in routine laboratories is usually limited to a few active hormones and precursors, leaving the overall steroidome picture largely uncovered. Mass spectrometry has contributed enormously to

current knowledge about the metabolism and action of steroid hormones (176). Today, the technology of choice for the study of steroids is liquid chromatography-tandem mass spectrometry (LC-MS/MS). This technique has high specificity and sensitivity compared to immunometric tests and allows the analysis of different molecules in the same analytical run (multiplexing). The application of this technology in routine clinical laboratories for steroid analysis is a reality in centers of excellence in Europe. In Italy, however, its use is still rare and limited to a few steroids. The Endocrinology research group of the Department of Medical and Surgical Sciences has been using LC-MS/MS since 2007 to develop quantitative methods for steroid panels in different biological fluids, applying them to the study of large populations and numerous endocrine and non-endocrine diseases (195) (196). LC-MS/MS has already proven useful for measuring steroid drugs in serum and saliva. However, only a few studies have evaluated the presence of exogenous and endogenous steroids simultaneously, and only a few applications were reported in DBS (197) (198). DBS are widely and successfully used for newborn screening: however, in this application, LC-MS/MS analysis is not properly quantitative but mainly focused on determining analyte absence/presence or very large variation from the normal levels (199).

In the present study, preliminary developmental work was performed for the optimization of LC-MS/MS methods for the simultaneous quantification of a large number of exogenous and endogenous steroids in DBS. Two analytical panels were developed, based on the favorite ionization polarity of the analytes of interest, one in ESI-, and one in ESI+, the first including 16 compounds and the second 18 compounds. These included precursors, metabolites and active hormones from all steroid classes as well as steroid drugs such as prednisone, prednisolone, methylprednisolone, dexamethasone, budesonide and beclomethasone.

As mentioned above, the accurate measurement of steroids is challenging, due to their structural similarity. Accordingly, a crucial hamper to overcome during the developmental phase consisted in the chromatographic separation of steroidal compounds that generated cross-reactive signals in the MS/MS detection. The chromatographic optimization was initially performed using a Kinetex® Luna C8 100 Å (2.6 µm, 100 × 3 mm), which is a core-shell chromatographic column, commonly used for the separation of hydrophobic compounds. Thanks to the solid, non-porous core surrounded by a thin, porous shell of stationary phase material design, it allows for the separation of molecules with similar structures such as steroids. Nevertheless, under this stationary phase, the isobars cortisone and prednisolone, as well as cortisol, 20α-dihydrocortisone and 20β-dihydrocortisone, were not baseline-separated.

Attempts to optimize the chromatographic gradient to determine the separation of these molecules were insufficient, therefore, the Kinetex® Biphenyl 100 Å (2.6 µm, 100 × 3 mm) column was tested for the ESI- panel, which resulted in the effective separation of the analytes of interest. C8 columns are based on purely hydrophobic interactions; biphenyl columns, on the other hand, have an aromatic stationary phase, with two benzene rings linked to a silane group: this also allows π-π and dipolar interactions. Steroids have conjugated or isolated double bonds in certain cases, carbonyl, hydroxyl, and local unsaturated groups, and rigid planar surfaces that allow π-π or stacking interactions with the biphenyl phase. As a result, the biphenyl column "recognizes" small structural differences better than C8 columns (184) (200) (201). After the definition of these two analytical panels for steroids, the additive to the mobile phase ammonium fluoride was evaluated at different concentrations as enhancer of the sensitivity of the methods. Ammonium fluoride is a recently introduced common additive in ESI-MS, reported in the literature across applications as an effective volatile compound, hypothesized to work as a sequestration agent. During the ESI process, ammonium fluoride can complex with interfering ions, enhancing the formation of the desired protonated or deprotonated molecular species (202). During the developmental phase, results showed that the use of ammonium fluoride was essential to achieve the required sensitivity of the two methods, with a maximum reached with the concentration level of 50 µM. However, prolonged use of ammonium fluoride caused frequent LC column failures and compromised the integrity of the current HPLC system, mainly because of back-pressure issues. These technical difficulties created a "stop-and-go" workflow, which is one of the reasons that limited the possibility to fulfill a complete validation of the developed methods. In this context, the concentration of ammonium fluoride was ultimately settled at 10 µM for the analysis, representing the compromise between the sensitivity of the methods and the viability of the HPLC system. With such a compromise, a preliminary assessment of linearity, accuracy, and precision was performed thereby supporting the effectiveness of the developed methods. The evidence and know-how gathered so far represent a solid background for the future transfer of the methods to a new generation UPLC-triple quadrupole platform, expected in 2026 in our department, and for the thorough validation complying with current guidelines.

Given that the analytical performance of the method is not solely determined by chromatographic or instrumental parameters, but also by the efficiency of sample preparation, subsequent work focused on optimizing the extraction of steroids from DBS. According to the literature, DBS soaking in solvent approach is the prevalent strategy. Therefore, in the first

attempts, several combinations of acetonitrile, methanol and water were tested, coupled to mechanical agitation, like vortex and/or ultrasound bath (179) (199) (203) (204). Among these, the best procedure was using acetonitrile: methanol 80:20 (v/v) and sonication. This could be due to the fact that acetonitrile is less polar than methanol or water, so it may better extract neutral or moderately polar compounds from matrices. Acetonitrile, especially when mixed with methanol, causes protein denaturation and precipitation, thereby ensuring the release of compounds bound to proteins or the matrix. Nevertheless, this extraction procedure alone did not provide satisfactory overall efficiency, prompting the evaluation of additional purification strategies. LLE with MTBE showed high recovery for neutral steroids but caused substantial losses of sulfated species, likely due to their poor partitioning into the organic phase; on the other hand, SPE provided a more homogeneous recovery across both neutral and conjugated steroids, balancing selectivity and reproducibility, presumably removing interfering elements, such as phospholipids. Overall, the development of an extraction protocol for DBS remains a highly challenging task due to the complexity of the matrix and the need for accurate quantitative measurements. Several instrumental and methodological challenges were encountered and addressed during this preliminary phase. While the optimized workflow described here represents a promising starting point, full analytical validation according to current guidelines will be completed with the installation of a new generation UPLC-MS/MS platform in 2026, which will allow further refinement and improvement of the entire analytical workflow.

9.2. CIRCADIAN STEROID PROFILING AND COMPLEMENTARY METHOD DEVELOPMENT AT THE UNIVERSITY OF GENEVA (UNIGE)

9.2.1. CHARACTERIZATION OF THE CIRCADIAN STEROIDOME IN DBS

When steroid hormones undergo metabolism within tissues, they generate an extensive group of resulting molecules present in biological fluids; this entire set is referred to as the steroidome. To obtain a more complete picture of the steroidome, two main strategies can be adopted: untargeted and targeted analysis. Untargeted analysis, often using LC coupled with High-Resolution Mass Spectrometry (LC-HRMS), offers the benefit of faster method setup and

allows for compound annotation or identification after the data has been collected, even permitting retrospective analysis (205). However, this approach faces significant challenges when dealing with steroids. The fragmentation patterns and collision cross sections of steroids are typically non-specific, making it hard to reliably identify them in untargeted screens based solely on HRMS, MS/MS, or even Ion Mobility Spectrometry (IMS) data (206). Furthermore, the low concentration and poor ionization efficiency of many steroids pose a major limitation for these untargeted methods. Therefore, the most robust and effective approach is to combine a highly efficient LC separation, which provides known and stable retention times, with a multi-targeted analysis workflow. This method utilizes Multiple Reaction Monitoring (MRM) with unique, distinctive fragments for each individual steroid metabolite, offering an accurate and sensitive profile of formally identified steroids in biological samples. This powerful multi-targeted strategy can also be extended to provide precise absolute quantification of selected compounds (185). Absolute quantification in metabolomics is crucial for several key objectives: comparing metabolite levels against established reference intervals, establishing and validating effective disease biomarkers, and gaining a mechanistic understanding of biological responses triggered by diseases and medical treatments (207) (208). The standard method for determining a metabolite's concentration-response relationship involves using an external calibration curve. This approach enables the calculation of analyte unknown concentration of a sample (209). However, a major difficulty arises when analyzing endogenous compounds, those naturally present in biological matrices; because these compounds are already present, it becomes practically arduous to use a truly "blank" matrix to create the necessary external calibration curve, which is a significant constraint in this type of analysis. Therefore, an appealing and straightforward option that bypasses the complex requirement of assessing matrix similarity is the internal calibration approach (210). The fundamental principle of this method is to use stable isotope labeled compounds as internal standards and internal calibrants at the same time (211) (187). According to the internal calibration strategy recently proposed by the group of Prof. Serge Rudaz of the University of Geneva (Biomedical and Metabolomics Analysis Group, BMA) (185), these isotopes are used to quantify their corresponding endogenous analytes through a one-point calibration performed directly within the biological sample itself. Scientific interest in internal calibration strategy is growing because it is easy to implement and highly efficient at delivering quantitative results, even when analyzing a limited number of samples (187) (212). Despite its clear potential, however, it has yet to be formally adopted into international guidelines for analytical method

validation, as external calibration remains the current recommended approach by the FDA and EMA.

A method for the detection of up to 200 among steroid hormones, bile acids and oxysterols, is available at the Biomedical and Metabolomics Analysis Group the University of Geneva, also allowing the absolute quantification of eight steroids by internal calibration (185). Within this essential methodological background, the present study's aim was formulated to assess the applicability of this advanced multi-targeted method to DBS sampling. The objective was to execute a proof-of-concept of the feasibility of detecting a broad steroid panel from DBS samples while maintaining the necessary high-throughput and ease-of-quantification for major steroids. This assessment was conducted on a total of 54 DBS samples derived from 6 subjects, 3 males and 3 females, stratified by body mass index class in 3 normal-weight and 3 overweight/obese. The application of this multi-targeted LC-MS/MS approach to DBS samples allowed for the assessment of 34 endogenous compounds, confirming the feasibility of this strategy for comprehensive steroid profiling. The method also proved its ability to detect the expected diurnal variations of circulating levels of key glucocorticoids and androgens, in line with their known physiological circadian patterns. Among the quantified glucocorticoids, cortisol, cortisone and 11-deoxycortisol displayed a clear circadian rhythmicity, consistent with the well-established secretion pattern governed by the HPA axis, which peaks in the early morning and declines throughout the day, confirming that DBS sampling of capillary blood is capable to capture daily fluctuations. Furthermore, the precision of the method further allowed to detect the post-prandial peak, which is coherent with the metabolic and carbohydrate stimulation subsequent to meals (213) (214). The circadian fluctuation of testosterone and androstenedione were found to be more pronounced in males than females. Progesterone and 17-hydroxyprogesterone concentrations did not exhibit significant temporal variation. When analyzed by sex, 17-hydroxyprogesterone showed a modest but significant circadian fluctuation in males. In males, circulating progestogens are derived almost exclusively from the adrenal glands. Progesterone is produced in much smaller quantities than glucocorticoids, so the diurnal fluctuation is weak and easily masked by interindividual variations or analytical noise. On the other hand, androgen and progestogen circulating levels in women are influenced by the menstrual phase. Morning-to-evening decrease in androgen and progestogen levels was previously demonstrated in women in follicular phase by our group and others (215). However, in the present study, women participation was not standardized at the follicular phase. Therefore, ovarian secretion may have obscured the HPA-related daily fluctuation. In future,

by enlarging the analyzed cohort, we will be able to address menstrual phase-dependent changes in steroid fluctuations (216).

The exploratory evaluation of detected but non-quantified metabolites provided additional insights into the temporal fluctuation of the steroidome. The vast majority of the detected glucocorticoids, such as 18-hydroxycortisol, 20α-hydroxycortisol, 20β-hydroxycortisol, 5α-hydroxycortisol, 5β-hydroxycortisol, 20α-cortolone, 20β-cortolone, 20αdihydrocortisone, 20βdihydrocortisone, presented the typical HPA-related diurnal fluctuations described for cortisol and cortisone, such as reinforcing the concept that glucocorticoid metabolism itself is under circadian regulation. These metabolites arise from sequential enzymatic conversions, mainly involving 11β-HSD, 5α/β-reductase, and 20α/β-HSD activities, whose expression and activity have been reported to fluctuate throughout the day (217) (218) (219). Therefore, the rhythmicity observed is likely a reflection of the synchronized action of these enzymatic systems, downstream of the primary cortisol rhythm. In agreement with recent literature and with its exclusive adrenal source, we found that levels of 11βOH-androstenedione, the major 11-oxo-androgen, parallel glucocorticoid fluctuation (220). Regarding sex hormones, the scenario was variegated. Androstenediol is an endogenous weak androgen and estrogen, acting as an intermediate in the biosynthesis of testosterone from DHEA (221). Estrone is produced by aromatization of androstenedione and serves as precursor of the more potent estradiol, further exerting its own biological activity. 17,20-Dihydroprogesterone is a precursor of the back-door pathway of dihydrotestosterone (222). Interestingly, the circulating fluctuation of these metabolites, with high levels at awakening, U-shaped decrease in late morning, and slow increase toward the late afternoon and evening, is possibly reflecting the result of combined diurnal adrenal secretion, gonadal secretion along with enzymatic interconversion and peripheral metabolism (223). Androsterone-3α-glucuronide is a phase II metabolite, that is a conjugation reaction product, in which a polar endogenous molecule is attached to a molecule with the purpose of increasing the polarity and water solubility of the compound, facilitating its excretion, mainly via kidneys (224). 11βOH-etiocholanolone is a 3-hydroxy steroid and has its role as androgen (225). The temporal trend of these two metabolites is such that their levels increase along afternoon and evening: the accumulation of this metabolite during the evening could mirror the hepatic metabolism of androgens secreted earlier in the day.

Overall, these results demonstrate that DBS sampling coupled with a multi-targeted LC-MS/MS approach not only enables accurate quantification of endogenous steroids but also allows the detection of temporal fluctuations of a consistent part of the steroidome. Hence, the

pursued approach could in future, after extensive validation, represent a valuable tool for investigating steroid metabolism in the context of pathophysiology of the circadian rhythms.

9.2.2. ESTROGEN ANALYSIS IN SERUM

Estrone and estradiol are the main circulating estrogens in humans and perform numerous physiological functions. Estriol, or 16-hydroxyestradiol, the third most common form in humans, can be derived from both estradiol and estrone, via the intermediate 16-hydroxyestrone (226). Some tissues can synthesize estrogens on demand from major androgen precursors thanks to the action of the aromatase enzyme (227). During female reproductive age years, ovaries are the main site of estrogen production, while, after menopause, peripheral tissues such as adipose tissue take on a more important role (228). Estradiol is predominant in premenopausal women, while estrone is more abundant in postmenopausal women and in males, where it is derived from adrenal androstenedione (229). Estriol increases significantly during pregnancy, as it is produced in the placenta. The aromatic oxidation of estrone and estradiol leads to the formation of hydroxylated metabolites, which are subsequently converted into methoxylated compounds; however, the circulating levels of each metabolite remain largely unknown and poorly studied (230). Epidemiological and experimental studies have also linked estrogens to various diseases: high levels in women are associated with an increased risk of breast, endometrial, and ovarian cancer while, in men, an imbalance between androgens and estrogen appears to contribute to the development of aggressive forms of prostate cancer (231) (232) (233) (234). Recent evidence also suggests a role for estrogen metabolism in the development of diabetes, somehow explaining why obesity is a major risk factor for breast cancer (235). In this context, it is crucial to accurately and precisely quantify estrogens and their metabolites, not only for the comprehension of their physiology and alteration in different biological conditions, but also to investigate their potential in diseases related to metabolism and hormonal disorders.

Estrogens circulate in the bloodstream at very low concentrations, particularly in postmenopausal women and in children, which poses significant challenges for their accurate measurement. Conventional immunoassays, commonly used in clinical laboratories, often lack sufficient specificity and sensitivity (236) (237). To overcome these limitations, LC-MS/MS has been increasingly employed, offering high analytical performance with excellent

specificity and sensitivity. Given the inherently low ionization efficiency of estrogens, derivatization strategies are typically necessary to achieve detection at the picogram per milliliter level (238). Given these analytical challenges, the present study performed in the laboratory of Biomedical and Metabolomics Analysis Group of the University of Geneva, under the guidance of Serge Rudaz, implemented a dedicated LC-MS/MS method for estrogen quantification in serum, employing derivatization with dansyl chloride. Dansylation was found to be more effective than derivatization with 2-fluoro-1-methylpyridinium p-toluene sulfonate (FMPTS). Additionally, the choice of catalyst during derivatization proved crucial: triethylamine, initially tested for its volatility and minimal interference in mass spectrometry, produced excessive matrix effects, whereas sodium bicarbonate significantly enhanced signal intensity and was therefore adopted in combination with dansyl chloride. Estrogen detection further necessitated maximal serum purification, as matrix effect was found to be a major issue. The initial extraction strategy relied on the laboratory pre-existing steroid protocol, which involved solid-phase extraction (SPE) using Oasis PRIME cartridges. However, this approach resulted in poor recovery and substantial matrix effects. Switching to LLE with MTBE allowed for a cleaner extract, substantially improving recovery, matrix suppression, and overall signal quality. Using this optimized LLE-dansylation workflow, estrone, estradiol, and estriol were reliably detected and quantified across a wide dynamic range (0.1-100ng/mL), overcoming the limitations of low ionization efficiency and matrix effects. This approach demonstrates that careful optimization of both extraction and derivatization steps is essential for sensitive and selective estrogen profiling in human serum, paving the way for future studies investigating their physiological and pathological roles, and applying this approach to DBS.

9.3. VALIDATION OF TARGETED METABOLOMIC ANALYSIS IN DBS

Metabolomics is a discipline whose informative potential is constantly and impressively increasing, as it is influenced by technological advances in the field of LC-MS. Furthermore, the high sensitivity of the latest platforms allows this science to be applied to increasingly smaller volumes of blood samples. In this sense, our study, which applied LC-MS/MS to the analysis of a wide panel of metabolites in DBS, is pioneering in the current scientific landscape. Although still underutilized, DBS is an extremely advantageous micro-sampling technique, as it is inexpensive, non-invasive, and can be performed independently by the patient, allowing for multiple collections throughout the day. It is therefore an ideal device for conducting studies on the circadian rhythm. To date, the information available in the literature on circadian fluctuations of metabolites levels is extremely limited. The study by Dallmann R. et al (182) reported that 15% of the amino acids measured in saliva show diurnal variation. On the other hand, a recent study conducted by members of our group showed that chronic hypercortisolism is characterized by lower basal plasma levels of branched-chain amino acids, along with histidine, tyrosine, and kynurenine and, in the case of Cushing's syndrome, by higher levels of spermidine and taurine (183). However, to date, there is no information on the possible impact of hypercortisolism and the associated loss of circadian rhythm on the fluctuation of circulating levels of amino acids and biogenic amines. Besides, no information is available on the physiological fluctuation of metabolites from other classes involved in energy metabolism.

Based on these assumptions, we designed a study that aimed to validate the applicability of DBS for the study of amino acids, biogenic amines, acylcarnitines, glycerophospholipids, and sphingomyelins, by means of a technology nowadays recommended for its intrinsic high sensitivity, specificity and for its multitargeting potential, such as LC-MS/MS.

An important element of the protocol for this study is that all participants were placed on a isocaloric Mediterranean diet throughout the week preceding the day of observation, with the aim of smoothing out inter-individual differences in terms of nutrient and overall calorie intake. This validation study aimed to verify the comparability of the information obtained from the quantitative DBS analysis compared to that which can be obtained from a traditional venous serum sample. The two types of samples differ in many ways. Serum is obtained from venous blood, while DBS is obtained from capillary blood from the fingertip: the levels of certain molecules may vary as the blood travels from the peripheral to the large vessels, depending on

the contribution of tissue metabolism. Furthermore, serum is the acellular component of blood, while DBS represents whole blood, consisting of blood cells, plasma, and interstitial fluid (239). Serum and whole blood may also show very different concentration levels for certain analytes, depending on the specific partition coefficient between the cellular and acellular components. Additionally, the different mechanisms that can undermine the stability of compounds in serum and DBS should not be underestimated. Another difference between the two types of matrices is that serum is a liquid, while DBS is a dry sample: this poses different pre-analytical and analytical difficulties.

Although the Biocrates p180 kit was initially validated for use with plasma and serum, it had already been applied to DBS samples, as reported in an application note (www.biocrates.com). However, although promising, only a few studies are available in literature about the consistency or complementarity of molecular information gathered from the two specimens. Among these, Chiu et al. found that nearly half of all metabolites, including amino acids, and carnitines among others, showed strong plasma-to-DBS agreement, indicating the feasibility of DBS for metabolomic profiling (240). The development of certified reference materials for amino acids in DBS further supports the analytical validity of measuring these compounds in DBS (241).

To evaluate the preservation of the information conveyed by DBS in respect to serum, we performed a paired collection of these samples in order to analyze the correlation between metabolite levels in each fluid. Moreover, in order to verify whether this comparability is changing according to circadian rhythm, we collected samples at 6 time points. The moderate to strong correlations observed for amino acids, particularly branched-chain amino acids such as isoleucine, leucine, valine, and biogenic amines such as serotonin and spermine between DBS and serum are consistent with recent literature (240). The absence of association we observed between DBS and serum levels of polar amino acids such as aspartate, glutamate and glutamine also aligns with what reported in the same study (240).

With regard to acylcarnitines, we found stronger correlations between DBS and serum levels of short chain compounds, lowering with the length of the chain. Similar data were reported by Yang et al. (242). This might be due to the increasing affinity of acylcarnitine with longer chain for plasma membrane of red blood cell, which might limit their release in plasma (243). In line with this, we documented a 2-fold increase in DBS compared to serum concentration of the two longest chain acylcarnitines detected by our method, C18:1 and C18:2.

Concerning glycerophospholipids, the study by Koulman et al. (244) validated a lipid-profiling approach in DBS and reported that, despite spotting and drying may cause oxidation and hydrolysis, the major lipid classes (including phosphatidylcholines and sphingomyelins) maintained comparable inter-subject differences and precision relative to plasma (244). Taking note of this, our observation that many glycerophospholipid species (LysoPCs, PC aa/ae) show moderate to strong correlations between DBS and serum is consistent with the notion that DBS can preserve relative quantitation of these lipid classes under optimized conditions. However, the weaker correlation for very long-chain PCs and LysoPCs in our analysis aligns with the caution expressed in the work of Koulman: spotting, drying, and minor oxidative modifications can differentially affect lipid species, particularly those prone to oxidation or with poor recovery extraction (244). Additionally, similarly to acylcarnitines, long chain lipids might be poorly available in serum as they remain embedded in the erythrocyte membranes. In line with this a fold increase in DBS vs serum concentrations of 1.29 to 4.55 was found for PC of 38 or more C atoms.

Altogether, the validation results confirm the feasibility of using DBS for large-scale targeted metabolomics studies, although analyte-dependent variability still requires careful consideration in study design and data interpretation, paving the way for further investigations. The information potential of metabolites not displaying a significant association between DBS and serum levels may nonetheless maintain a complementary biomarker value as they represent intracellular dynamics of circulating cells.

9.4. CIRCADIAN METABOLIC PROFILING IN HEALTH AND IN STATES OF CORTISOL RHYTHM DERANGEMENT

Chronic hypercortisolism is a condition that is harmful to health, increasing the risk of cardiovascular, metabolic, neoplastic, neurological, and immunological diseases (245). Although the negative effects of hypercortisolism are evident and well described in Cushing's syndrome, they are still poorly characterized in intermediate conditions, such as in patients with adrenal lesions with MACS, and in opposite conditions, such as adrenal insufficiency (AI), the so-called Addison disease. Currently, the diagnosis of MACS itself is still complex and poorly standardized (245) (189). Recent studies by our group and others (183) have shown that even individuals with chronic hypercortisolism who do not present clinical stigmata have a high risk of long-term adverse events compared to the general population. Therefore, it would be important to recognize chronic hypercortisolism early, characterize its metabolic alterations in depth, and intervene in a tailored manner to limit its consequences. Among the numerous biochemical processes that are altered by hypercortisolism and the loss of circadian rhythm, protein metabolism plays a central role. It is well known that patients with Cushing's syndrome experience severe alterations in glucose metabolism and insulin sensitivity, a condition that predisposes them to use proteins as an energy source. This leads to the risk of severe sarcopenia, a trait that is one of the classic clinical manifestations of Cushing's syndrome. Although the clinical consequences of this biochemical alteration are well known, the exact molecular mechanisms involved are far from being well characterized. In addition to the well-known catabolic impact of cortisol on protein metabolism, numerous studies show that chronic hypercortisolism also profoundly alters lipid metabolism, leading to dyslipidemia, redistribution of body fat, and changes in phospholipid composition (246) (247).

Adrenal insufficient secretion of glucocorticoid is a life-threatening condition requiring life-long replacement therapy. Unfortunately, all the available replacement approaches fail to reproduce a physiological rhythmicity in cortisol availability, exposing the patient to over- as well as to under-treatment within the same day. In the long term, AI patients develop clinical morbidity similar to hypercortisolism, featured by sarcopenia, dysmetabolism as well as sleep deprivation (181).

Based on these considerations, the present study aimed at applying the previously validated targeted metabolomics approach on DBS to clinical cohorts represented by patients affected by

AI under glucocorticoids replacement therapy, MACS and CS, and healthy subjects, to investigate metabolic signatures able to characterize these cortisol imbalance conditions. In this context, the circadian metabolic profiling performed in DBS revealed distinct molecular patterns that discriminated between healthy subjects and patients with CS. Such group of informative molecules not only differed in circulating levels but also, more interestingly, in the daily fluctuation pattern. Two main metabolic signatures emerged: Pattern A, dominated by phosphatidylcholines (PCs), and Pattern B, characterized by acylcarnitines, amino acids, and biogenic amines. These two patterns appear to capture lipid and amino acids dynamics as energetic fuels, in which cortisol is closely involved. The U-shaped circadian profile observed in healthy individuals likely describes the physiological rhythmicity of lipid and amine metabolism, which presents higher levels in the morning, that decrease throughout the day and finally increase at night, presumably explaining day/night variations in glucose availability, lipid and energy requests for membrane turnover and for the anabolic-catabolic balance of cells.

The flattening and general decrease of PC levels observed in CS may suggest a loss of rhythmic lipid turnover under chronic excessive glucocorticoid exposure, consistent with the derangement of lipid metabolism exerted by cortisol in such condition (247) (248). In literature, an overall increase in glycerophospholipids, and in particular PCs, in the serum of patients with Cushing's syndrome was reported and interpreted as the result of increased hepatic lipogenesis and altered phospholipase-mediated degradation (249). However, the molecular species detected by that study are different from ours. Hence, our results offer a complementary perspective, highlighting not only quantitative differences but, above all, alterations in the temporal regulation of lipid metabolism. This behavior can be explained by considering the chronic effects of hypercortisolism on lipid metabolism: chronic exposure induces glucocorticoid desensitization and dysregulation of the Kennedy and Lands cycles (249), resulting in impaired normal glycerophospholipid turnover. In this context, the loss of the circadian rhythm of PCs represents an index of functional decoupling between cortisol secretion and peripheral lipid remodeling processes. Accordingly, our data suggests that chronic hypercortisolism not only causes a quantitative alteration in the lipid profile, but also a deep temporal disorganization of phospholipid metabolism, which could contribute to the metabolic and cardiovascular burden typical of Cushing's syndrome. In physiological conditions, protein catabolic processes are reduced during the day, resulting in lower levels of amino acids in the bloodstream, along with a predominant use of glucose and fatty acids as substrates to fuel energy expenditure. Conversely, in CS, pattern B metabolites displayed

higher overall concentrations and a loss of physiological oscillation. These data substantially agree with the findings previously reported in the 2017 study by Di Dalmazi et al. (183), which indicates that clinically manifest hypercortisolism has a direct impact on the biochemical pathways involving polyamines. The data concerning polyamines could be explained by the direct induction of the enzyme limiting polyamine synthesis, ornithine decarboxylase, by cortisol, with a consequent increase in their production (250). In fact, the promoter of this gene has a hormone-regulated region on which cortisol could act. Polyamines act as mediators in multiple biological processes involving biosynthesis, catabolism, and cellular homeostasis. Furthermore, consistent with the manifestations of Cushing's syndrome, they are involved in oxidative stress and the cortisol-induced inflammatory response.

Interestingly, AI patients under once-a-day glucocorticoid replacement showed morning oscillation of PCs and the sharp rise in the evening, which are likely linked to exogenous cortisol intake after awakening. While the replacement therapy can transiently restore cortisol availability, it fails to replicate the physiological pattern of cortisol endogenous secretion (181). As to amine compounds in pattern B, AI patients displayed physiological concentrations, though with increased morning variability, again, possibly related to the pharmacokinetic peak of replacement therapy.

Finally, MACS patients exhibited an intermediate phenotype, with PC levels similar to those of CS but retaining a rhythmic profile more similar to HS. The preservation of PC rhythm could reflect the flattened but preserved cortisol rhythm in MACS. A moderate increase of amines representing pattern B was also found in MACS, suggesting a dose-response effect of cortisol exposure on amine regulation. In line with the partially preserved cortisol rhythm the fluctuation of these compounds was found to be deranged in the evening, when it parallels the one found in CS, but not in the morning, when it parallels the one found in HS. Overall, our findings reinforce the concept that MACS represents a continuum within the spectrum of cortisol excess, with subtle but measurable metabolic derangements that may help define the actual metabolic risk and a tailored therapeutic approach.

It is worth noting that clinical variables such as age, BMI, and waist circumference significantly differed among groups, with MACS patients being older and CS patients displaying higher adiposity indexes compared to healthy subjects. These differences could partly contribute to the observed metabolic variability, suggesting that future analyses might benefit from adjusting

for these covariates to better isolate the specific contribution of cortisol imbalance to the metabolic phenotype.

Substantially, these findings highlight distinct metabolic signatures associated with different degrees of cortisol imbalance, providing novel insights into the investigation of these conditions.

10. CONCLUSION

The presented PhD work aimed to develop and apply advanced LC-MS/MS methods applied to dried blood spots (DBS) for studying steroid and metabolic circadian profiles in different endocrine contexts. The pursued approach allowed for the integration of analytical and clinical aspects and contributed to the consolidation of mass spectrometry as a reference tool for empowered steroidomic and metabolomic characterization. The expansion of steroid panels and the optimization of the extraction procedure from DBS have made it possible to obtain accurate and reproducible analyses even from extremely small sample volumes. This result supports the validity of DBS as an alternative matrix to serum, with significant advantages in terms of practicality, minimal invasiveness, and the possibility of serial sampling. At the same time, the development of a highly sensitive method for quantifying estrogens has made it possible to overcome one of the main critical issues in the analysis of these compounds, opening up new perspectives for the study of these hormones even in DBS. The application of optimized targeted metabolomics protocols to DBS from cohorts of patients with alterations in cortisol secretion or rhythm has made it possible to identify specific metabolic patterns associated with different degrees of hyper- or hypocortisolism. These results underscore the importance of an integrated approach, capable of correlating the hormonal with the metabolic profile, in order to better understand the systemic effects of cortisol dysfunction.

On balance, the work has provided a significant methodological and translational contribution, demonstrating how the combination of LC-MS/MS, non-invasive sampling, and targeted analysis can represent a powerful and innovative strategy for endocrine and metabolic investigation. Future prospects include the complete validation of methods on next-generation platforms and their application in large-scale clinical studies, with the aim of translating this evidence into increasingly accurate and personalized diagnostic and monitoring tools.

Bibliography

1. **Ettre, L. S., & Zlatkis, A.** *75 Years of Chromatography: A Historical Dialogue.* s.l. : Elsevier Scientific Publishing Company. (Journal of Chromatography Library, Vol. 17). , 1979.

2. **Snyder, L. R., Kirkland, J. J., & Dolan, J. W.** *Introduction to Modern Liquid Chromatography.* s.l. : John Wiley & Sons, 2010.

3. **McMaster, M. C.** *LC/MS: A Practical User's Guide.* s.l. : John Wiley & Sons, Inc., 2005.

4. **Dolan, J. W., & Snyder, L. R.** *Troubleshooting LC Systems. A Comprehensive Approach to Troubleshooting LC Equipment and Separations.* s.l. : Springer Science+Business Media, LLC , 1989.

5. **Watson, D. G.** *Pharmaceutical Analysis: A Textbook for Pharmacy Students and Pharmaceutical Chemists, Fourth Edition.* s.l. : Elsevier, 2017.

6. **Meyer, V. R.** *Practical High-Performance Liquid Chromatography.* s.l. : John Wiley & Sons, 2010.

7. **Rouessac, F., & Rouessac, A.** *Chemical Analysis: Modern Instrumentation Methods and Techniques Second Edition.* s.l. : John Wiley & Sons Ltd, 2007.

8. **Fritz, J. S., & Gjerde, D. T.** *Ion Chromatography 4th, Completely Revised and Enlarged Edition.* s.l. : John Wiley & Sons, 2009.

9. **Weiss, J.** Anion-Exchange Chromatography (HPIC). *Handbook of Ion Chromatography.* s.l. : Wiley, 2016, pp. pp 29-152.

10. **Miller, J. M., & Miller, J. N.** *Statistics and Chemometrics for Analytical Chemistry Fifth Edition.* s.l. : Pearson Education, 2005.

11. *Separation techniques: Chromatography.* **O., Coskun.** 2016, North Clin Istanb., pp. 3(2):156-160.

12. **David S. Hage.** Chromatography and electrophoresis. *Contemporary Practice in Clinical Chemistry.* s.l. : William Clarke, Mark A. Marzinke, Academic Press, 2012.

13. **Striegel, R. C., Yau, W. W., & Kirkland, J. J.** *Modern Size-Exclusion Liquid Chromatography: Practice of Gel Permeation and Gel Filtration Chromatography.* s.l. : John Wiley & Sons, 2009.

14. **Wu, C.-S. .** *Handbook Of Size Exclusion Chromatography And Related Techniques: Revised And Expanded (2nd ed.).* s.l. : CRC Press, 2003.

15. **Lloyd R. Snyder, Joseph J. Kirkland, Joseph L. Glajch.** *Practical HPLC Method Development.* s.l. : John Wiley & Sons, 1997.

16. **Kevin Robards, P. E. Jackson, Paul A. Haddad.** *Principles and Practice of Modern Chromatographic Methods.* s.l. : Academic Press, 1994.

17. **Ardrey, Robert E.** *Liquid Chromatography - Mass Spectrometry: an introduction .* s.l. : John Wiley & Sons, 2003.

18. **Dong, M. W.** *Modern HPLC for Practicing Scientists.* s.l. : John Wiley & Sons, 2006.

19. **Poole, C. F.** *The Essence of Chromatography.* s.l. : Elsevier Science, 2003.

20. **Neue, U. D.** *HPLC Columns: Theory, Technology, and Practice.* s.l. : John Wiley & Sons, 1997.

21. **Kromidas, Stavros.** *HPLC Made to Measure: A Practical Handbook for Optimization.* s.l. : Wiley-VCH Verlag GmbH & Co. KGaA, 2006.

22. **E. Hywel Evans, Mike E. Foulkes.** *Analytical Chemistry: A Practical Approach.* s.l. : OUP Oxford, 2019.

23. **Niessen, W. M.** *Liquid Chromatography–Mass Spectrometry.* s.l. : CRC Press, 2006.

24. **Instruments, Shimadzu Scientific.** What is HPLC? *www.ssi.shimadzu.com.* [Online] https://www.ssi.shimadzu.com/service-support/technical-support/analysis-basics/basic/what_is_hplc.html.

25. **Oscar Bodansky, A.L. Latner.** *Advances in Clinical Chemistry Volume 15.* s.l. : Academic Press, 1972.

26. *Liquid chromatography tandem-mass spectrometry (LC-MS/MS) --technique and applications in endocrinology.* **Vogeser M, Parhofer KG.** 2007 Oct, Exp Clin Endocrinol Diabetes, pp. 115(9):559-70. 17943689.

27. **Cole, R. B.** *Electrospray Ionization Mass Spectrometry: Fundamentals, Instrumentation, and Applications.* s.l. : Wiley-Interscience, 1997.

28. *Electrospray ionization for mass spectrometry of large biomolecules.* **Fenn, J. B., Mann, M., Meng, C. K., Wong, S. F., & Whitehouse, C. M.** 1989, Science, pp. 246(4926), 64-71.

29. *From ions in solution to ions in the gas phase - the mechanism of electrospray mass spectrometry.* **Kebarle, P., & Tang, L.** 1993 : s.n., Analytical Chemistry, pp. 65(22), 972A-986A.

30. *Electrospray Ionization Mass Spectrometry: A Technique to Access the Information beyond the Molecular Weight of the Analyte.* **Shibdas Banerjee, Shyamalava Mazumdar.** 2012, International Journal of Analytical Chemistry. 2012(8):282574.

31. **Hari Nair, William Clarke.** *Mass Spectrometry for the Clinical Laboratory.* s.l. : Academic Press, 2017.

32. **Gross, J. H.** *Mass Spectrometry: A Textbook (3rd ed.).* s.l. : Springer Cham, 2017.

33. *Advantages of atmospheric pressure photoionization mass spectrometry in support of drug discovery.* **Cai Y, Kingery D, McConnell O, Bach AC 2nd.** 2005, Rapid Commun Mass Spectrom, pp. 19(12):1717-24.

34. *Atmospheric pressure photoionization mass spectrometry.* **Andrea Raffaelli, Alessandro Saba.** 2003, Mass Spectrom Rev, pp. 22(5):318-31.

35. *Atmospheric Pressure Photoionization: An Ionization Method for Liquid Chromatography−Mass Spectrometry.* **Damon B. Robb, Thomas R. Covey, Andries P. Bruins.** 2000, Anal. Chem., pp. 72, 15, 3653–3659.

36. *Assessing analytical specificity in quantitative analysis using tandem mass spectrometry.* **Kushnir MM, Rockwood AL, Nelson GJ, Yue B, Urry FM.** 2005, Clin Biochem, pp. 38(4):319-27.

37. *Strategies for the assessment of matrix effect in quantitative bioanalytical methods based on HPLC-MS/MS.* **Matuszewski BK, Constanzer ML, Chavez-Eng CM.** 2003, Analytical Chemistry, pp. 75(13) 3019-3030.

38. **Skoog, D. A., West, D. M., Holler, F. J., & Crouch, S. R.** *Fundamentals of Analytical Chemistry.* s.l. : Cengage Learning, 2021.

39. *Method for Internal Standard Introduction for Quantitative Analysis Using On-Line Solid-Phase Extraction LC−MS/MS.* **Yazen Alnouti, Ming Li, Olga Kavetskaia, Honggang Bi, Cornelis E. C. A. Hop, Arkady I. Gusev.** 2006, Anal Chem, pp. 78, 4, 1331–1336.

40. *CLSI C62-A: A New Standard for Clinical Mass Spectrometry.* **KL., Lynch.** 2016, Clin Chem, pp. 62(1):24-9.

41. *Bioanalytical Method Validation: Guidance for Industry.* **Administration, U.S. Food and Drug.** 2018.

42. *Guideline on bioanalytical method validation. European Medicines Agency. EMEA/CHMP/EWP/192217/2009.* **European Medicines Agency, Committee for Medicinal Products for Human Use (CHMP).** 2011.

43. *Q2(R2) Validation of Analytical Procedures.* **(ICH), International Council for Harmonisation.** 2023.

44. *Dried Blood Spot in Laboratory: directions and prospects.* **Malsagova K, Kopylov A, Stepanov A, Butkova T, Izotov A, Kaysheva A.** 2020, Diagnostics, Vol. 10, p. 248.

45. *Dried blood spot sampling in combination with LC-MS/MS for quantitative analysis of small molecules.* **Li W, Tse FL.** 2010, Biomed Chromatogr, Vol. 24, pp. 49-65.

46. *Influence of Hematocrit and Total-Spot Volume on Performance Characteristics of Dried Blood Spots for Newborn Screening.* **Hall EM, Flores SR, De Jesús VR.** 2015, Int. J. Neonatal Screen, Vol. 1, pp. 69-78.

47. *Influence of hematocrit and localisation of punch in dried blood spots on levels of amino acids and acylcarnitines.* **Holub M, Tuschl K, Ratschmann R, Strnadová KA, Mühl A, Heinze G, Sperl W, Bodamer OA.** 2006, Clin Chim Acta, Vols. 373(1-2), pp. 27-31.

48. *Inborn errors of metabolism and expanded newborn screening: Review and update.* **Mak CM, Lee HC, Chan AY, Lam CW.** 2013, Crit Rev Clin Lab Sci., Vol. 50(6), pp. 142-62.

49. *Dried blood spot analysis with liquid chromatography and mass spectrometry: Trends in clinical chemistry .* **Skogvold HB, Rootwelt H, Reubsaet L, Elgstøen KBP, Wilson SR.** 2023, J Sep Sci, Vol. 46(15):e2300210.

50. *Performance of LC/MS/MS in Analyzing Multiple Amino Acids and Acylcarnitines in Dried Blood Spot of Very Low Birth Weight, Low Birth Weight, and Normal Weight Neonates.* **Yu T, Han Y, Pu X, Duan H, Zhi L, Zhang Y, Lei L, Zhao Y, Cao Q, Xu H.** 2018, Clin Lab, Vol. 64(9), pp. 1333-1339.

51. *Dried blood spots in HIV monitoring: applications in resource-limited settings.* **A, Johannessen.** 2010, Bioanalysis, Vol. 2(11) , pp. 1893-908.

52. **Michael H. Ross, Wojciech Pawlina.** *Histology a Text and Atlas with correlated cell and molecular biology.* s.l. : Lippincott Williams & Wilkins, 2015.

53. *Intraadrenal Interactions in the Regulation of Adrenocortical Steroidogenesis.* **Monika Ehrhart-Bornstein, Joy P. Hinson, Stefan R. Bornstein, Werner A. Scherbaum, Gavin P. Vinson.** 1998, Endocrine Reviews, Vols. Volume 19, Issue 2, pp. 101–143.

54. *Endocrinology: An Integrated Approach.* **Stephen Nussey, Saffron Whitehead.** s.l. : Oxford: BIOS Scientific Publishers, 2001.

55. *The molecular biology, biochemistry, and physiology of human steroidogenesis and its disorders.* **Miller WL, Auchus RJ.** 2011, Endocr Rev, Vol. 32(1), pp. 81-151.

56. *Overview of steroidogenic enzymes in the pathway from cholesterol to active steroid hormones.* **Payne AH, Hales DB.** 2004, Endocr Rev, Vol. 25(6), pp. 947-70.

57. *The biology of the glucocorticoid receptor: new signaling mechanisms in health and disease.* **Oakley RH, Cidlowski JA.** 2013, J Allergy Clin Immunol, Vol. 132(5), pp. 1033-44.

58. *The multifaceted mineralocorticoid receptor.* **Gomez-Sanchez E, Gomez-Sanchez CE.** 2014, Compr Physiol, Vol. 4(3), pp. 965-94.

59. **Eroschenko, Victor P.** Figure 17.11: Adrenal (Suprarenal) Gland: Cortex and Medulla. *DiFiore's Atlas of Histology with Functional Correlations (11th ed.).* s.l. : Wolters Kluwer Health Lippincott Williams & Wilkins, 2008, pp. 404–5.

60. **Litwack, Gerald.** *Hormones 4th Edition.* s.l. : Academic Press, 2022. p. 41.

61. *Regulation of the Adrenal Androgen Biosynthesis.* **Rainey WE, Nakamura Y.** 2008, J. Steroid Biochem. Mol. Biol, Vols. 108 (3–5), pp. 281–6.

62. *Corticotropin-releasing hormone as adrenal androgen secretagogue.* **Ibáñez L, Potau N, Marcos MV, de Zegher F.** 1999, Pediatric Research, Vol. 46 (3), pp. 351–3.

63. *A case of 17 alpha-hydroxylase deficiency.* **Kim SM, Rhee JH.** 2015, Clin Exp Reprod Med, Vol. 42 (2), pp. 72–6.

64. **John E. Hall, Michael E. Hall.** *Guyton and Hall Textbook of Medical Physiology.* s.l. : Elsevier, 2025.

65. *Adrenal responses to stress.* **DS, Goldstein.** 2010, Cell Mol Neurobiol, Vol. 30(8), pp. 1433-40.

66. *Tyrosine Hydroxylase. The initial step in norepinephrine biosyinthesis* . **Nagatsu T, Levitt M, Udenfriend S.** 1964, J Biol Chem, Vol. 239, pp. 2910-7.

67. *Catecholamine metabolism: a contemporary view with implications for physiology and medicine.* **Eisenhofer G, Kopin IJ, Goldstein DS.** 2004, Pharmacol Rev, Vol. 56(3), pp. 331-49.

68. **Kim E. Barrett, Susan M. Barman, Scott Boitano, Heddwen L. Brooks.** *Ganong's Review of Medical Physiology Twenty-Third Edition.* s.l. : McGraw Hill Medical, 2010.

69. *International Union of Pharmacology nomenclature of adrenoceptors.* **D B Bylund, D C Eikenberg, J P Hieble, S Z Langer, R J Lefkowitz, K P Minneman, P B Molinoff, R R Ruffolo, U Trendelenburg.** 1994, Pharmacological Reviews, Vols. Volume 46, Issue 2, pp. 121-136.

70. *Biochemical Diagnosis of Chromaffin Cell Tumors in Patients at High and Low Risk of Disease: Plasma versus Urinary Free or Deconjugated O-Methylated Catecholamine Metabolites.* **Eisenhofer G, Prejbisz A, Peitzsch M, Pamporaki C, Masjkur J, Rogowski-Lehmann N, Langton K, Tsourdi E, Pęczkowska M, Fliedner S, Deutschbein T, Megerle F, Timmers HJLM, Sinnott R, Beuschlein F, Fassnacht M, Januszewicz A, Lenders JWM.** 2018, Clin Chem, Vol. 64(11), pp. 1646-1656.

71. *Diagram of the pathways of human steroidogenesis.* **Häggström, Mikael and Richfield, David.** 2014, WikiJournal of Medicine.

72. *The diagnosis of Cushing's syndrome: an Endocrine Society clinical practice guideline.* **Nieman LK, Biller BM, Findling JW, Newell-Price J, Savage MO, Stewart PM, Montori VM.** 2008, J Clin Endocrinol Metab, Vol. 93(5), pp. 1526-1540.

73. *Cushing's syndrome.* **Newell-Price J, Bertagna X, Grossman AB, Nieman LK.** 2006, Lancet, Vol. 367(9522), pp. 1605-17.

74. *Consensus on diagnosis and management of Cushing's disease: a guideline update.* **al., Fleseriu M et.** 2021, Lancet Diabetes Endocrinol, Vol. 9(12), pp. 847-875.

75. *European Society of Endocrinology clinical practice guidelines on the management of adrenal incidentalomas, in collaboration with the European Network for the Study of Adrenal Tumors.* **Fassnacht M, Tsagarakis S, Terzolo M, Tabarin A, Sahdev A, Newell-Price J, Pelsma I, Marina L, Lorenz K, Bancos I, Arlt W, Dekkers OM.** 2023, Eur J Endocrinol, Vol. 189(1), pp. G1-G42.

76. *Adrenal Hypercortisolism: A Closer Look at Screening, Diagnosis, and Important Considerations of Different Testing Modalities.* **Chiodini I, Ramos-Rivera A, Marcus AO, Yau H.** 2019, J Endocr Soc, Vol. 3(5), pp. 1097-1109.

77. *Approach to the Patient: Diagnosis of Cushing Syndrome.* **Savas M, Mehta S, Agrawal N, van Rossum EFC, Feelders RA.** s.l. : J Clin Endocrinol Metab, 2022, pp. 107(11):3162-3174.

78. *Differential Diagnosis of ACTH-Dependent Cushing Syndrome.* **Filippo Ceccato, Mattia Barbot, Alessandro Mondin, Marco Boscaro, Maria Fleseriu, Carla Scaroni.** s.l. : The Journal of Clinical Endocrinology & Metabolism, 2023, Vols. Volume 108, Issue 5, pp. e178–e188.

79. *Medical management pathways for Cushing's disease in pituitary tumors centers of excellence (PTCOEs).* **Giustina A, Uygur MM, Frara S, Barkan A, Biermasz NR, Chanson P, Freda P, Gadelha M, Haberbosch L, Kaiser UB, Lamberts S, Laws E, Nachtigall LB, Popovic V, Schilbach K, Lely AJV, Wass JAH, Melmed S, Casanueva FF.** 2025, Pituitary, Vol. 28(1), p. 23.

80. *Update in the medical therapy of Cushing's disease.* **LK., Nieman.** 2013, Curr Opin Endocrinol Diabetes Obes, Vol. 20(4), pp. 330-4.

81. *Improved Clinical Outcomes During Long-term Osilodrostat Treatment of Cushing Disease With Normalization of Late-night Salivary Cortisol and Urinary Free Cortisol.* **Newell-Price J, Fleseriu M, Pivonello R, Feelders RA, Gadelha MR, Lacroix A, Witek P, Heaney AP, Piacentini A, Pedroncelli AM, Biller BMK.** 2024, J Endocr Soc, Vol. 9(1), p. bvae201.

82. *Osilodrostat Treatment of Cushing Syndrome in Real-World Clinical Practice: Findings From the ILLUSTRATE study.* **Fleseriu M, Auchus RJ, Huang W, Spencer-Segal JL, Yuen KCJ, Dacus KC, Padgett J, Babler EK, Das AK, Campos C, Broder MS, Ioachimescu AG.** 2025, Journal of the Endocrine Society, Vols. Volume 9, Issue 5, p. bvaf046.

83. *Osilodrostat: A Review of Recent Clinical Studies and Practical Recommendations for its Use in the Treatment of Cushing Disease.* **KCJ, Yuen.** 2021, Endocr Pract, Vol. 27(9), pp. 956-96.

84. *Long-term efficacy and safety of subcutaneous pasireotide alone or in combination with cabergoline in Cushing's disease.* **Feelders RA, Fleseriu M, Kadioglu P, Bex M, González-Devia D, Boguszewski CL, Yavuz DG, Patino H, Pedroncelli AM, Maamari R, Chattopadhyay A, Biller BMK, Pivonello R.** 2023, Front Endocrinol (Lausanne), Vol. 14, p. 1165681.

85. *Cabergoline for Cushing's disease: a large retrospective multicenter study.* **Ferriere A, Cortet C, Chanson P, Delemer B, Caron P, Chabre O, Reznik Y, Bertherat J, Rohmer V, Briet C, Raingeard I, Castinetti F, Beckers A, Vroonen L, Maiter D, Cephise-Velayoudom FL, Nunes ML, Haissaguerre M, Tabarin A.** 2017, Eur J Endocrinol, Vol. 176(3), pp. 305-314.

86. *Relacorilant or surgery improved hemostatic markers in Cushing syndrome.* **Simeoli C, Di Paola N, Stigliano A, Lardo P, Kearney T, Mezosi E, Ghigo E, Giordano R, Mariash CN, Donegan DM, Feelders RA, Hand AL, Araque KA, Moraitis AG, Pivonello R.** 2025, J Endocrinol Invest, Vol. 48(3), pp. 671-680.

87. *Age-dependent and sex-dependent disparity in mortality in patients with adrenal incidentalomas and autonomous cortisol secretion: an international, retrospective, cohort study.* **al., Timo Deutschbein et.** 2022, The Lancet Diabetes & Endocrinology, Vol. 10(7), pp. 499-508.

88. *Urine steroid metabolomics for the differential diagnosis of adrenal incidentalomas in the EURINE-ACT study: a prospective test validation study.* **al., Bancos I et.** 2020, Lancet Diabetes Endocrinol, Vol. 8(9), pp. 773-781.

89. *Cardiometabolic Disease Burden and Steroid Excretion in Benign Adrenal Tumors : A Cross-Sectional Multicenter Study.* **al., Prete A. et.** 2022, Ann Intern Med, Vol. 175(3), pp. 325-334.

90. *Adrenocortical carcinomas and malignant phaeochromocytomas: ESMO-EURACAN Clinical Practice Guidelines for diagnosis, treatment and follow-up.* **Fassnacht M, Assie G, Baudin E, Eisenhofer G, de la Fouchardiere C, Haak HR, de Krijger R, Porpiglia F, Terzolo M, Berruti A.** 2020, Ann Oncol, Vol. 31(11), pp. 1476-1490.

91. *The Management of Primary Aldosteronism: Case Detection, Diagnosis, and Treatment: An Endocrine Society Clinical Practice Guideline.* **Funder JW, Carey RM, Mantero F, Murad MH, Reincke M, Shibata H, Stowasser M, Young WF Jr.** 2016, J Clin Endocrinol Metab, Vol. 101(5) , pp. 1889-916.

92. *Diagnosis and treatment of primary aldosteronism.* **Reincke M, Bancos I, Mulatero P, Scholl UI, Stowasser M, Williams TA.** 2021, Lancet Diabetes Endocrinol, Vol. 9(12), pp. 876-892.

93. **Ashley B. Grossman, Glenn D. Braunstein.** Secondary Aldosteronism. *MSD Manuals.* [Online] https://www.msdmanuals.com/professional/endocrine-and-metabolic-disorders/adrenal-disorders/secondary-aldosteronism.

94. *Treatment of primary aldosteronism.* **Quinkler M, Stewart PM.** 2010, Best Pract Res Clin Endocrinol Metab, Vol. 24(6), pp. 923-32.

95. *A comparison of the aldosterone-blocking agents eplerenone and spironolactone.* **Karagiannis A, Athyros VG, Mikhailidis DP.** 2009, Clin Cardiol, Vol. 32(4), p. 230.

96. *Safety profile of mineralocorticoid receptor antagonists: Spironolactone and eplerenone.* **Lainscak M, Pelliccia F, Rosano G, Vitale C, Schiariti M, Greco C, Speziale G, Gaudio C.** 2015, Int J Cardiol, Vol. 200, pp. 25-9.

97. *Comparison of different medical treatments for primary hyperaldosteronism: a systematic review and network meta-analysis.* **Ho WY, Hsiao CC, Wu PH, Chen JY, Tu YK, Wu VC, Chen JJ.** 2024, Ther Adv Chronic Dis, Vol. 15 , p. 20406223241239775.

98. *Familial hyperaldosteronism: an European Reference Network on Rare Endocrine Conditions clinical practice guideline.* **Mulatero P, Scholl UI, Fardella CE, Charmandari E, Januszewicz A, Reincke M, Gomez-Sanchez CE, Stowasser M, Dekkers OM.** 2024, Eur J Endocrinol, Vol. 190(4), pp. G1-G14.

99. *Congenital adrenal hyperplasia.* **Speiser PW, White PC.** 2003, N Engl J Med, Vol. 349(8), pp. 776-88.

100. *Congenital adrenal hyperplasia* . **El Maouche D, Arlt W, Merke DP.** 2017, Lancet, Vol. 390(10108), pp. 2194-2210.

101. *Adrenal steroidogenesis and congenital adrenal hyperplasia.* **Turcu AF, Auchus RJ.** 2015, Endocrinol Metab Clin North Am, Vol. 44(2), pp. 275-96.

102. *Congenital Adrenal Hyperplasia Due to Steroid 21-Hydroxylase Deficiency: An Endocrine Society Clinical Practice Guideline.* **Speiser PW, Arlt W, Auchus RJ, Baskin LS, Conway GS, Merke DP, Meyer-Bahlburg HFL, Miller WL, Murad MH, Oberfield SE, White PC.** 2018, J Clin Endocrinol Metab, Vol. 103(11), pp. 4043-4088.

103. *MANAGEMENT OF ENDOCRINE DISEASE: Congenital adrenal hyperplasia due to 21-hydroxylase deficiency: update on the management of adult patients and prenatal treatment.* **Bachelot A, Grouthier V, Courtillot C, Dulon J, Touraine P.** 2017, Eur J Endocrinol, Vol. 176(4), pp. R167-R181.

104. *Diagnosis and Treatment of Primary Adrenal Insufficiency: An Endocrine Society Clinical Practice Guideline.* **Bornstein SR, Allolio B, Arlt W, Barthel A, Don-Wauchope A, Hammer GD, Husebye ES, Merke DP, Murad MH, Stratakis CA, Torpy DJ.** 2016, J Clin Endocrinol Metab, Vol. 101(2), pp. 364-89.

105. *Clinical review 130: Addison's disease 2001.* **Ten S, New M, Maclaren N.** 2001, J Clin Endocrinol Metab, Vol. 86(7), pp. 2909–22.

106. *Adrenal insufficiency.* **Charmandari E, Nicolaides NC, Chrousos GP.** 2014, Lancet, Vol. 383(9935), pp. 2152-67.

107. *European Society of Endocrinology Clinical Practice Guideline for long-term follow-up of patients operated on for a phaeochromocytoma or a paraganglioma.* **P F Plouin, L Amar, O M Dekkers, M Fassnacht, A P Gimenez-Roqueplo.** 2016, Eur J Endocrinol, Vol. 174(5), pp. G1-G10.

108. *Comprehensive Molecular Characterization of Pheochromocytoma and Paraganglioma.* **Fishbein L, Leshchiner I, Walter V, Danilova L, Robertson AG, Johnson AR, Lichtenberg TM, Murray BA, Ghayee HK, Else T, Ling S, Jefferys SR, de Cubas AA, Wenz B, Korpershoek E, Amelio AL, Makowski L, Rathmell WK, Gimenez-Roqueplo AP, Giordano TJ et al.** 2017, Cancer Cell, Vol. 31(2), pp. 181-193.

109. *Update on Adrenal Tumours in 2017 World Health Organization (WHO) of Endocrine Tumours.* **AK, Lam.** 2017, Endocr Pathol, Vol. 28(3), pp. 213-227.

110. *Pheochromocytoma and Paraganglioma: An Endocrine Society Clinical Practice Guideline.* **Jacques W. M. Lenders, Quan-Yang Duh, Graeme Eisenhofer, Anne-Paule Gimenez-Roqueplo, Stefan K. G. Grebe, Mohammad Hassan Murad, Mitsuhide Naruse, Karel Pacak, William F. Young,.** s.l. : J Clin Endocrinol Metab, 2014, Vol. 99(6), pp. 1915–1942.

111. **Stillwell, William.** Bioactive Lipids. *An Introduction to Biological Membranes (Second Edition).* 453-478 : Elsevier, 2016.

112. *Multiple actions of steroid hormones- a focus on rapid, nongenomic effects.* **Falkenstein E, Tillmann H-C, Christ M, Feuring M, Wehling M.** 2000, Pharmacol Rev, Vol. 52(4), pp. 513-56.

113. **David L Nelson, Michael M Cox.** *Lehninger Principles of Biochemistry.* s.l. : W.H.Freeman & Co Ltd, 2017.

114. *Plasma steroid-binding proteins: primary gatekeepers of steroid action.* **Hammond, G. L.** 2016, J Endocrinol, Vol. 230(1), pp. R13-25.

115. *Transcriptional regulation by the nuclear receptor superfamily.* **Yu VC, Näär AM, Rosenfeld MG.** 1992, Curr Opin Biotechnol, Vol. 3(6), pp. 597-602.

116. *Steroid receptor interactions with heat shock protein and immunophilin chaperones.* **Pratt WB, Toft DO.** 1997, Endocr Rev, Vol. 18(3), pp. 306-60.

117. *The coregulator exchange in transcriptional functions of nuclear receptors.* **Glass CK, Rosenfeld MG.** 2000, Genes Dev, Vol. 14(2), pp. 121-41.

118. *SF-1: a key regulator of development and function in the mammalian reproductive system.* **Y., Ikeda.** 1996, Acta Paediatr Jpn, Vol. 38(4), pp. 412-9.

119. *Nongenomic actions of steroid hormones.* **Lösel, R., Wehling, M.** 2003, Nat Rev Mol Cell Biol, Vol. 4(1), pp. 46–56.

120. *Endocrinology of the stress response.* **Charmandari E, Tsigos C, Chrousos G.** 2005, Annu Rev Physiol, Vol. 67, pp. 259-84.

121. *Regulation of the Hypothalamic-Pituitary-Adrenocortical Stress Response.* **Herman JP, McKlveen JM, Ghosal S, Kopp B, Wulsin A, Makinson R, Scheimann J, Myers B.** 2016, Compr Physiol, Vol. 6(2), pp. 603-21.

122. *Role of glucocorticoid negative feedback in the regulation of HPA axis pulsatility.* **Gjerstad JK, Lightman SL, Spiga F.** s.l. : Stress., 2018, pp. 21(5):403-416.

123. *Cortisol Awakening Response, Internalizing Symptoms, and Life Satisfaction in Emerging Adults.* **Li Shen Chong, Michelle Thai, Kathryn R Cullen, Kelvin O Lim, Bonnie Klimes-Dougan.** 2017, Int J Mol Sci, Vol. 18(12), p. 2501.

124. *The Functional and Clinical Significance of the 24-Hour Rhythm of Circulating Glucocorticoids.* **Oster H, Challet E, Ott V, Arvat E, de Kloet ER, Dijk DJ, Lightman S, Vgontzas A, Van Cauter E.** 2017, Endocr Rev, Vol. 38(1), pp. 3-45.

125. *Resetting of circadian time in peripheral tissues by glucocorticoid signaling.* **Balsalobre A, Brown SA, Marcacci L, Tronche F, Kellendonk C, Reichardt HM, Schütz G, Schibler U.** 2000, Science, Vol. 289(5488), pp. 2344-7.

126. *Glucocorticoids and the circadian clock.* **T., Dickmeis.** 2009, J Endocrinol, Vol. 200(1), pp. 3-22.

127. *Perfect timing: circadian rhythms, sleep, and immunity - an NIH workshop summary.* **Haspel JA, Anafi R, Brown MK, Cermakian N, Depner C, Desplats P, Gelman AE, Haack M, Jelic S, Kim BS, Laposky AD, Lee YC, Mongodin E, Prather AA, Prendergast BJ, Reardon C, Shaw AC, Sengupta S, Szentirmai É, Thakkar M, Walker WE, Solt LA.** 2020, JCI Insight, Vol. 5(1), p. e131487.

128. *Acute and chronic regulation of aldosterone production.* **Hattangady NG, Olala LO, Bollag WB, Rainey WE.** 2012, Mol Cell Endocrinol, Vol. 350(2), pp. 151-62.

129. *The Renin-Angiotensin System in the Central Nervous System and Its Role in Blood Pressure Regulation.* **Nakagawa P, Gomez J, Grobe JL, Sigmund CD.** 2020, Curr Hypertens Rep, Vol. 22(1), p. 7.

130. *Mineralocorticoid receptors: distribution and activation.* **JW, Funder.** 2005, Heart Fail Rev, Vol. 10(1), pp. 15-22.

131. *Revisiting steroidogenesis and its role in immune regulation with the advanced tools and technologies.* **Chakraborty S, Pramanik J, Mahata B.** 2021, Genes Immun, Vol. 22(3), pp. 125–140.

132. **McEwan IJ, Brinkmann AO.** Androgen Physiology: Receptor and Metabolic Disorders. *NIH National Library of Medicine-National Center for Biotechnology Information* . [Online] 2021. https://www.ncbi.nlm.nih.gov/books/NBK279028/.

133. *Progesterone: A Steroid with Wide Range of Effects in Physiology as Well as Human Medicine.* **Kolatorova L, Vitku J, Suchopar J, Hill M, Parizek A.** 2022, Int J Mol Sci, Vol. 23(14), p. 7989.

134. *The Roles of Androgens in Humans: Biology, Metabolic Regulation and Health.* **Alemany, M.** Int J Mol Sci, Vol. 23(19), p. 11952.

135. *On the role of sex steroids in biological functions by classical and non-classical pathways. An update.* **Pillerová M, Borbélyová V, Hodosy J, Riljak V, Renczés E, Frick KM, Tóthová Ľ.** 2021, Front Neuroendocrinol, Vol. 62, p. 100926.

136. *Role of estrogen receptors in health and disease.* **Chen P, Li B, Ou-Yang L.** 2022, Front Endocrinol, Vol. 13, p. 839005.

137. *Systemic distribution of progesterone receptor subtypes in human tissues.* **Asavasupreechar T, Saito R, Miki Y, Edwards DP, Boonyaratanakornkit V, Sasano H.** 2020, J Steroid Biochem Mol Biol, Vol. 199, p. 105599.

138. *Mass spectrometry and immunoassay: how to measure steroid hormones today and tomorrow.* **Taylor AE, Keevil B, Huhtaniemi IT.** 2015, Eur J Endocrinol, Vol. 173(2), pp. D1–D12.

139. *Some problems of radioimmunoassay control.* **Závada, M., Šafarčik, K. & Topolčan, O.** 1978, J. Radioanal. Chem, Vol. 46, pp. 57-66.

140. *Clinical steroid mass spectrometry: A 45-year history culminating in HPLC–MS/MS becoming an essential tool for patient diagnosis.* **Shackleton, Cedric.** 2010, J Steroid Biochem Mol Biol, Vols. 121(3-5), pp. 481-490.

141. *Metabolomics–the link between genotypes and phenotypes.* **Fiehn, Oliver.** 2002, Plant Mol Biol, Vols. 48(1-2), pp. 155-171.

142. *Metabolomics and lipidomics strategies in modern drug discovery and development.* **Astarita G, Kelly RS, Lasky-Su J.** 2023, Drug Discov Today, Vol. 28(10), p. 103751.

143. *Metabolomics enables precision medicine: 'a white paper, community perspective'.* **Beger RD, Dunn W, Schmidt MA, Gross SS, Kirwan JA, Cascante M, Brennan L, Wishart DS, Oresic M, Hankemeier T, Broadhurst DI, Lane AN, Suhre K, Kastenmüller G, Sumner SJ, Thiele I, Fiehn O, Kaddurah-Daouk R.** s.l. : Metabolomics, 2016, Vol. 12(10), p. 149.

144. *Opinion: understanding 'global' systems biology: metabonomics and the continuum of metabolism.* **J.K. Nicholson, I.D. Wilson.** 2003, Nat Rev Drug Discov, Vol. 2(8), pp. 668-676.

145. *Targeted metabolomics.* **Roberts, L. D., Souza, A. L., Gerszten, R. E., Clish, C. B.** 2012, Curr Protoc Mol Biol, Vol. Chapter 30:Unit 30.2, pp. 30, 1–24.

146. *LC-MS-based metabolomics.* **Zhou B, Xiao JF, Tuli L, Ressom HW.** 2012, Mol Biosyst, Vol. 8(2), pp. 470-81.

147. *Contribution of Untargeted Metabolomics for Future Assessment of Biotech Crops.* **Christ B, Pluskal T, Aubry S, Weng JK.** 2018, Trends Plant Sci, Vol. 23(12), pp. 1047-1056.

148. *Biogenic Amines Formation Mechanism and Determination Strategies: Future Challenges and Limitations.* **Ahmad W, Mohammed GI, Al-Eryani DA, Saigl ZM, Alyoubi AO, Alwael H, Bashammakh AS, O'Sullivan CK, El-Shahawi MS.** 2020, Crit Rev Anal Chem, Vol. 50(6), pp. 485-500.

149. *Neurochemistry and defects of biogenic amine neurotransmitter metabolism.* **K, Hyland.** 1999, J Inherit Metab Dis, Vol. 22(4), pp. 353-63.

150. *The mitochondrial carnitine/acylcarnitine carrier: function, structure and physiopathology.* **Indiveri C, Iacobazzi V, Tonazzi A, Giangregorio N, Infantino V, Convertini P, Console L, Palmieri F.** 2011, Mol Aspects Med, Vols. 32(4-6), pp. 223-233.

151. *A student centric method for calculation of fatty acid energetics: Integrated formula and web tool.* **Jain P, Singh S, Arya A.** 2021, Biochem Mol Biol Educ, Vol. 49(3), pp. 492-499.

152. *Plasma acylcarnitine profiles suggest incomplete long-chain fatty acid beta-oxidation and altered tricarboxylic acid cycle activity in type 2 diabetic African-American women.* **Adams SH, Hoppel CL, Lok KH, Zhao L, Wong SW, Minkler PE, Hwang DH, Newman JW, Garvey WT.** 2009, J Nutr, Vol. 139(6), pp. 1073-1081.

153. *Acylcarnitines--old actors auditioning for new roles in metabolic physiology.* **McCoin CS, Knotts TA, Adams SH.** 2015, Nat Rev Endocrinol, Vol. 11(10), pp. 617-625.

154. *Long-chain acylcarnitines and cardiac excitation-contraction coupling: links to arrhythmias.* **Aitken-Buck HM, Krause J, Zeller T, Jones PP, Lamberts RR.** 2020, Front Physiol, Vol. 11, p. 577856.

155. *Postprandial changes in plasma acylcarnitine concentrations as markers of fatty acid flux in overweight and obesity.* **Ramos-Roman MA, Sweetman L, Valdez MJ, Parks EJ.** 2012, Metabolism, Vol. 61(2), pp. 202-212.

156. *Disorders of mitochondrial long-chain fatty acid oxidation and the carnitine shuttle.* **Knottnerus SJG, Bleeker JC, Wüst RCI, Ferdinandusse S, IJlst L, Wijburg FA, Wanders RJA, Visser G, Houtkooper RH.** Rev Endocr Metab Disord, Vol. 19(1), pp. 93-106.

157. *Fat and fatty acid terminology, methods of analysis and fat digestion and metabolism: a background review paper.* **Ratnayake WM, Galli C.** s.l. : Ann Nutr Metab, 2009, pp. 8-43.

158. *Free fatty acid receptors in health and disease.* **Kimura I, Ichimura A, Ohue-Kitano R, Igarashi M.** s.l. : Physiol Rev, 2020, pp. 171-210.

159. *Kinetics, pharmacokinetics, and regulation of L-carnitine and acetyl-L-carnitine metabolism.* **CJ, Rebouche.** s.l. : Ann N Y Acad Sci, 2004, Vol. 1033, pp. 30-41.

160. *Enzymology of the carnitine biosynthesis pathway.* **Strijbis K, Vaz FM, Distel B.** 2010, IUBMB Life, Vol. 62(5), pp. 357-362.

161. *Carnitine transport and fatty acid oxidation.* **Longo N, Frigeni M, Pasquali M.** 2016, Biochim Biophys Acta, Vol. 1863(10), pp. 2422-2435.

162. *Acylcarnitines: Nomenclature, Biomarkers, Therapeutic Potential, Drug Targets, and Clinical Trials.* **Dambrova M, Makrecka-Kuka M, Kuka J, Vilskersts R, Nordberg D, Attwood MM, Smesny S, Sen ZD, Guo AC, Oler E, Tian S, Zheng J, Wishart DS, Liepinsh E, Schiöth HB.** 2022, Pharmacol Rev, Vol. 74(3), pp. 506-551.

163. *Membrane Lipids: Where They Are and How They Behave.* **Van Meer G., Voelker D. R., and Feigenson G. W.** 2008, Nat Rev Mol Cell Biol, Vol. 9(2), pp. 112–124.

164. *Structure and Mechanism in Membrane Trafficking.* **Hughson FM, Reinisch KM.** 2010, Curr Opin Cell Biol, Vol. 22(4), pp. 454–460.

165. **William Dowhan, Mikhail Bogdanov, Eugenia Mileykovskaya.** CHAPTER 1 - Functional roles of lipids in membranes. *Biochemistry of Lipids, Lipoproteins and Membranes (Fifth Edition).* s.l. : Elsevier, Dennis E. Vance, Jean E. Vance, pp. 1-37.

166. *Glycerophospholipids: Roles in Cell Trafficking and Associated Inborn Errors.* **Lamari F, Rossignol F, Mitchell GA.** 2025, J Inherit Metab, Vol. 48(2), p. e70019.

167. *Concise Synthesis of Glycerophospholipids.* **Tufan K Mukhopadlhyay, Dirk Trauner.** 2023, J. Org. Chem., Vol. 88, p. 11253−11257.

168. **Pulok Kumar Mukherjee, Sayan Biswas, Amit Kar, Nanaocha Sharma, Pallab Kanti Haldar.** Chapter 4 - Phospholipid complexation: A versatile technique for delivery of phytomedicine. *Evidence-Based Validation of Herbal Medicine (Second Edition).* 2022, pp. 65-108.

169. *Molecular properties of various structurally defined sphingomyelins -- correlation of structure with function.* **J, Peter Slotte.** 2013, Prog Lipid Res, Vol. 52(2), pp. 206-19.

170. *Cardiovascular Implications of Sphingomyelin Presence in Biological Membranes.* **Kikas P, Chalikias G, Tziakas D.** 2018, Eur Cardiol, Vol. 13(1), pp. 42-45.

171. *The importance of hydrogen bonding in sphingomyelin's membrane interactions with co-lipids.* **JP, Slotte.** 2016, Biochim Biophys Acta, Vol. 1858(2), pp. 304-10.

172. *Structure and dynamics of sphingomyelin bilayer: insight gained through systematic comparison to phosphatidylcholine.* **Niemelä P, Hyvönen MT, Vattulainen I.** 2004, Biophys J, Vol. 87(5), pp. 2976-89.

173. *Effect of sphingomyelin composition on the phase structure of phosphatidylcholine-sphingomyelin bilayers.* **Bar LK, Barenholz Y, Thompson TE.** Biochemistry : s.n., 1997, Vol. 36(9), pp. 2507-16.

174. *Biological functions of sphingomyelins.* **JP, Slotte.** 2013, Prog Lipid Res, Vol. 52(4), pp. 424-37.

175. *Liquid chromatography–tandem mass spectrometry applications in endocrinology.* **Kushnir MM, Rockwood AL, Bergquist J.** 2010, Mass Spectrom Rev, Vol. 29(3), pp. 480-502.

176. *LC–MS/MS analysis of steroids in the clinical laboratory.* **Keevil, Brian G.** 2016, Clin Biochem, Vols. 49(13-14), pp. 989-997.

177. *A liquid chromatography-tandem mass spectrometry (LC-MS/MS)-based assay to profile 20 plasma steroids in endocrine disorders.* **Wang Z, Wang H, Peng Y, Chen F, Zhao L, Li X, Qin J, Li Q, Wang B, Pan B, Guo W.** 2020, Clin Chem Lab Med, Vol. 58(9), pp. 1477-1487.

178. *Dried Blood Spot Multiplexed Steroid Profiling Using Liquid Chromatography Tandem Mass Spectrometry in Korean Neonates.* **Choi R, Park HD, Oh HJ, Lee K, Song J, Lee SY.** 2019, Ann Lab Med, Vol. 39(3), pp. 263-270.

179. *Steroid profiling by UHPLC-MS/MS in dried blood spots collected from healthy women with and without testosterone gel administration.* **Salamin O, Nicoli R, Xu C, Boccard J, Rudaz S, Pitteloud N, Saugy M, Kuuranne T.** 2021, J Pharm Biomed Anal, Vol. 204, p. 1142.

180. *Predictive, personalized, preventive, participatory (P4) cancer medicine.* **Hood L, Friend SH.** 2011, Nat Rev Clin Oncol, Vol. 8(3), pp. 184-7.

181. *Monitoring adrenal insufficiency through salivary steroids: a pilot study.* **Tucci L, Fanelli F, Improta I, Bissi V, Lena C, Galante G, Mezzullo M, Magagnoli M, Lalumera AB, Colombin G, Coscia K, Rotolo L, Vicennati V, Pagotto U, Di Dalmazi G.** 2024, Eur J Endocrinol, Vol. 190(4), pp. 327-337.

182. *The human circadian metabolome.* **Dallmann R, Viola AU, Tarokh L, Cajochen C, Brown SA.** 2012, Proc Natl Acad Sci USA, Vol. 109(7), pp. 2625-2629.

183. *Cortisol-related metabolic alterations assessed by mass spectrometry assay in patients with Cushing's syndrome.* **Di Dalmazi G, Quinkler M, Deutschbein T, Prehn C, Rayes N, Kroiss M,**

Berr CM, Stalla G, Fassnacht M, Adamski J, Reincke M, Beuschlein F. 2017, Eur J Endocrinol, Vol. 177(2), pp. 227-237.

184. *Substantial benefits of an inert biphenyl column for the analysis of steroids and their phase II metabolites in biological samples.* **Galmiche M, Monat MA, Lopez DA, Lamboley C, Connolly P, Girel S, Guillarme D, Meister I, Rudaz S.** 2024, J Sep Sci, Vol. 47(16), p. e2400436.

185. *Extended Steroid Profiling in Human Serum and Plasma with Simultaneous Quantitative Determination Using One-Point Internal Calibration.* **Galmiche M, Strassel O, Monat MA, Meister I, Boccard J, Rudaz S.** 2025, J Sep Sci, Vol. 48(4), p. e70147.

186. *Estimation of the Volume of Blood in a Small Disc Punched From a Dried Blood Spot Card.* **Hewawasam, E., Liu, G., Jeffery, D.W., Gibson, R.A. and Muhlhausler, B.S.** 2018, Eur. J. Lipid Sci. Technol, Vol. 120, p. 1700362.

187. *Multitargeted Internal Calibration for the Quantification of Chronic Kidney Disease-Related Endogenous Metabolites Using Liquid Chromatography–Mass Spectrometry.* **Visconti G, de Figueiredo M, Strassel O, Boccard J, Vuilleumier N, Jacques D, Ponte B, Rudaz S.** 2023, Anal Chem, Vol. 95(36), pp. 13546-13554.

188. *Derivatization of estrogens enhances specificity and sensitivity of analysis of human plasma and serum by liquid chromatography tandem mass spectrometry.* **Abdullah M.M. Faqehi, Diego F. Cobice, Gregorio Naredo, Tracy C.S. Mak, Rita Upreti, Fraser W. Gibb, Geoffrey J. Beckett, Brian R. Walker, Natalie Z.M. Homer, Ruth Andrew,.** 2016, Talanta, Vol. 151, pp. 148-156.

189. *Sublinical Cushing's syndrome.* **De Leo M, Cozzolino A, Colao A, Pivonello R.** 2012, Best Pract Res Clin Endocrinol Metab, Vol. 26(4), pp. 497-505.

190. *Feature Selection with the Boruta Package.* **Kursa, M. B., & Rudnicki, W. R.** 2010, Journal of Statistical Software, Vol. 36(11), pp. 1–13.

191. *The varimax criterion for analytic rotation in factor analysis.* **Kaiser, H.F.** 1958, Psychometrika, Vol. 23, pp. 187–200.

192. **farmaco, AIFA-Agenzia italiana del.** L'uso dei farmaci in Italia - Rapporto OsMed 2019. [Online] 2020. https://www.aifa.gov.it/web/guest/-/rapporto-osmed-2019.

193. —. L'uso dei farmaci in Italia - Rapporto OsMed 2023. [Online] 2024. https://www.aifa.gov.it/-/l-uso-dei-farmaci-in-italia-rapporto-osmed-2023.

194. *The Use of Mass Spectrometry to Analyze Dried Blood Spots.* **Wagner M, Tonoli D, Varesio E, and Hopfgartner G.** 2016, Mass Spec Rev, Vol. 35 (3), pp. 361–438.

195. *Female and male serum reference intervals for challenging sex and precursor steroids by liquid chromatography - tandem mass spectrometry.* **Mezzullo M, Pelusi C, Fazzini A, Repaci A, Di Dalmazi G, Gambineri A, Pagotto U, and Fanelli.** 2020, J Steroid Biochem, Vol. 197 , p. 105538.

196. *Serum steroid profiling by isotopic dilution-liquid chromatography-mass spectrometry: comparison with current immunoassays and reference intervals in healthy adults.* **Fanelli F, Belluomo I, Di Lallo VD, Cuomo G, De Iasio R, Baccini M, Casadio E, Casetta B, Vicennati V, Gambiner A et al.** 2011, Steroids, Vol. 76, pp. 244-253.

197. *Determination of unbound prednisolone, prednisone and cortisol in human serum and saliva by on-line solid-phase extraction liquid chromatography tandem mass spectrometry and potential implications for drug monitoring of prednisolone and prednisone saliva.* **Ruiter AFC, Teeninga N, Nauta J, Endert E, Ackermans MT.** 2012, Biomed Chromatogr, Vol. 26, pp. 789–96.

198. *Steroid hormone concentrations in dried blood spots: A comparison between capillary and venous blood samples.* **Olthof A, de Kleijne VH, Boelen A, Heijboer AC.** 2025, Clin Chim Acta, Vol. 567, p. 120099.

199. *Measuring Steroids from Dried Blood Spots Using Tandem Mass Spectrometry to Diagnose Congenital Adrenal Hyperplasia.* **Qasrawi DO, Boyd JM, Sadrzadeh SMH.** 2021, Clin. Chim. Acta, Vol. 520, pp. 202–207.

200. *Biphenyl based stationary phases for improved selectivity in complex steroid assays.* **Lindner JM, Vogeser M, Grimm SH.** 2017, J Pharm Biomed Anal., Vol. 142, pp. 66-73.

201. *Robust Extraction, Separation and Quantitation of Structural Isomer Steroids From Human Plasma by SPE with LC-MS/MS Detection.* **Scientific, Thermo Fisher.** 2019. Improved separation of steroid isomers using an Accucore Biphenyl column [Poster] Pittcon Conference & Expo, Philadelphia, PA, USA.

202. *Assessment of ammonium fluoride as a mobile phase additive for sensitivity gains in electrospray ionization.* **Jeremy Ryan McFadden, David Michael Ames.** 2023, Anal Sci Adv, Vols. 4 (11-12), pp. 347-354.

203. *Determination of a steroid profile in heel prick blood using LC-MS/MS.* **Boelen A, Ruiter AF, Claahsen-van der Grinten HL, Endert E, Ackermans MT.** 2016, Bioanalysis, Vol. 8(5), pp. 375-84.

204. *Evaluation of a Two-Tier Screening Pathway for Congenital Adrenal Hyperplasia in the New South Wales Newborn Screening Programme.* **Lai F, Srinivasan S, Wiley V.** 2020, Int J Neonatal Screen, Vol. 6(3), p. 63.

205. *From a single steroid to the steroidome: Trends and analytical challenges.* **Olesti E, Boccard J, Visconti G, González-Ruiz V, Rudaz S.** 2021, J Steroid Biochem Mol Biol, Vol. 206, p. 105797.

206. *Interlaboratory and Interplatform Study of Steroids Collision Cross Section by Traveling Wave Ion Mobility Spectrometry.* **Hernández-Mesa M, D'Atri V, Barknowitz G, Fanuel M, Pezzatti J, Dreolin N, Ropartz D, Monteau F, Vigneau E, Rudaz S, Stead S, Rogniaux H, Guillarme D, Dervilly G, Le Bizec B.** 2020, Anal Chem, Vol. 92(7), pp. 5013-5022.

207. *Recent Advances in LC-MS-Based Metabolomics for Clinical Biomarker Discovery.* **Chen CJ, Lee DY, Yu J, Lin YN, Lin TM.** 2023, Mass Spectrometry Reviews, Vol. 42(6), pp. 2349-2378.

208. *Approaches in Metabolomics for Regulatory Toxicology Applications.* **Olesti E, González-Ruiz V , Wilks MF , Boccard J , Rudaz S.** 2021, Analyst, Vol. 146(6), pp. 1820-1834.

209. *Tutorial Review on Validation of Liquid Chromatography-Mass Spectrometry Methods: Part II.* **Kruve A, Rebane R, Kipper K, Oldekop ML, Evard H, Herodes K, Ravio P, Leito I.** 2015, Analytica Chimica Acta, Vol. 870, pp. 8–28.

210. *Improving Quantitative Precision and Throughput by Reducing Calibrator Use in Liquid Chromatography-Tandem Mass Spectrometry.* **Rule GS, Rockwood AL.** 2016, Analytica Chimica Acta, Vol. 919, pp. 55-61.

211. *Internal Calibration as an Emerging Approach for Endogenous Analyte Quantification: Application to Steroids.* **Visconti G, Olesti E, González-Ruiz V, Glauser G, Tonoli D, Lescuyer P, Vuilleumier N, Rudaz S.** 2022, Talanta, Vol. 240, p. 123149.

212. *Isotope Dilution With Isotopically Labeled Biomass: An Effective Alternative for Quantitative Metabolomics.* **Fitz V, Panzenboeck L, Schoeny H, Foels E, Koellensperger G.** 2024, Analytica Chimica Acta, Vol. 1318, p. 342909.

213. *A mid-day surge in cortisol levels.* **Quigley ME, Yen SS.** 1979, J Clin Endocrinol Metab, Vol. 49(6), pp. 945-7.

214. *Diurnal cortisol peaks and their relationships to meals.* **Follenius M, Brandenberger G, Hietter B.** 55(4), 1982, J Clin Endocrinol Metab, pp. 757-61.

215. *Parallel diurnal fluctuation of testosterone, androstenedione, dehydroepiandrosterone and 17OHprogesterone as assessed in serum and saliva:validation of a novel liquid chromatography-tandem mass spectrometry method for salivary steroid profiling.* **Mezzullo M, Fazzini A, Gambineri A, Di Dalmazi G, Mazza R, Pelusi C, Vicennati V, Pasquali R, Pagotto U, Fanelli F.** 2017, Clin Chem Lab Med, Vol. 55(9), pp. 1315-1323.

216. *Progesterone and human cognition.* **VW, Henderson.** 2018, Climacteric, Vol. 21(4), pp. 333-340.

217. *Alteration in glucocorticoids secretion and metabolism in patients affected by cystic fibrosis.* **Podgórski R, Sumińska M, Rachel M, Fichna M, Fichna P, Mazur A.** 2022, Front Endocrinol (Lausanne), p. 13:1074209.

218. *11β-Hydroxysteroid Dehydrogenases: Intracellular Gate-Keepers of Tissue Glucocorticoid Action.* **Karen Chapman, Megan Holmes, Jonathan Seckl.** 2013, Physiological Reviews, Vol. 93(33), pp. 139-206.

219. *Steroid Metabolism in Children and Adolescents With Obesity and Insulin Resistance: Altered SRD5A and 20α/20βHSD Activity.* **Sumińska M, Podgórski R, Fichna P, Fichna M.** 2021, Front. Endocrinol, Vol. 12, p. 759971.

220. *11-Oxygenated androgens in health and disease.* **Turcu AF, Rege J, Auchus RJ, Rainey WE.** 2020, Nat Rev Endocrinol, Vol. 16(5), pp. 284-296.

221. **Database, Human Metabolome.** Human Metabolome Database-Androstenediol. [Online] https://www.hmdb.ca/metabolites/HMDB0003818.

222. *Exploring the human chorionic gonadotropin induced steroid secretion profile of mouse Leydig tumor cell line 1 by a 20 steroid LC-MS/MS panel.* **Fanelli F, Magagnoli M, Mezzullo M, Lispi M, Limoncella S, Tommasini A, Pelusi C, Santi D, Simoni M, Pagotto U, Casarini L.** 2023, J Steroid Biochem Mol Biol, Vol. 229, p. 106270.

223. *Estrogen and androgen receptor mediated stimulation and inhibition of proliferation by androst-5-ene-3 beta,17 beta-diol in human mammary cancer cells.* **Hackenberg R, Turgetto I, Filmer A, Schulz KD.** 1993, J Steroid Biochem Mol Biol, Vol. 46 (5), pp. 597–603.

224. *Androgen glucuronides, instead of testosterone, as the new markers of androgenic activity in women.* **Labrie F, Bélanger A, Bélanger P, Bérubé R, Martel C, Cusan L, Gomez J, Candas B, Castiel I, Chaussade V, Deloche C, Leclaire J.** 2006, J Steroid Biochem Mol Biol, Vols. 99(4-5), pp. 182-8.

225. **National Center for Biotechnology Information, Pubchem.** PubChem Compound Summary for CID 101849, 11beta-Hydroxyetiocholanolone. Retrieved October 30, 2025. [Online] October 2025. https://pubchem.ncbi.nlm.nih.gov/compound/11beta-Hydroxyetiocholanolone.

226. *The structural biology of oestrogen metabolism.* **Thomas MP, Potter BV.** 2013, J Steroid Biochem Mol Biol, Vol. 137, pp. 27-49.

227. *Genetic variation in the estrogen metabolic pathway and mammographic density as an intermediate phenotype of breast cancer.* **Li J, Eriksson L, Humphreys K, Czene K, Liu J, Tamimi RM, Lindström S, Hunter DJ, Vachon CM, Couch FJ, Scott CG, Lagiou P, Hall P.** 2010, Breast Cancer Res, Vol. 12(2), p. R19.

228. *Estrogen Metabolism in Abdominal Subcutaneous and Visceral Adipose Tissue in Postmenopausal Women.* **Hetemäki N, Savolainen-Peltonen H, Tikkanen MJ, Wang F, Paatela H, Hämäläinen E, Turpeinen U, Haanpää M, Vihma V, Mikkola TS.** 2017, J Clin Endocrinol Metab, Vol. 102(12), pp. 4588-4595.

229. *Current strategies for quantification of estrogens in clinical research.* **Denver N, Khan S, Homer NZM, MacLean MR, Andrew R.** 2019, J Steroid Biochem Mol Biol, Vol. 192, p. 192:105373.

230. *The Role of Sex in the Pathophysiology of Pulmonary Hypertension.* **Docherty CK, Harvey KY, Mair KM, Griffin S, Denver N, MacLean MR.** 2018, Adv Exp Med Biol, Vol. 1065, pp. 511-528.

231. *Estrogen metabolites and breast cancer.* **Santen RJ, Yue W, Wang JP.** 2015, Steroids, Vol. 99(Pt A), pp. 61-6.

232. *Estrogen Metabolism and Risk of Postmenopausal Endometrial and Ovarian Cancer: the B ~ FIT Cohort.* **Dallal CM, Lacey JV Jr, Pfeiffer RM, Bauer DC, Falk RT, Buist DS, Cauley JA, Hue TF, LaCroix AZ, Tice JA, Veenstra TD, Xu X, Brinton LA and Group, B~FIT Research.** 2016, Horm Cancer, Vol. 7(1), pp. 49-64.

233. *Circulating Estrogens and Postmenopausal Ovarian Cancer Risk in the Women's Health Initiative Observational Study.* **Trabert B, Brinton LA, Anderson GL, Pfeiffer RM, Falk RT, Strickler HD, Sliesoraitis S, Kuller LH, Gass ML, Fuhrman BJ, Xu X, Wentzensen N.** 2016, Cancer Epidemiol Biomarkers Prev, Vol. 25(4), pp. 648-56.

234. *Sex steroid hormone metabolism in relation to risk of aggressive prostate cancer.* **Black A, Pinsky PF, Grubb RL 3rd, Falk RT, Hsing AW, Chu L, Meyer T, Veenstra TD, Xu X, Yu K, Ziegler RG, Brinton LA, Hoover RN, Cook MB.** 2014, Cancer Epidemiol Biomarkers Prev, Vol. 23(11), pp. 2374-82.

235. *Estrogen: an emerging regulator of insulin action and mitochondrial function.* **Gupte AA, Pownall HJ, Hamilton DJ.** 2015, J Diabetes Res, Vol. 2015, p. 916585.

236. *An LC/MS/MS method for analyzing the steroid metabolome with high accuracy small serum samples.* **Yuan T-F, Le J, Wang S-T, Li Y.** 2020, J Lipid Res, Vol. 61(4), pp. 580–6.

237. *Measurement of estradiol in human serum by LC-MS/MS using a novel estrogen-specific derivatization reagent.* **Keski-Rahkonen P, Desai R, Jimenez M, Harwood DT, Handels man DJ.** 2015, Anal Chem, Vol. 87(14), pp. 7180–6.

238. *Development and validation of LC-MS/MS method for quantification of bisphenol A and estrogens in human plasma and seminal fluid.* **Vitku J, Chlupacova T, Sosvorova L, Hampl R, Hill M, Heracek J, Bicikova M, Starka L.** 2015, Talanta, Vol. 140, pp. 62-67.

239. *Therapeutic drug monitoring by dried blood spot: progress to date and future directions.* **Wilhelm AJ, den Burger JC, Swart EL.** 2014, Clin Pharmacokinet, Vol. 53(11), pp. 961-73.

240. *A comparative study of plasma and dried blood spot metabolomics and its application to diabetes mellitus.* **Chiu HH, Lin SY, Zhang CG, Tsai CC, Tang SC, Kuo CH.** 2024, Clin Chim Acta, Vol. 552, p. 117655.

241. *Development of Certified Reference Material for Amino Acids in Dried Blood Spots and Accuracy Assessment of Disc Sampling.* **Woo S, Rosli N, Choi S, Kwon HJ, Yoon YA, Ahn S, Lee JY, Hong SP, Jeong JS.** 2022, Anal Chem, Vol. 94(28), pp. 10127-10134.

242. *Direct and quantitative analysis of underivatized acylcarnitines in serum and whole blood using paper spray mass spectrometry.* **Yang Q, Manicke NE, Wang H, Petucci C, Cooks RG, Ouyang Z.** 2012, Anal Bioanal Chem, Vol. 404(5), pp. 1389-97.

243. *Differences between acylcarnitine profiles in plasma and bloodspots.* **de Sain-van der Velden MG, Diekman EF, Jans JJ, van der Ham M, Prinsen BH, Visser G, Verhoeven-Duif NM.** 2013, Mol Genet Metab, Vols. 110(1-2), pp. 116-21.

244. *The development and validation of a fast and robust dried blood spot based lipid profiling method to study infant metabolism.* **Koulman A, Prentice P, Wong MCY, Matthews L, Bond NJ, Eiden M, Griffin JL, Dunger DB.** 2014, Metabolomics, Vol. 10(5), pp. 1018-1025.

245. *Possible, probable, and certain hypercortisolism: A continuum in the risk of comorbidity.* **Araujo-Castro M, Pascual-Corrales E, Lamas C.** 2023, Ann Endocrinol (Paris), Vol. 84(2), pp. 272-284.

246. *Glucose metabolism in Cushing's syndrome.* **Sharma A, Vella A.** 2020, Curr Opin Endocrinol Diabetes Obes, Vol. 27(3), pp. 140-145.

247. *Glucose and lipid metabolism abnormalities in Cushing's syndrome.* **Salehidoost R, Korbonits M.** 2022, J Neuroendocrinol, Vol. 34(8), p. e13143.

248. *The effects of glucocorticoids on adipose tissue lipid metabolism.* **Peckett AJ, Wright DC, Riddell MC.** 2011, Metabolism, Vol. 60(11), pp. 1500-10.

249. *Endogenous cortisol excess confers a unique lipid signature and metabolic network.* **Vega-Beyhart A, Iruarrizaga M, Pané A, García-Eguren G, Giró O, Boswell L, Aranda G, Flores V, Casals G, Alonso C, Mora M, Halperin I, Carmona F, Enseñat J, Vidal O, Hu T, Rojo G, Gomis R, Hanzu FA.** 2021, J Mol Med (Berl), Vol. 99(8), pp. 1085-1099.

250. *Synergistic Effect of Cortisol and Growth Hormone on Hepatic Ornithine Decarboxylase Activity 1.* **R. Richman, L. Underwood, J. V. Van Wyk, S. Voina.** 1971, Proc Soc Exp Biol Med, Vol. 138(3), pp. 880-4.

251. **Douglas A. Skoog, F. James Holler e Stanley R. Crouch.** *Principles of Instrumental Analysis.* s.l. : 5th Ed., p.726, 1971.

252. **ScienceDirect Topics, s.d.** Mass Spectrometer. *ScienceDirect* . [Online] https://www.sciencedirect.com/topics/engineering/mass-spectrometer.

253. **Instruments, Shimadzu Scientific.** Interfaces for LC-MS. [Online] https://www.ssi.shimadzu.com/service-support/technical-support/analysis-basics/fundamental/interfaces_for_lcms.html#section2.

254. **Lloyd R. Snyder, Joseph J. Kirkland, John W. Dolan.** *Introduction to Modern Liquid Chromatography.* s.l. : Wiley, 2011.

256. *Bioanalytical LC-MS/MS validation of therapeutic drug monitoring assays in oncology.* **van Nuland M, Rosing H, Schellens JHM, Beijnen JH.** s.l. : Biomed Chromatogr., 2020, p. 34(1):e4623.

257. *The Multifaceted Mineralocorticoid Receptor.* **E Gomez-Sanchez, C.E. Gomez-Sanchez.** s.l. : Comprehensive Physiology, 2014, pp. 965-994.

258. *Adrenocortical carcinoma.* **Else T, Kim AC, Sabolch A, Raymond VM, Kandathil A, Caoili EM, Jolly S, Miller BS, Giordano TJ, Hammer GD.** s.l. : Endocr Rev, 2014, pp. 35(2):282-326.

259. *metaP-Server: A Web-Based Metabolomics Data Analysis Tool.* **Gabi Kastenmüller, Werner Römisch-Margl, Brigitte Wägele, Elisabeth Altmaier, Karsten Suhre.** s.l. : Clinical and Epidemiological Metabonomics, 2011.

260. *Steroid profiling by UHPLC-MS/MS in dried blood spots collected from healthy women with and without testosterone gel administration.* **Olivier Salamin, Raul Nicoli, Cheng Xu, Julien Boccard, Serge Rudaz, Nelly Pitteloud, Martial Saugy, Tiia Kuuranne.** s.l. : Journal of Pharmaceutical and Biomedical Analysis, 2021, Vol. 204.

261. **Products, Clinical Lab.** Implementing Dried Blood Spot (DBS) Testing in the Clinical Laboratory. [Online] 2022. https://clpmag.com/diagnostic-technologies/anatomic-pathology/specimen-collection-handling/implementing-dried-blood-spot-dbs-testing-in-the-clinical-laboratory/.

262. *Postprandial Dried Blood Spot-Based Nutritional Metabolomic Analysis Discriminates a High-Fat, High-Protein Meat-Based Diet from a High Carbohydrate Vegan Diet: A Randomized Controlled Crossover Trial.* **McNairn M, Brito A, Dillard K, Heath H, Pantaleon M, Fanter R, Pilolla K, Amin S, La Frano MR.** s.l. : J Acad Nutr Diet, 2021, pp. 121(5):931-941.e2. .

263. *Diurnal pattern of protein and energy metabolism in man.* **Garlick PJ, Clugston GA, Swick RW, Waterlow JC.** s.l. : J Clin Nutr, 1980, pp. 33(9):1983-6.

264. **eMedicine, Pediatric Adrenal Insufficiency (Addison Disease) at.** [Online]

265. **Products, Clinical Lab.** Implementing Dried Blood Spot (DBS) Testing in the Clinical Laboratory. [Online] April 05, 2022. https://clpmag.com/diagnostic-technologies/anatomic-pathology/specimen-collection-handling/implementing-dried-blood-spot-dbs-testing-in-the-clinical-laboratory/.

266. *LC–MS-based metabolomics: an update.* **Zhong-Ze Fang, Frank J Gonzalez.** 2014, Arch Toxicol, pp. 88(8):1491–1502.

267. *Glucose and lipid metabolism abnormalities in Cushing's syndrome.* **Salehidoost R, Korbonits M.** 2022, J Neuroendocrinol, Vol. 34(8), p. e13143.